Studies into endothelial cell migration in corneal models: towards application of ROCK inhibitor in treatment

Thesis submitted to Cardiff University for the degree of Doctor of Philosophy (Ph.D.)

2018

Alina Akhbanbetova

School of Optometry and Vision Sciences
Cardiff University

Abstract

A clear cornea comprising the front surface of the eye is essential for normal vision. In part, a single layer of corneal endothelial cells located on the inner surface of the cornea helps regulate corneal transparency. In corneal endothelial dysfunctions such as Fuchs' endothelial corneal dystrophy (FECD), however, deteriorating endothelial cells lead to corneal cloudiness and a progressive loss of vision. FECD is currently treated via corneal replacement surgeries, which generally are successful but are associated with some potentially problematic issues, including donor shortage and graft rejections. Thus, there is a pressing need for new, less-invasive medical treatments for corneal endothelial dysfunction and the resultant loss of vision. Recently, there has been a growing interest in selective inhibitors of a Rho-associated kinase (ROCK) as agents that can help dysfunctional endothelial cells recover.

The research described in this thesis has as its main focus an investigation of new treatment options for corneal endothelial diseases such as FECD. As a baseline, corneal endothelial development is studied because some biological processes in corneal healing have been reported to recapitulate those in corneal embryogenesis. Following this, an assessment is made of the human corneal endothelium and the morphologic changes that occur in FECD.

Next, to judge potential new therapeutic approaches to treat vision loss caused by corneal endothelial dysfunction, experiments to assess the potential of transcoreal freezing were conducted. These identified the optimal use of a newly designed cryoprobe and its application for transcorneal freezing to reproducibly damage corneal endothelial cells that line the inner aspect of the cornea. Ingress into the cornea of dyes and medicinal agents was also tested. The concept of this approach is to eliminate the diseased corneal endothelial cells, prior to the medicinal encouragement of more peripheral corneal endothelial cells to regenerate the ablated area.

Current research in many laboratories indicates that inhibitors of the Rho kinase pathway within cells lead to them becoming more fibroblast-like in their phenotype, accelerating the migration and inhibit cell death encouraging the endothelial wound healing. This study suggests that a less invasive transcorneal freezing using a 3.4 mm-diameter cryoprobe can be used for reproducible and targeted endothelial cell destruction to be followed by selective ROCK inhibitor application to treat corneal endothelial pathologies such as FECD and potentially other corneal endothelial dysfunctions.

.

Acknowledgements

It is my great honour to thank the Life Sciences Research Network Wales - Ser Cymru studentship for funding the research of this thesis.

I wish to express my immeasurable appreciation to my supervisors, Professor Andrew Quantock and Dr Rob Young, for their generosity in sharing their skills and knowledge, their understanding and assistance, without which this work would not have been possible.

Huge thanks to Prof Noriko Koizumi, Dr Naoki Okumura for supervising me during my visit to Doshisha University in Japan. It is also my great honour to have the opportunity to give special thanks to Nigel Fullwood for carrying out scanning electron microscopy for a study in my thesis. Thank you to my advisor, Dr Craig Boote, for the valuable input during our meetings.

Many thanks also to the members of the School of Optometry and Vision Sciences, all the past and present members of the Structural Biophysics Research Group for being supportive and friendly. I want to especially thank Dr Elena Koudouna for her kindness and taking good care of me during my visit to Japan.

I am enormously grateful to my precious family members, especially, mother, aunt, and sister for their unconditional love, belief in me and encouragement at all times. My studies were partly funded by my dear aunt, Professor Zoya Tuiebakhova, who I am incredibly grateful for making this life-changing opportunity of studying in the UK possible for me.

Last but not least, I wish to thank my wonderful husband, Neil Emery, for his caring love and support always. I also thank my beloved mother in law for being my family away from home.

I am thankful for everyone who was involved in this beautiful journey.

List of publications

Chan, W., **Akhbanbetova, A**., Quantock, A. J. and Heard, C. M. (2016) 'Topical delivery of a Rho-kinase inhibitor to the cornea via mucoadhesive film', *European Journal of Pharmaceutical Sciences*, 91. doi: 10.1016/j.ejps.2016.05.016.

Akhbanbetova, A., Nakano, S., Littlechild, S.L., Young, R.D., Zvirgzdina, M., Fullwood, N.J., Weston, I., Weston, P., Kinoshita, S., Okumura, N. and Koizumi, N. (2017). A surgical cryoprobe for targeted transcorneal freezing and endothelial cell removal. *Journal of Ophthalmology*, 2017.

Table of contents

List of figures

List of tables

List of abbreviations

ARVO	The Association for Research in Vision and Ophthalmology
BDMA	Benzyl Dimethylamine
BSA	Bovine Serum Albumin
CRD	Cysteine-rich domain
DAPI	4′,6-diamidino-2-phenylindole
DDSA	Dodecenyl succinic anhydride
DLK	Deep lamellar keratoplasty
DM	Descemet’s membrane
DMEK	Descemet’s membrane endothelial keratoplasty
DMEM	Dulbecco's modified Eagle’s medium
DSAEK	Descemet’s stripping automated endothelial keratoplasty
DSEK	Descemet’s stripping endothelial keratoplasty
ECM	Extracellular matrix
EMT	Endothelial-mesenchymal transition
ER	Endoplasmic reticulum
FECD	Fuchs endothelial corneal dystrophy
GAG	Glycosaminoglycan
IHC	immunohistochemistry
IL	Interleukin
MAPK	Mitogen-activated protein kinase
MLC	Myosin light chain
PBS	Phosphate-buffered saline
PH	Plekstrin homology
PI	Propodium iodide
PRDX	Peroxiredoxin
RBD	Receptor binding domain
ROCK	Rho-associated protein kinase
ROS	Reactive oxygen species
SBF-SEM	serial block face scanning electron microscopy
SEM	Scanning electron microscope
TEM	Transmission electron microscope
TGFβ	Transforming growth factor beta
UV	Ultraviolet

Chapter 1: Introduction

1.1 Introduction

A clear cornea comprising the front surface of the eye is essential for normal vision. In part, a single layer of corneal endothelial cells located on the inner surface of the cornea helps regulate corneal transparency. In corneal endothelial dysfunctions such as Fuchs' endothelial corneal dystrophy (FECD), however, deteriorating corneal endothelial cells lead to corneal cloudiness and a progressive loss of vision. Corneal diseases are one of the primary causes of blindness in the world after cataract and glaucoma, according to the World Health Organisation (WHO, 2018) Corneal endothelial dysfunction, such as FECD in particular, affects approximately 5% of the United States population that is over the age of 40 years (Lorenzetti *et al.*, 1967; Baratz *et al.*, 2010). This prevalence is higher in countries such as Singapore (7%), Iceland (10%), and some small American Islands (22%) (Kitagawa *et al.*, 2002; Zoega *et al.*, 2006; Eghrari *et al.*, 2012). FECD is more common in females within a population of over 40 years of age (Friedenwxald and Friedenwvald, 1925; Goar, 1934; Krachmer *et al.*, 1978; Okumura, Hayashi and Koizumi, 2018), although the condition may occur in men and younger age (early-onset) groups (Magovern *et al.*, 1979; Biswas *et al.*, 2001). It is also known to be intensified by mechanical injuries (Hayashi *et al.*, 1996).

Currently, corneal replacement via graft surgery is the predominant treatment option for the endothelial diseases such as FECD. Corneal blindness caused by FECD is the foremost indication for more than 46,000 corneal transplant operations performed in the USA each year, a pattern that is mirrored in most developed countries worldwide (Lang and Naumann, 1987; Ramsay, Lee and Mohammed, 1997; Baratz *et al.*, 2010; Musch *et al.*, 2011; Keenan *et al.*, 2012; Wieben *et al.*, 2012; Tan *et al.*, 2014; Park *et al.*, 2015; Robert *et al.*, 2015; Le *et al.*, 2017). These transplants, though effective, can lead to numerous complications (Patel, Hodge and Bourne, 2005). Another issue with corneal transplantations is the shortage of donor corneas (Hara and Cooper, 2011). Thus there is a need for a new medical treatment strategy for FECD and other corneal endothelial dysfunctions.

The aims of this thesis are two-fold. First, to further investigate the normal morphology and morphologic changes of the corneal endothelium during embryonic development and following endothelial pathology. Second, to elucidate the possibility of deleting diseased endothelial cells by transcorneal freezing using a newly designed cryoprobe, and the potential for a Rho-associated kinase (ROCK) inhibitor to promote healing of a damaged corneal endothelium as a prospective alternative approach to treat corneal endothelial dysfunctions, such as FECD. To achieve my objectives, corneas from a range of species were utilised; embryonic chick for the development studies, post-operative human FECD tissue to more fully characterise the pathology, *in vitro* pig eyes for the transcorneal freezing experiments, and rabbit corneas, *in vivo* and *in vitro* for the post-freeze healing experiments and initial studies of the influence of a ROCK inhibitor on corneal endothelial healing.

1.2 The anatomy of the eye

The human eye is a complex sense organ that comprises multiple structures, as indicated in Figure. 1.1, which work together to provide us with the ability to see. As described at its most basic level, light enters the eye through the cornea and is focused by a combination of the cornea and the lens onto the retina at the back of the eye. Here, it is converted into electrical nerve impulses by the retina. The retina absorbs the light by distinct photoreceptors, involving cones and rods for absorption of bright and monochrome colours, respectively. The visual processing parts of the brain then interpret collected information contained in nerve impulses as an image. The cornea is often thought of as the eye's "window" to the world that overlies the eye's transparent interior components such as the anterior aqueous humour, lens, and vitreous humour (Figure 1.1). Evidently, if the cornea is not clear, vision is compromised. As well as allowing light to be transmitted into the eye, the cornea, owing to its convex profile, acts as the eye's main refractive component, accounting for approximately two-thirds of its total refractive power.

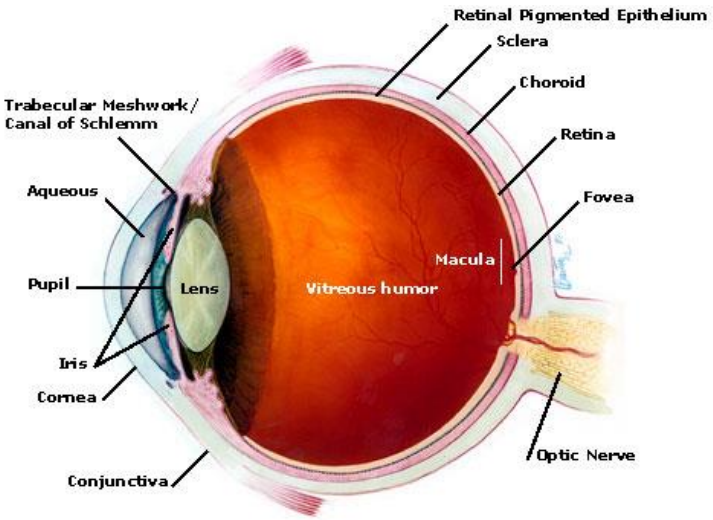

Figure 1.1 Diagram of a sagittal section of human eye anatomy. (http://www.eyecare-for-you.com/anatomy-of-the-eye.php).

1.3 Cornea

The cornea's optical transparency is dependent on distinctive physiologic features and interplay between its multiple cellular and macromolecular components, such as the highly specific arrangement of extracellular matrix proteins and delicately balanced hydration in the corneal stroma. In human adults, a healthy cornea is a little over 500 µm thick in the central pre-pupillary zone, and around 650 µm thick at its periphery. In cross-section, the cornea consists of five distinct layers, which listed from the outside to the inside of the eye are the epithelium, Bowman's layer, stroma, Descemet's membrane, and endothelium (Figure 1.2).

The surface *epithelial layer* is formed of 5–7 layers of cells and is around 50 µm thick (Reinstein *et al.*, 2008). This stratified squamous epithelium possesses a defensive function, protecting the eye from various infectious agents. It is continuously replenished throughout life, owing to the continual inward migration of new corneal epithelial cells originating from corneal limbal epithelial stem cell niche. The latter has been found to localise at the juncture between the peripheral region of the cornea and sclera, called

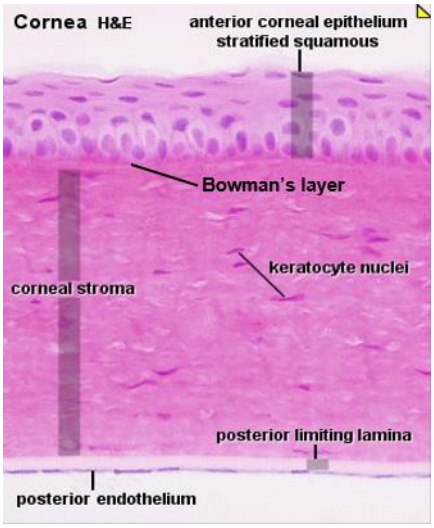

Figure 1.2 Cross-section of rat cornea stained with haematoxylin and eosin. Distinct layers can be seen: an anterior layer of the cornea consist of stratified squamous epithelium, proceeded by stroma, Bowman's layer and ending with inner endothelium after limiting lamina, also called Descemet's membrane. The stroma contains flattened keratocytes (http://www.lab.anhb.uwa.edu.au/mb140/corepages/eye/eye.htm).

limbus, which provides self-replacement of corneal epithelium when damaged or sloughed off (Cotsarelis *et al.*, 1989).

Located immediately below the surface epithelium is *Bowman's layer*, which is a dense acellular network of thin collagen fibrils. The function of Bowman's layer is thought to be as protection from external injuries due to its structural strength (Germundsson *et al.*, 2013). The average thickness of this layer is around 8 - 10 μm, which thins with age.

Next, is the thickest corneal layer, *the stroma*, which comprises nearly 90 percent of the whole cornea. The corneal stroma maintains strength as well as the refractive shape of the cornea and its transparency for light transmission toward retina. It consists of clear fluid, flat stromal cells called keratocytes, thin collagen fibrils (~30 nm thick), and sulphated proteoglycans. The cornea is transparent owing to the precise tissue-specific organisation of collagen fibrils (Maurice, 1957; Meek and Boote, 2004). The light waves that scatter from the collagen fibrils meet each other and interact via interference phenomena meaning that a significant proportion of light is transmitted through the cornea into the eye. It is crucial that the stroma remains relatively dehydrated because glycosaminoglycan (GAG) molecules that comprise the proteoglycans that are attached to the corneal collagen fibrils are highly hydrophilic, so water molecules are attracted to GAGs and can disrupt the particular collagen fibril arrangement by swelling the stroma. The swollen stroma can increase light scattering and reduce corneal transparency (Meek, Dennis and Khan, 2003).

A membrane lying beneath the stroma is posterior limiting lamina, termed *Descemet's membrane* (DM) (~ 3 μm thick at birth). It consists of an extracellular matrix produced by the cells of the endothelium (Murphy, Alvarado and Juster, 1984). DM is formed of the following two layers: anterior banded layer and the posterior non-banded layer. The former develops during pregnancy, while the latter is formed after birth (Waring *et al.*, 1982). The thickness of the DM, therefore, increases up to 10 μm in adulthood (Johnson, Bourne and Campbell, 1982).

Table 1.1 Summary of thicknesses of individual corneal layers.

No.	Corneal layer	Thickness
1	Epithelium	~ 50 μm
2	Bowman's membrane	~ 8–10 μm
3	Stroma	~ 450 μm
4	Descemet's membrane	~ 2–10 μm
5	Endothelium	~ 4–6 μm

The innermost layer of the cornea is the *corneal endothelium*, composed of about 4–6 μm thick and 15–25 μm wide endothelial cells. The majority of which are hexagonal (when looking from the posterior surface) and uniform in size (Tuft and Coster, 1990). Despite being the thinnest cellular layer of the cornea, the endothelium plays a crucial role in regulating corneal hydration. Therefore, endothelial cells are described in more detail in the next section.

1.3.1 Corneal endothelial cells

At birth, the number of human corneal endothelial cells (HCECs) is approximately 300,000 in each cornea, which is equivalent to about 6000 cells/mm^2 (Waring *et al.*, 1982; Bourne, 2003). After birth, however, the number of endothelial cells continuously reduces at a rate of 0.3-0.6 % per year, but normally remains above about 2000 cells per mm^2 (Geroski *et al.*, 1985; Bourne, Nelson and Hodge, 1997). The slow reduction of endothelial cell density throughout life occurs because these cells are terminally differentiated, arrested in the G1 phase of the cell cycle, and unable to divide mitotically *in vivo* (Joyce, Meklir, *et al.*, 1996; Joyce, Navon, *et al.*, 1996). Hence, the regenerative ability of HCECs to maintain endothelial function is limited to a compensating process of cell reorganisation: following cell loss during life or following injury, healthy adjacent cells spread by enlarging to preserve the continuous monolayer and cover a bare space on Descemet's membrane. These cells alter their dimensions possessing varied sizes (up to 1500 μm) (termed *polymegethism*) and varied shapes (termed *pleomorphism*) changing characteristic hexagonal morphology (Laing *et al.*, 1976; Kaufman and Katz, 1977; Carlson *et al.*, 1988; Bourne, Nelson and

Hodge, 1997). This way, an unbalanced incursion of the anterior chamber fluid – the aqueous humour – into the corneal stroma is hindered.

However, when the density of endothelial cells reaches a critical point of approximately 500 cells per mm^2 (Ventura, Wälti and Böhnke, 2001), a functional threshold is reached below which the 'pump-leak' mechanism that normally filters excess water out of the corneal stroma cannot keep the cornea in a balanced hydration state. As a consequence the cornea will imbibe fluid, which can result in severe swelling, opacification of the cornea and a loss of vision (Ventura, Wälti and Böhnke, 2001; Armitage, 2003).

1.3.2 "Pump-leak" mechanism

Cornea has no blood vessels, enabling the transparency of this tissue to prevail. Therefore, it is reliant on the contact of the endothelium with the aqueous humour, a clear plasma-like physiological liquid, from where the essential nutrients are diffused through interendothelial cell gaps. This mechanism then activates downstream pathways responsible for transport of nutrients inside the corneal cells (Bonanno, 2012). A key function of the corneal endothelial cells is to drive the "pump-leak" mechanism to maintain the corneal hydration at a required level (below 3.5 mg H_2O/mg) to allow corneal transparency (Bonanno, 2012). This equates to a physiologically

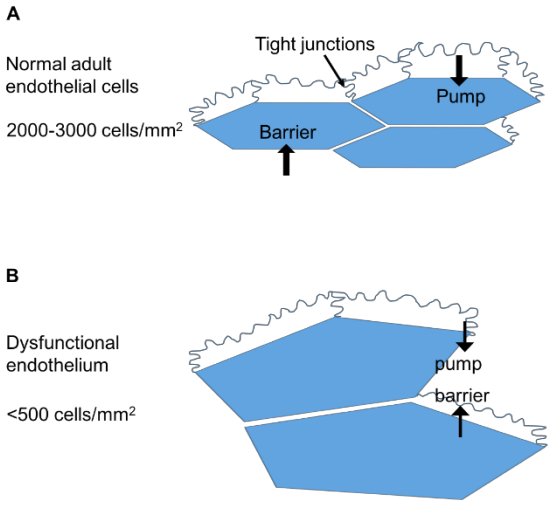

Figure 1.3 Diagram of the pump-leak mechanism.
(A-B) Shown is a relationship between endothelial cell density and metabolic pump function. B) Corneal decompensation takes place when endothelial cell reserve passes the threshold of 500 cells/mm^2.

normal hydration (H) of a transparent cornea of around 3.2, when H is defined as the ratio of the wet weight of the cornea to its dry weight (i.e. H = (wet weight – dry weight)/dry weight), or around 74% fluid (Meek *et al.*, 1991).

According to the 'pump-leak' theory, there is a direct relationship between the rate of liquid flow into the cornea and that of the released out through the endothelium (Bourne, 1998). This mechanism is mostly controlled by the regulation of sodium-potassium (Na^+-K^+) channel activity on the endothelial cell membranes, the important component of which is sodium-potassium-adenosine triphosphatase (Na^+-K^+-ATPase) a transmembrane protein. The average rate of the pump function is between 25-40 $\mu L/cm^2/hr$ (Dikstein, 1973). If the endothelial pump-leak balance becomes imbalanced, owing to a loss of cells or lack of healthy corneal cells as happens in diseases of the corneal endothelium such as FECD, stromal hydration increases above normal values, the characteristic arrangement of the stromal collagen fibrils breaks-down and corneal light scattering and opacification occur.

1.4 Fuchs' Endothelial Corneal Dystrophy

The deterioration of the corneal endothelium may occur in numerous conditions, including various eye diseases. Several corneal dystrophies that share functional and morphological disorders of endothelium include FECD, posterior polymorphous corneal dystrophy, congenital hereditary endothelial dystrophy, and X-linked endothelial corneal dystrophy. Among these conditions, FECD, which was first described, as "dystrophia epithelialis corneae", by Ernst Fuchs' in 1910, is one of the most prevalent causes of corneal transplantation surgery worldwide (Fuchs, 1910; Baratz *et al.*, 2010; Wieben *et al.*, 2012). Although corneal epithelial cells are affected in later disease stages, the primary defects seen in FECD are changes in endothelial cell morphology and function, accompanied by the localised thickening of Descemet's membrane and the deposition of extracellular matrix between Descemet's membrane and the corneal endothelium.

1.4.1 Aetiology and pathogenesis of FECD

Understanding the underlying mechanisms of a disease is a critical element in it's study, which potentially can lead to the discovery of new treatment

approaches to prevent a loss of vision. Although the precise cause and development mechanism of the FECD are still to be determined, it is likely that the condition is caused by a combination of various factors (Figure 1.4). This section describes several hypotheses of the aetiology and pathogenesis of the FECD.

1.4.2 Genetic basis

Like many disorders, FECD has a hereditary component. Although the condition can occur asymmetrically - more profound in one eye than in the other - the genetic nature of FECD suggests that, if not treated, both eyes may be affected and result in a total blindness (Goar, 1934; Waring, Rodrigues and Laibson, 1978; Waring *et al.*, 1982).

To date, several genes have been associated with the condition. Although, some cases are of sporadic inheritance (Sundin, Broman, *et al.*, 2006), cumulative evidence indicates that FECD is caused by an autosomal dominant pattern of inheritance (Cross, Maumenee and Cantolino, 1971; Krachmer *et al.*, 1978; Magovern *et al.*, 1979; Rosenblum *et al.*, 1980; Iliff, Riazuddin and Gottsch, 2012). The first gene mutation found to be associated with FECD in the autosomal dominant pattern was COL8A2 (encoding α2 subunit of collagen type VIII) located on chromosome 1 (Biswas *et al.*, 2001; Gottsch, Sundin, *et al.*, 2005; Gottsch, Zhang, *et al.*, 2005; Liskova *et al.*, 2007; Mok, Kim and Joo, 2009). However, this mutation has only been found in the rare, early-onset form of FECD (affecting people earlier than 40 years of age), and not in the common, late-onset FECD form (Kobayashi *et al.*, 2004; Aldave *et al.*, 2006; Hemadevi *et al.*, 2010). Further, FCD1, FCD2, FCD3, and FCD4 were identified as linked to the late-onset FECD occurring in chromosome 13, 18, 5, and 9, respectively (Sundin, Broman, *et al.*, 2006; Sundin, Jun, *et al.*, 2006; Riazuddin *et al.*, 2009; A S Riazuddin *et al.*, 2010). Additionally, more evidence has suggested that mutations occur in FECD patients in the 18th chromosome in a gene called TCF4, which encodes a protein called E2-2 (Baratz *et al.*, 2010; Li *et al.*, 2011).

Gene mutations associated with other diseases have also been identified in FECD. For example, mutations of SLC4A11 (that encodes membrane-bound sodium borate cotransport protein) and TCF8 (that encodes ZEB1 protein), which are causative for two less common endothelial dystrophies -- congenital hereditary endothelial dystrophy and polymorphous posterior corneal dystrophy, respectively – have been found in the late-onset FECD (Vithana *et al.*, 2008; A S Riazuddin *et al.*, 2010; A S. Riazuddin *et al.*, 2010). Additionally, the TCF4 gene, which is found in some FECD patients, has also been associated with schizophrenia (Steinberg *et al.*, 2011). This may suggest that individuals suffering from schizophrenia could have an additional risk to develop FECD and vice versa, however, there is limited information in the literature regarding this possibility.

Despite these genetic studies, however, the significance of the above-mentioned mutations in the development of FECD (i.e. the molecular pathways associating the genetic transmutations with the clinical manifestations) is yet to be determined. The water is further muddied by the possibility of ethnic differences as suggested by a recent multi-generational study on a Chinese pedigree with late-onset FECD, which did not show any changes in either COL8A2, SLC411, or TCF4 (Tang *et al.*, 2016). Nevertheless, several theories have been suggested regarding the way in which FECD might develop.

1.4.3 Epithelial-mesenchymal transformation and endoplasmic reticulum (ER) stress

Based on clinical and microscopy findings, the most recognisable pathologic feature of FECD is the presence of corneal guttae (Chiou *et al.*, 1999). Also known as corneal guttata, these are focal thickenings of the posterior surface of Descemet's membrane. In addition, the overall thickness of Descemet's membrane in FECD may reach up to 20 μm, while in non-diseased eyes it only thickens to approximately 10 μm by the age of 80 years (Gottsch, Zhang, *et al.*, 2005). Consistent evidence suggests that the guttae appear due to excessive production, release, and accumulation of extracellular matrix (ECM) (Waring *et al.*, 1982; Gottsch, Sundin, *et al.*, 2005; Vithana *et al.*, 2008; Engler *et al.*, 2010). Iwamoto (1970) and Waring (1978) also

reported that FECD-affected endothelial cells display changes in their cell-to-cell contacts, desmosomes, and tight intercellular junctions, accompanied by atypical features such as dilated endoplasmic reticulum (ER), swollen mitochondria, and the presence of cytoplasmic filaments. It was suggested that these changes were due to a tendency of dystrophic endothelial cells to transform to more fibroblast-like cell phenotype that leads to overproduction of the extracellular fibrous matrix that is occasionally seen between Descemet's membrane and the endothelium during FECD. In agreement, a study by Hidayat and Cockerham (2006) demonstrated that FECD endothelial cells may exhibit epithelial and fibroblastic phenotypes based on immunohistochemical staining characteristics.

Recently, the concept of metaplasia – i.e. the reversible transformation of one differentiated cell type to another differentiated cell type – in FECD was supported by several lines of genetic evidence based on the upregulation of specific genes (*ZEB1* and *Snail1*) associated with the development of fibrous connective tissues, known as epithelial-mesenchymal transition (EMT) genes (Lechner *et al.*, 2013; Gupta *et al.*, 2015; Okumura, Minamiyama, *et al.*, 2015). It was suggested that mutated genes may disrupt cell homeostasis, including the correct protein folding mechanisms in the ER. This phenomenon of ER stress is thought to lead to the accumulation of unfolded proteins in Descemet's membrane. The abnormal Descemet's membrane, on which the corneal endothelium sits, is postulated to negatively influence cell-cell connectivity and lead to endothelial cell thinning, pleomegathism, polymorphism and a resultant loss of function. The prolonged aggregation of unfolded proteins in Descemet's membrane is also thought to activate an unfolded protein response that eliminates affected cells via apoptosis (Schröder and Kaufman, 2005; Meng *et al.*, 2013; Okumura, Hashimoto, *et al.*, 2017).

1.4.4 Oxidative stress

As was mentioned previously, mature human corneal endothelial cells are in a post-mitotic condition (arrested in the G1 phase of the cell cycle); thus, susceptibility to oxidative stress due to continuous exposure to light and high metabolic activity (pump function) increases with age (Joyce, Zhu and Harris,

2009). Therefore, the role of chronic oxidative stress has also been proposed in FECD pathogenesis (Buddi *et al.*, 2002; Wang *et al.*, 2007; Jurkunas *et al.*, 2010). The cornea is rich in antioxidant enzymes that inhibit endothelial cell death by removing free radicals and reactive oxygen species (ROS) (Buddi *et al.*, 2002). The findings of a proteomic analysis of endothelium reported by Jurkunas and colleagues (2010) demonstrated the decreased expression of antioxidants such as peroxiredoxin (PRDX) in FECD cells, compared to normal endothelial cells that have an anti-apoptotic function by removing hydrogen peroxide. It is unclear, however, whether the oxidative stress is the cause or the effect of FECD and needs further investigations.

FECD thus involves corneal endothelial cell death followed by the failure of the corneal endothelium to function as a barrier between the aqueous humour and corneal stroma and regulate water levels of the cornea, hence, clinical manifestations such as corneal swelling leading to opacification and reduced visual acuity.

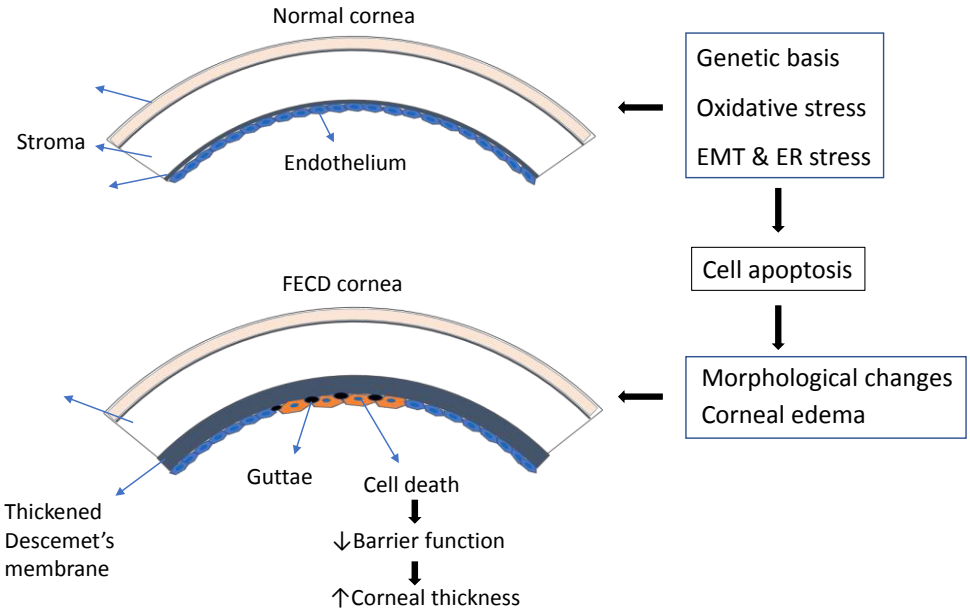

Figure 1.4 Schematic diagram of possible pathological mechanisms of FECD. Genetic factors combined with oxidative stress and ER stress may lead to morphological changes in corneal endothelium, cell death and corneal oedema seen in FECD.

1.4.5 Clinical manifestations of FECD

FECD is generally diagnosed by an eye exam, involving measurements of corneal thickness and specular imaging of the corneal endothelium (Chiou *et al.*, 1999). This condition has been categorised into four clinical stages (Waring, Rodrigues and Laibson, 1978; Adamis *et al.*, 1993; Weiss *et al.*, 2015).

Absence of symptoms

In the first stage, the FECD patients do not have any complaints, although characteristic small elevations that appear as dark drop-like spots on the back of the cornea, termed guttae (plural of 'gutta', translated as *'*drop' from Latin terminology), can be observed on the backside of the cornea during regular specular microscopy examination;

Presence of corneal swelling

Guttae begin to accumulate from the central corneal area and as the disease progresses symptoms include a thickening of the cornea in the central area overlying the abnormal endothelial cells. In the second symptomatic phase, patients have light glares, photophobia, and feel less comfortable in the mornings. This eases throughout the day due to aqueous evaporation from the overly hydrated cornea while the eyelids are open;

Painful epithelial bullous ruptures

As the disease evolves, haziness of vision is present the whole time. In subsequent stages, clear blisters produced from the stored liquid can appear in the corneal epithelium, causing severe pain when they rupture (bullous keratopathy);

Impaired sensitivity (painless) decompensated state of the cornea.

Eventually, irreversible morphological changes such as scarring and subepithelial fibrosis occur on cornea and vision becomes impaired during the final phase, resulting in vision loss and the need for surgical intervention.

1.5 Current Treatment of Endothelial Dysfunction

1.5.1 Symptomatic Therapy

Approaches to treating vision reduction caused by endothelial dysfunction in the initial stages of FECD involve various symptomatic approaches to relieve the swelling of the cornea. These include a topical application of hypertonic saline solution drops, ointments, or even cool temperature hair-dryer use from lateral sides of the face to help water to evaporate from the ocular surface (Tuft and Coster, 1990). Although these procedures can be beneficial temporarily, they do not alleviate the cause of the disease and its progression through pathologic stages. Once the above-mentioned attempts to treat developed symptoms fail to help control the corneal thickness and transparency, endothelial replacement therapy is generally required to promote visual recovery.

1.5.2 Corneal Graft Surgery

In its later stages, FECD is typically treated via a corneal transplantation (Tan *et al.*, 2012). The graft of a full-thickness donor cornea, a surgery known as a penetrating keratoplasty, has been the traditional surgical treatment for people with severe corneal endothelial dysfunctions for nearly a century. Around 50,000 patients experience corneal transplants to replace diseased or injured corneas in the United States of America every year (Park *et al.*, 2015). Even though the success rate of penetrating keratoplasties is relatively high, there is a risk of inducing irreversible mechanical or functional impairment of the desired endothelial tissue during the surgical interruption (Pineros *et al.*, 1996; Thompson *et al.*, 2003). However, one of the most frequent complications has been identified as a graft rejection, in which the corneal endothelium can become detached, resulting in endothelial graft failure with a continuous decrease in endothelial cell density (Dandona *et al.*, 1997; Armitage, 2003; Patel, Hodge and Bourne, 2005; Terry *et al.*, 2008). Questions have also been raised regarding the long-term survival of a donor tissue after the transplantation (Akanda *et al.*, 2015). Furthermore, patients must be maintained by immunosuppressing steroid medicine for an extended period following graft surgery, as it can take from months to years after surgery for the corneal wound to heal (Yureeda and Hamrah, 2013).

Prolonged administration of immunosuppressant's, in turn, may contribute to side effects such as secondary infections. In addition to risks associated with graft failure, corneal graft surgery for FECD can be hampered by difficulties obtaining transplantable corneal tissue, which is accentuated by the fact that significant numbers of donated corneas (up to 30% by some estimates) are discarded to variety of reasons including insufficient endothelial cells density (Armitage *et al.*, 1990). Other potential complications of penetrating keratoplasty include suture-related haemorrhages and the induction of an irregular corneal surface causing high astigmatism (Tan *et al.*, 2012).

Based on the sub-optimal nature of penetrating keratoplasty as a treatment for FECD, certain improvements have been achieved in surgical approaches by developing partial-thickness (lamellar) keratoplasty (Melles *et al.*, 1999; Bahar, Kaiserman and Mcallum, 2008). These methods involve selective replacement of only the pathologic corneal layer leaving the healthy layers of the recipient's cornea untouched. Anterior lamellar keratoplasty surgeries are used to treat diseases of the anterior cornea or even diseases of the stroma in the case of DLK (deep lamellar keratoplasty) which dissects away the whole thickness of the cornea down to the level of Descemet's membrane). Posterior lamellar corneal grafts are technically more challenging for the surgeon because they involve intraocular manipulation of tissue using specialised instruments. However, these are becoming increasingly popular and surgeries such as Descemet's stripping (automated) endothelial keratoplasty (DS(A)EK) or Descemet's membrane endothelial keratoplasty (DMEK) have become preferred methods to treat endothelial dystrophies such as FECD, due to a lower risk of graft rejection, faster recovery rates, and improved visual quality (Keenan *et al.*, 2011; Lichtinger *et al.*, 2012; Galvis *et al.*, 2013; Robert *et al.*, 2015; Le *et al.*, 2017).

Despite the contemporary popularity of posterior lamellar keratoplasties for FECD, difficulties acquiring suitable donor corneas still exist as do potential complications due to the invasiveness of the procedure. For instance, injuries associated with inserting, unfolding and positioning of the graft corneal layers may occur. Also, the risk of unsutured graft detachment is high and development of endophthalmitis, an inflammatory infection of the

endothelium, may necessitate repeated surgeries (Nieuwendaal *et al.*, 2006; Lee *et al.*, 2009). Evaluation studies show that although DSEK surgeries generally have good outcomes, the duration of these expectations is only a short-term (Stocker and Irish, 1969; Borderie *et al.*, 2009). Furthermore, many countries with restricted access to donor corneas would benefit from a therapy alternative to transplantation (Gain *et al.*, 2016).

Since the corneal endothelium is arrested in the post-mitotic state and has a restricted regenerative capacity *in vivo* (Joyce, Meklir, *et al.*, 1996; Joyce, Navon, *et al.*, 1996), it has long been considered essential to replace the diseased corneal endothelial layer with donor endothelial layer during the DSEK/DMEK procedures (Dirisamer *et al.*, 2011). Surprisingly, however, several case reports have described a spontaneous corneal endothelial recovery and improved visual outcomes despite graft detachments (Watson, Abiad and Coroneo, 2006; Balachandran *et al.*, 2009; Zafirakis *et al.*, 2010; Shah, Randleman and Grossniklaus, 2012; Ziaei, Barsam and Mearza, 2013; Kymionis *et al.*, 2017). For instance, a spontaneous corneal endothelial repopulation and improved visual acuity was reported in patients diagnosed with FECD after removing detached endothelial graft (Shah, Randleman and Grossniklaus, 2012). These cases suggest that either remaining healthy host endothelial cells or cells that had become detached from the donor tissue may have the ability to migrate onto the bare central area of Descemet's membrane from which diseased endothelial cells had been surgically removed and reproduce an integrated endothelial barrier. This led to further case reports of keratoplasty without a donor endothelial replacement, where a smaller area of endothelium was stripped (3-4 mm) in an FECD patient resulting in a complete corneal clearing within four months (Kymionis *et al.*, 2017).

Another less-invasive approach, currently under investigation is a cell-based therapy, whereby a cultivated cell suspension derived from post-mortem donor corneal endothelium combined with a trophic pharmaceutical agent, ROCK inhibitor, is directly injected into the anterior chamber (Okumura *et al.*, 2012, 2018; Okumura, Sakamoto, *et al.*, 2016). This has been shown to have success in small-scale human trials to treat corneal endothelial disease

(Kinoshita *et al.*, 2018a); however, issues still exist with cultivation of endothelial cells *in vitro* due to limited proliferative ability. The above-mentioned studies have encouraged more ideas for modification of the existing surgical interventions towards simplifying the management of corneal endothelial diseases without using a donor corneal tissue to reduce potential post-operational complications.

1.6 Transcorneal freezing

One alternative approach that has been used to remove diseased corneal endothelial cells from eyes with corneal endothelial dysfunction is via cryosurgery, using a minimally invasive procedure to locally destroy diseased cells by freezing. Cryosurgery has been used, historically, to treat a variety of tissues which are easily accessible to the surgeon such as skin defects, oral cancers, and corneal conditions including endothelial dysfunctions (Yeh, 2000; Okumura *et al.*, 2011, 2013; Chang and Yu, 2013; Koizumi *et al.*, 2013, 2014). For example, Koizumi and colleagues (2013) used first-in-man transcorneal freezing on a 52-year old male to destroy guttae caused by FECD. A 2-mm steel rod immersed in liquid-nitrogen was directly applied onto the central corneal surface of the patient for a duration of 15 seconds. This was followed by topical administration of Y-27632 ROCK inhibitor in the form of eye drops to stimulate remaining cells to recover. A week of treatment with the ROCK inhibitor applied in the form of eye drops six times a day demonstrated major improvement in the patient's visual acuity and function of the endothelial cells, with a significant and maintained reduction in corneal thickness back to normal levels.

Despite the potential of this approach it is likely that endothelial damage of diseased FECD cells via the application of a liquid-nitrogen-cooled steel rod for an arbitrary period cannot achieve surgical consistency, as the wound is dependent on the instrument features such as rod diameter and temperature, and the duration of freezing (Okumura *et al.*, 2011). Although a controlled transcorneal freezing could potentially be an appropriate alternative procedure to remove diseased corneal endothelial cells in FECD patients, there is no optimised reproducible procedure to be used in a clinical setting.

Thus, promising results of the combination of transcorneal freezing with the ROCK inhibitor eye drop administration have produced an incentive to engage further experiments on improving the transcorneal freezing technique as well as to study endothelial cell responses toward the ROCK inhibitor treatment.

1.7 ROCK inhibitor application

Recent mounting evidence suggests that activation of the ROCK pathway occurs in the pathogenesis of numerous systemic diseases, such as, cancer, neurodegenerative, and cardiovascular diseases, which raises the prospects of this molecule to be pursued as a therapeutic target (Itoh *et al.*, 1999; Fukata *et al.*, 2001; Mukai *et al.*, 2001; Lingor *et al.*, 2008). For example, the important role of a selective ROCK inhibitor has been demonstrated in arterial hypertension development (Mukai *et al.*, 2001). Also, Fukata (2001) suggested that ROCK plays a crucial role in the Ca2+ sensitisation of smooth muscle contraction involved in hypertension. A study on cultivated human embryonic stem cells by Watanabe and colleagues (2007) demonstrated that ROCK inhibitor Y27632 has anti-apoptotic activity as well as an effect on the differentiation of the cells. Despite the involvement of ROCK signalling in multiple cells and tissues, until recently, only one drug, Fasudil, has been clinically approved (in Japan and China in 1995) and is marketed as a selective and potent inhibitor of Rho-kinase for human cerebral vasospasm (Uehata *et al.*, 1997).

1.7.1 ROCK inhibitor application in the eyes

Owing to the demonstrable value of ROCK inhibitors, the discovery of them has attracted high interest in various research and medical fields including in the ophthalmology community. One successful discovery regarding the effect of ROCK inhibitors in the field of ocular pathology resulted in the eye drop solution, Ripasudil (ROCK inhibitor, also named as Glatanec, K-115), being approved in Japan in 2014 for the treatment of glaucoma and ocular hypertension. The investigators found that ROCK inhibitor reduces the intraocular pressure by increasing outflow of aqueous humour through the trabecular meshwork (Garnock-Jones, 2015).

Despite the approval of Ripasudil for clinical use, its mechanism of action continues to be explored in relation to glaucoma as well as other eye disorders, including corneal endothelial dysfunctions. An increasing number of studies have been conducted in recent years, which have focused on the beneficial effects of ROCK inhibitors on corneal endothelial cells in multiple models including cell cultures, animal models, and early-stage human clinical trials. These have shown some results of promise in clinical setting (Okumura *et al.*, 2009, 2012; Li *et al.*, 2013; Pipparelli *et al.*, 2013; Peh *et al.*, 2015).

According to Okumura (2012), the selective ROCK inhibitor, Y27632, has a beneficial effect when cultivating monkey corneal endothelial cells by increasing cell survival, cell adhesion, and cell proliferation *in vitro* with normal expression of endothelial function-related markers. This led to the concept of the potential use of human cultivated endothelial cells as a cell-based therapy for the endothelial dysfunctions, such as those resulting from FECD or a complicated cataract surgery. Li (2013) and Lee (Lee *et al.*, 2016) studied cultured bovine and porcine corneal endothelial cells in the presence of Y27632 and suggested that the ROCK inhibitor remarkably benefits cell cultures by promoting corneal endothelial cell proliferation, migration, whilst also preventing cell death. The proliferative and wound healing effects of the

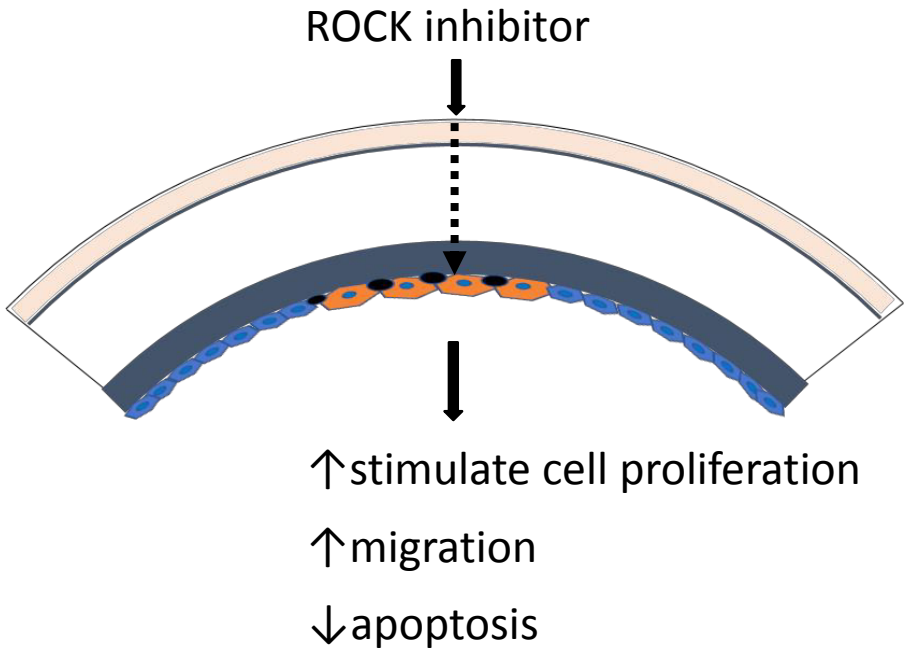

Figure 1.5 Effect of ROCK inhibitors on corneal endothelial cells.

ROCK inhibitors were supported by further studies involving administration of the Y27632 inhibitor on *in vivo* rabbit and monkey eyes, delivered in the form of eye drops (Okumura *et al.*, 2011, 2013, 2014; Okumura, Okazaki, *et al.*, 2016). The same group of researchers has carried out more advanced studies that implicated human clinical trial using the ROCK inhibitor eye drops on diseased corneal endothelium (Koizumi *et al.*, 2013, 2014; Okumura *et al.*, 2013).

1.8 Aims and Objectives

As mentioned at the start of this chapter, the overarching aims of this doctoral research are to provide improved knowledge about the dynamics of corneal endothelial development as a natural model of endothelial cell migration, and the changes that occur in late-stage corneal endothelial disease (FECD) in two- and three-dimensions and at high magnification using advanced electron optical imaging technologies not previously applied to corneal endothelia (*Chapters 2 and 3*). The cornea's response, in pig eyes *in vitro* and in rabbit eyes *in vivo*, to a series of newly designed cryoprobes for transcorneal freezing to be used as part of a new minimally invasive surgical treatment for FECD (*Chapters 4 and 5*) were also investigated. The effect on endothelial cell behaviour of the Y27643 ROCK inhibitor as a therapeutic agent and new potential ways of delivering it to the cornea were also investigated (*Chapters 4 and 6*).

Chapter 2: Early Development of the Corneal Endothelium

2.1 Introduction

To be able to treat corneal endothelial dysfunction effectively, it is important to first understand factors involved in the process of cell migration from regions of intact endothelial integrity and function, to repopulate damaged areas from which viable cells are missing. Useful information on the mechanisms and events influencing corneal endothelial cell migration might be gained from observations on the initial establishment of the endothelial monolayer in the embryo. Several studies have already been published on the subject of corneal development, but the majority of these - using a number of approaches, including scanning and transmission electron microscopies - have focussed on epithelial and stromal development (Trelstad and Coulombre, 1971; Wulle, 1972; Linsenmayer *et al.*, 1998; Hirsch *et al.*, 1999; Koudouna, Mikula, *et al.*, 2018; Koudouna, Winkler, *et al.*, 2018). Significant additional work remains to be carried out, therefore, before we fully understand the events sequence and control mechanisms involved in the process of corneal endothelial development. To comprehend the formation of endothelial cells in the cornea, it is helpful first to consider in the context of how the eye itself develops. A brief description of how eye develops will be covered in the following sections of this chapter.

After progressively dividing from two cells, embryonic cells form a blastula characterised by an outer epithelial layer, called the blastoderm, which during gastrulation forms three layers: ectoderm, mesoderm, and endoderm. The eye originates from the ectodermal derivatives (surface ectoderm, neural crest, and neural ectoderm) starting at prenatal week 3 (embryonic day 22) by forming an optic groove first, then an optic vesicle (Figure 2.1A). Then in weeks 4 and 5 the lateral walls of optic vesicles expand towards the surface ectoderm and invaginate to form a two-layered optic cup (Figure 2.1B). The inner layer of the optic cup gives rise to the retina, ciliary body epithelium, iris, and the optic nerve, while the outer layer gives rise to the lens structure, the corneal and conjunctival epithelium, and eyelids with the lacrimal system. When the free edges of the optic cup merge together, the lens separates from the ectoderm creating an anterior chamber (Figure 2.1C). Finally, in the 7th week of gastrulation, invasion of mesenchymal cells takes place to form corneal endothelium and stroma by a two-step cell migration from the neural crest, which originates from the area where the surface ectoderm and neural ectoderm fuse. First, the crest cells migrate to central cornea to form endothelium. The second wave then migrates to the space between epithelium and endothelium to differentiate into stromal cells, keratocytes, to form a highly collagenous stroma.

Avian corneal development is known to involve the analogous two-step migration of the mesenchyme cells from the neural crest to develop the

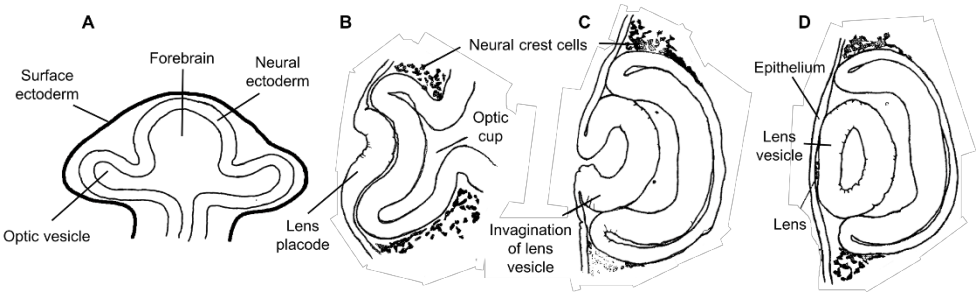

Figure 2.1 Diagram of the stages of early eye development.
A: Formation of optic vesicle; B: Invagination of lens placode and formation of optic cup; C: Invagination of lens vesicle; D: Separation of lens from surface ectoderm (adapted from Hay and Revel, 1969)

endothelial layer (Hay and Revel, 1969). Some other animals such as mice and rabbits, however, have only a 1-step migration (Cintron, Covington and Kublin, 1988; Kidson *et al.*, 1999). Owing to the similarity between human and avian ocular embryogenesis and easier accessibility of the chick tissue than that of human origin, morphology of embryonic avian development has been studied widely (Hay and Revel, 1969; Johnston *et al.*, 1979; Hay, 1980). In addition, because corneal development occurs more rapidly in chick compared to that in humans, the avian eye was chosen as the most suitable model in which to investigate corneal development.

The first migration of neural crest-derived cells to the proximal surface of the primary stroma in developing avian corneas occurs between embryonic day 4 and 5 (E4 and E5). N-cadherin has been reported to be expressed as the first marker of the presumptive endothelial cells in a 3-day old chick cornea. It is thought to aid the mesenchymal-to-endothelial transition from the neural crest to endothelial monolayer during the avian eye development (Hatta and Takeichi, 1986; Reneker *et al.*, 2000). As seen in Figure 2.2, by the end of

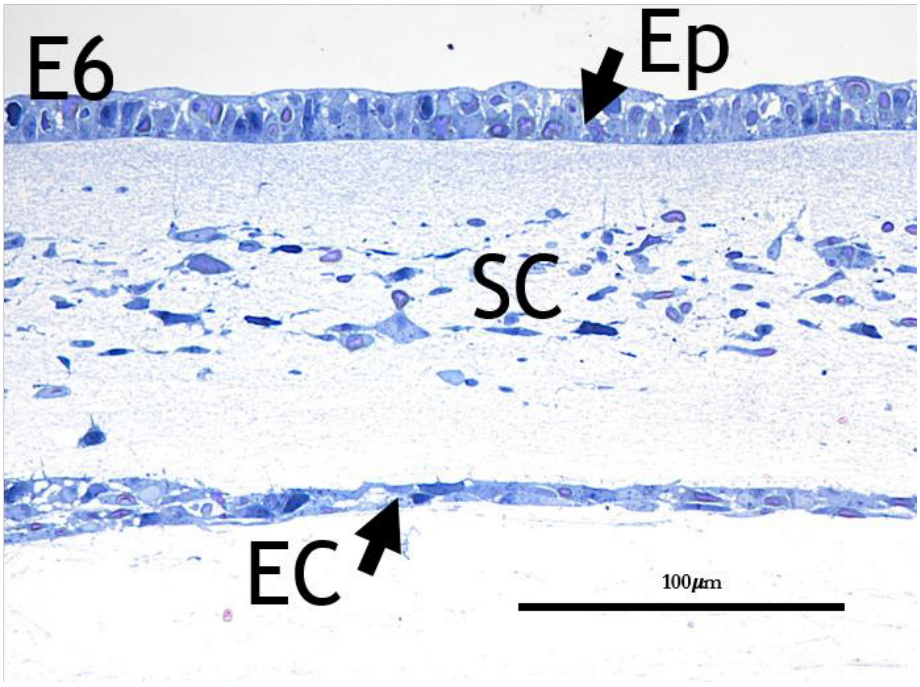

Figure 2.2 Light micrograph illustrating all distinct layers of the chick cornea at embryonic day 6 (E6):
Epithelium (Ep), stroma containing migrating stromal cells (SC) and endothelial layer (EC) migrated from the periphery. The image was kindly provided by Dr Rob Young (Cardiff University). Scale bar, 100μm.

E6 the endothelium has formed a continuous sheet across the proximal corneal surface but does not yet represent an organised cell monolayer at this stage. Keratocyte invasion from the periphery forms a continuous cell population in the mid-depth stroma, which is surfaced by stratifying epithelial layer. As the keratocytes develop, the stroma will become denser, containing less fluid to help maintain the transparency. These events form a highly organised cornea with three distinct layers of epithelium, stroma, and endothelium.

The emphasis in this study is placed on morphological events that underlie corneal development that will give an understanding of endothelial cell migration. Intensive research has been carried out on corneal endothelial cells leading to identification of their major function and mechanisms involved in maintaining corneal transparency. However, the formation of endothelial cells into a monolayer is not completely clear.

In the work described below, morphogenesis of corneal endothelial cells was investigated in chick cornea at days three to five of embryonic development using serial block face scanning electron microscopy (SBF-SEM) to visualise, for the first time in three-dimensional (3D) reconstructions, the events in endothelial cell migration. The underlying premise was that knowledge of endothelial migration in the embryo cornea could provide insights into the mechanism by which endothelial cells might be stimulated to respond in repair processes following injuries, such as scrape wounds or transcorneal freezing, for example.

2.2 Materials and Methods

This section describes experimental materials and methods that were used in this study.

2.2.1 Experimental models

Embryonic chick cornea

Chick embryos were selected in this study as the most suitable experimental model in which to investigate corneal development on account of the ready

availability of tissue, obtained at specific stages of development in the course of a relatively rapid 21-day incubation period. In addition, the endothelial layer is known to develop in analogous way in both birds and humans. Therefore, the findings can be comparable and relevant to human corneal development.

To capture the sequence of events involved in migration of presumptive endothelial cells from periphery to the central cornea, chicks between embryonic days 3 (E3) and 5 (E5) were used. It was considered that these observations on how endothelial cells spread to form a coherent population in the embryo might also provide some clues towards the mechanisms of induced endothelial repair following wounding or disease in adult healing tissue. The migration of the endothelial cells occurs rapidly during the first days of embryonic development, and individual corneas can develop at a slightly variable rate. Based on this, considering this outcome, an additional time-point at day 4 (E4) + 12 hours was chosen to include in the representing the logical order of events and capture the phase of endothelial migration.

Fertilised chicken eggs were obtained from a commercial hatchery (Henry Stewart & Co Limited, Louth, UK). After a 'rest period' of 1-3 days following receipt from the supplier, to reach the desired developmental stage (E3 – E5) the eggs were placed in a humidified atmosphere (~60% relative humidity) inside a Brinsea Octagon 100 incubator (Brinsea Products Ltd, Sandford, UK) at temperatures of 37 to 38° C. At E3, E4, E4 + 12 h, and E5, eggs were removed from the humidified chamber and processed further for serial block face scanning electron microscopy.

2.2.2 Experimental methods

Excision of chick embryos

At the completion of the required incubation time (E3, E4, E4 + 12 hours, and E5), developing eye tissue was obtained from the chick embryos using a filter paper template as described by Chapman (2001) (Figure 2.3). First, an eggshell was gently cracked by tapping and rolling the egg's side on a solid bench surface. The intact egg contents were then carefully released directly into a petri dish. The middle of a filter paper was centred over the embryo,

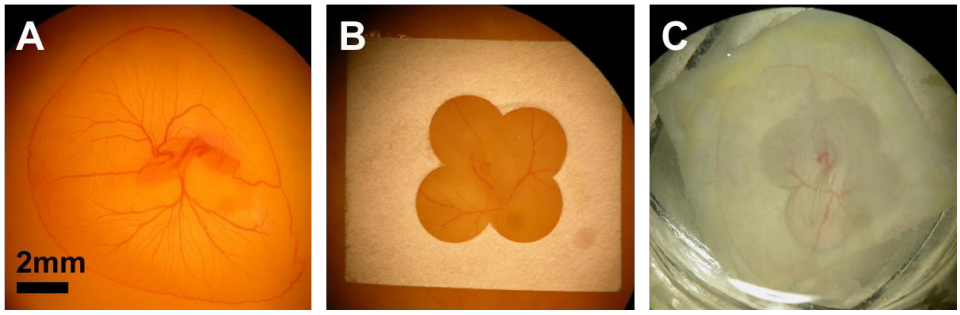

Figure 2.3 Isolation of early stage chick embryo (E3).
A: High magnification of chick embryo at E3 by light microscopy; B: filter paper centred over the embryo; C: embryo attached to the filter paper transferred to a fresh petri dish with saline solution to wash away excess yolk.

placed gently onto the surface of the yolk sac after which the membrane around the filter paper was cut using scissors. After ensuring the attachment of the embryo to the filter paper, the embryonic tissue was pulled away using forceps to detach from the rest of the yolk membrane. The excised embryo was then transferred to a glass embryo dish filled with a fixative solution as described below.

Fixation

The extracted portion of a chick embryo was immersed in 2.5% glutaraldehyde and 2% paraformaldehyde in 0.1 M sodium cacodylate buffer, pH 7.2, for 3 hours.

Staining and Embedding

Preservation of the whole corneas started with post-fixation in fresh fixative for 2 hours, after which chick embryo specimens were washed with cacodylate buffer 5 times for 3 min each time. To increase the contrast of cellular structures within the fixed corneas, the specimens were post-fixed with 1% osmium tetroxide and 1.5% potassium ferricyanide in 0.1 M sodium cacodylate buffer. After washing 5 times for 3 min each in the buffer, this was followed by immersion of the specimens in 1% tannic acid for 2 hours. The samples were then replaced with a fresh 1% tannic acid solution for another 2-hour incubation. After washing specimens for 5 x 3 min in a distilled water, they were immersed in 1% osmium tetroxide for 40 min, then in 1% uranyl acetate for 1 hour, following washes of 3 times for 5 min each.

The samples were then dehydrated by immersion in a graded ethanol series of 50%, 70%, 90%, and 100% in distilled water for 10 min at each step. Specimens were then infiltrated with Araldite CY212 resin, placed in labelled embedding moulds and polymerised at 60° C for 72 hours.

Making glass knives

Glass knives were used first to cut semithin sections for light microscopy and then ultrathin sections for SBF-SEM investigation. Knives were made with an EM KMR2 glass knifemaker (Leica Microsystems (UK) Ltd). Initially, glass squares were prepared from a clean 6.4 mm thick glass strip (Leica) of 200 mm in length placed onto the cover plate of the knife-maker and secured by the locking lever. Then the scoring shaft was pulled out to score the glass at a pre-set position. Next, the breaking knob was turned clockwise until the glass was broken into a square. This was followed by making two triangular glass pieces from the prepared square glass by rotating it by 45°and securing it with both front and rear clamping holders. Then a line was scored in the middle of the glass square via the scoring shaft before the square was broken again via the breaking knob. After several triangular glass knives were prepared, a piece of aluminium tape was attached around the top of the glass knife to form a 'boat' to hold a small volume of Millipore–filtered distilled water for collecting cut sections. The knife boats were sealed to the glass knives using warmed paraffin wax and kept in a dust-free environment in a special box until ready to use for sectioning.

Ultramicrotomy

First, a polymerised specimen block was firmly fixed in the sample holder, and the binocular eyepiece of the ultramicrotome (Ultracut E, Reichert-Jung) zoomed in to focus on the block surface. A glass knife was then introduced into the knife block, set with a cutting angle of 6º and clamped in place ready for sectioning. Following this, the specimen block was trimmed into a trapezium shape via using a razor blade to remove excess resin and expose the corneal tissue. The block surface was planed and polished by a glass knife using first the coarse then fine manual advance controls for the knife stage. Then the knife boats were filled with filtered distilled water to catch the cut sections. Then several semi-thin sections of around 2-4 µm in thickness

were cut and transferred onto a microscope slide for the primary observation via light microscope to ensure the area of interest was exposed on the cut section prior to SBF-SEM investigation.

Light microscopy

After cutting semi-thin sections, they were transferred onto a drop of distilled water on a microscope slide. The cut sections were then dried on a hotplate (Stuart, UK) at approximately 60 ºC. Sections were stained on the hotplate for a few minutes with 1% toluidine blue in 1% sodium tetraborate. Excess stain on the microscope slide was gently rinsed off using a wash bottle filled with distilled water. The rinsed glass slide was then air-dried before examination on a light microscope (Olympus BH-2).

Serial Block Face Scanning Electron Microscopy (SBF-SEM)

To enable critical events in corneal endothelial morphogenesis in detail, SBF-SEM was carried out using a Zeiss Sigma VP FEG scanning electron microscope equipped with a Gatan 3View2 system. This is a powerful

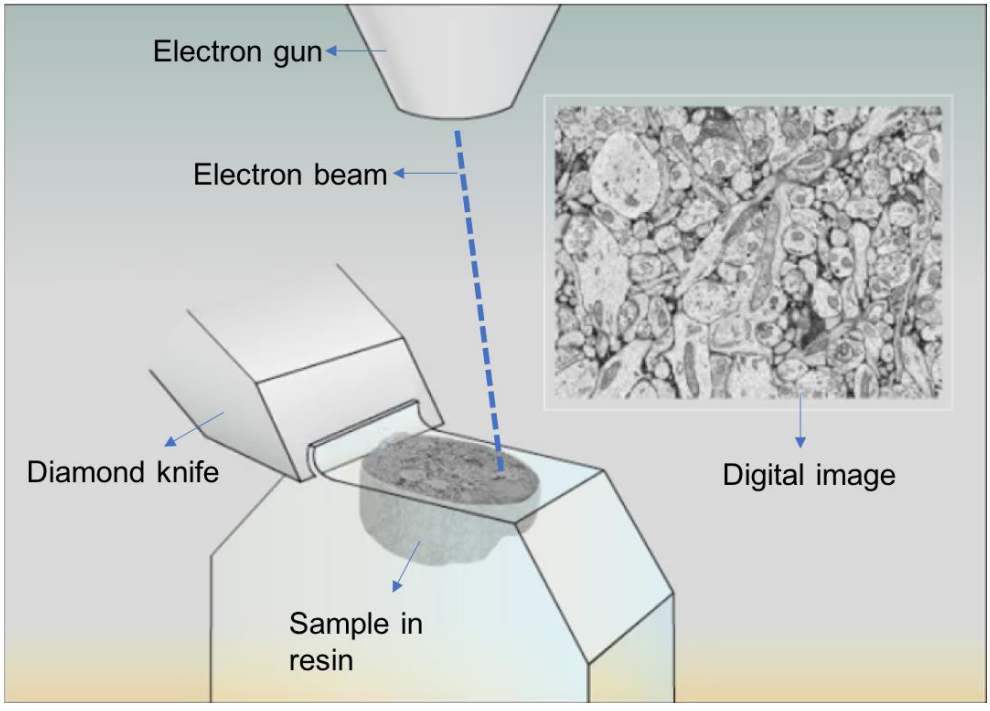

Figure 2.4 Schematic diagram showing set up of SBF-SEM.
An electron beam scans the resin block surface automatically producing a digitalised image (inset). Then an ultrathin slice of the block surface is cut by diamond knife and a stack of images is obtained in a reproducible manner. Image was obtained from a video at: http://www.gatan.com/products/sem-imaging-spectroscopy/3view-system.

scientific approach to view microstructures of samples at high resolution with the potential to generate a specific 3D reconstruction of the sample. The 3D images add new information about a sample compared to the 2D imaging capabilities of conventional transmission electron microscopes, which can help better understand a material, solve research problems, and contribute to new knowledge. The SBF-SEM operates in a similar approach to conventional scanning and transmission electron microscopes (TEM), as the name implies, however, rather than imaging a sliced ribbon of sections on a specimen support grid as in TEM, the instrument scans and collects images of the block surface, alternating with removal of a surface slice by the Gatan 3View ultramicrotome inside the microscope chamber. SBF-SEM also has the advantage of high-resolution imaging at the level of cellular organelles and collagen fibrils normally requiring TEM for their visualisation. The thickness of each slice cut via the ultramicrotome with a diamond knife is adjustable (100 nm was selected in this study). After the knife cuts off a slice of the block to reveal a new surface, the block is raised up to a focal point and is scanned by the electron beam over again, until a sequence of images of the complete desired tissue volume is obtained.

Preparation for SBF-SEM

After finding the area of interest by light microscopy, the trimmed sample was glued onto an aluminium specimen pin using conductive epoxy adhesive (2400 Circuit Works Conductive Epoxy Kit, Agar Scientific). Then, to avoid electrostatic charging of the sample, it was coated with a 6 nm layer of gold in an EM ACE 200 Sputter coater (Leica Microsystems (UK) Ltd, Milton Keynes, UK).

Acquisition of images

Each image sequence of approximately 1000 serial images at embryonic days E4 and E5, including additional E4 + 12 hours was collected every 100 nm at 4 kV with a dwell time of 10 ms. The scan resolution was 4096 x 4096, or approximately 10 nm per pixel.

Three-dimensional reconstruction

Once the datasets of images of embryonic chick corneas were collected between embryonic days E4 and E5, including additional time-point of E4 + 12 hours, 3D models were generated using ImageJ/Fiji and Amira 6.2 software. In ImageJ/Fiji, image sequences of each developmental stage were "*Imported*", then *"Inverted",* and then the *"Brightness/Contrast"* settings were adjusted for the differential contrast between structural elements of developing eye cells. Using the *"3D Viewer"* plugin, a 3D illustration of the selected image sequence was generated. Finally, the data was "*Saved*" or "*Recorded"* as a movie, when a representative view was identified.

In Amira, the raw sequential data was imported, and modules such as *"Ortho Slice"* and *"Volren"* were utilised to form a three-dimensional reconstruction of the sample.

2.3 Results

This section includes findings of developing chick cornea via imaging techniques involving light microscopy and 3-View SBF-SEM.

2.3.1 Light microscopy

Light microscopical observations at low magnification of early stages (days 3-5) of anterior eye development in toluidine blue-stained semi-thin sections showed the progress of endothelial cell invasion along the primary stroma at the inner surface of the forming cornea in the chick embryo.

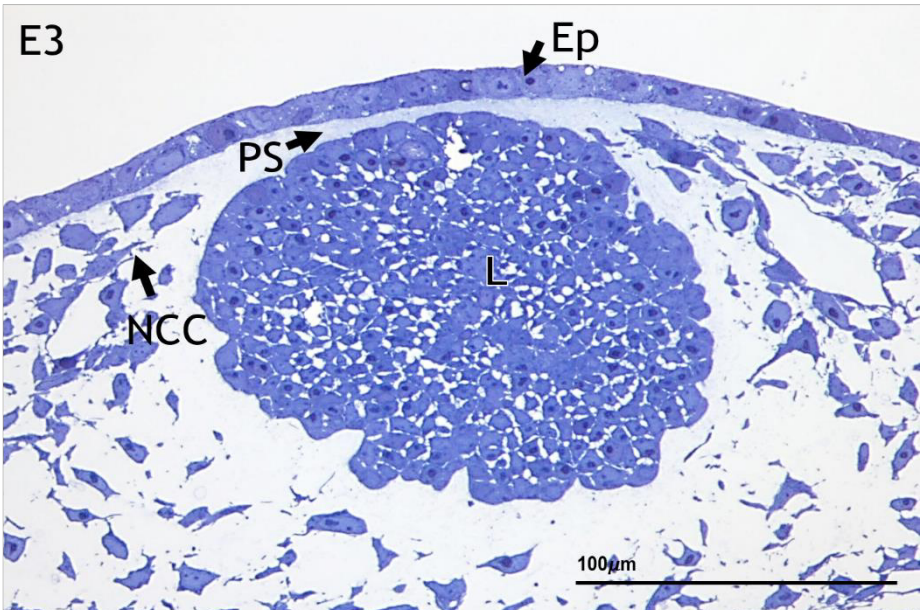

Figure 2.5 Toluidine blue light micrograph showing early eye development stage of chick embryo at E3.
Surface ectoderm formed a presumptive continuous corneal epithelium (Ep) and detached lens (L). A thin primary stroma (PS) stained lightly with a toluidine blue is indicated between the surface epithelium (Ep) and the lens (L). Neural crest cells (NCC) are evident peripheral to the lens. Scale bar, 100 µm.

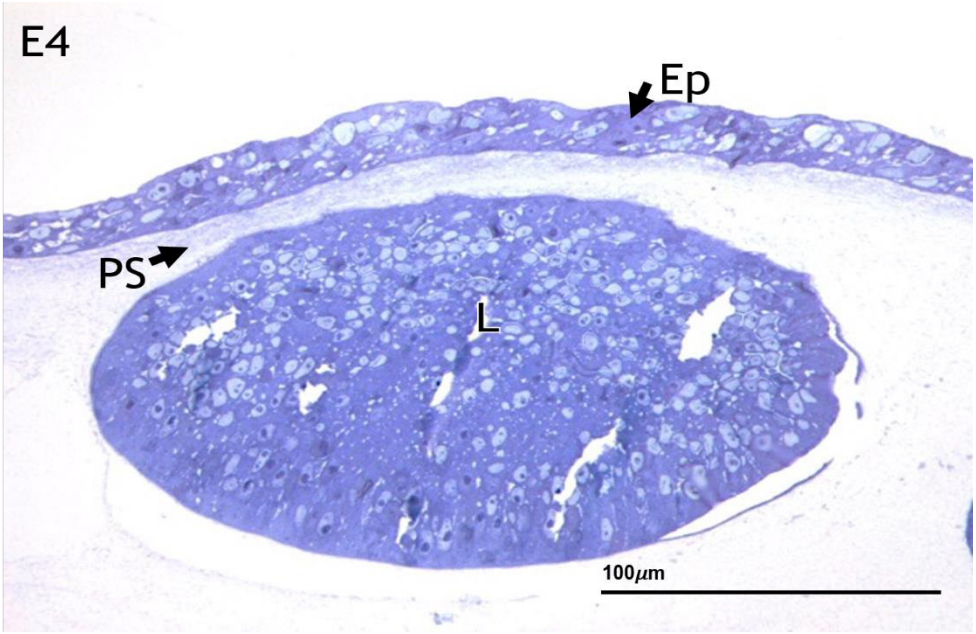

Figure 2.6 Light micrograph of corneal development at E4.
Presumptive multi-layered epithelium (Ep), acellular primary stroma (PS) between the epithelium and the lens (L) are indicated. Scale bar, 100 μm.

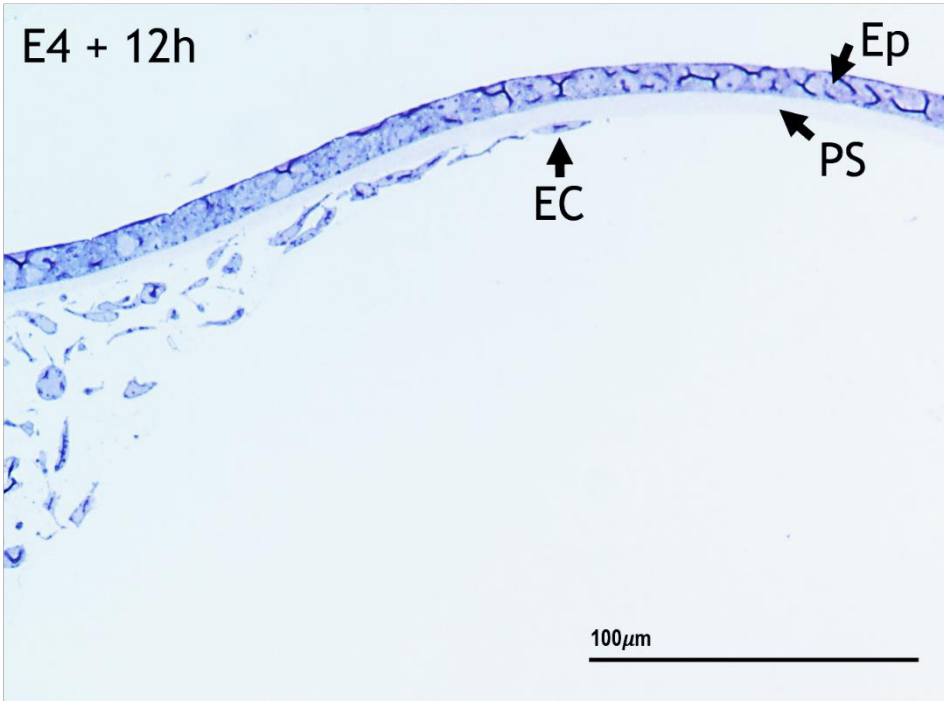

Figure 2.7 Light micrograph of chick corneal development at the embryonic stage between day 4 and 5 (i.e. E4 + 12 hours).
Presumptive corneal endothelial cell (EC) progress towards the central corneal area on the posterior surface of primary stroma (PS). Scale bar, 100 μm.

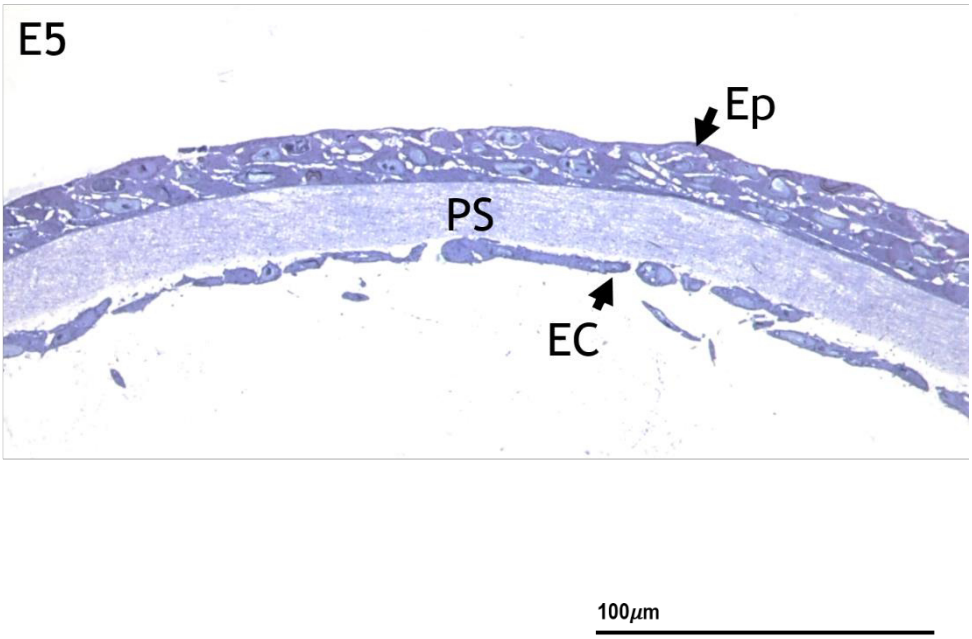

Figure 2.8 Light micrograph of chick embryo showing corneal development at E5. Endothelial cells (EC) appear to cover the inner surface of the corneal primary stroma (PS) in a discontinuous manner with some gaps. Scale bar, 100 μm.

Light microscopy of endothelial cells during corneal development indicated stages when endothelium starts to enter the corneal inner surface. As light micrographs were obtained from different samples of fertilised eggs, corneas sometimes were found to have developed slightly differently. Thus the thickness of the corneas at each stage did not always match precisely. These small individual variations between embryos presumably reflect slightly different rates of development at these early stages post-fertilisation.

At day 3 of incubation, as illustrated in Figure 2.5, structures of ectodermal origin were evident, including a continuous, surface epithelium and subepithelially, the formative lens, separated by the primary stroma. Between E4 and E5 endothelial cells became evident, first peripherally, then extending towards the centre and appearing in these 2D images to cover the entire proximal surface of the primary stroma.

In summary, these light microscopical observations confirm cell migration to form the presumptive endothelium between days 4 and 5 of chick embryonic development. Although several previous studies have described endothelial development in the cornea using 2D microscopy, the nature of endothelial

cell interactions and establishment of the corneal endothelial monolayer has not before been examined at high resolution in 3D.

In the next section, this approach is explored through the results of 3D reconstructions from data acquired by 3-View SBF-SEM.

2.3.2 3-view serial block face scanning electron microscopy

This section presents 3D reconstructions generated from data obtained from 3View SBF-SEM using ImageJ/Fiji to demonstrate morphology of endothelial cells during development at early stages of days 4 to 5: at E4, E4+12 h, E5.

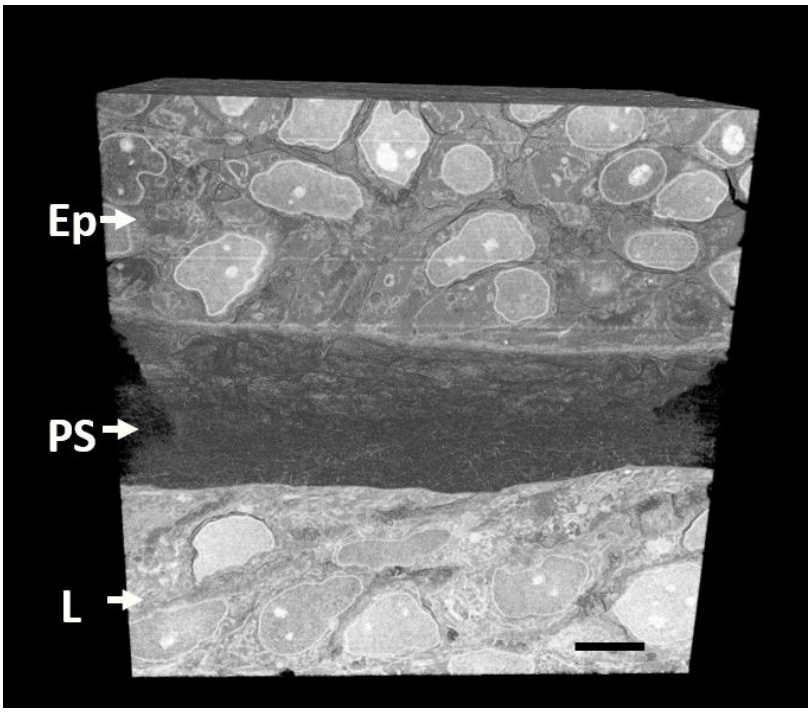

Figure 2.9 Snapshot of 3D reconstruction of developing chick cornea at E4. Corneal structures formed prior to the appearance of endothelial cells: presumptive corneal epithelium (Ep), primary stroma (PS) and lens (L) are indicated. This image corresponds to the light microscopy image in Figure 2.6. A three-dimensional reconstruction movie is available at: https://figshare.com/s/d90fa231776e1edf8a0a. Scale bar, 5 µm.

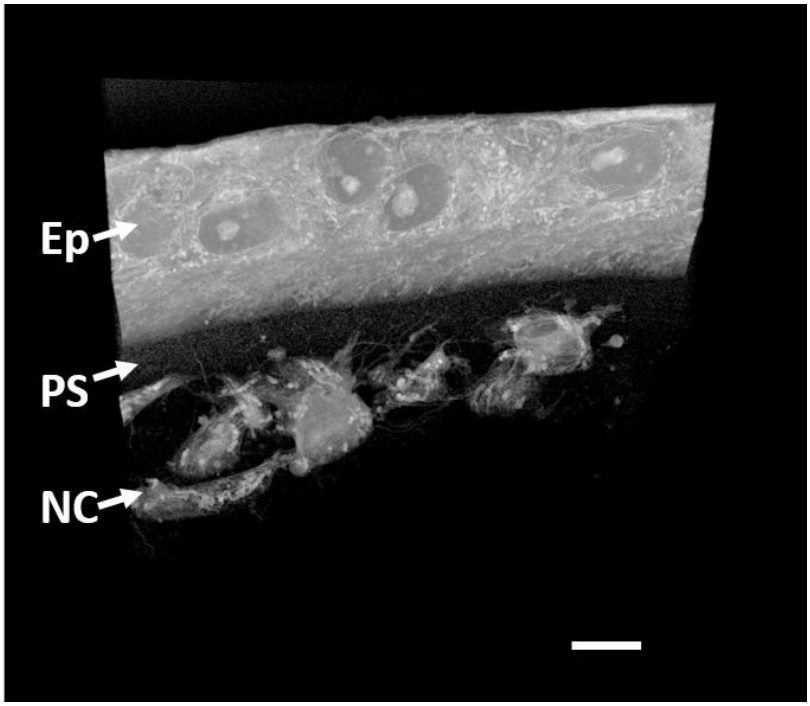

Figure 2.10 Snapshot of 3D reconstruction of developing chick cornea at E4+12 hours.
The beginnings of migration of presumptive endothelial cells (NC) toward the central cornea. Epithelium (Ep); Primary stroma (PS). The image corresponds to Figure 2.7. 3D movie available at: https://figshare.com/s/9315bda9907202cab428. Scale bar, 5 μm.

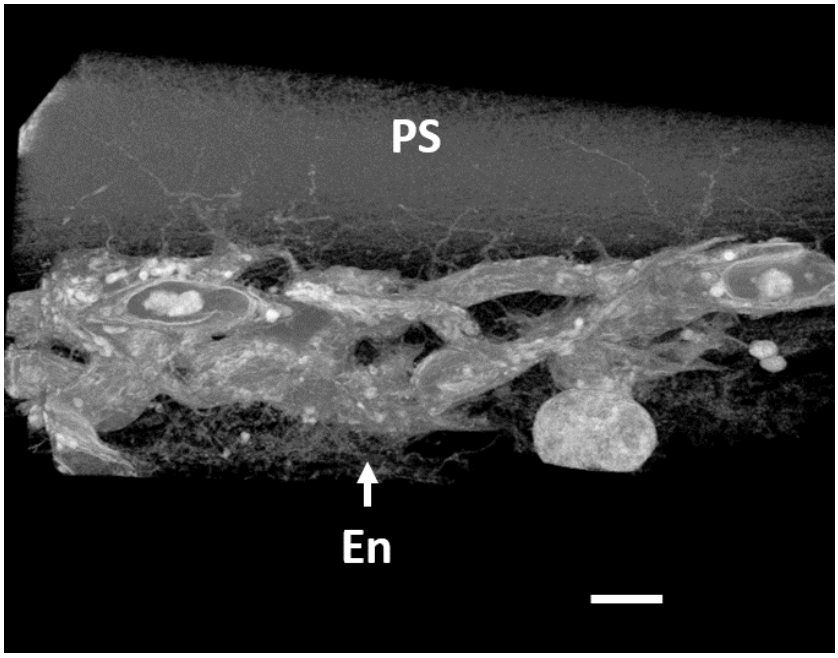

Figure 2.11 Snapshot of 3D reconstruction of chick embryo corneal endothelium at E4 + 12 hours.
Epithelium (Ep) and endothelial cells (En) migrating from the periphery to the central cornea are demonstrated. A sheet of irregular shaped endothelial cells is present at this stage but consolidation as a monolayer has not yet occurred. The cells exhibit numerous filamentous processes, which extend both into the overlying primary stroma (PS) and proximally into the anterior chamber. Orientation: epithelium towards top and the lens is below, both out of field of view. The image refers to Figure 2.8. 3D movie available at: https://figshare.com/s/e126be80ef2ffea4fe65. Scale bar, 5 μm.

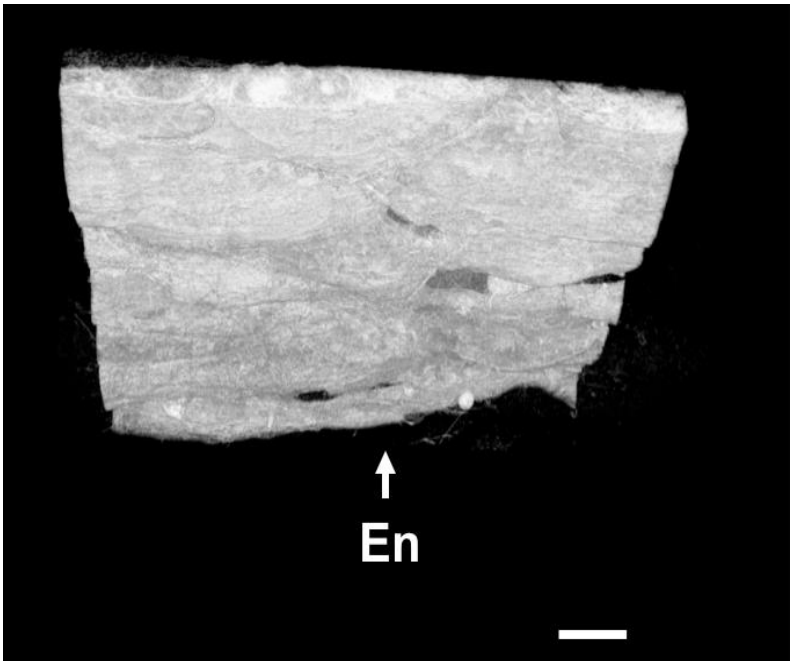

Figure 2.12 Snapshot of 3D reconstruction of developing chick corneal endothelial monolayer at E5.
Hexagonal morphology of the cells is becoming apparent in the 5-day old avian embryonic cornea (angle looking from the posterior side). 3D movie reconstruction available at: https://figshare.com/s/e9b1da724bf40cb46306. Scale bar, 5 μm.

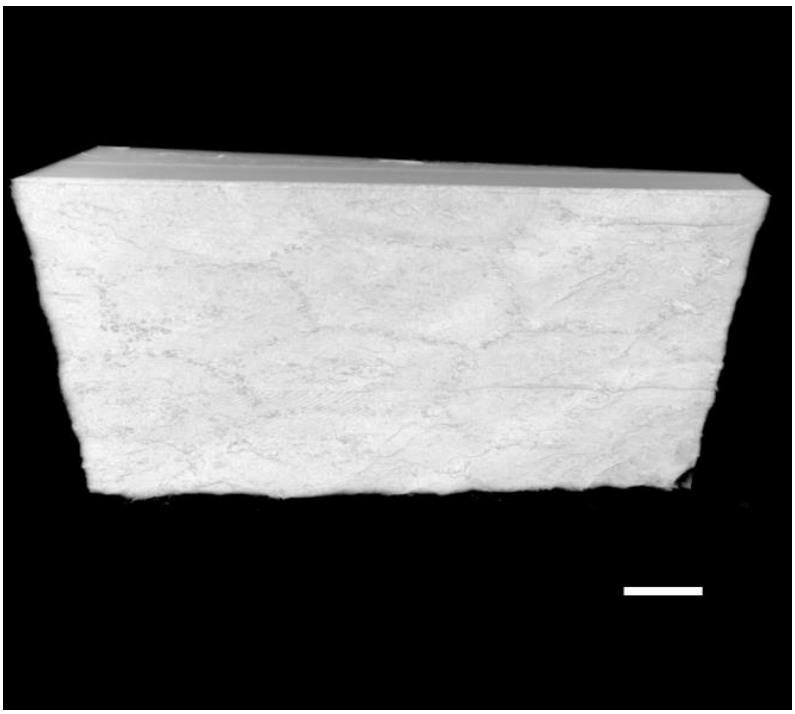

Figure 2.13 Snapshot of 3D reconstruction of the mature porcine corneal endothelium.
The similarity of the characteristic hexagonal shape of the endothelial cells with those of the E5 chick cornea is evident. 3D movie reconstruction is available at: https://figshare.com/s/cc2f4363a2ae674cf406. Scale bar, 5 μm.

Electron microscopical reconstructions in 3D showed that at early embryonic stages (i.e. E4) no endothelial cells had arrived at the inner corneal surface. Surface epithelium appears multi-layered, and its cells bear a resemblance morphologically and ultrastructurally to those of the lens, both of which have common origin. Epithelial cells seem to be still differentiating as evidenced by similar cell and nuclear morphology with no evidence of columnar, basal or wing cell characteristics, which is typical of a well-formed stratified corneal epithelium. Sandwiched between the two components, epithelium and lens, a fine fibrillar extracellular matrix representing the primary stroma was evident (Figure 2.9).

Figure 2.10 demonstrates endothelial cell migration from the peripheral limbal region towards the central inner corneal surface at E4+12 hours. This three-dimensional image corresponds to the light micrograph shown in Figure 2.7. Surface epithelium appears to consist of up to two layers of cells, thinner than the example of an earlier phase at E4. Endothelial cells are moving from the peripheral limbal area towards the central cornea (right of field of view).

Looking at Figure 2.11, it is clear that endothelial cells of irregular shape have reached the central posterior corneal surface forming a sheet. This has not yet consolidated as a continuous monolayer, however. An interesting morphological feature of the endothelial cells at this stage is the presence of long, thin, cell processes that extend in several directions: some are directed into the primary stroma towards the epithelium, whereas others extend towards the lens. Fine filamentous material is also seen at this time weaving its way into the primary stroma in the direction of the epithelium.

Observations on chick embryo cornea at E5 clearly reveal the development of hexagonal endothelial cell morphology (Figure 2.12), characteristic of adult avian and mammalian corneas, and illustrated in the example of porcine cornea shown in Fig. 2.13.

2.4 Discussion

Several novel features of migrating endothelial cells were identified in the course of this study using large-volume 3D reconstructions, previously only examined in 2D.

The familiar polygonal or hexagonal shape of cells in the mature endothelial monolayer is not evident in cells of the neural crest origin which migrate around E4.5 from the periphery of the growing chick cornea to populate the posterior surface of the primary stroma. The cells do not appear to migrate as a coherent layer, as do cells growing from an explant *in vitro*, but resemble more a wave of closely associated but individual entities. By E5 they extend across the full extent of the posterior stroma but are not continuous, exhibit wide intercellular spaces, and have not established a proper complement of intercellular junctions at that time. In general, the cells are flattened in the plane of the stroma, but not to the same extent as appears later when they spread to exclude the intercellular spaces.

A conspicuous feature of the cells throughout their migration to the corneal centre is the presence of numerous fine cell processes, filopodia, which extend both proximally into the newly forming anterior chamber and also distally to project well into the primary stroma. These structures were originally identified by Hay & Revel (1969) in early seminal studies of developing chick cornea although, without the advantage of 3D imaging, their extent was not fully appreciated and they were considered to normally terminate on the primary stromal surface, or on adjacent cells. SBF-SEM clearly showed that instead, they extend for some distance from the cell of origin to penetrate into the loose collagenous matrix of the stroma or appear freely exposed in the expanding space of the anterior chamber. Filopodia are considered typical of migrating cells, are rich in actin and common, for example, in neurite growth cones, and are thought to have a role in detection of extracellular cues, influencing cell orientation and motility (Kim, Kolodziej and Chiba, 2002; Mattila and Lappalainen, 2008).

Endothelial cells appear to be highly sensitive to environmental stimuli. Human endothelial cells of vascular origin grown in an *in vitro* culture model were found to develop several corneal cell characteristics, such as hexagonal shape and expression of the bicarbonate pump enzyme, sodium/potassium adenine triphosphatase, in response to different substrate topographies (Chua, Liew and Yim, 2013).

In the chick embryo, the neural crest cells destined to become the endothelium migrate between the lens surface and the posterior surface of the primary stroma, mainly attaching to the latter (Bard and Hay, 1975). This substrate likely presents very different topographical cues for the cells compared to that of the nanoscale fibre and pore microsurface of Descemet's membrane upon which spreading or healing adult endothelial cells are supposed to move and attach. At E4 the primary stroma is not thought to exhibit substantial orthogonal collagen fibril order which might be expected to provide an obvious conduit for cell alignment and movement. Maybe, therefore, the most significant signals for embryonic cell movement are derived from cues in the fluid environment at the interface between the primary stroma and the lens?

Distal projecting filopodia may facilitate detection of subtle changes in stromal matrix composition towards E5, such as levels of expression of type II and type IX collagens (Fitch *et al.*, 1988), as signals for consolidation of the endothelium through alterations in cell shape and synthesis of intercellular junction components. There is currently great interest in understanding potential routes for stimulation of endothelial cell mitosis and migration from the standpoint of developing new therapies to promote endothelial repair and to treat endothelial dysfunction in the clinic. This has resulted in numerous studies revealing factors which influence endothelial cell activity. Filopodial cell processes reaching into the anterior chamber probably enables exposure of the cell to growth factors, such as TGFβ, known to increase endothelial cell migration through activation of p38 MAPK (mitogen-activated protein kinase) signalling (Joko *et al.*, 2017). Interleukin-1β (IL-1β) has also been shown to have a similar effect on endothelial cell motility, but through Wnt5a induction (Lee and Heur, 2014). IL1-β appears to

act on mature human endothelial cell activity through stimulation of fibroblast growth factor2, but this is believed to lead to transition of endothelial cells to mesenchymal cells capable of fibrotic activity, via activation of transcription factor pathways involving SNAI1, CDK2 and ZEB1 (Lee, Jung and Heur, 2018). These mechanisms are probably suppressed during development; otherwise, the biosynthesis of a collagen type I-rich retro corneal membrane might be the outcome. A recent study has implicated the Ephrin receptor signalling pathway in corneal endothelial cell migration acting through effects on cadherin expression (Walshe *et al.*, 2018). Whether embryonic cell filopodial membranes show enrichment for receptors to these molecules remains to be investigated, although EphA1 and EphA2 receptors were detected on endothelial cells by Walshe *et al*. (2018).

An interesting observation at E4.5 was the apparent interaction of migrating corneal endothelial cells with connective tissue structures within the overlying primary stroma. ‘Interactions’ were present as close associations between these structures and the processes of the migrating cells. The structures appeared as ‘strands’ or ‘cords’ of condensed matrix material extending in a distal to proximal orientation. These matrix strings are presumed to be the same as structures first identified by Bee *et al*. (1988), and later termed ‘strings’ (Fitch *et al.*, 1991; Linsenmayer *et al.*, 1998). These previous studies showed the matrix strings to label positively with antibodies specific for fibronectin and type VI collagen, and they seemed to be connected to the basement membrane of the epithelial cells. It was speculated that they might have a role in the acquisition of transparency by the developing stroma, but this has never been fully confirmed, and their precise function is currently unknown. Association between these structures and the presumptive endothelium suggests that they may fulfil some function in cell guidance, perhaps providing navigational cues to the migrating neural crest cells.

One important and accepted, yet largely under-researched, source of stimulatory control of neural crest cell differentiation in the anterior segment of the embryonic eye, including endothelial growth, is represented by the lens (Beebe and Coats, 2000; Alkatan, 2017). It has been known for many years

that if the lens is ablated at E4, the endothelium fails to form (Zinn, 1970), being replaced instead by a multi-layered mass of disorganised mesenchymal cells. Signals from the lens are apparently vital for expression of the cell adhesion molecule N-cadherin by endothelial cells (Beebe and Coats, 2000), and other research suggests that if the endothelium fails to form normally, development of the anterior chamber also does not proceed (Kidson *et al.*, 1999; Reneker *et al.*, 2000). The influence of lens-derived signals on embryonic endothelial cell morphogenesis is known to persist until at least E15 in the chick (Beebe and Coats, 2000). However, it seems unlikely that regulatory molecules, whatever their nature, would be available from this source for regulation of endothelial regeneration in the adult eye.

Similar to TEM, one of the limitations of the 3view SBF-SEM imaging technique is that this only provides for observation of static stages at selected developmental timepoints. Continuous observation throughout the entire process of endothelial morphogenesis is the ultimate objective, but demands live cell imaging, which has rarely been attempted (Bard and Hay, 1975), and was beyond the capabilities of the present research project.

Chapter 3: Mature Corneal Endothelial Cells in Health and Disease

3.1 Introduction

Human corneal endothelial cells are terminally differentiated cells lining the inner surface of the cornea and forming a monolayer attached to Descemet's membrane with its apical surface exposed to the aqueous humour. Corneal endothelium allows fluid to enter the stroma from the aqueous, but has an essential function in controlling stromal hydration, and thus corneal transparency, by actively pumping water back into the anterior chamber in the form of bicarbonate. A recent study in rabbits showed that stromal water currents determined by the endothelium exist in the horizontal plane from centre to periphery challenging the long-held concept of dynamic flow solely in the vertical plane (Inoue *et al.*, 2014). Potential implications of these findings on the dynamics of pump activity and ultrastructure of cells across the endothelium have yet to be investigated. Water currents cease upon deactivation of the endothelial pump, and stromal swelling rapidly ensues clearly indicating the importance of the endothelium in corneal integrity and the severe consequences of endothelial disease such as Fuchs' endothelial corneal dystrophy (FECD).

The pathogenic mechanisms underlying FECD are still not well-understood. This investigation was undertaken to examine diseased corneal endothelial

cells and compare their fine structure to that in normal, healthy tissue. Earlier studies identified some intracellular changes at the organelle level associated with the diseased condition. In the present study, it was postulated that additional ultrastructural changes might be expressed by organelles in endothelial cells in FECD, which could throw further light on the nature of disease mechanisms. Observations presented in this section were made to compare endothelial cell ultrastructure in normal human cornea with that in Fuchs' endothelial corneal dystrophy. Comparisons were also made with corneal endothelium in the pig eye, widely considered to be closer equivalent anatomically to human (Lee *et al.*, 2014; Choi *et al.*, 2015) and thus an invaluable experimental model.

3.2 Materials and Methods

Various imaging techniques were used to examine samples of pig and human corneal endothelium (healthy and FECD-diseased), including transmission electron microscopy and three-view serial block face scanning electron microscopy.

3.2.1 Experimental models

Human corneal tissues

To better understand the pathophysiology of FECD, the samples of the healthy and FECD-diseased human corneas were used for comparison on an ultrastructural level. The archived specimens were obtained from corneal surgeries carried out in Addenbrookes Hospital, Cambridge, UK. Thus, already processed and embedded to preserve the subcellular structure and ready for ultramicrotomy for further transmission electron examination.

Pig corneal tissue

To compare corneal endothelial structures with those of humans, porcine cornea was chosen as an animal model to investigate normal endothelial ultrastructure using transmission and 3D viewing scanning electron microscopy. Pig eyes were obtained from a regional abattoir, W.T. Maddock (Maddock Kembery Meats, Maesteg) within 6 hours of slaughter and

transported on ice to the laboratory for dissection of corneas and further processing.

3.2.2 Experimental methods

Transmission Electron Microscopy (TEM)

To study ultrastructure of corneal samples TEM was employed. To protect delicate tissue ultrastructure from the destructive effects of high vacuum and electron beam irradiation inside the column of the electron microscope, the samples were processed prior to the TEM examination by conventional methods for biological material. The main steps of preparation for TEM investigation involved preservation of *in vivo* appearance of the samples using fixation, infiltration with resin, sectioning, and staining as described below.

Sample processing

Initially, corneal samples were fixed using a modification of the method introduced by Karnovsky (Karnovsky, 1965) in 2.5% glutaraldehyde and 2% paraformaldehyde in 0.1 M cacodylate buffer, pH 7.2 -7.4 for 2-3 hours. Before the secondary fixation with osmium tetroxide, they were washed with the cacodylate buffer in two changes for 10 minutes each. The specimens were then placed in a secondary fixative of 1% osmium tetroxide in 0.1 M sodium cacodylate buffer for 1 hour. Followed by three washes in distilled water three times for 5 minutes each, they were then placed in 0.5% aqueous uranyl acetate solution for another hour. To completely replace the water within the specimen tissue, gradual dehydration steps were then carried out with a series of ethanol solutions (EtOH) of 70%, 90%, and twice with absolute ethanol (100%). The specimens were placed in each EtOH concentration for 10-15 minutes. Because epoxy resin is not miscible mix with ethanol, a transitional solvent, propylene oxide, that mixes with both ethanol and resin, was used for further dehydration; tissues were twice replaced into propylene oxide-resin mixture for 15 minutes, and 1 hour in 1:1 propylene oxide : Araldite CY212 resin mixture on a rotary mixer. The specimens were then placed into fresh resin three times for approximately 2 hours each, prepared as described below. After the third resin infiltration, the samples were left on the rotator in the fume hood overnight and subsequently

replaced with fresh resin three further times for 1 hour each. After tissues were infiltrated with resin, they were placed into further resin in moulds and cured in an oven at 60°C for at least 24 hours to polymerise the resin. The polymerised resin containing corneal tissue was then ready for section cutting using glass knives. A pig cornea was similarly processed for examination of the mature corneal endothelium by SBF-SEM.

Preparation of resin

To embed the corneal tissue, Araldite CY212 epoxy resin mixture (approximately 3 ml per sample) was prepared. First, 14 ml of Araldite monomer CY212 was put in a prewarmed conical flask, then prewarmed 16 ml of Dodecenyl succinic anhydride (DDSA) hardener and 0.6 ml Benzyl dimethylamine (BDMA) accelerator were added and thoroughly mixed by swirling before use.

Light microscopy

To ensure that the cut section area was appropriate for subsequent examination using the transmission electron microscope, the samples were observed by the conventional light microscopy (Olympus BH-2). To expose the corneal tissue, the blocks with samples were first trimmed with a razor blade. Once the tissue region of interest was bared, several semi-thin sections of 2-4 μm thickness were sliced using a glass knife attached to the ultramicrotome (Ultracut E, Reichert Jung).

Specimen collection for TEM

Once the area of interest was found by light microscopy, ultrathin sections of 70-90 nm in thickness were cut. As sections came off the knife edge to float on the water surface, they were stretched by exposure to the vapour from a piece of filter paper soaked in chloroform held in the proximity to the knife boat. After cutting several sections, they were picked up using a meshed specimen grid made of copper (G300 HEX-C3 Hexagonal mesh, Gilder Grids) (Figure 3.1).

Following collection of corneal sections onto copper grids, they were 'stained' to generate electron contrast in the microscope with solutions of heavy metals, as described below.

Staining and TEM examination

To obtain differential contrast in transmission electron micrographs, copper grids containing ultrathin sections were stained in aqueous solutions of uranyl acetate followed by lead citrate as described below.

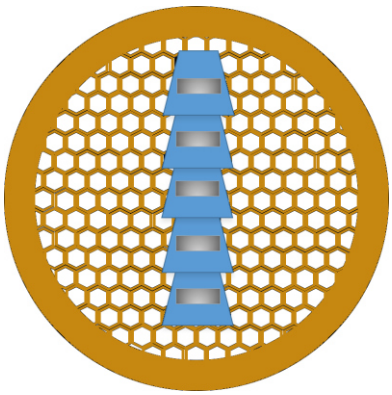

Figure 3.1 Schematic diagram of corneal specimen collection.
The area of interest (grey) in trapezoid-shaped resin (blue) section is collected on a copper grid, 3.05 mm in diameter, before staining and examining using the transmission electron microscope.

First, to get rid of any precipitates, prepared stain solutions were transferred into microcentrifuge tubes and spun down in the centrifuge (MIKRO 120 Hettich zentrifugen, Andrea Hettich GmbH & Co.KG, Germany) at 14000 rpm for 5 min. The staining process was carried out in the clean dust-free environment using parafilm, on which droplets of the uranyl acetate and lead citrate stains were dripped (Figure 3.2). Once the samples were stained, the grids were air dried and stored in a covered grid holder until ready to be examined on the TEM (JEOL JEM-1010 Electron microscope). Finally, transmission electron micrographs were digitalised by the 11megapixel 14 bit CCD camera (Orius SC1000, Gatan) (Figure 3.3).

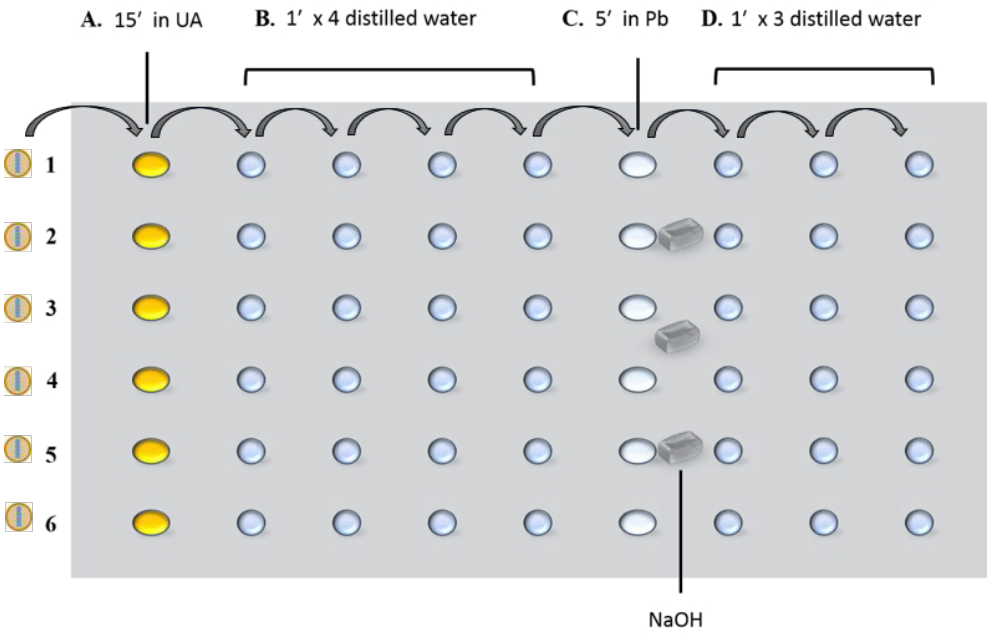

Figure 3.2 Schematic diagram showing of the staining process
Staining steps on example of six grids are shown above (A-D). A: the grids were first dipped using forceps in uranyl acetate (UA) solution for 15 minutes; B: the grids were then transferred in water droplets for 1 minute each; C: next, lead citrate (Pb) for 5 minutes; D: final washing step. To prevent Pb precipitation by scavenging carbon dioxide molecules, sodium hydroxide (NaOH) pellets were placed onto the parafilm between lead citrate droplets

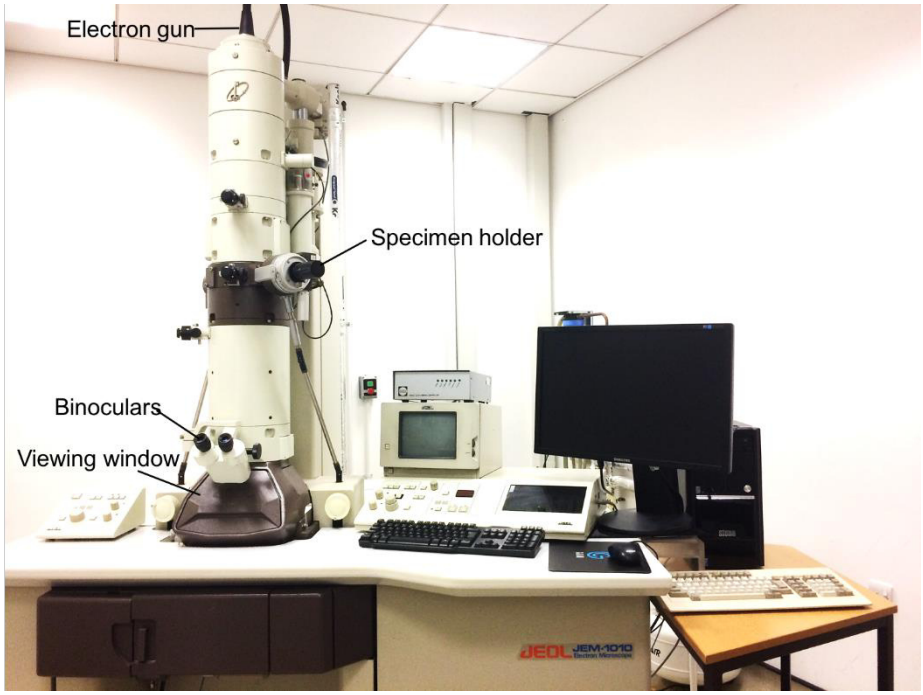

Figure 3.3 Image of transmission electron microscope set up.
The main components of the TEM are shown: Electron gun; specimen holder; binoculars; viewing window.

3.3 Results

This section includes the results of the TEM examination of three different samples including normal human corneal endothelium, corneal tissue from FECD patient, and porcine corneal endothelial cells.

3.3.1 Normal human corneal endothelial cells

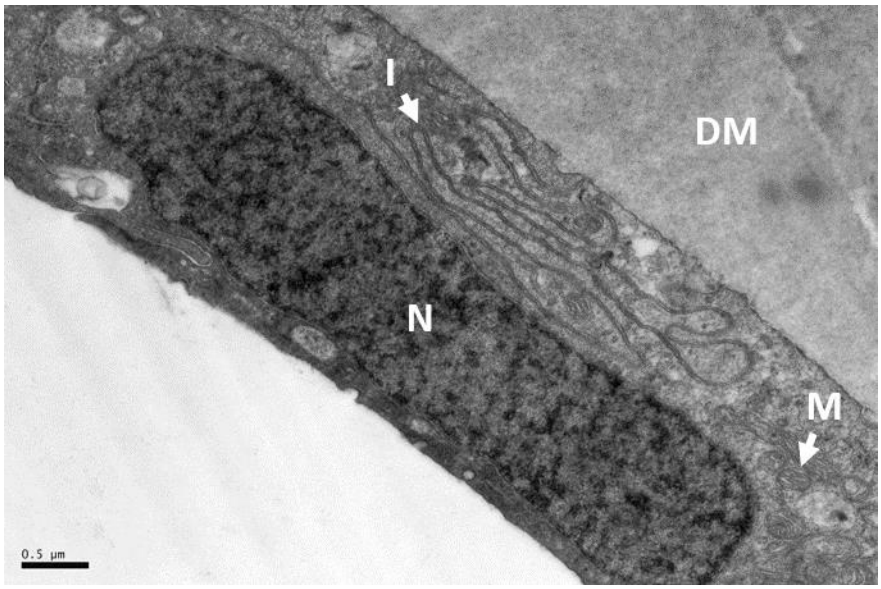

Figure 3.4 Transmission electron micrograph of normal human cornea.
Endothelial cell cytoplasm containing typical intracellular organelles is shown: oval shaped nucleus (N), mitochondria (M), and Descemet's membrane (DM). Extensive interdigitation (I) between adjacent cells typical to corneal endothelial cells is visible. Scale bar, 0.5 µm.

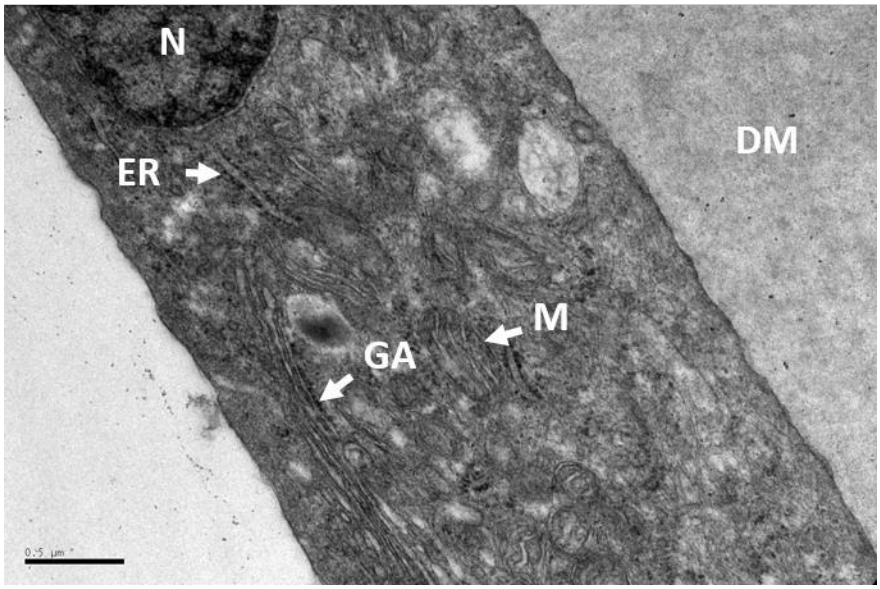

Figure 3.5 Higher magnification of transmission electron micrograph of normal human cornea.
Nucleus (N), multiple mitochondria (M), endoplasmic reticulum (ER), and Golgi apparatus (GA) are present in the endothelial cytoplasm. Scale bar, 0.5 µm.

3.3.2 Human Fuchs' endothelial corneal dystrophy

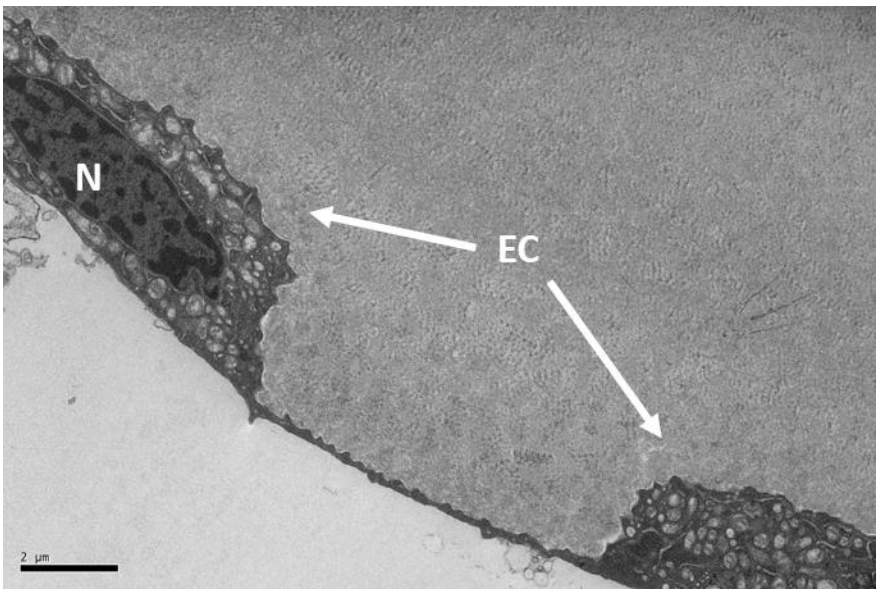

Figure 3.6 Transmission electron micrograph of human FECD endothelium. Irregularly attenuated endothelial layer is shown. Nucleus (N) of endothelial cell is visible and the cells are packed with vesicles. A gutta, typical of FECD is present as an extension of Descemet's membrane and covered by thin processes from the cells. Scale bar, 2 µm.

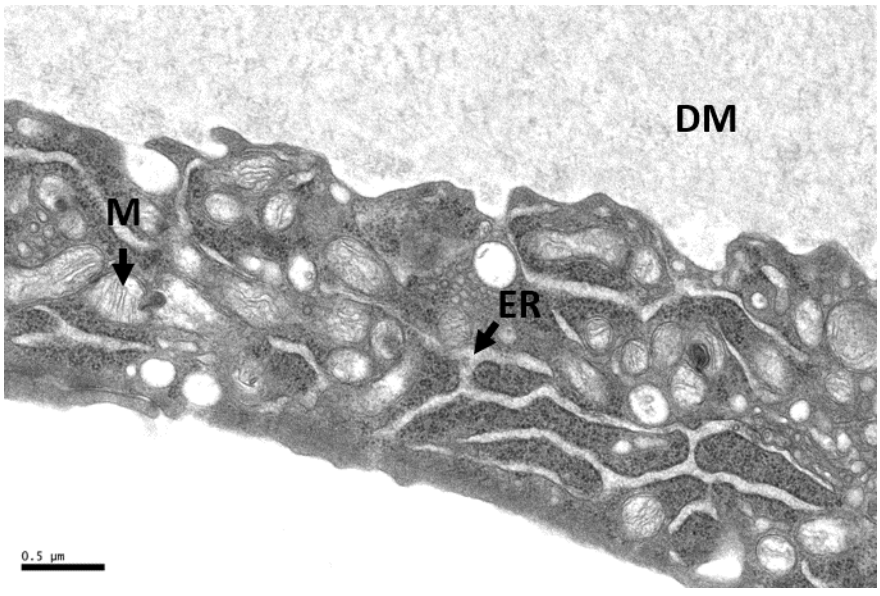

Figure 3.7 Higher magnification transmission electron micrograph of human FECD corneal endothelium.
Dilated endoplasmic reticulum (ER) and mitochondria (M) are evident. The endothelial cell basal membrane shows pathological irregular profile where it adjoins Descemet's membrane (DM). Scale bar, 0.5 µm.

3.3.3 Normal pig corneal endothelial cells

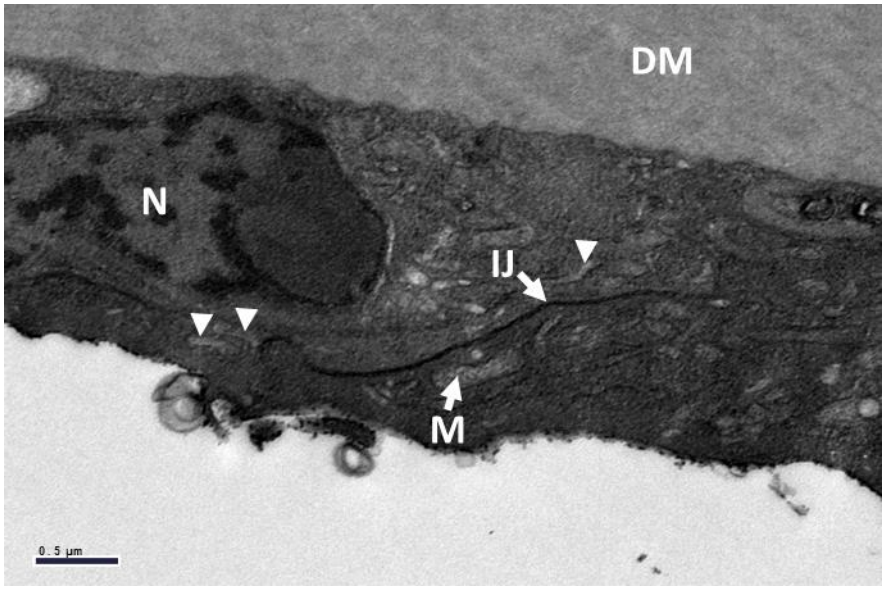

Figure 3.8 Transmission electron micrograph of pig corneal endothelium. Cytoplasmic organelles including nucleus (N), mitochondria (M), and endoplasmic reticulum (arrowheads) are comparable to those of normal human cornea. Fixation in the presence of Ruthenium red provides additional contrast to intercellular junctions (IJ). DM – Descemet's membrane. Scale bar, 0.5 µm.

3.3.4 Three-dimensional reconstruction of normal pig cornea

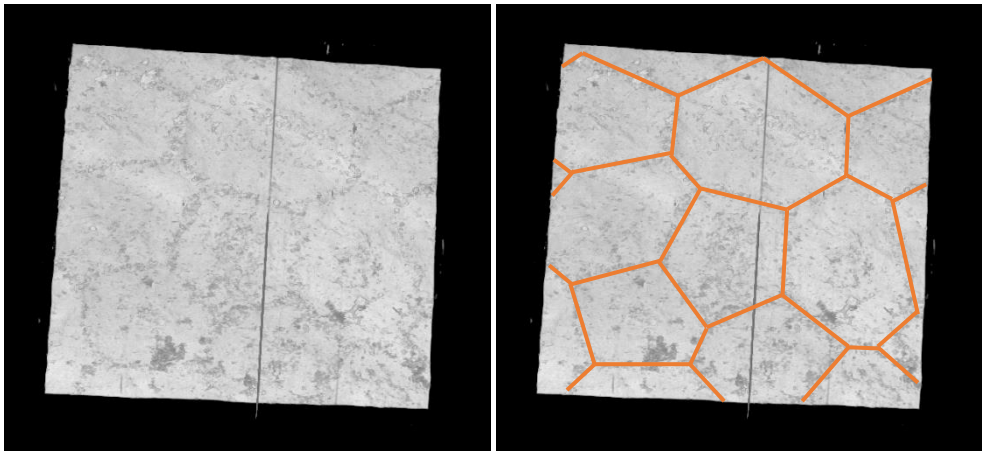

Figure 3.9 Three-dimensional reconstruction of mature pig cornea. Original snapshot (left panel). Right panel indicating hexagonal shaped cells characteristic to normal human corneal endothelial cells.

3.3.5 Transmission electron microscopy of corneal endothelium

The ultrastructures of corneal endothelium in normal pig and human corneas were compared and contrasted with pathological changes seen in a specimen of a human cornea with FECD. Ultrathin sections of all tissue specimens were stained via the same procedure with uranyl acetate and lead citrate and prepared for TEM examination as described in Materials and Methods section 3.2.2. A pig corneal sample was fixed in the presence of ruthenium red to provide additional contrast to endothelial cell intercellular junctions.

The examination of the normal corneal endothelium by TEM demonstrated a continuous endothelial monolayer formed from flattened cells tightly apposed to Descemet's membrane. The mean thickness of the layer was approximately 3–4 μm. Figure 3.4 presents some of the main morphological characteristics indicating that corneal endothelial cells interdigitate extensively at their periphery with the membranes of neighbouring cells. At high magnification, multiple profiles of endoplasmic reticulum were detected in the cytoplasm. In addition, vesicles were very numerous in endothelial cells, clearly seen at higher magnification (Figure 3.7).

An FECD corneal sample studied by TEM revealed a grossly irregular inner corneal surface composed of impaired endothelial cells. Endothelial cells were depleted and even absent in some areas. The approximate range of endothelial thickness was between 0–3 μm, while Descemet's membrane was at least 12 μm. There was an evident difference in the intracellular component from that present in normal corneal endothelium, in particular in the endoplasmic reticulum which appeared clearly increased in thickness.

3.4 Discussion

In agreement with previous studies (Wulle, 1972; Ringvold, Davanger and Olsen, 1984), endothelial cells in normal human and pig corneas formed an integrated layer, tightly apposed to Descemet's membrane, but without apparent specialised membrane attachments to this structure. The appearance of abundant mitochondria and conspicuous, well-developed

Golgi complexes and mitochondria were all features associated with a highly metabolically-active cell population, consistent with its role in supporting an active fluid pumping mechanism responsible for maintaining stromal hydration and thickness.

It was considered that further information on the ultrastructural anatomy of cellular interactions within the corneal endothelium might be achieved by three-dimensional imaging of the monolayer. In order to achieve this, as no fresh human material was available, samples of pig cornea were processed for serial block face scanning electron microscopy. Fixation was carried out in the presence of ruthenium red to induce enhanced contrast in the intercellular junctions.

The flat, hexagonal appearance of corneal endothelial cells seen in two-dimensional imaging by transmission electron microscopy, is evidently more complex when viewed in 3D reconstructions generated from serial data sets acquired by 3View SBF-SEM. Lateral interdigitations of the peripheral cell membrane of adjacent endothelial cells presumably increase the surface area of the cells perhaps as a specialisation associated with membrane transport during fluid transport.

In contrast to normal endothelial cells, morphology was significantly altered in the FECD cornea examined, with greatly attenuated cell shape, some areas of Descemet's membrane completely devoid of cells, and substantial localised thickening of the membrane, so-called guttae, where adjacent cells were thinned and barely maintaining the integrity of the endothelial layer. Characteristic alterations in cytoplasmic organelles within FECD endothelium were consistent with those already reported in the literature, including dilation of endoplasmic reticulum and an increase in size and apparent number of mitochondria**.** The endoplasmic reticulum dilation is thought to indicate to the ER stress caused by overproduction of extracellular matrix, which leads to protein aggregation resulting in cell death (Iwamoto and Devoe, 1970; Engler *et al.*, 2010; Okumura, Hashimoto, *et al.*, 2017). Previously, high expression levels of ER chaperons that help protein folding, GRP78 phosphorylated eIF2α and CHOP, were found in FECD corneal

endothelial cells (Engler *et al.*, 2010; Okumura, Kitahara, *et al.*, 2017). Also, caspase 9 and caspase 3 levels were reported to be increased through ER stress mechanism suggesting the connection between the ER stress and induction of apoptosis in FECD pathology (Engler *et al.*, 2010).

Even using two-dimensional TEM imaging, the extensive nature of endothelial cellular interactions can be seen to be greatly perturbed in FECD. Examination of these changes in 3D reconstructions is highly desirable to fully characterise them, but unfortunately, a fresh sample of FECD cornea was not available for processing via the high contrasting method essential for successful imaging by SBF-SEM.

To conclude, this study demonstrated the ultrastructural differences between corneal endothelial cells in normal and FECD corneas. The markedly-increased amount of endoplasmic reticulum within the diseased corneal endothelium supports the hypothesis of the involvement of ER stress during the pathogenesis of FECD.

Chapter 4: Transcorneal Freezing for Corneal Endothelial Cell Removal: *In Vitro* Porcine Eye Studies

4.1 Introduction

Surgical intervention in the form of penetrating keratoplasty is the main treatment route for severe corneal oedema and the accompanying loss of vision caused by Fuchs' endothelial corneal dystrophy (FECD). The scarcity of donor corneas and frequency of post-operative complications with the corneal transplantation such as graft rejection continue to limit the success of this invasive procedure, despite the availability of approaches for selective replacement of the endothelium, which are now more commonly used, such as Descemet's stripping (automated) endothelial keratoplasty (DS(A)EK) and Descemet's membrane endothelial keratoplasty (DMEK). To improve surgical methods and outcomes, eye researchers continue to seek less invasive alternative treatment options for endothelial dysfunctions. One such approach, pioneered by our surgical collaborators in Kyoto Prefectural University of Medicine and Doshisha University in Kyoto, Japan, was based on the pharmacological encouragement of non-diseased corneal endothelial cells to regenerate and resurface the damaged central area of the cornea in patients with FECD following the removal of the diseased and dysfunctional endothelial cells lining the central region of the posterior cornea.

Conceptually, this could have been achieved by intraocular surgery and the mechanical scraping off of these cells via a full thickness peripheral corneal incision. However, to make the surgery less invasive, transcorneal freezing was selected as a way of destroying the diseased FECD cells at the cornea's inner surface (Koizumi *et al.*, 2013, 2014; Okumura *et al.*, 2013). Of course, the corneal epithelial and stromal cells will also be damaged by the cryo-injury, but these are expected to regenerate. In the first-in-man experimental surgeries conducted in Kyoto, a stainless steel rod that had been immersed in liquid nitrogen was used to induce the transcorneal freezing. If this surgical approach is to be more widely adopted into medical practice, however, the freezing would likely need to be achieved in a more controlled manner, thus the reason for the investigations described in this chapter.

Various cryoprobes have been used for therapeutic purposes in the medical field to remove diseased tissue, and methodologies have exploited a variety of materials and cooling agents to achieve low temperature. Extreme low temperature has a destructive effect on tissues because of extremely rapid heat transfer from the cells and extracellular matrix to the cryo-agent, which can break cell membranes by disrupting their structural integrity via the formation of ice crystals that breach the cell membrane, eventually leading to cell death. Damage can also occur owing to the conversion of liquid water to ice crystals, which leads to an unsustainable osmotic imbalance that can render a cell non-functional. In the ophthalmic field, the response of cells to freezing is described by Fraunfelder (2008) in his comprehensive review of corneal cryotherapy.

Cryoprobes for use in ophthalmic surgery do exist. However, these were not designed for corneal use, and are more commonly used for cataract extraction via a "freeze-grip" mechanism whereby the cold probe adheres to the cataractous lens, enabling the surgeon to manipulate and remove it (Ben-nun and Barkana, 2002). The use of such probes would not be desirable for transcorneal freezing to damage dysfunctional corneal endothelial cells in our proposed FECD surgery since adherence of the cold probe to the corneal surface would be an unwanted effect. Also, existing cryoprobes tend to have a convex curved probe-tip profile, so were thought by us not be optimal for

transcorneal freezing and that a concave curved probe-tip surface would be preferable and result in better freezing.

Freezing of corneal tissue has been used experimentally as a modality to induce an injury to facilitate basic research into corneal wound healing (Maumenee and Kornblueth, 1948; Chi and Kelman, 1966; Faure, Kim and Graf, 1971; Buco *et al.*, 1973; Minkowski *et al.*, 1984; Tuft, Williams and Coster, 1986; Ichijima *et al.*, 1993; Fullwood *et al.*, 1996; Petroll *et al.*, 1997; Mimura, Yamagami, Yokoo, Yanagi, *et al.*, 2005; Mimura, Yokoo, *et al.*, 2005; Han *et al.*, 2013). But, if corneal freezing is to be used in a clinical setting (either for the destruction of diseased cells in the central endothelium prior to ROCK inhibitor eye drop application for FECD, as described above, or to pre-treat the cornea prior to targeted drug delivery to combat conditions such as fungal keratitis as an additional potential use), it needs to be achieved in a more sophisticated, reliable and reproducible manner than that achieved with an immersion-cooled steel rod. In this chapter, investigations into the effects on the porcine eye of a new cryoprobe for transcorneal freezing in FECD surgery are described.

4.2 Materials and Methods

4.2.1 Experimental materials

Cryoprobe development

A console that uses nitrous oxide as a cryogen was designed and manufactured specifically for use as a tool to achieve transcorneal freezing as a treatment for FECD. It was designed and manufactured in collaboration with a medical device company based in Ripon, North Yorkshire (Network Medical Products Ltd., UK) (Figure 4.1). A patent has been granted in Japan (No. 6104249) for the device and a European patent application currently under examination. Cardiff University holds this intellectual property (IP). Two prototypes exist, one in Cardiff University and the other in our collaborator's laboratory at Doshisha University, Kyoto, Japan. The console is attached to a hand-held cryoprobe, which was used for corneal freezing. Enclosed nitrous oxide gas expanded within a tip and

was recycled inside the tip of the cryoprobe, achieving a low temperature based on the Joule/Thomson effect.

To allow good contact with the cornea's surface the tip of the cryoprobe was not convex (as it the case for existing ocular cryoprobes), but was designed either to be flat or to be concave with a similar average radius of curvature of the human cornea itself (approx. 8 mm) around the probe's main axis, and several designs were tested with probe tips measuring 1.8 mm, 2.4 mm, or 3.4 mm in diameter laterally. The tips are made of silver for high thermal conductivity. Probe tip diameters larger than 3.4 mm were not considered because it was decided that if relatively large areas of tissue needed to be treated, then multiple freezing procedures could take place.

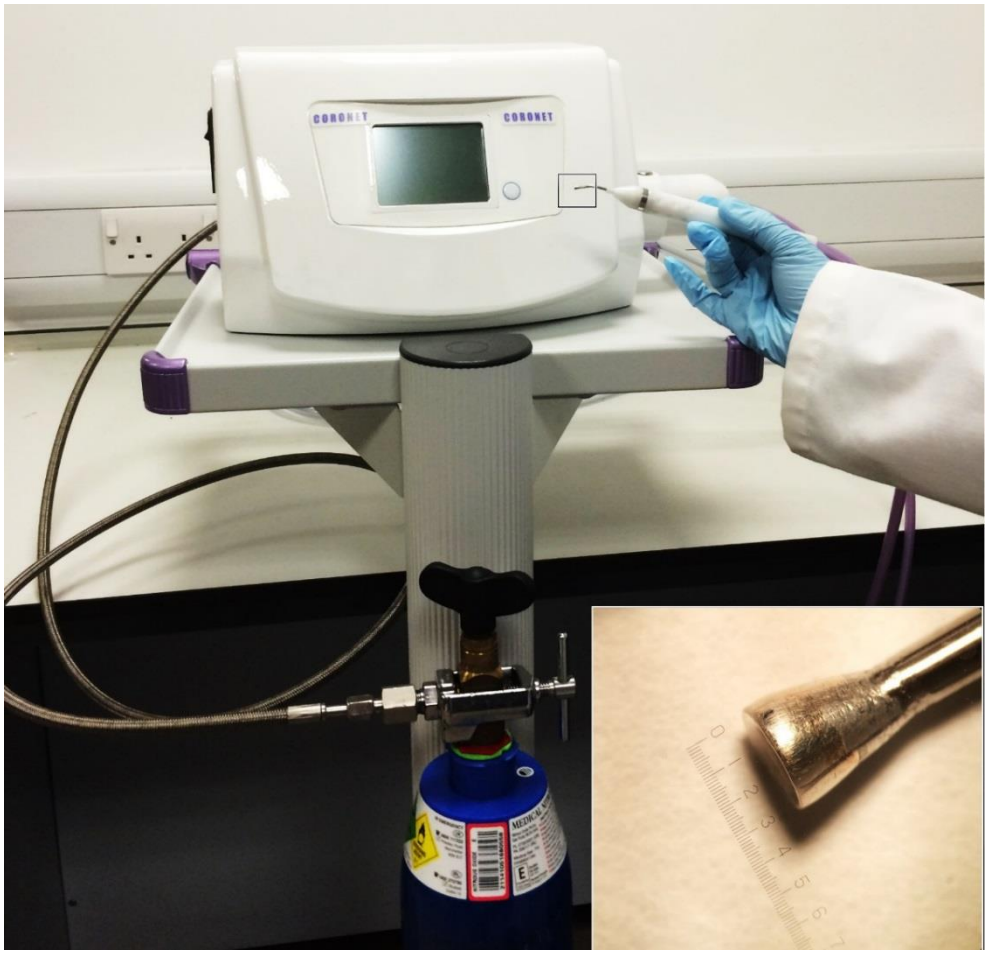

Figure 4.1 The transcorneal freezing machine, attached to a cylinder of medical grade nitrous oxide (the cryogen).
The machine comprises of a main console with a monitor screen that displays freeze time, cryogen levels and readiness for freeze plus interchangeable probe tips, and a footswitch (not shown). Inset: the 3.4 mm diameter concave probe tip manufactured from silver for high thermal conductivity.

For ease of use, a foot-pedal was incorporated into the design, which initiates cooling at the cryoprobe tip and maintains the reduced temperature throughout the whole time the pedal is depressed. Freezing temperature at the probe tip (approximately -50°C, according to the manufacturer), is reached within 2 seconds of depressing the foot-pedal; after its release, ambient temperature is achieved within seconds concomitant with a thawing effect. The hand-held cryoprobe has an ergonomic angled design to allow easy application to the corneal surface (Figure 4.1).

4.2.2 Experimental models

This chapter describes a series of *in vitro* experiments in pig eyes to ascertain the optimal surgical parameters using a newly designed corneal cryoprobe needed to induce corneal endothelial cell removal via transcorneal freezing, as well as the permeability of the cornea to a topically applied solution (potentially a therapeutic pharmaceutical agent) following transcorneal freezing.

The porcine eye was used as an experimental model to evaluate the impact of various designs of cryoprobe tip attached to the newly-manufactured cryoprobe. On average the human cornea is about 550 μm thick, though some small ethnic differences have been reported (Ma *et al.*, 2018). The pig cornea, on the other hand, tends to be approximately 670 μm thick (Hatami-Marbini, Etebu and Rahimi, 2013; Guindolet *et al.*, 2017). A comprehensive study by Repp and colleagues has shown that owing to the corneal stromal swelling that occurs as a result of the corneal endothelial dysfunction in FECD the central corneal thickness (in 118 patients included in Repp's study) was 652 ± 61 μm, compared to the average thickness in 267 normal corneas they measured, which was 559 ± 31 μm ($P<0.001$) (Repp *et al.*, 2013). Serendipitously then, it appears that, based on average central corneal stromal thickness, the pig cornea is a representative proxy of the human FECD cornea. For the studies described here, intact pig eyeballs with associated extraocular tissues were obtained from bacon-weight pigs within 6 hours of slaughter at a local abattoir (W.T. Maddock, Kembery Meats, Maesteg, Wales, UK) delivered by a dedicated technician for the laboratory.

These were transported to the laboratory on ice and experiments began within 8–9 hours of the animals' death.

4.2.3 Experimental methods

Reducing Corneal Thickness

When the porcine eyes arrived at the home laboratory, measurements of central corneal thickness were taken with an ultrasound pachymeter (Tomey SP-100), which revealed that the corneas had thickened post-mortem to approximately 1000 µm-thick, compared to published *in vivo* values in the 600–700 µm range (Ruiz-Ederra *et al.*, 2005; Faber *et al.*, 2008). Preliminary experiments suggested that intraocular pressure was low in enucleated eyes. Thus 500 µl of 0.9% saline solution was injected with a syringe into the vitreous chamber via the optic nerve. Additionally, the corneal surface of each eye was dampened with droplets (approx. 1 ml each) of the saline solution prior to pachymetry measurements to mimic the tear film and help avoid any abrasive damage caused by the application of a dry device (i.e. pachymeter and/or tonopen) to the cornea's surface. The average thickness of the cornea was evaluated by taking eight readings from the same location on the central corneal surface. An initial analysis revealed that the average corneal thickness of the pig eyes that had arrived on ice from the abattoir was in the region of 1000 µm (average 1079 ± 64.6, n=7). Evidently, this was not appropriate for experiments on corneal tissue that was intended to mimic a typical human FECD cornea, so steps needed to be taken to de-swell the corneas in the intact pig eyes prior to the experiments being conducted.

Several different approaches have been used by other researchers to reduce the corneal thickness for *in vitro* experimentation, including positioning the anterior surface of an eyeball in a dextran solution to allow osmotic effects to thin the cornea (Thuret *et al.*, 2005; Zhao *et al.*, 2008; Wolf *et al.*, 2009). Attempts to optimise the de-swelling of the porcine corneas using an 8% dextran solution and immersion time of up to 24 hrs, however, failed to sufficiently thin the corneas to thicknesses that resembled normal pig corneal thicknesses/human FECD corneal thicknesses. Humidified dehydration at high temperature was thus chosen as an alternative mechanism by which to thin the pig corneas to usable thicknesses. A series of empirical tests

disclosed that placing the intact pig eyes in a humidified incubator (Brinsea Octagon 100 Incubator, Brinsea Products Ltd, Sandford, UK) at 45ºC for 30 - 45 min was able to reverse the post-mortem swelling and obtain a suitable thickness for all subsequent experiments.

Transcorneal Freezing

Transcorneal freezing was achieved by placing the cryoprobe tip on the central corneal surface and initiating cooling by pressing down on the foot-pedal to control the flow of nitrous oxide gas. The cryoprobe design team advised that 2 sec was needed for the probe tip to reach the low temperature subsequent to the foot pedal being depressed. Thus, initial experiments to ascertain whether or not freezing time influenced the extent of endothelial cell damage were conducted, and freezing times of 3 sec, 5 sec, 9 sec, and 13 sec were tested. An additional 2 sec was included for the freezing temperature to be reached. Thus, a 3-sec freeze required a 5-sec application and foot-pedal depression of the foot pedal. The cryo-console has a light-emitting diode (LED) time display that counts upwards in seconds, plus an audible beep, to allow the operator to conduct the freeze for the designated time.

Epithelial On/Off Testing

The pig eyes I used were from animals that had not undergone hot water immersion scalding, as happens in some abattoirs. This makes the eyes much more relevant for experimentation, and there was a likelihood that the corneal epithelium would still be present. To investigate whether or not the presence of this cell layer might have an effect on corneal endothelial damage via transcorneal freezing, experiments were conducted from which the epithelial layer had been removed in 20 eyes using a sponge to gently debride the corneal epithelium from the ocular surface prior to application of the cryoprobe. The intactness of the corneal endothelium was then assessed using the cell viability test described below.

Pre-Cool or not Pre-Cool

To establish whether or not the cryoprobe tip should be cooled prior to application to the cornea or cooled after it was in contact with the cornea,

tests were conducted on eyes with pre-cooled and non-precooled probe tips. The intactness of the corneal endothelium was then assessed using the cell viability test described below.

Cell Viability Test

Following transcorneal freezing, the *in vitro* pig corneas were carefully excised at the limbus, retaining a peripheral rim of anterior sclera, after which staining solutions of 0.2% alizarin red (approx.1 ml) and 0.25% trypan blue were applied sequentially to the endothelial surface for 60 - 90 sec each to identify live and dead cells. The stains were gently rinsed off using approximately 5 ml of buffer solution and left in the corneal cup until light microscopy examination.

Light Microscopy

Digital images of the corneal endothelial surface were captured on a Zeiss Stemi 1000 light microscope (Carl Zeiss) via a digital camera (Nikon Coolpix 4500 4MP). The magnification was calibrated during every set of experiments using the image of an eyepiece graticule. The trypan-blue-stained endothelial wound area in each corneal image was manually traced and measured using ImageJ/Fiji software (http://imagej.nih.gov/ij/). Averages of three measurements were calculated, and data were further collated using Microsoft Excel software (Microsoft Corporation).

Statistical Analysis

Statistical analysis was carried out operating IBM SPSS Statistics software (Version 23.0, IBM Corporation). For the evaluation of the success rate of transcorneal freezing using each probe, only images with circular shaped endothelial wound areas that mirrored the probe were included. Spearman's rank order correlation test was run to determine the relationship between central corneal thickness and endothelial wound areas induced by the freezing.

Scanning Electron Microscopy

To investigate the endothelial cell damage caused by transcorneal freezing in the *in vitro* pig eye model in more detail, four treated corneas were

examined by scanning electron microscopy (SEM). Immediately after excision, the corneas were fixed in 2.5% glutaraldehyde, 2% paraformaldehyde in 0.1 M sodium cacodylate buffer, pH 7.3, for at least 2 h. Samples in fresh fixative were then sent to Lancaster University, UK to be further processed for SEM examination where they were first washed free from fixative in phosphate-buffered saline (PBS). This was followed by gradual dehydration through a graded ethanol series (from 50% to 100% in 30 min steps), after which the ethanol was replaced by the sublimation dehydrating agent, hexamethyldisilazane for 20 min to minimise the shrinkage of the specimens. After drying, the corneas were placed on aluminium specimen stubs (Agar Scientific) and sputter coated with gold (Edwards S150 sputter coater, Edwards High Vacuum Co. International) to allow imaging in a JEOL JSM 5600 scanning electron microscope (JEOL Company) with a beam accelerating voltage of 15.0 kV. Final sample processing and SEM data acquisition in this part of the study was kindly conducted by Dr Nigel Fullwood, Lancaster University, UK.

Corneal Permeability

To investigate whether transcorneal freezing enhances penetration of a solution (potentially, a pharmaceutical agent) across the stroma to the inner endothelial layer, 12 corneas were studied. As reported below, the 3.4 mm diameter concave profile cryoprobe tip was found to be the most effective in inducing prominent endothelial damage in the porcine eye *in vitro*. Thus, cryofreezing was carried out on six of the twelve *in vitro* pig eyes using the 3.4 mm diameter concave probe for a total of 5 sec following the procedure described above. The six eyes that were not exposed to transcorneal freezing acted as controls. Methylene blue is readily visible to the naked eye and on light microscopy, and was used as a visual guide of solution penetration into the cornea after transcorneal freezing, and this was either delivered in the form of eye drops or was incorporated into a thin contact lens-like polymeric film that could be placed on the corneal surface for the slow release of the agent into the cornea. The polymeric mucoadhesive films were pliable and 0.1 mm thick approximately, and were developed by colleagues in the School of Pharmacy and Pharmaceutical Sciences, Cardiff University (Chan, Akhbanbetova, A. J. A. J. Quantock, *et al.*, 2016).

4.3 Results

4.3.1 Transcorneal freezing of porcine cornea in vitro: freezing time and epi-on or epi-off.

Experiments into the extent of endothelial damage caused by transcorneal freezing induced by the 2.4 mm diameter/concave profile cryoprobe tip revealed that the time of cryoprobe tip contact with the corneal surface did not affect the area of endothelial damage, seen as a blue stained area of the corneal endothelium, with freezing times of 3, 5, 9, or 13 seconds tested (Figure 4.2).

This indicated that the endothelial damage was more consistent when the cryoprobe tip was in contact with the corneal surface prior to the initiation of cooling, whereas precooling of the tip for 2 seconds before surface application resulted in an unreliable removal of endothelial cells. A series of epi-off/epi-on tests revealed that removing the corneal epithelium prior to a

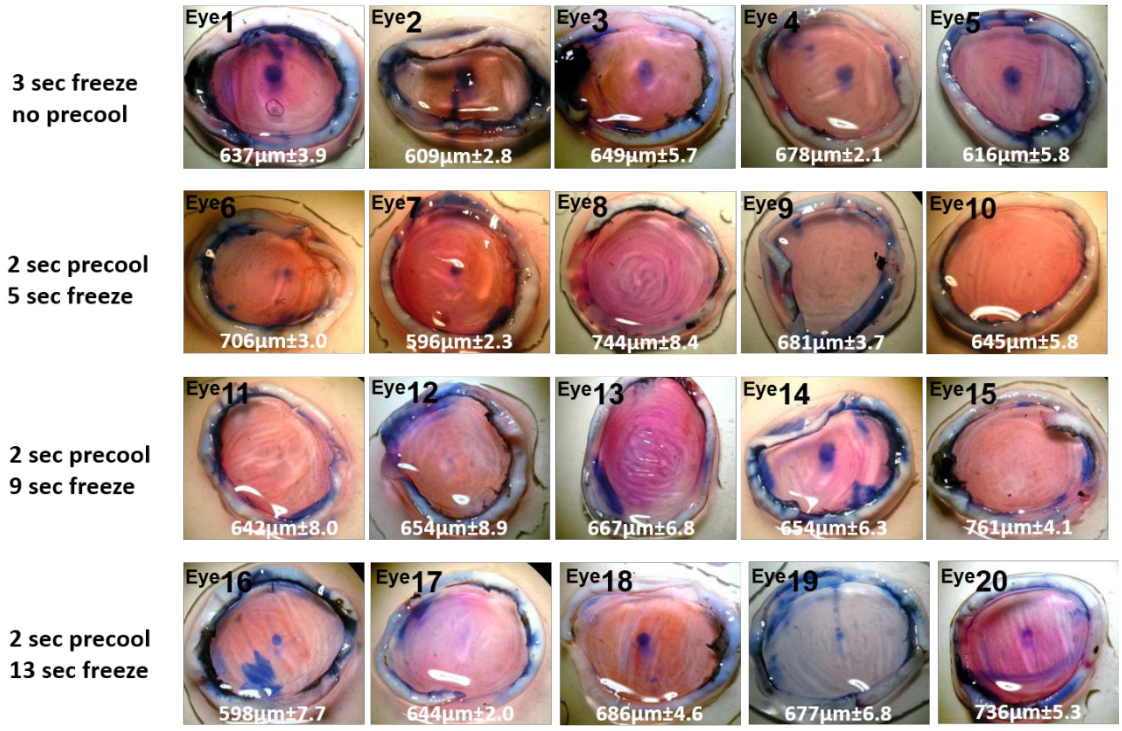

Figure 4.2 Table of images show the effect of 3-second freeze with no precool and 2 second precool with different freeze times (3,5, 9,13 seconds) on pig corneal endothelium.
The 2.4 mm cryoprobe tip with concave shape was used. Endothelial damage as a result of freeze-thaw effect is indicated by blue stain.

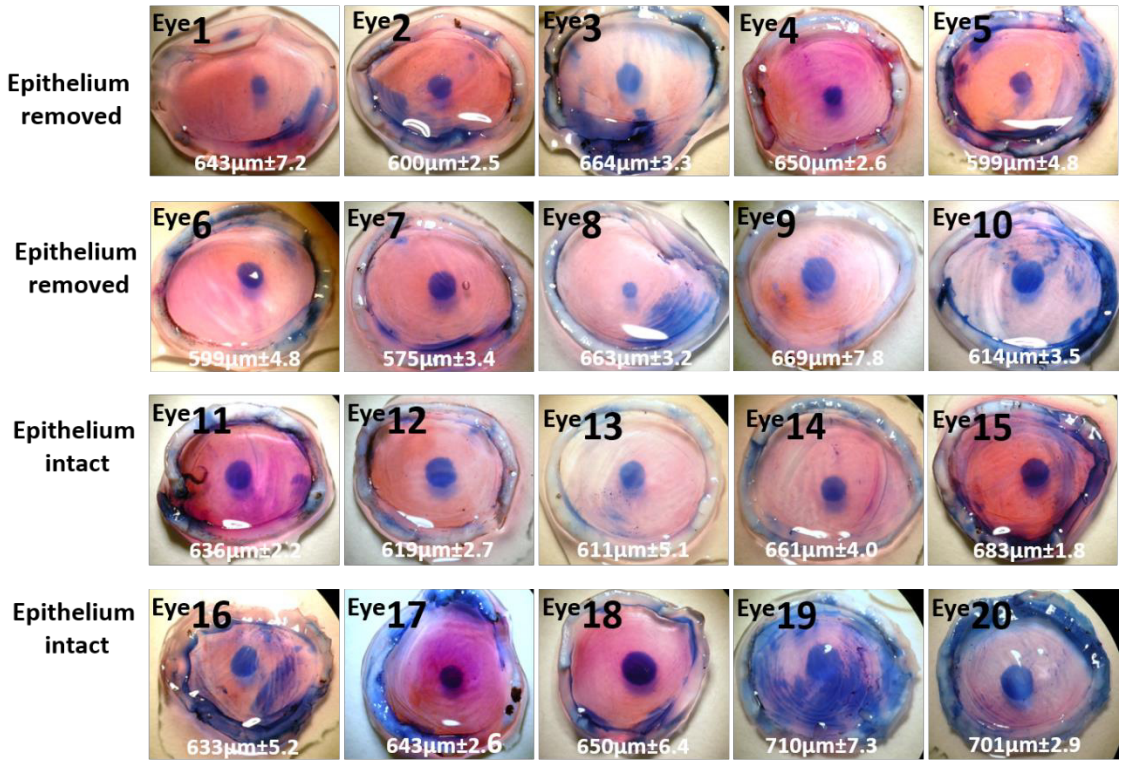

Figure 4.3 Effect of epithelial scrape removal prior to 3 sec freeze using the 2.4 mm diameter concave probe tip on porcine corneas.
No observable difference was seen in the extend of endothelial damage following removal of corneal epithelial cells compared to the endothelial damage in eyes from which the epithelium had not been removed prior to the freeze. Endothelial damage is indicated by blue stain.

transcorneal freeze caused no observable difference in corneal endothelial cell damage. Thus, for the all further experiments, the cryoprobe tip was not pre-cooled, and the corneal epithelium was not removed.

4.3.2 Transcorneal freezing on porcine cornea in vitro: An optimisation of probe design.

Based on the experiments described above, a freezing time of 3 seconds with no cryoprobe tip pre-freeze was chosen for the experiments described in this section to ascertain the best performing tip design.

Light microscopy of the endothelial surfaces of post-freeze, trypan blue-stained corneas indicated the area of cell damage caused by the four different probes used in these experiments. Representative images of 426 technical replicates, denoting the typical extent of endothelial damage, are shown in Figure 4.4, with examples of what were considered to be successful

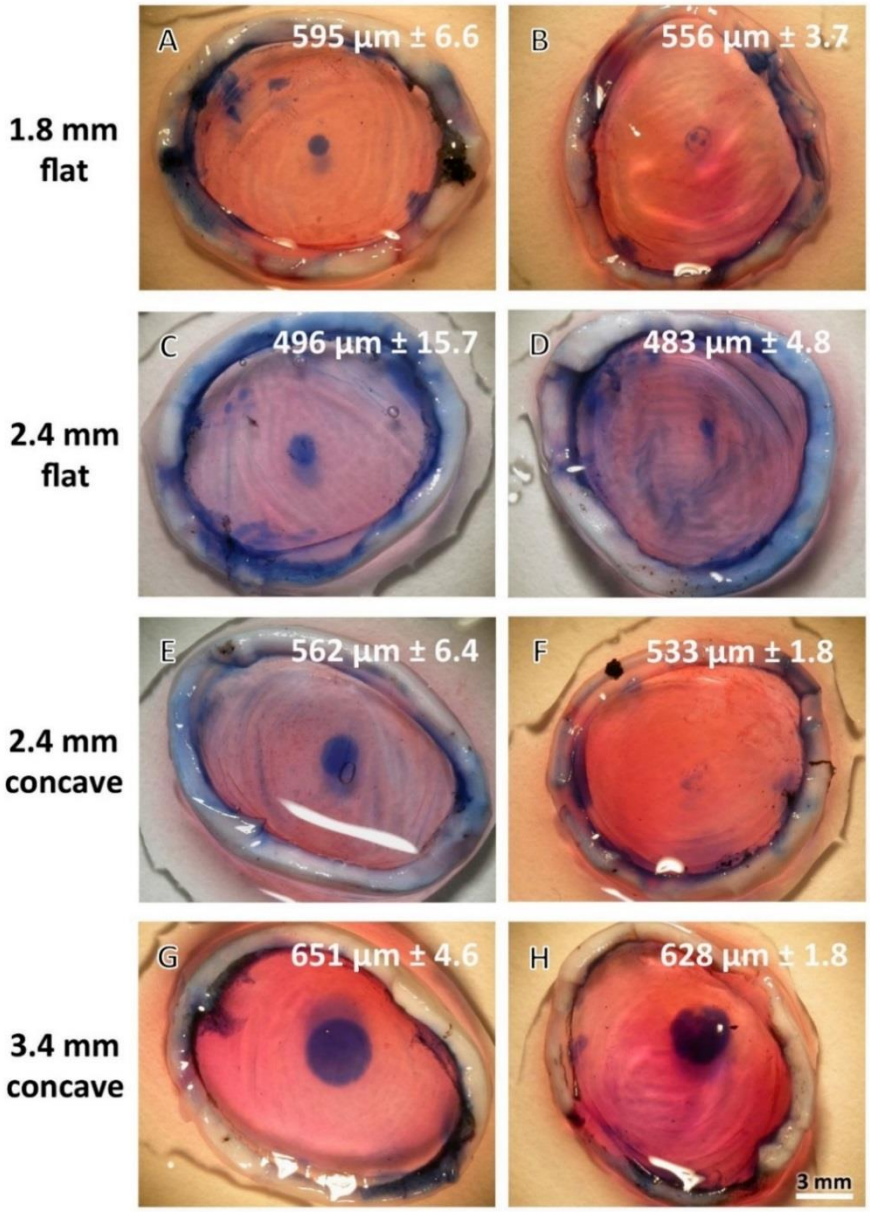

Figure 4.4 Representative images of corneal endothelial freeze-injury on pig eye *in vitro* induced by a 3 sec freeze with four different cryoprobe tips and assessed by trypan blue staining.
The thickness of each cornea is indicated on each panel (±SD) based on eight pachymetry readings. The area of cell damage is seen via blue stain and successful and non-/less successful freeze injuries are shown in the left and right columns, respectively. Freezing with the 1.8-mm diameter/flat profile probe only rarely resulted in a reproducible wound (A, B). Endothelial freeze injury was more reliably achieved with 2.4 mm diameter probe tips with flat or concave profiles (C-F), but the optimal result and best consistency were achieved using the 3.4 mm diameter/concave profile cryoprobe (G, H). Scale bar, 3 mm. See table 4.1, also.

or unsuccessful freeze injuries. A successful freeze injury was defined as one that resulted in a well-delineated circular area of cell damage; whereas an unsuccessful one was considered to have occurred, either when there

was no evidence of any cell damage, or when the area of induced damage was irregular. Based on these criteria only 14 of 102 eyes (14%) treated with the 1.8 mm flat probe were judged to have been successfully wounded, whereas 78 of 108 (73%) treated with the 2.4 mm flat probe displayed successful endothelial injuries, as did 76 eyes of 108 (70%), treated with the 2.4 mm concave probe. The 3.4 mm concave cryoprobe, however, resulted in the most reproducible endothelial damage with 90 eyes of 108 (83%) being successfully wounded in a reproducible manner (Table 4.1).

To quantify the extent of endothelial cell damage, ImageJ/Fiji software was used to manually trace around each wound deemed to have been successfully created (i.e. n=258 of 426 technical replicates). The area of each wound was calculated, which, perhaps unsurprisingly, disclosed that larger probe tips led to more extensive endothelial damage (Table 4.1). All of the 426 corneas examined were subjected to multiple pachymetry measurements immediately prior to transcorneal freezing. This revealed that the average corneal thickness was 649 µm (±61.4 standard deviation (SD)), which is a fair representative value for corneal oedema in humans with endothelial dysfunction (Koizumi, Okumura and Kinoshita, 2012; Repp *et al.*, 2013). Moreover, when the corneal thickness of individual corneas was taken into account, a statistical Spearman's rank order correlation test identified that there was a weak relationship between central corneal thickness and endothelial damage when treated with the smallest and largest probes (1.8-mm (r=–0.208, n=102, p=0.408) and 3.4-mm (r=–0.258, n=108, p=0.007),

Table 4.1 Summary of transcorneal freezing for 3 seconds on porcine eyes.

Probe tip (mm)/type	No. eyes	No. eyes with successful freeze (%)	Mean/SD damaged area (mm^2)	Mean diameter (mm)	Mean/SD corneal thickness (µm)	Spearman's correlation coefficient (rs)
1.8/Flat	102	14 (13.73)	0.79/0.4	1.0	642/63.7	–0.208
2.4/Flat	108	78 (72.89)	2.12/1.0	1.6	650/71.2	–0.433
2.4/Concave	108	76 (70.37)	2.29/1.0	1.6	651/60.1	–0.466[|]
3.4/Concave	108	90 (83.33)	6.91/1.9	2.9	654/59.4	–0.258[#]

but a stronger relationship using 2.4-mm probe tips with concave and flat profiles ($r=-0.433$, $n=108$, $p<0.001$; $r=-0.466$, $n=108$, $p<0.001$, respectively) (Table 4.1).

To provide higher resolution information as to the status of the cells after freeze injury in the *in vitro* pig eye model, a series of SEM studies were conducted (Figure 4.5). This indicated that the corneal endothelial monolayer was severely disrupted in the central portion of the cornea beneath the site of a cryoprobe injury with a 2.4 mm-diameter concave-profile tip. Injured cells tended to become damaged and/or disassociated from each other, whereas non-injured cells adjacent to the area of damage exhibited a classic hexagonal endothelial cell morphology.

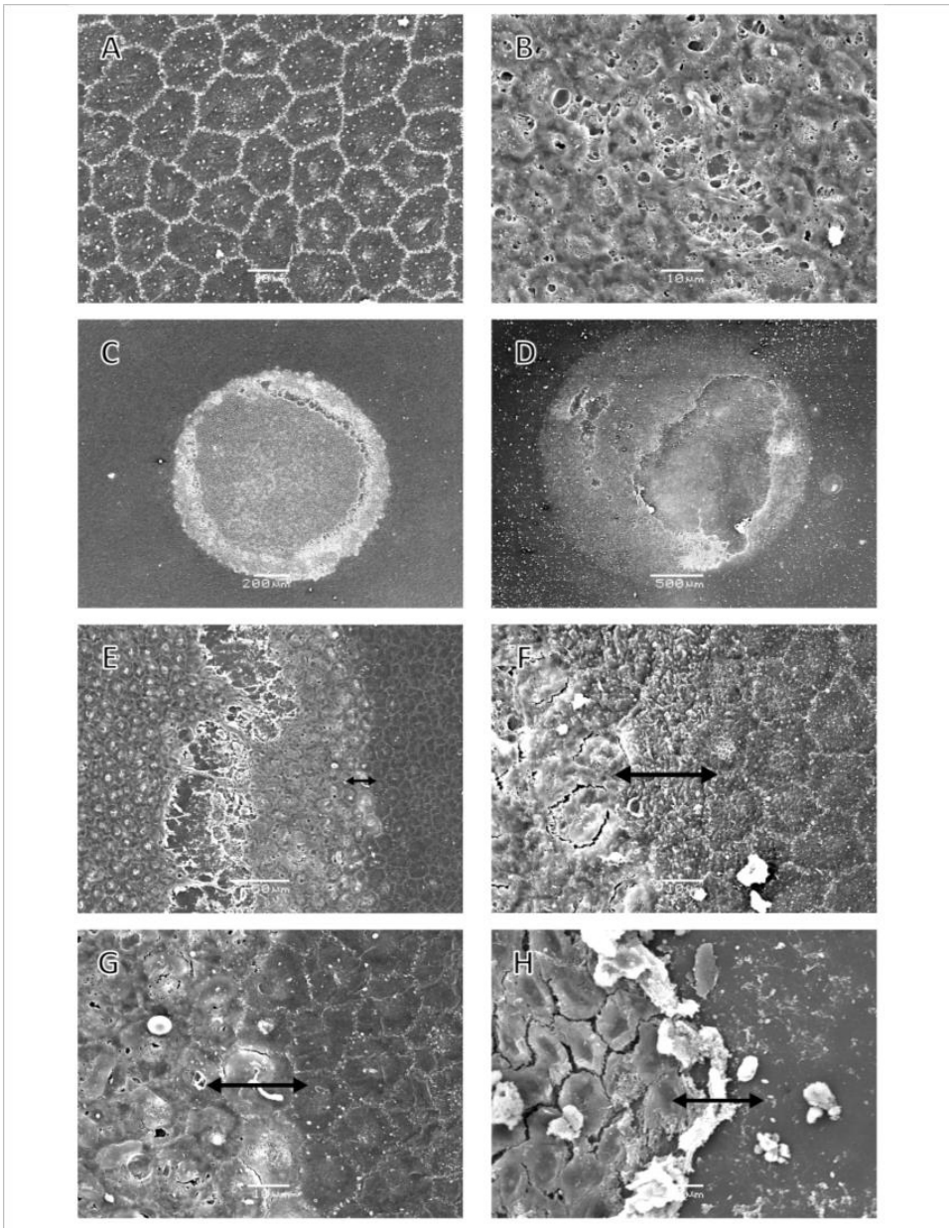

Figure 4.5 SEM of the endothelium of pig corneas after transcorneal freezing. (A) An untreated pig cornea with cell borders in white showing a characteristic hexagonal mosaic. The outline of the cell nucleus is evident as a slightly lighter area within each cell. Scale bar, 10 μm. (B) A representative image taken at the same magnification of the freeze damaged area after treatment with a 2.4 mm diameter/concave profile tip, illustrating severe damage to endothelial cells by freezing. Scale bar, 10 μm (C, D) Lower magnification images of endothelial freeze injury showing circular areas of endothelial cell damage including some endothelial debridement, exposing Descemet's membrane (C: 2.4 mm diameter/concave profile cryoprobe (scale bar, 200 μm); D: 3.4 mm diameter/concave profile cryoprobe (scale bar, 500 μm)) As expected the larger probe induces more widespread damage (see Table 4.1 also). (E-H) Transition zones (double headed arrows) between unfrozen endothelial cells and those that were destroyed by freeze injury are often sharp (E and G); same area, but different magnification. Scale bars, 10 μm, apart from G which is 50 μm.

Interestingly, there appear to be two transitional zones between healthy non-frozen cells and the more central damaged ones. The immediate transition at the inner edge of the morphologically normal cells was fairly abrupt, and in some cases, this was on a micron scale (Figure 4.5 E, F, G). More centrally there was evidence of cellular dissociation (Figure 5 E), and also the total removal of large areas of frozen endothelial cells, exposing a bare Descemet's membrane (Fig. 4.5 D, H).

Transcorneal freezing on porcine cornea in vitro to test 'drug' infiltration

The corneal endothelium is the layer intended to be treated via transcorneal freezing followed by ROCK inhibitor application to the corneal surface. Therefore, it was important that the ability of an agent to penetrate the cornea and reach the posterior endothelial region should be assessed. To do this a blue stain, methylene blue was used a visible proxy of a medicated solution. This was incorporated for slow release from a thin mucoadhesive polymeric film that was applied to the surface of the *in vitro* intact or cryoprobe-treated pig cornea overnight.

As illustrated in Figure 4.6, it is evident that methylene blue is released from the thin mucoadhesive film into the cornea. The whole thickness of the porcine cornea, including the posterior endothelial layer was visibly blue in colour in the central area, suggesting that an agent reaches the targeted posterior cornea following the transcorneal freezing. These studies demonstrate not only that the transcorneal freezing is a promising topical

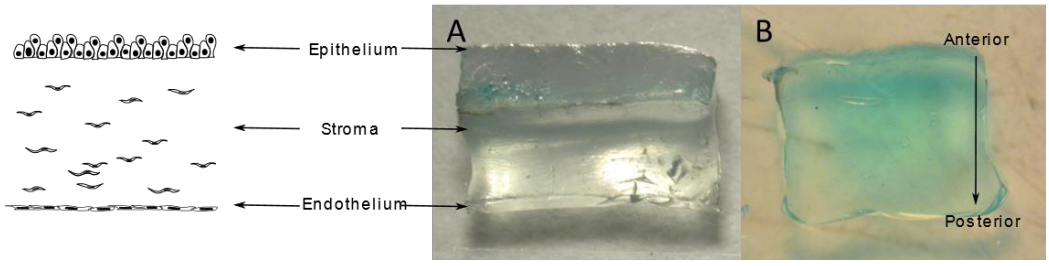

Figure 4.6 Cross sections of porcine corneas topically treated with thin mucoadhesive film incorporated with methylene blue solution for overnight: (A) intact porcine cornea prior to treatment, (B) treated following transcorneal freezing. It is evident with that the methylene blue penetrated through all corneal layers reaching the posterior layer, endothelium in cryoprobe-treated sample, unlike (A) intact control.

approach to remove the endothelial cells, but also helps a potential pharmaceutical agent to be delivered.

4.4 Discussion

A number of investigative surgical procedures that utilise the selective ROCK inhibitor, Y27632, to combat FECD and bullous keratopathy are under investigation, including cell-injection therapy (Koizumi et al., 2013, 2014; Okumura et al., 2013; Okumura, Okazaki, et al., 2015). Indeed, a recent fairly high-profile paper has reported promising results when donor-derived cultivated in a solution containing Y27632 ROCK inhibitor were injected into the anterior chambers of the eye of 11 patients with bullous keratopathy (Kinoshita *et al.*, 2018b). However, an alternative less-invasive approach for corneal endothelial dysfunction owing to FECD or bullous keratopathy, which doesn't require intraocular surgery or the need to obtain post-mortem donor eye tissue and inject cultivated allogenic corneal endothelial cells into the patient's eye, involves freezing the central cornea using a cold probe to damage corneal endothelial cells beneath the surface contact area. This is then followed by the short-term delivery, for one week, of Y27632 in eye drop formulation (Koizumi et al., 2013, 2014; Okumura et al., 2013). In these surgeries, conducted by colleagues with whom I worked, freezing was achieved by touching the corneal surface with a stainless-steel rod, which had been immersed in liquid nitrogen. An arbitrary freezing time of 15 sec was chosen for these experiments, along with a 2-mm diameter for the steel rod used. Encouragingly, the outcomes of these surgeries showed promise, but if the approach was to be adopted more widely by the ophthalmic community the corneal freeze would probably need to be achieved in a more reliable manner and with more knowledge of the nature and extent of the freeze damage. Thus, the experiments described here.

Historically, and up to the present day, corneal freezing has been carried out by a variety of methods, most of which use it to induce an experimental injury for research into corneal endothelial wound healing and regeneration (Maumenee and Kornblueth, 1948; Faure, Kim and Graf, 1971; Van Horn and Hyndiuk, 1975; Van Horn *et al.*, 1977). Freezing studies tend either to

employ a brass rod or dowel, which had been immersed in liquid nitrogen (Buco *et al.*, 1973; Van Horn *et al.*, 1977; Minkowski *et al.*, 1984; Mimura, Yamagami, Yokoo, Araie, *et al.*, 2005; Mimura, Yokoo, *et al.*, 2005) or similarly cooled steel ones (Ichijima *et al.*, 1993; Fullwood *et al.*, 1996; Petroll *et al.*, 1997) Retinal cryoprobes have also been used in investigational studies of transcorneal freezing (Tuft, Williams and Coster, 1986)(Olsen and Davanger, 1984).

In this chapter, the design and manufacture of a corneal cryoprobe that uses circulating nitrous oxide as a cryogen and the type of freeze damage it induces are reported. Typically, the tips of cryoprobes that use high-pressure gas as a cryogen are made of stainless-steel owing to the need to contain high-pressure gas safely. In the new design, however, the use of stainless steel would have resulted in a freeze that started in the centre of the tip and thereafter spread, albeit quickly, to its outer circumference at a speed which relies on the thermal conductivity of the metal. To achieve a more uniform cooling across the probe tip, a cryoprobe tip was manufactured out of silver, which has a higher thermal conductivity than that of steel. The benefit of this design feature is that the diameter of the freeze in the cornea is based on the expansion and internal recycling of nitrous oxide inside the cryoprobe tip. At the point of its transition from liquid to gas inside the cryoprobe tip, nitrous oxide exists at a temperature of - 88.5ºC, and this transition, which occurs inside the probe tip, of course, rapidly cools it. Owing to thermal conductivity within the whole probe and thermal loss at ambient room temperature, an equilibrium is reached, which in this novel design means that the temperature at the outer surface of the probe tip reaches - 50ºC.

Cryobiology is an area of study that investigates the response of biological cells and tissue to low temperature. Here, the focus is in how low temperature can destroy diseased cells in the human corneal endothelium in FECD or bullous keratopathy to allow the recovery of an intact function corneal endothelium by healthy peripheral endothelial cells away from the diseased area, perhaps encouraged to recover the endothelium via the action of the Y27643 ROCK inhibitor. Armitage (2009) describes corneal freezing from the opposite perspective, however, showing how careful freezing using time-

mediated freeze-thaw protocols accompanied by the use of cryoprotectants can lead to cell survival (Armitage 2009). For example, with rapid freezing techniques, such as high-pressure freezing, the structure of cells is preserved, and non-crystalline, amorphous ice is produced instead of crystals preventing cell membranes from damage. Cells and tissue can also be protected by being immersed in cryoprotectants and cooled and thawed at controlled rates. Indeed, Armitage and associates, experimenting on excised rabbit corneas, have shown how ice-free cryopreservation of the corneas by vitrification to temperatures as low as -110°C can be achieved in the presence of a cryoprotectant and with cooling and rewarming rates of 7°C/min and 12°C/min, respectively, in which some corneal endothelial cell function was retained (Armitage, Hall and Routledge, 2002). These sophisticated freeze-thaw protocols, however, are the flip side of the coin of our approach, which is a purposely seeks to damage by freeze-injury the diseased corneal endothelial cells of the central cornea in FECD. The concept is to remove them from the inner surface of the cornea, with cell fragments floating away into the aqueous humour and to be later removed from the eye via the regular ocular outflow pathway. An exposed Descemet's membrane will then remain (as seen in Figure 4.5) on which peripheral, non-diseased corneal cells can migrate prompted by the presence of Y27632 ROCK inhibitor to recover corneal endothelial function. The data presented in this chapter clearly show that a 3.4 mm-diameter cryoprobe tip with a concave profile that approximates the radius of curvature of the corneal surface results in the optimal amount of reproducible freeze damage to the corneal endothelium. It is also, evident that the corneal epithelium need not be chemically or mechanically removed before the transcorneal freezing procedure and that the desired effect can be achieved with a brief, 3 sec, freeze, with prolonged freezing times not required.

Experiments described here also found that if the foot pedal was depressed to initiate the cooling of the probe tip before it was brought into contact with the corneal surface, then no appreciable endothelial freeze damage was seen, even if the cryoprobe was kept in contact with the cornea for periods of up to 15 sec. It is not immediately clear why this is the case, but perhaps frosting of the probe tip, when it is cooled in air, is the reason, reducing the

efficiency of cooling rate on corneal contact. This possible lack of frosting, when the tip is cooled after application, also might help facilitate the easy release of the probe tip from the corneal surface after the foot-switch is released, which happens within a second or two of the cryogenic circulation being suspended.

According to the Spearman's correlation test results, the area of damage caused by transcorneal freezing was inversely dependent statistically on the increasing thickness of the cornea. It was expected that there would be a negative correlation between corneal thickness and endothelial wound area as the stromal layer likely has some conductive properties, which would explain the gradual reduction of cooling effect on the endothelium. Thus, the thicker the cornea, the less damage, it warms the cryogen, thus having less cryo-damaging effect on the endothelium. Therefore, application of the largest probe with 3.4 mm diameter seems likely to be more effective in removing diseased endothelial cells in FECD patients with the swollen corneas.

As the endothelium is the target for a potential pharmaceutical strategy in endothelial dysfunction, it is essential that an agent applied via the corneal surface is delivered into the posterior cornea. Incubation with methylene blue in the mucoadhesive thin film evidently demonstrated that a potential agent for endothelial repair can reach the posterior cornea following transcorneal freezing. This is most likely due to loosening of intercellular spaces and structures located anteriorly to the endothelium, as a result of the transcorneal freezing. Therefore, this study proposes that destroying the dysfunctional endothelial cells is as important as to provide the route for targeted drug delivery, proposing a promising approach to treat FECD.

The data presented here show that endothelial cells can be functionally damaged and/or removed by the application to the corneal surface of a cryogenic cold probe and that this can be done in a targeted and reproducible manner with cell damage restricted to the area below the surface contact. Use of the 3.4-mm-diameter cryoprobe with a concave profile was discovered to be the optimal design of those tested. It thus has the potential

to rapidly and reliably induce damage to the human corneal endothelium via transcorneal freezing. The approach using a patented new device has the potential to be used prior to the application of ROCK inhibitors to the eye in the form of eye drops (Koizumi *et al.*, 2013, 2014; Okumura *et al.*, 2013), or as slow-release chemicals from thin films (Chan, Akhbanbetova, A. J. Quantock, et al., 2016) to aid the recovery of corneal endothelial function.

Chapter 5: Transcorneal Freezing for Corneal Endothelial Cell Removal: *In vivo* Rabbit Eye Studies

5.1 Introduction

The previous chapter described the rationale for the desire to destroy diseased corneal endothelial cells as part of a minimally invasive treatment for vision loss owing to corneal dysfunction in conditions such as FECD and bullous keratopathy. The *in vitro* studies using pig eyes, which had corneas of a similar thickness to pathologically swollen FECD corneas, were instrumental in establishing preferred treatment modalities and identified the 3.4 mm-diameter cryoprobe tip with a concave surface as the optimal one to achieve the best endothelial cell damage. This work also showed that prior removal of the corneal epithelium had no beneficial effect on the outcome of the procedure, that the cryoprobe tip should only be cooled after brought into contact with the corneal surface and that prolonged freezing times beyond 3 sec were of no advantage. Of course, *in vitro* experiments such as these can tell us nothing about the biological response of the living eye to transcorneal freezing, thus in this chapter, a small number of rabbits were used to ascertain some healing characteristics of eyes post-transcorneal freeze.

Rabbits are fairly widely used in the field of corneal research, and whilst not a perfect proxy for understanding human corneal biology, they represent a highly valuable model to augment data acquired from studies on mice, rats, and chicks and less commonly tree-shrews, mini-pigs and primates due to similar corneal structure. Due to increased regenerative ability of rabbit corneas, wound healing, in particular, is a field that often utilises rabbits to study the cornea's response to interventions such as corneal refractive surgery (Kivanany *et al.*, 2018), ultraviolet A (UVA)-induced corneal crosslinking (Bradford *et al.*, 2018), implantation of tissue-engineered constructs (Cui *et al.*, 2018; Jia *et al.*, 2018) and even the use of human-derived stem cells as potential therapeutic materials for the corneal epithelium and endothelium (Hayashi *et al.*, 2016; Yamashita *et al.*, 2018). Thus, rabbits were utilised for the experiments described in this chapter, the main aim of which was to assess the healing response to transcorneal freezing via a series of clinical and morphological examinations of the cornea with a focus on the structural integrity of the corneal epithelial basement membrane, corneal stroma and central and peripheral regions of the corneal endothelium. These *in vivo* investigations were conducted in the laboratories of Professor Noriko Koizumi and Dr Naoki Okumura in the Department of Biomedical Engineering, Doshisha University, Kyoto, Japan, where the author spent time as part of this doctoral research. The 3.4-mm diameter concave cryoprobe tip was found to be most suitable to achieve reliable endothelial destruction in the *in vitro* pig studies described in Chapter 4. However, owing to the fact that the rabbit cornea is thinner than that of the pig, at <400 μm thick compared to >600 μm in the pig, the smaller, 2.4 mm diameter, concave tip was used in the *in vivo* rabbit experiments described here.

5.2 Materials and Methods

5.2.1 In vivo transcorneal freezing

To investigate the corneal wound healing response to transcorneal freeze, experiments on a small number of rabbit corneas were conducted in Doshisha University, Japan, using the second prototype of the newly-designed cryoprobe that was used for porcine *ex vivo* experiments, adjusted

for Japanese power differences. At all stages, the animals were treated in accordance with the Association for Research in Vision and Ophthalmology (ARVO) Statement for the use of Animals in Ophthalmic and Vision Research and the research was approved by the Doshisha University. The surgical procedure mimicked that used for the *in vitro* experiments on pig corneas (i.e. no epithelial scrape, a 3-sec freeze, and freeze initiation after contact). For these investigations, a 2.4 mm diameter concave profile cryoprobe tip was used rather than the 3.4 mm concave one owing to the relative thinness (approximately 350–400 μm) of rabbit cornea, compared to that of the pig (approximately 660 μm). The transcorneal freezing treatments were conducted by Mr Shinichiro Nakano, who had spent time in Cardiff University observing and assisting with the i*n vitro* porcine transcorneal work, and who was thus highly familiar with the operation of the cryoprobe. It was performed on one eye of each rabbit (each was under general anaesthesia). The contralateral eyes of all three rabbits represented untreated controls, which is in line with best practice as bilateral experimental corneal surgeries are not permitted in Japan based on animal welfare grounds. The treatments were overseen by an experienced corneal surgeon, Dr Naoki Okumura, Associate Professor of Biomedical Engineering in Doshisha University.

Following transcorneal freezing, at the 24-hr, 10-day, and 30-day time-points, the anterior segment of each rabbit eye was assessed with a slit-lamp microscope, which showed that the procedure had not resulted in any severe general adverse effects. Corneal thicknesses were also determined at these times using an ultrasound pachymeter (SP-2000, Tomey), and the mean of eight measured values was calculated. Two rabbits were euthanised (one at 24 hrs, the other 30 days) after transcorneal freezing by intravenous injection of 64.8 mg/kg pentobarbital sodium solution (Somnopenthyl, Kyoritsu Yakuhin Corporation). Corneas were excised from treated and untreated eyes and prepared for transmission electron microscopy as described below.

5.2.2 Transmission Electron Microscopy (TEM)

Rabbits were euthanised 24 hrs and 30 days following *in vivo* transcorneal freezing. After excision at the limbus, the corneas were fixed in 2.5% glutaraldehyde and 2% paraformaldehyde in 0.1 M Sorensen buffer (pH

7.2—7.4) overnight at 4ºC. Samples in a fresh buffer solution were then sent to Cardiff to be further processed for TEM as described previously (Chapter 3.2.2).

5.3 Results

5.3.1 Transcorneal freezing on rabbit eyes in vivo

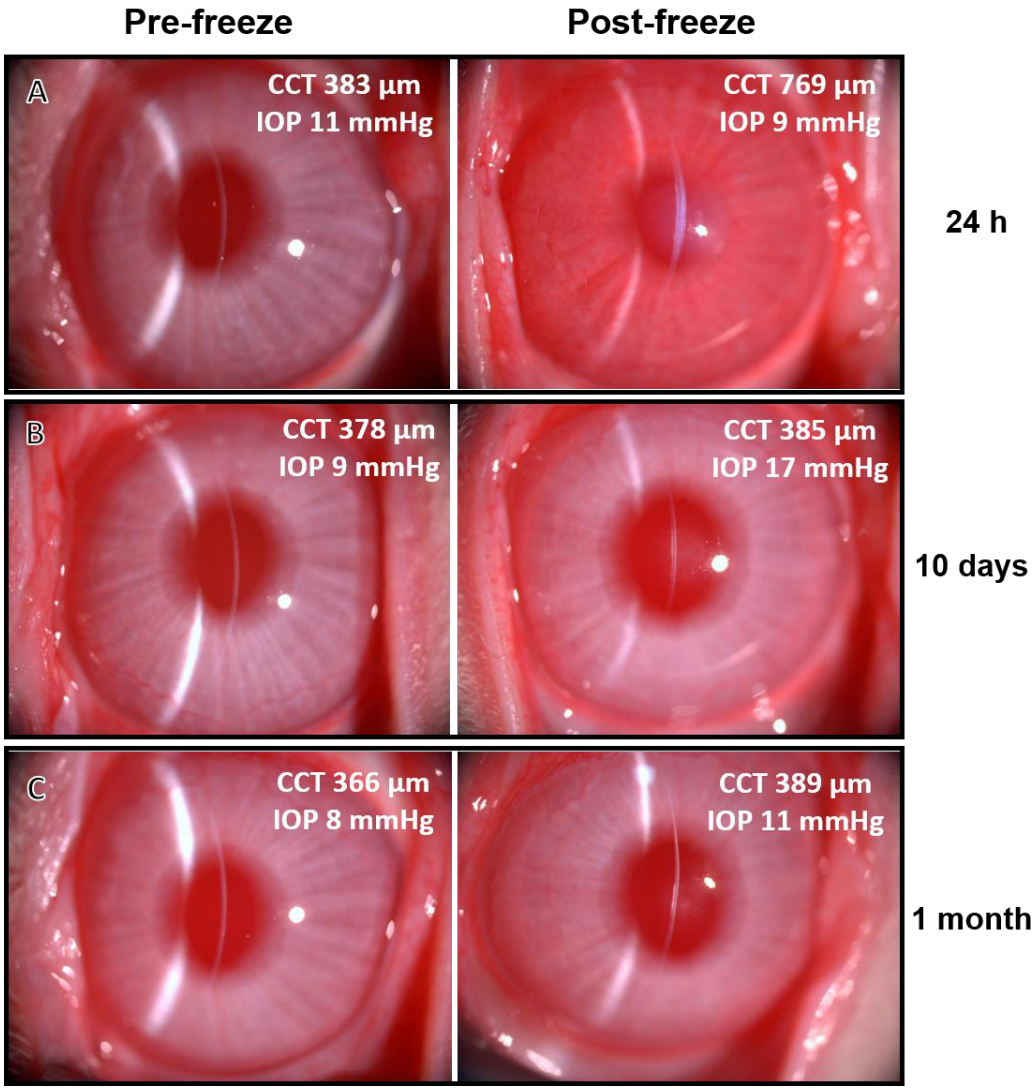

Figure 5.1 Slit lamp microscopy images showing effects of 3 sec freeze on rabbit cornea *in vivo* using 2.4 mm diameter/concave profile cryoprobe tip.
(A) 24 h after freeze, central corneal thickness (CCT) is increased considerably (769 µm) compared to before freeze (383 µm) and the cornea is hazy, indicative of corneal endothelial damage, as well as epithelial and stromal cell damage. (B) 10 days after a freeze injury (in a different animal) CCT was at normal levels. (C) This was the case also, 1 month after treatment. (B, C) Some corneal haziness at the level of the posterior stroma or Descemet's membrane is evident at 10 days and 1 month.

Transcorneal freezing using 2.4 mm diameter concave cryoprobe revealed that one day after a 3-sec surface freeze the rabbit cornea had become significantly oedematous, with its thickness approximately twice the normal value (Figure 5.1 A). The central corneal thickness returned to normal values by day 10, and this was maintained up to one-month post-freeze (Figure 5.1 C). Transcorneal freezing did not induce any general health adverse effects in rabbits. Slit-lamp images of three cryo-treated rabbit eyes showed some evidence of corneal haze at the level of the posterior stroma or Descemet's membrane at 10 days and 1 month (Figure 5.1 B and C).

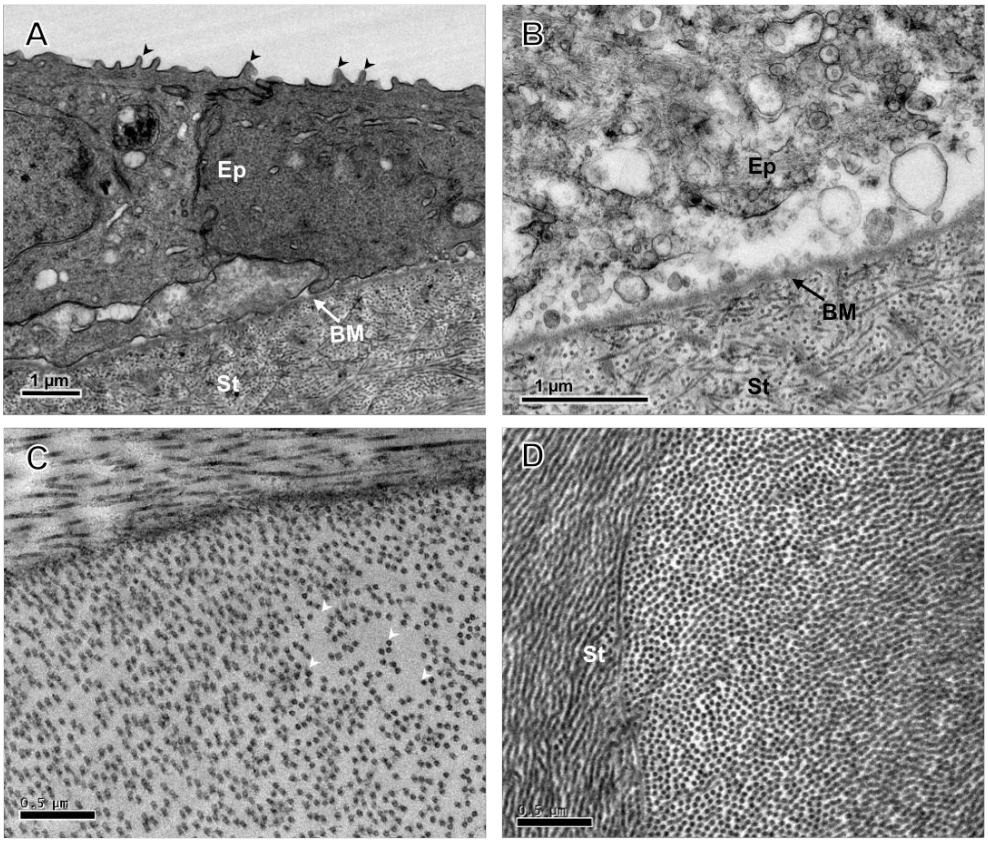

Figure 5.2 TEM of the corneal epithelium (Ep), epithelial basement membrane (BM), and stroma (St) following a 3 sec transcorneal freeze injury using 2.4 mm diameter/concave profile cryoprobe on rabbit cornea *in vivo*.
(A) The wound periphery surface at 24 hrs is epithelialized. Arrowheads indicate microvilli on the apical surface of epithelial cells. (B) Intact basement membrane is observed in the central freeze-injured area 24 hrs post-freeze. (C) After 24 hr freeze-injury, occasional focal regions of stromal matrix disruption were evident in the cornea, manifesting as tissue regions with increased spacing between collagen fibrils. (D) One month after the freezing, throughout the cornea, the spacing between collagen fibrils appeared normal. Scale bars, 1 µm (A, B) and 0.5 µm (C, D).

TEM examinations of one rabbit cornea 24 hrs after transcorneal freeze indicated that the corneal epithelium peripheral to the wound area was structurally normal, with typical epithelial stratification, cell-cell contact and surface microvilli (Figure 5.2 A). In all likelihood, these healthy-looking cells, or a sub-set of them, are migrating inwardly to repopulate the denuded area of the central corneal epithelium. As expected, the corneal epithelium was severely damaged in the central freeze-injured region of the cornea. Notably, though, the corneal epithelial basement membrane remained intact, which presumably is important to aid subsequent epithelial resurfacing of the wound area (Figure 5.2 B). In the deep stroma, increased collagen fibril spacing and disorder in the collagen fibril arrangement were apparent 24 hr post-freeze (Figure 5.2 C), but this had resolved by the 1-month timepoint by

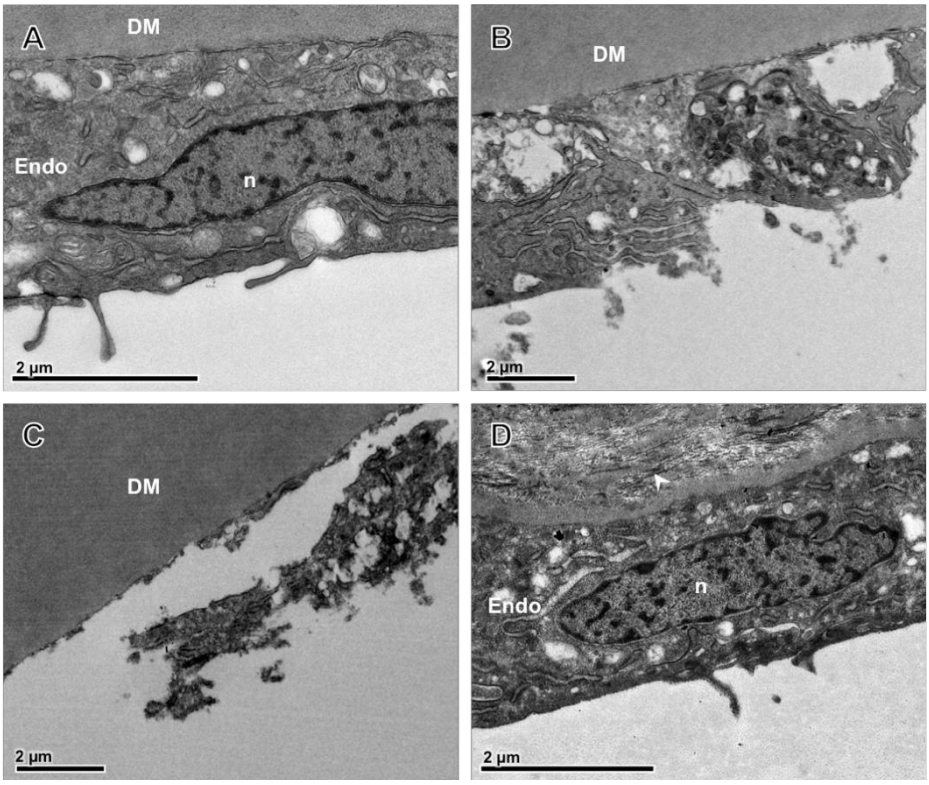

Figure 5.3 TEM of corneal endothelium following a 3 sec transcorneal freeze injury using 2.4 mm diameter/concave profile cryoprobe on rabbit cornea *in vivo*.
(A) An endothelial cell (Endo) at 24 h post- freeze in a region peripheral to the freeze-injured area appeared morphologically normal, with normal organelles and nucleus (n). It adhered to Descemet's membrane (DM). (B) Closer to the region below the cryoprobe surface application there were clear signs of cell damage. More centrally (C), the cell damage was more extreme revealing a bare Descemet's membrane. (D) 30 days after the transcorneal freezing was performed, the central region of the inner cornea contained fairly normal endothelial cells that were sometimes accompanied by extracellular matrix material (white arrowheads) in the area posterior to Descemet's membrane. Scale bar, 2 µm.

which time the stromal architecture appeared normal (Figure 5.2 D). These structural matrix changes likely contribute to the increased corneal thickness and opacity seen at 24 hrs after transcorneal freeze (Figure 5.1 A).

Similar to the epithelium, the corneal endothelium in the periphery of the cornea away from the region of the tissue under the surface wound zone remained unaffected 24 hrs after the transcorneal freeze of the central rabbit cornea (Figure 5.3 A). In this region, cells appeared morphologically normal with typical intracellular structures and were adhered to Descemet's membrane. The endothelium more centrally, however, began to exhibit clear signs of damage (Figure 5.3 B), including the destruction of the cell membrane. The central endothelium (Figure 5.3 C) was found to be fully debrided with a bare Descemet's membrane consistent with the SEM analysis of *in vitro* pig corneas (Figure 4.5). One month after the freeze the central corneal endothelium had re-attained its normal character, although occasionally fibrous tissue deposition between Descemet's membrane and the recovered endothelium was observed (Figure 5.3 D).

5.4 Discussion

In the experiments described in this chapter describing the effect of transcorneal freezing on the corneas of three rabbits show that the central corneal epithelium was totally destroyed by the application of the cryoprobe. Of course, this would be fully expected. However, it is important to note that the corneal epithelial basement membrane remains intact (Figure 5.2 B). This apparent absence of epithelial basement membrane damage, based on TEM observations, will almost certainly be of benefit to the epithelial resurfacing of the debrided epithelial area. It is well known that corneal epithelial cells migrate inwardly from the limbal region at the edge of the cornea to continuously replenish the central superficial cells that are lost into the tear film as part of the natural turnover of the corneal epithelium (Kinoshita *et al.*, 2001). After injury, the inward migration of corneal epithelial cells also occurs, and having an intact basement membrane as a substratum on which to recover an epithelium is postulated to be beneficial. Previous studies conducted as part of the long-term collaboration between eye

researchers in Cardiff and Doshisha universities indicated that corneal epithelial recovery following an experimental injury in which the corneal epithelial basement membrane is surgically removed takes around five days (Yamamoto *et al.*, 2012). Unfortunately, this study is unable to provide comparable information about the early stage dynamics of epithelial resurfacing in the transcorneal freeze rabbit eyes, but the timeline is likely to be significantly shorter than that reported in the study by Yamamoto et al. (2012) because the corneal wound in their experiments was more substantial than the freeze wound described here, being 7.5 mm in diameter and including the removal of not only the epithelial basement membrane but some anterior stromal cornea too. That research also showed that the application of Y27632 ROCK inhibitor in eye drop form to the wounded corneal surface delayed, but did not prevent corneal epithelial resurfacing by a few days. Any delay in corneal epithelial recovery following transcorneal freezing is likely to be less pronounced owing to the retained epithelial basement membrane and the less extensive lateral extent of the initial wound.

Signs of ultrastructural disruption in the extracellular matrix are apparent in the stroma after the *in vivo* rabbit freeze-injury, but these are transient, and the increased collagen fibril separation and disorganisation which are seen 24 hrs after the treatment subsequently decrease as corneal thickness reduces. These results match those observed in earlier studies, where rabbit corneal endothelial cell density and thickness were reached normal values as prior to injury by day 13 following similar endothelial damage caused by transcorneal freezing (Van Horn *et al.*, 1977; Staatz and Van Horn, 1980). The obvious conclusion is that the initial freeze damage to the corneal endothelium leads to corneal oedema (evident in the thickness measurements in Figure 5.1 A) and that the healing corneal endothelium recovers this. It should be noted that *in vivo* corneal endothelial wound healing studies in rabbits, such as those reported here, do not fully reflect the situation in the human cornea because of the manifestly different behaviour of the endothelial cells and their constrained replicative ability in humans (Van Horn *et al.*, 1977). Pre-clinical experiments in primates closer replicate the situation in humans, and have been conducted to examine new

corneal endothelial surgeries, but these are limited in number owing to ethical concerns (Okumura *et al.*, 2013)

My examinations of the rabbit cornea treated by transcorneal freezing and examined by TEM one month after treatment discloses the presence of fibrotic extracellular matrix in the region of Descemet's membrane (Figure 5.3D). The presence of such an abnormal extracellular matrix is not totally unexpected, and such material has been fairly widely reported in rabbit corneas following a corneal wound (Leung *et al.*, 2000) and in human corneas that had experienced prolonged wounding or undergone multiple surgeries (Jakobiec and Bhat, 2010). I postulate that the presence of abnormal fibrous tissue in the deep corneal stroma following transcorneal freezing likely contributes to the deep stromal haze seen in the cornea at this time. Additional light scatters owing to a refractive index mismatch between freeze-injured stromal keratocytes, and their immediate surrounding matrix might also contribute to the reduction in corneal transparency it should be noted though. A contribution to the loss of corneal transparency because of collagen fibril disorganisation, such as that illustrated in Figure 5.2 seems to be unlikely, as the fibril alterations seen in the early 24-hrs stages were not detected later at one month.

Chapter 6: The Effect of ROCK Inhibitor on Injured Corneal Endothelial Cells

6.1 Introduction

It has been identified that the Rho subfamily of serine-threonine kinases, known as Rho GTPases, regulate numerous signal transduction pathways common for numerous critical cell activities in the body. One of the best characterised downstream pathways of the Rho GTPases is Rho-associated coiled-coil kinase (ROCK) that is known to play an essential role in signal transduction pathways common for numerous vital activities in cell life cycle. The most well-described roles of these molecules include regulation of intracellular actin cytoskeleton dynamics responsible for the shape and size of a cell as well as cell polarity, motility, adhesion, migration, proliferation, and apoptosis (Hodge and Ridley, 2016).

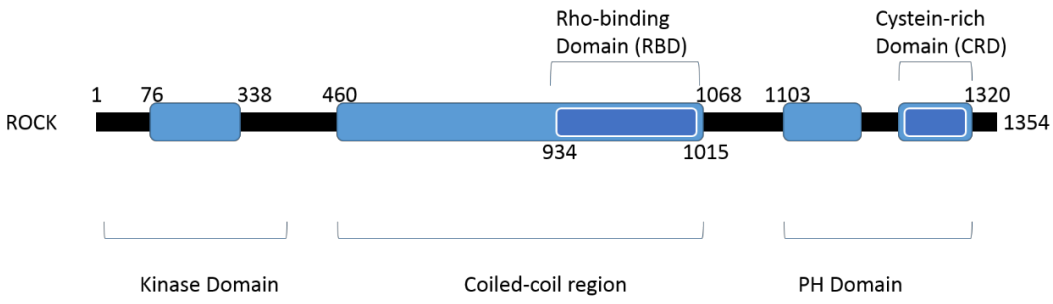

Figure 6.1 Schematic diagram of ROCK protein consisting of N-terminal kinase domain followed by a coiled-coil region including receptor binding domain (RBD), a C-terminal cysteine-rich domain (CRD), and a pleckstrin homology (PH) domain.

The ROCK gene is located in chromosome 18 and encodes 1354 amino acids. Having 158 kDa of molecular mass, a ROCK protein contains an amino-terminal kinase domain, followed by a mid-coiled-coil forming region including a Rho-binding domain (RBD) and a carboxy-terminal cysteine-rich domain (CRD) located in plekstrin homology (PH) domain (Sebbagh *et al.*, 2001). Several molecules regulate ROCK pathway via these multiple contact point domains. The activity of Rho-associated kinases is regulated by signals originating from various surface receptors such as G-protein-coupled, cytokine receptors, adhesion receptors. Molecular studies suggest that ROCK controls myosin light chain (MLC) phosphorylation which in turn switches on myosin ATPase to enhance production of energy and ability of cell contraction (Lai, Hsieh and Chang, 2003).

Recently, there is mounting interest in investigating the potential effects of employing the inhibition of the ROCK molecules to normalise cell activities, especially in diseased corneal endothelial cells (Okumura *et al.*, 2009, 2012; Li *et al.*, 2013; Pipparelli *et al.*, 2013; Peh *et al.*, 2015). Y27632 is a specific inhibitor of the ROCK signalling pathway that has been demonstrated to promote cell proliferation and adhesion of corneal endothelial cells, while restraining apoptotic process (Okumura *et al.*, 2011, 2013). However, the underlying mechanisms of action of their ROCK inhibitor remain unclear.

Based on the current understanding of the literature, it is expected that blocking the Rho-kinase signalling pathway using the selective ROCK inhibitor, Y27632, will accelerate endothelial cell migration for wound healing and suppress apoptosis following a damage. In order to test this, the current work attempts to elucidate the effect of the active treating agent, Y27632, on *in vitro* scrape and UV injured rabbit corneal endothelium by using the expression of related proteins that were analysed by confocal microscopy. This study would also bring more understanding on the regenerative mechanism of the Y27632 by investigating the ultrastructural changes in endothelial cells after treatment via inspection of the cells by transmission electron microscopy.

The study reported here was carried out as part of a collaboration between my group in Cardiff University and that of Professor Noriko Koizumi and Dr Naoki Okumura in Doshisha University, Kyoto, Japan, who have performed extensive research on the subject of blocking Rho-kinase signalling pathway for treating corneal endothelial dysfunctions.

6.2 Materials and Methods

6.2.1 Experimental models

To mimic pathologic changes that may affect the corneal endothelium as a result of cataract surgery, transcorneal freezing, or FECD, damage was induced by setting up two types of *in vitro* rabbit corneal endothelial injury models: 1) a mechanical scrape of the exposed corneal endothelial surface; 2) exposure of the endothelium to the ultraviolet light (UV) irradiation. In both situations, this was followed by treatment with Y27632 ROCK inhibitor at a concentration of 10 μM. To bring more understanding of the regenerative influence of the active agent, Y27632, on the damaged endothelium, the status of the endothelial cells and their ultrastructures were evaluated using immunohistochemistry and transmission electron microscopy. Vehicle-treated rabbit corneas were used as negative controls. In total ten in vitro corneas of New Zealand white rabbits were used in this study. The experiments were performed in duplicate. All animals that were used in this study were handled in accordance with the ARVO Statement for the Use of Animals in Ophthalmic and Vision Research.

6.2.2 Experimental methods

To obtain the corneas, rabbits were first euthanized by an intravenous injection of pentobarbital sodium solution (Somnopenthyl, Kyoritsu Yakuhin Corporation) into a marginal ear vein (64.8 mg/kg of body weight). Eyes were enucleated within 5 minutes after the euthanasia, and corneas excised and cultured in growth medium consisting of Dulbecco's modified Eagle’s medium (DMEM) with streptomycin (Nacalai Tesque) + 1% Penicillin-streptomycin.

Scrape wound injury on rabbit corneal endothelium

To have enough samples for the examinations and to reduce the number of rabbits used for the experiments, each cornea was bisected (endothelial side to epithelial side), then cut in quarters with a razor blade. A half of each cornea was prepared for the immunohistochemistry, and the other half was prepared for electron microscopy. To create an injury, a straight mechanical scrape wound was then created on the endothelial side of each corneal piece using a tip of 10 mL plastic pipette to bare the Descemet's membrane.

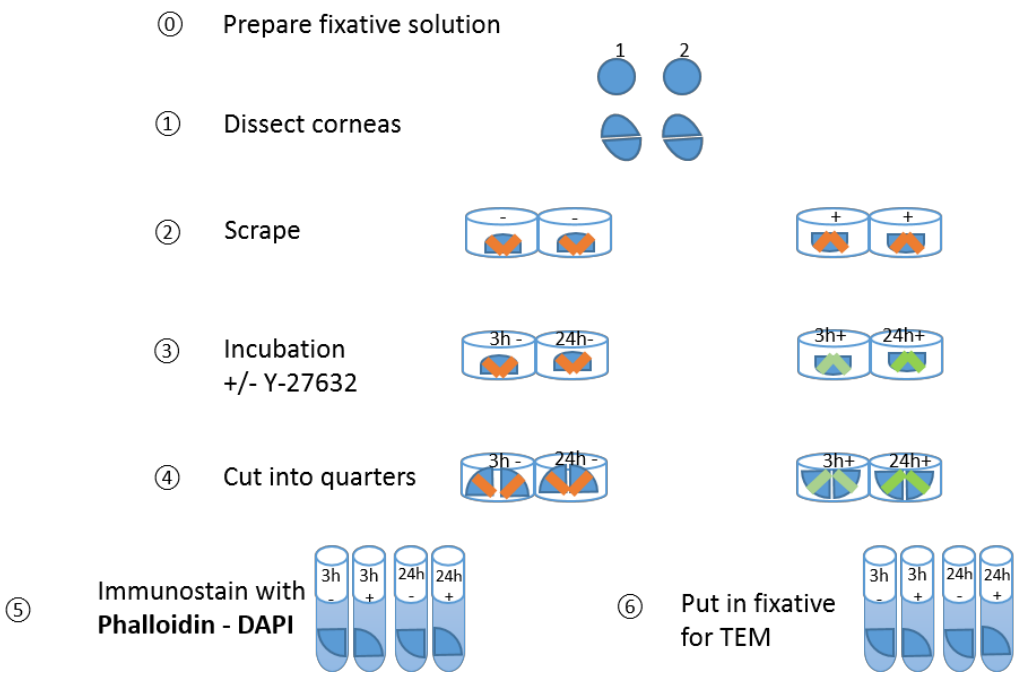

Figure 6.2 Schematic diagram of scrape injury experiment.

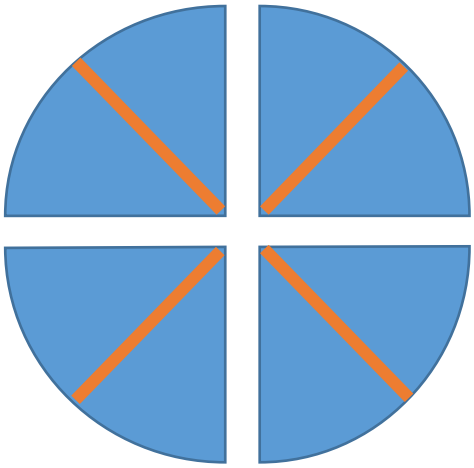

Figure 6.3 Schematic diagram of scrapes (orange) on each quarter of a rabbit corneal endothelium.

Following a mechanical scrape, corneas were transferred into a well plate containing culture medium of DMEM + 1% Penicillin/Streptomycin with or without Y27632 and incubated for 3 and 24 hours.

Immunostaining with Phalloidin – DAPI stain kit

To evaluate the cell response to the Y27632 treatment, the contraction of the scrape wound, and endothelial cell features were monitored using immunohistochemical analyses at various times of incubation.

To visualise the endothelial cell nucleus and cytoskeleton, scrape-injured corneas were stained using binding buffer (1% bovine serum albumin (BSA)): DAPI: Phalloidin 546 (Alexa Fluor, Invitrogen, USA) at ratio 1000:1:2.5 after the 3 and 24 hours of Y27632 treatment. The samples were first fixed in 4% paraformaldehyde in PBS for 10 minutes at room temperature. The specimens were then washed in PBS three times gently, not to further damage fragile endothelial cells. Specimens were then incubated in 0.5% Triton solution in PBS for 5 minutes after washing with PBS. This was followed by placing the corneas in a blocking solution of 1% BSA for 60 minutes at room temperature. Finally, after blocking step, the samples were placed in DAPI/Phalloidin in 1% BSA for 60 minutes, followed by embedding on a glass microscope slide ready to examine by confocal

microscopy. For the control, organ culture medium without the ROCK inhibitor was used.

Ultraviolet (UV) injury on rabbit corneal endothelium

UV light is suggested to be relatively safe in small portions, such as 60 J/cm2. In humans, 0.33 J/cm2 intensity is used during corneal cross-linking treatments, which is considered nontoxic for the corneal endothelium. However, when the exposure is increased over 70J/cm2, the survival of the endothelial cells decreases due to its destructive effect on cell DNA (Lichtinger *et al.*, 2011). To cause experimental damage to corneal endothelial cells via UV radiation, we chose the fluence of 100J/cm2. However, in an attempt to prevent complete endothelial cell death and increase chances of survival of some endothelial cells, corneas in this group were pre-treated in a culture medium comprising of DMEM with the Y27632 ROCK inhibitor (10 µm) for 2 hours at 37◦C. After the pre-treatment in the medium, corneas were gently washed by dipping them in a PBS solution. To induce the endothelial cell injury, irradiation of UV light of 100 J/cm^2 in UPV CrossLinker CX-2000 for 5 seconds was used.

Detection of apoptosis and necrosis in vitro using immunostaining with annexin V – propodium iodide (PI) stain kit.

To test the protective effect of the Y27632 ROCK inhibitor, endothelial cell death as a response to the UV irradiation was examined on in vitro rabbit cornea after 3, 6, and 24 hours of incubation, with or without the ROCK inhibitor, by immunohistochemical analysis. To evaluate the apoptotic and necrotic cell status, related antibody markers (annexin V and propidium iodide, respectively) were used (Medical and Biological Laboratories Co. LTD) at a ratio of 100:1:2.5. A stain solution with a binding buffer of 250 mL per well was prepared, and the specimens thereafter gently washed twice in

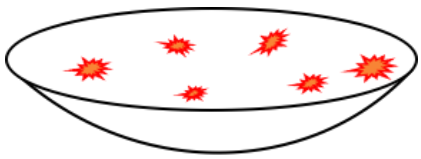

Figure 6.4 Schematic diagram of UV-induced damage on corneal endothelium (the endothelial side facing upwards).

PBS. The corneas were then fixed in 4% paraformaldehyde for 10 minutes. After additional washing with PBS corneas were incubated in 0.5% Triton, followed by blocking with 1% BSA for 60 minutes at room temperature.

6.2.3 Confocal fluorescence microscopy

Following treatment, experimental and control corneas were investigated by confocal fluorescence microscopy (Leica Microsystems Confocal Microscope) along with Leica Application Suite AF software. Before examining the samples, Beam Paths (Scans 1-5) were chosen according to the staining. Once the area of interest was found and the z-stack adjusted, digital images were acquired.

6.2.4 Transmission electron microscopy (TEM)

To examine the ultrastructural changes in corneal endothelial cells following both scrape and UV-induced injuries, and following treatment with Y27632 ROCK Inhibitor, images of the same samples were obtained by TEM. For this, Y-27632-treated and vehicle-only corneas were immersed in a fixative

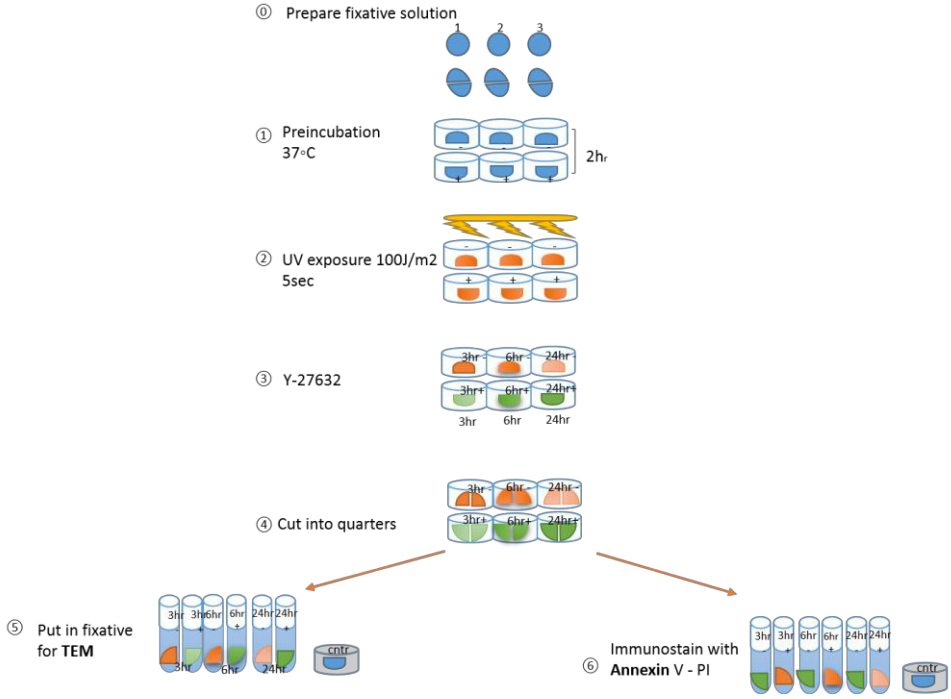

Figure 6.5 Schematic diagram of UV injury experiment.

solution of 2.5% glutaraldehyde and 2% paraformaldehyde in 0.1 M in Sorensen buffer for 2 hours at room temperature on a rotator. Following initial fixation, the specimens were rinsed with 0.1 M Sorensen buffer and then fixed with a fresh solution of 2.5% glutaraldehyde and 2% paraformaldehyde in 0.1 M in Sorensen buffer and stored in glass bottles in at 4 degrees C prior to dehydration, infiltration, and polymerisation with resin, sectioning, and staining steps described in detail in the Chapter 3.2.2.

6.3 Results

This section presents a comparison of Y27632-treated and vehicle-treated corneas following endothelial injury in vitro as examined by immunohistochemistry and electron microscopy imaging.

6.3.1 Confocal microscopy

Results below compare confocal micrographs of the wounded endothelial cells that were incubated with or without the presence of the Y27632 ROCK inhibitor.

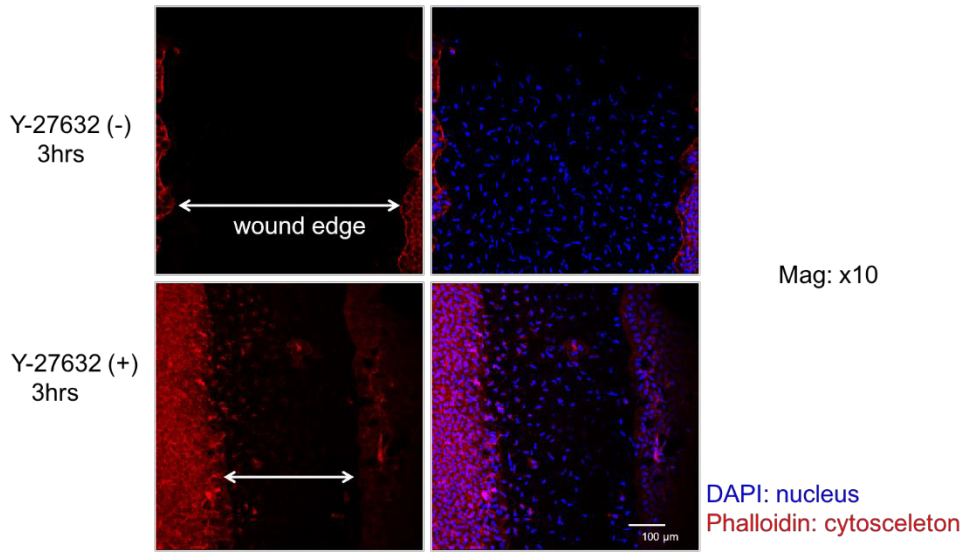

Figure 6.6 Immunohistochemical image of rabbit corneal endothelium observed via confocal microscopy.
Cell cytoskeleton (red fluorescence) and cell nuclei (blue fluorescence) in scraped wound areas of a corneal endothelium incubated for 3 hours with or without Y27632 are shown. The scrape wound area is visibly narrower in the Y27632-treated corneal endothelium (lower row panel) compared to the control (upper row panel). The width of scrape wound edges treated with Y27632 measured 295.5 µm, compared to 606.9 µm in the control cornea. Scale bar, 100 µm.

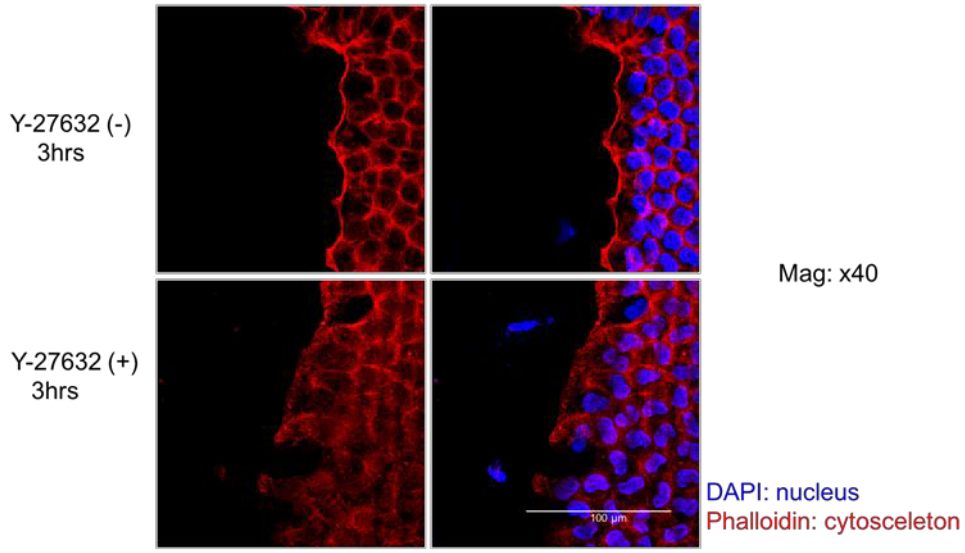

Figure 6.7 Higher magnification of immunohistochemical analysis via confocal microscopy revealing the cell cytoskeleton and nuclei in scraped wound areas in samples incubated with or without Y27632 for 3 hours.
Elongation of endothelial cells adjacent to the wound edge can be seen in the Y27632-treated corneal sample. The control sample (upper panel) seems to have tightly compacted endothelial cells and enlarged cells at the immediate edge of the wound. Scale bar, 100 µm.

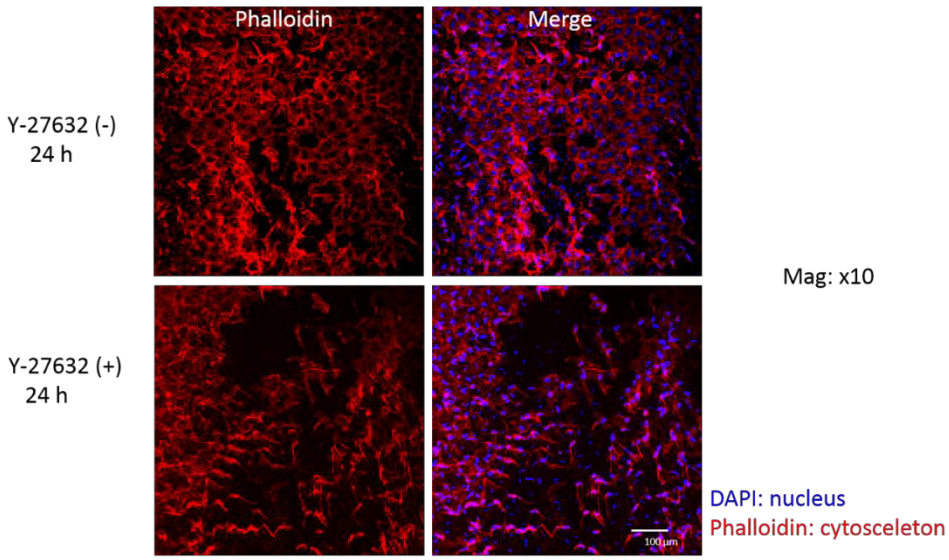

Figure 6.8 Low magnification confocal micrograph showing endothelial cells following a mechanical scrape incubated for 24 hours in the presence or absence of the ROCK inhibitor Y27632.
The lower panel shows that the endothelial cells assume a fibroblast-like irregular in shape when treated with Y27632. In the vehicle-treated sample (upper row), there seem to be less fibroblast-transformed cells and more hexagonal shaped cells characteristic of normal endothelial cells. Scale bar, 100 µm.

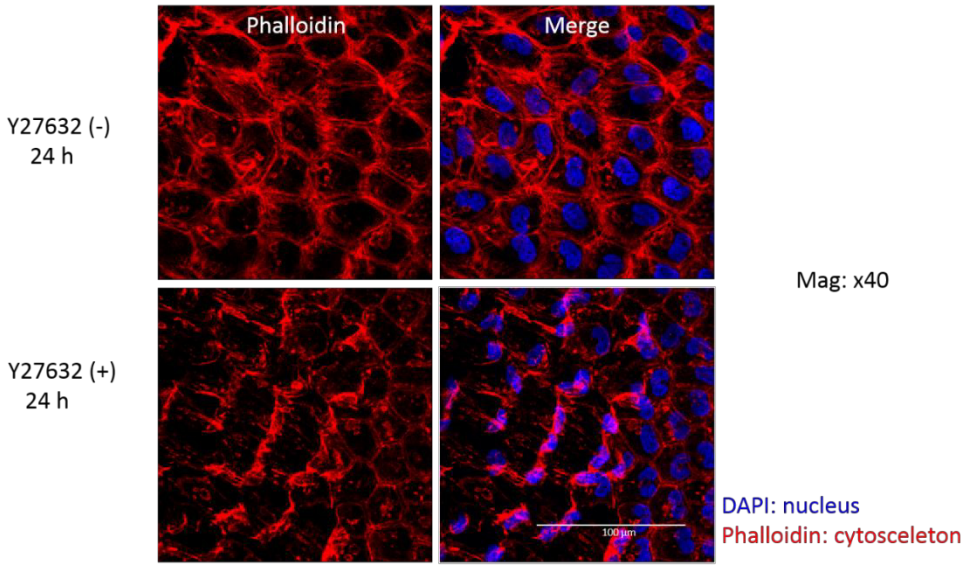

Figure 6.9 Higher magnification confocal micrograph showing outlines of endothelial cells following a mechanical scrape incubated for 24 hours of the treatment with (lower row) and without (upper row) ROCK inhibitor following a mechanical scrape injury.
The Y27632-treated cells appear irregular shape, while the cells of the control sample have a typical endothelial hexagonal mosaic pattern. Scale bar, 100 µm.

Summary for confocal microscopy results on scraped injured corneas

The results obtained from the immunohistochemistry analysis of scrape-injured corneas are presented in Figures 6.6–6.9. To assess the healing effect of ROCK inhibitor at covering the defect after a mechanical scrape, the gaps between two opposite wound edges were measured by ImageJ software (Figure 6.6). This showed that the wound had contracted to by about half in the presence of Y27632, (i.e. 295.5 µm compared to 606.9 µm in the control wound). Furthermore, in Figure 6.7, phalloidin staining shows that the cytoskeleton of the cells immediately adjacent to the wound edge appear to be altered from characteristic hexagonal shape to elongated shape in the presence of Y27632. In the control sample, the cells at the edge of the wound appear to be slightly enlarged in size. Closer inspection of this data also shows that endothelial cells retain their cell-cell contact in the vehicle-treated cornea and that more loose cells are seen in the ROCK inhibitor-treated cornea.

After 24 hour incubation, differences in wound areas were not obvious between the Y27632 and vehicle-treated groups. However, differences in the

morphological pattern of the cell cytoskeleton were more apparent compared to those that were incubated for 3 hours (Figures 6.8, 6.9). Corneas that were incubated with the ROCK inhibitor seemed to have a higher prevalence of contact inhibited fibroblastic-like cell phenotype, whereas in the control group the endothelial cells tended to retain the classic hexagonal outline.

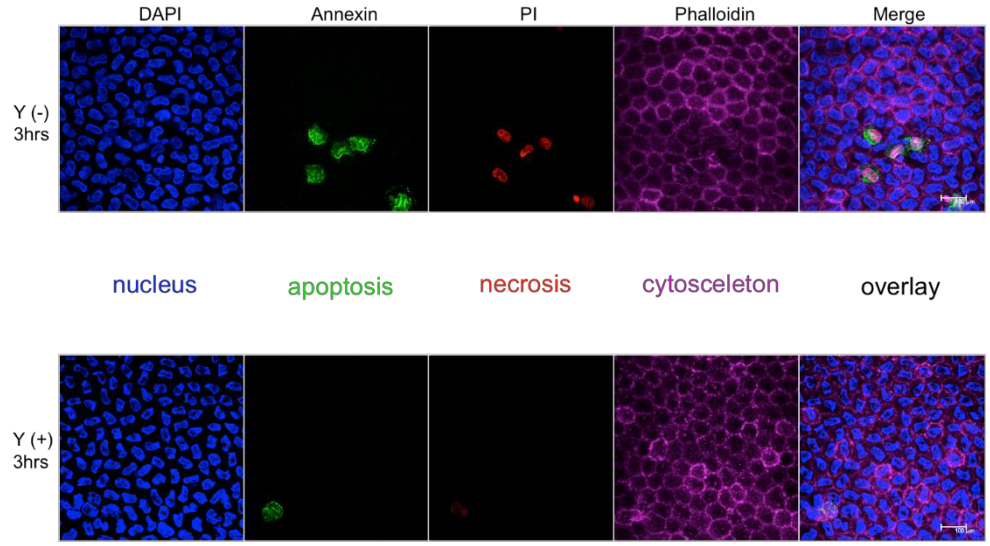

Figure 6.10 Immunohistochemical detection of apoptotic (green fluorescence) and necrotic (red fluorescence) endothelial cells after 3-hour incubation without [upper panel Y(-)] and with [lower panel Y(+)] Rho-kinase inhibitor, Y27632.
Actin cytoskeleton stained with purple phalloidin dye, demonstrated a hexagonal mosaic of the endothelial cells. It is evident that there were less apoptotic cells in the presence of Y27632 compared to the control of corneal endothelium after 3-hour incubation. Scale bar, 100 μm.

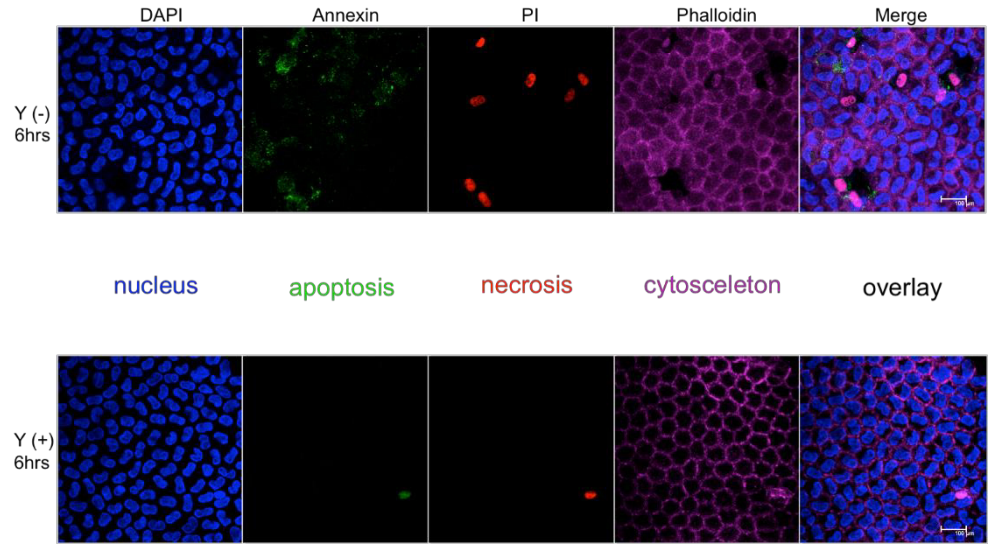

Figure 6.11 Further fluorescent staining of endothelial cells showing apoptotic and necrotic cells after 6-hour incubation with [Y(+)] or without [Y(-)] ROCK inhibitor. A decreased expression of apoptotic and necrotic markers was evident in Y27632-treated corneal endothelium. Scale bar, 100 μm.

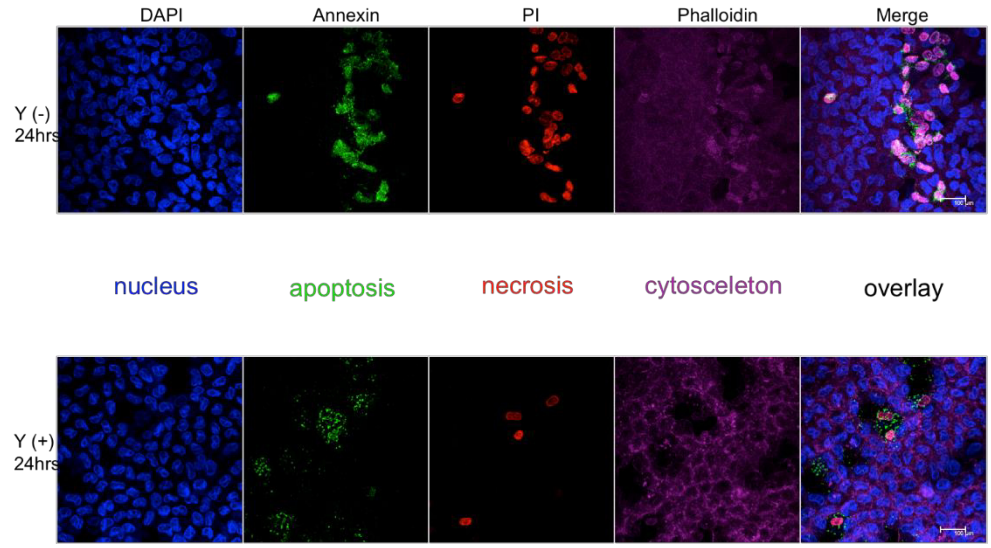

Figure 6.12 Immunoreactivity of apoptotic and necrotic endothelial cells after 24-hour incubation with or without ROCK inhibitor.
Similar to 3 and 6 hours post-treatment, more endothelial cells were damaged in the corneal samples incubated in the absence of the Y27632. Scale bar, 100 μm.

Immunohistochemical investigation of the corneal endothelial surface indicated that the incubation with ROCK inhibitor reduced cell death caused by UV irradiation in rabbit corneal endothelium. As shown in Figure 6.10, the Y27632-treated endothelial cells had a higher survival rate even after the first 3-hour treatment, suggesting that cell death is delayed in the presence of Y27632. As seen in the merged panel, the same cells were stained with both PI and annexin V. Being a membrane-impermeable dye, PI only enters the cell in membrane breakdown, meaning that the UV-induced apoptotic cells that were stained by annexin were in the late stage of the apoptosis and had irreversible damage to the cell membrane.

Further incubation for 6 hours led to more cell deaths in the control group, but not in the Y27632-treated group where the amount of cell death remained at the minimal level in the presence of the ROCK inhibitor. From the Figures 6.10-12 above, it can be seen that the proportions of cells stained for apoptosis and necrosis increased in vehicle-treated corneas in a time-dependent manner following UV irradiation, even in the ROCK inhibitor-treated cornea (Figure 6.12). The growing number of dead cells with time was expected due to a gradual deterioration of cells in the culture medium.

Analysis of corneas from ten animals showed that the UV light caused selective cell death of endothelial cells and, most importantly, that these apoptotic and necrotic cells were visibly reduced when the ROCK inhibitor was present in the culture medium throughout all incubation time periods of 3, 6, and 24 hours. These data suggest that Y27632 treatment prolongs cell survival by inhibiting cell death in rabbit corneal endothelium.

6.3.2 Transmission electron microscopy (TEM)

Results below compare electron micrographs of the wounded cells that were incubated with or without the presence of the Y27632 ROCK inhibitor. These TEM images refer to the same samples as in confocal micrographs above.

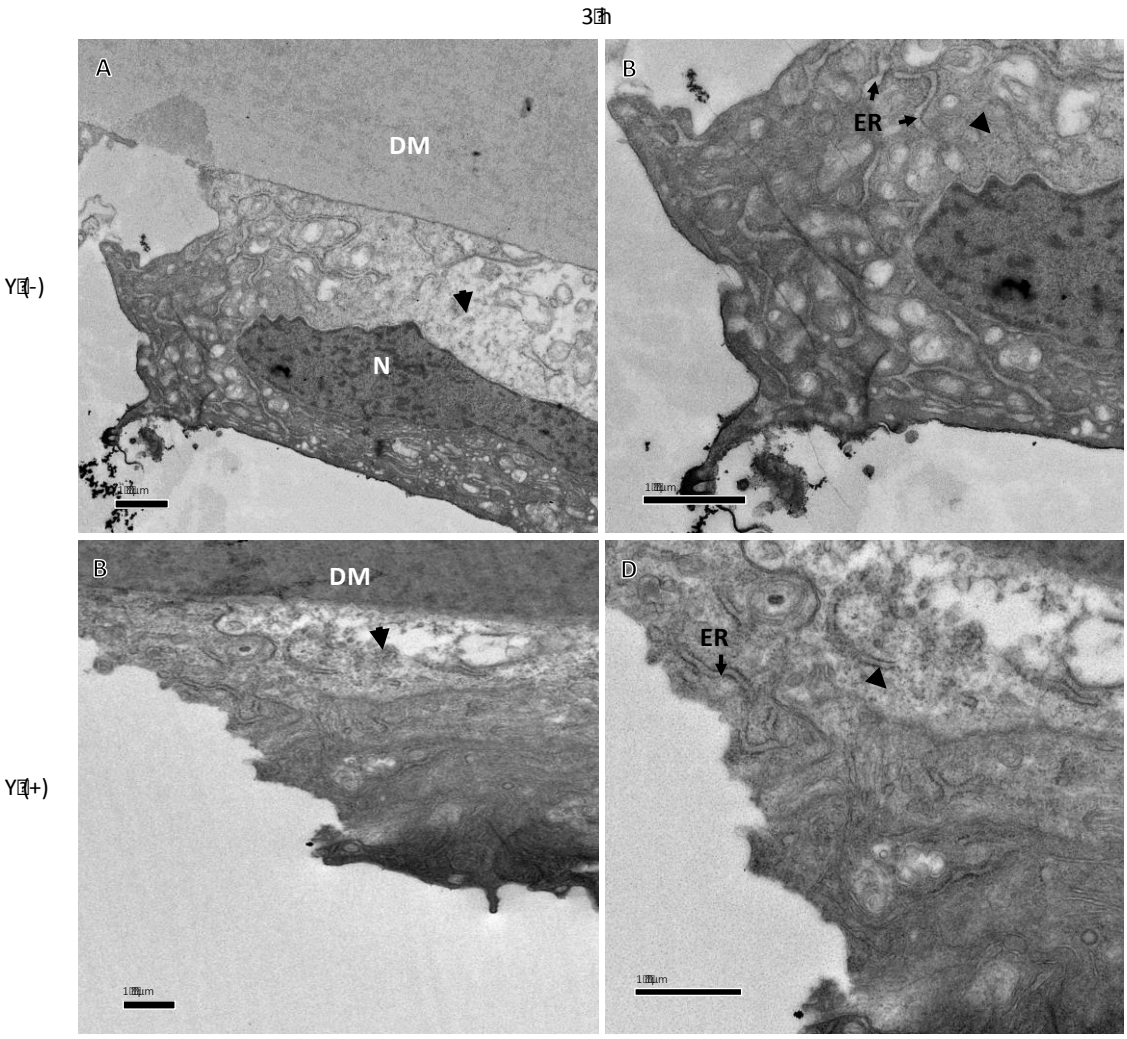

Figure 6.13 Transmission electron micrographs of scraped rabbit corneas after 3-hour incubation in culture medium without (A, B) or with (B, D) ROCK inhibitor at low and high magnifications showing what looks like the edges of the scrape wounds with endothelial cell with filopodia.
The part of the cytoplasm that attaches to Descemet's membrane (DM) has low contrast (arrowheads). The nuclei (N) appear normal. The low electron density areas have swollen endoplasmic reticulum in cells near the wound edge. Scale bar, 1 μm.

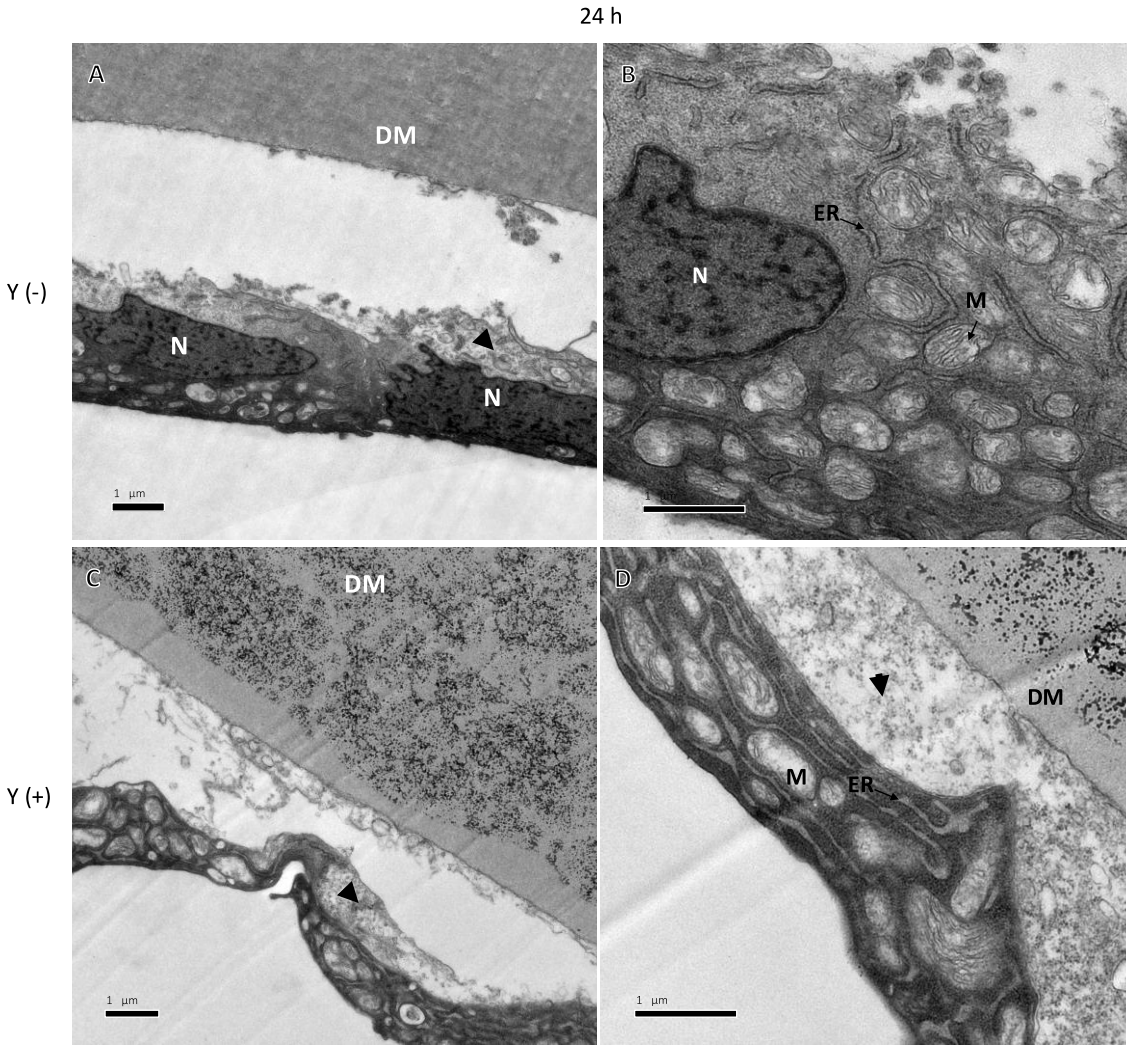

Figure 6.14 Low and high magnifications of endothelia that were induced by using a scrape wound after 24 hours in culture medium without (A, B) and with ROCK inhibitor treatment (C, D).
Panels A and B show cells that look like normal endothelial cells with normal nuclei (N) and cell structure, although detached from the Descemet's membrane (DM). C and D show corneal endothelial cells following 24-hour-treatment with ROCK inhibitor revealing an altered phenotype, with cells that appear thinner and have extended protrusion towards the adjacent cell (C). Also, the Y27632-treated endothelium (C, D) seems to have more than one cell layer. Arrows indicate to low electron dense cell layer (degenerating cell) between Descemet's membrane that is covered with another cell layer. Higher magnification transmission electron microscopy shows an elevated number of mitochondria in endothelia of both groups (B, D). Corneal endothelial cells treated with ROCK inhibitor show more elongated and enlarged mitochondria compared to the control. Scale bar, 1 µm.

Summary of TEM results for scraped injury

Transmission electron microscope results of scrape-injured rabbit corneal endothelium treated with or without ROCK inhibitor, Y27632, can be compared in Figures 6.13-14. Figure 6.13 shows what seems like a demarcated edge of the scrape wound in corneas that were treated for

3 hours. The endothelial cell with the filopodia appears to be edging toward the wound site in the control sample, although the apparent elongation of the endothelial cell is not visible in the Y27632-treated cornea. The images indicate that the region of the cell that attaches to Descemet's membrane has a low electron density, whereas the other side of the cells appears to have high electron density.

Further incubation for 24 hours with ROCK inhibitor showed cells that appear to be thinner and create more than one layer covering the degenerating cells (Figure 6.14). The figure also shows an endothelial cell that seems to have extension protruding towards a neighbouring cell where it is migrating on top of the deteriorating cell. Higher magnification micrographs of 24 hour-incubated corneas showed an increased number of enlarged mitochondria in both Y27632 and vehicle-treated cells, suggesting their elevated activity (Figure 12 B, D). No abnormal change in the nucleus or endoplasmic reticulum in either vehicle or Y27632-treated corneal endothelial cells was observed after 24 hours of incubation following scrape injury. As shown in Figure 6.14 D, there was a clear thinning of endothelial cells after ROCK inhibitor treatment. Thus, ROCK inhibitor treatment *in vitro* changes the ultrastructure of corneal endothelial cells, and the changes include cell thinning and elongation as well as abundant mitochondrial activity.

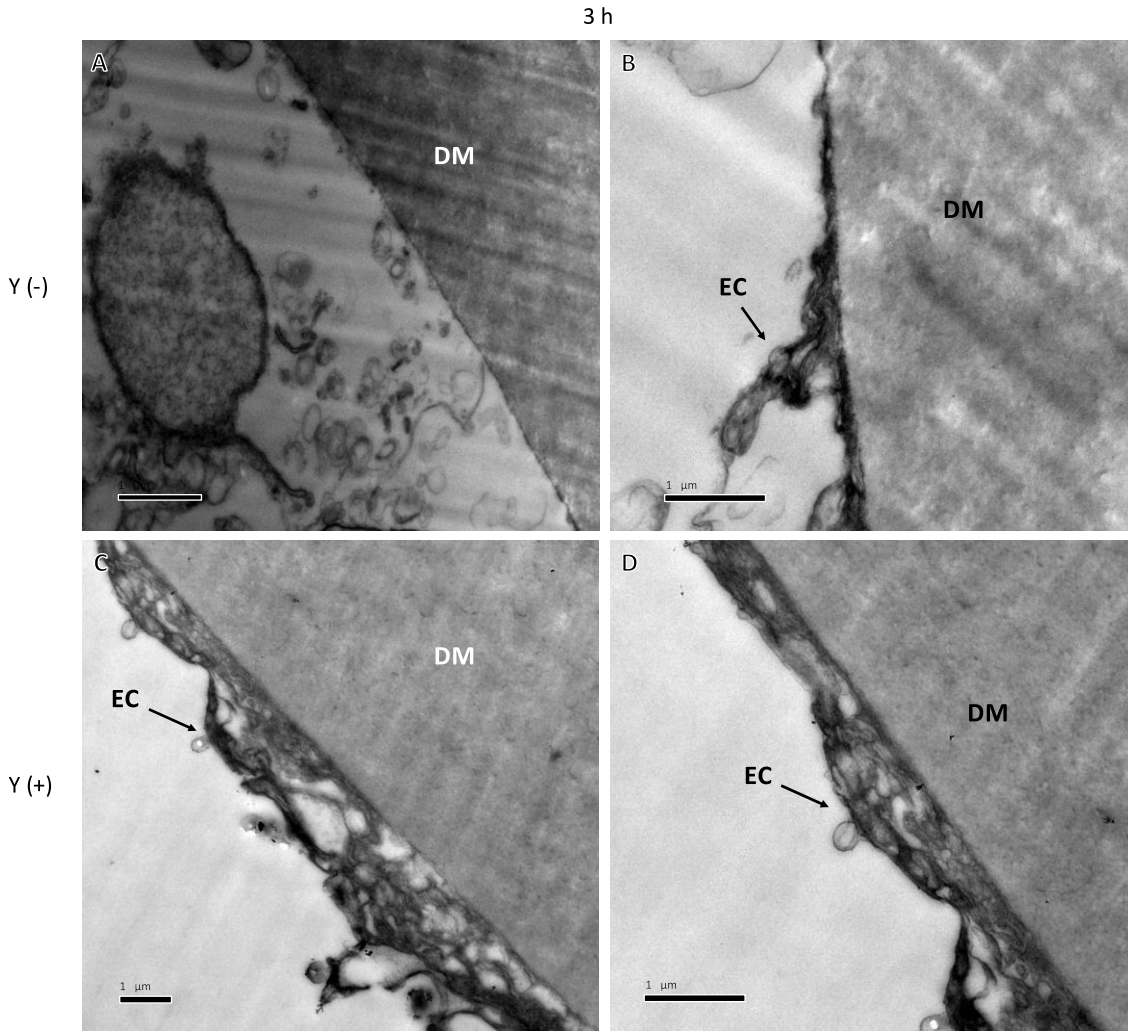

Figure 6.15 Transmission electron micrographs showing endothelial cells 3 hours after UV irradiation followed by vehicle-treatment (upper panel - A, B) and ROCK inhibitor-treatment (lower panel - C, D).
Panel A shows a cell-free area on the vehicle-treated cornea and detached cellular organelle remnants are visible floating underneath bare Descemet's membrane (DM) in the cornea treated without the ROCK inhibitor. Lower panel, which was treated with the ROCK inhibitor the endothelial cells appear thicker compared to control sample (upper panel). Panels C and D show that some endothelial cell structures are still attached to Descemet's membrane in Y27632-treated corneas, despite having altered morphology (blebs). Scale bar, 1 µm.

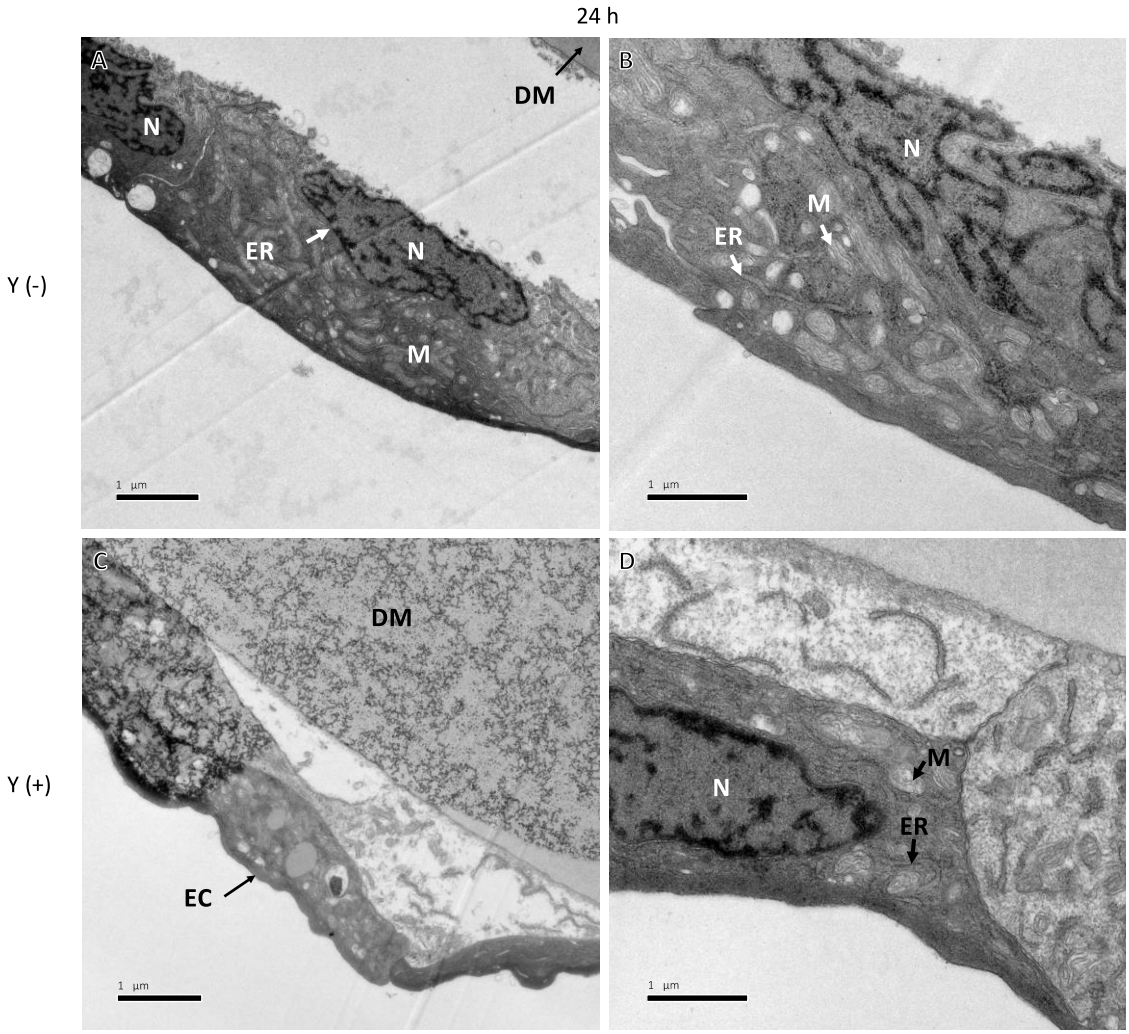

Figure 6.16 Transmission electron micrograph showing vehicle-treated (A, B) and Y27632-treated (C, D) rabbit corneal endothelial cells 24 hours following UV exposure.
In panels A and B the endothelial cells seem to have separated from Descemet's membrane (DM). The organelles of the vehicle-treated rabbit cornea (A, B) appeared normal. Higher magnification of rabbit corneal endothelial cells shows regularly sized mitochondria (M) and endoplasmic reticulum (ER). In ROCK inhibitor-treated sample (C and D), the endothelial cells seem to have two layers instead of one, with a low electron dense cell layer close to Descemet's membrane. In panel C, there is an artefact of staining covering Descemet's membrane. Scale bar, 1 µm.

Summary of results of the UV-injured cornea

Following UV-injury, pathologic changes in endothelial cell morphology are seen (e.g. Figure 6.15), and this is evident to varying degrees including in cells treated for 3 hours in the presence of ROCK inhibitor. Fluctuating cellular organelles are evident, suggesting cell damage. This is most likely a consequence of the destructive imprint of UV light leading to plasma membrane breakdown and leakage of components of the cell underneath

Descemet's membrane. In contrast, micrographs in Figure 6.15 C, D demonstrate that numerous endothelial cells survived the UV impact in the Y27632-treated cornea, despite some morphological alteration. Figure 6.15 B, D compares the 3 hour treated corneas at higher magnification and reveals that endothelial cells survived better in the presence of the ROCK inhibitor compared to the control group. Vehicle-treated posterior cornea (Figure 6.16 A, B) appears similar to a normal endothelial cell, apart from the fact that it is detached from Descemet's membrane, unlike the Y27632-treated cornea (Figure 6.16 C, D). What is interesting in the ROCK inhibitor-treated sample, is that the endothelial cell has an altered ultrastructure, appearing thinner and more elongated and covering a degenerating cell underneath.

6.4 Discussion

Previous studies demonstrated the enhanced migration of corneal endothelial cells in a culture to cover a linear defect (Okumura *et al.*, 2011, 2014). As was expected, the results of confocal microscopy in this study suggested that the wound healing rate through the migration of rabbit corneal endothelial cells was accelerated when subjected to ROCK inhibitor treatment following an injury compared to wound healing in control vehicle-treated corneas. Transmission electron micrographs also indicated that endothelial cells transformed their phenotype to more fibroblast-like cells. Fibroblast-like morphological changes and a proliferative effect of the ROCK inhibitor, Y27623, in corneal endothelial cells were also reported previously in corneal endothelial cell cultures by Li (2013) and Okumura (Okumura, Okazaki, *et al.*, 2015), suggesting that the Y27632 may inhibit cell-cell contact between endothelial cells and allow them to transform into thin, active, elongated cells, which likely have an increased cell motility to promote wound healing.

The role of the ROCK kinase as a regulator of cell cytoskeleton architecture through downstream molecules such as myosin light chain (MLC) activity is well recognised. MLC is phosphorylated by ROCK activity resulting in the contraction of a cell by actin, with a myosin interaction area sacrificing their neural-crest-like phenotype (Kimura *et al.*, 1996). Possibly, there are various

other effectors of ROCK kinase that are also involved in endothelial cell behaviour resulting in wound healing. For example, LIM kinase, which can also contribute to the actin cytoskeleton reorganisation and cell shape transformations through cofilin phosphorylation (Maekawa, 1999). These signalling pathways may explain the prevalence of a fibroblast-like cell phenotype exhibited by the endothelial cells treated with the Y27632. The epithelial-mesenchymal transition (EMT) may also reflect the increased motility of the cells (Savagner, 2001). One of the features of the EMT transformation is the loss of cell-cell contact due to disruption of intercellular junctions, which may explain the enhanced wound contraction encouraged by application of the ROCK inhibitor to a wounded endothelium, by perhaps triggering active endothelial cells to migrate to the wounded cell-free area. Similar cellular transformations in the endothelium were observed in ROCK inhibitor-treated corneas in rabbits, as well as in glaucoma patients that showed temporary guttae on clinical observation (Okumura, Okazaki, *et al.*, 2015). However, the abnormal cell transformation was transient, and a normal cell phenotype was regained once the administration of the Y27632 was discontinued. Perhaps, after discontinuing ROCK inhibitor administration, the endothelial cells slow down their motility and migration and reconnect to adjacent cells using typical proliferation mechanism through stretching.

Both in scraped and UV injured endothelial cells, the detachment of endothelial cells from Descemet's membrane was evident in the control samples. This could be an artefact of physical handling during cutting corneas or tissue preparation for microscopy. However, most likely, the attachment of the endothelial cells to the Descemet's membrane on Y27632-treated samples suggests that the cells are better adhered with the ROCK inhibitor. The increase in endothelial cell adhesion by ROCK inhibitor is also supported by previous studies (Okumura *et al.*, 2009, 2012; Pipparelli *et al.*, 2013).

The next question this study sought to address was the possible protective effect of Y27632 ROCK inhibitor against the UV radiation. Findings of TEM showed that despite the same pre-treatment, more endothelial cell death was seen in the vehicle-treated corneas compared to those treated in the

presence of Y27632. This occurred at all time-points. This suggests that the ROCK inhibitor slows down the apoptotic mechanism in endothelial cells induced by UV exposure. A possible explanation for this might be that the inhibition of the ROCK signalling pathway acts as a survival signal, defending cells from the activation of apoptosis. This effect could potentially occur through the activation of complex cellular signalling that involves caspase 3 induced apoptosis (Liu *et al.*, 2016). Lack of internal survival signals combined with an external damage-provoking agent like excess UV irradiation, leading to subcellular reaction such as cell shrinkage may also be involved in FECD endothelial cell death. One possible implication of this is that ROCK inhibitor applied as a preventative measure may help reduce endothelial degeneration, particularly in elderly patients with the predisposition for FECD who had extended exposure of their corneas to UV light during their lifetime.

Clearly, there are differences in cell stress induced by FECD and UV, such as the initiation of guttae in the central cornea during FECD, while in our experiment the cells were damaged regardless of which area of the corneal endothelium, central or peripheral, in which they existed. The nature of the pathology of FECD which starts centrally would allow the possibility of removing the diseased endothelial cells in the central corneal region by transcorneal freezing for subsequent application of the ROCK inhibitor treatment, as discussed earlier in this thesis. According to clinical studies, an injury itself (e.g. scraping, stripping) can initiate the proliferative reaction of the endothelial cells, where corneal transparency can be recovered following descemetorhexis procedures or subsequent to detached endothelial grafts (Zafirakis *et al.*, 2010; Shah, Randleman and Grossniklaus, 2012; Kymionis *et al.*, 2017). Nevertheless, it appears that in the presence of ROCK inhibitor, the recovery of a corneal endothelial wound is enhanced.

It is widely accepted that, unlike humans, rabbit corneal endothelial cells have the regenerative ability *in vivo* (Van Horn *et al.*, 1977). Although animal organ culture may be a better approximation to the human endothelial environment *in vivo* than cell culture systems, my findings may be somewhat limited by *in vitro* conditions, fairly small sample size, and the likelihood that

the effect of ROCK inhibitor on rabbit cells will differ from those of human cells *in vivo*. It has been shown, however, that human cultured endothelial cells have proliferative activity *in vitro* (Joyce and Harris, 2010; Peh *et al.*, 2015). Also, clinical study shows that human corneal endothelial cells can regenerate with the help of ROCK inhibitor *in vivo* when there is sufficient endothelial reserve to help the defect areas to be covered (Koizumi *et al.*, 2013).

Another possible limitation is that damage caused by a scrape wound and by FECD might elicit a different endothelial response. In FECD, cells start to degenerate from the central corneal endothelium, and are not removed from the surface completely as was the case in the scrape injury. Endothelial injuries similar to the mechanical scrape are sometimes caused by cataract surgery (Lundberg, Jonsson and Behndig, 2005). It can therefore be assumed that patients who have undergone cataract surgery, which result in complications associated with traumatic endothelial cell loss could possibly benefit from the ROCK inhibitor to promote regeneration and, eventually, reduce the demand for donor corneal transplantation.

To conclude, the results of the present experiments confirm that ROCK inhibitor, Y27632, can promote the proliferative ability of endothelial cells, provide cell adhesion to Descemet's membrane, and extend the survival rate of corneal endothelial cells. Findings in this chapter propose that ROCK inhibitors that are used for therapeutic or research purposes are agents that have the potential to be involved in innovative treatments for corneal endothelial dysfunctions as FECD. These results confirm that the therapeutic use of Y27632 can be a promising approach to help regenerate cells in FECD patients where central endothelial cells need replacement due to degeneration. For this, an approach like transcorneal freezing, as described in the previous chapter, can be used to remove the deteriorating cells and then administer the ROCK inhibitor treatment as a solution to repair the defect faster.

Chapter 7: Conclusion

The overarching purpose of the research described in this thesis was to consolidate and improve our knowledge of corneal endothelial cell behaviour during development, maturity and disease, and to investigate the potential of transcorneal freezing as a minimally invasive approach to destroy dysfunctional/diseased corneal endothelial cells in corneas that are oedematous and hazy due to endothelial pathology. The proliferative and protective efficiency of a ROCK inhibitor, Y27632, was also studied in an attempt to help discover the effects of alternative treatment procedures for corneal dysfunctions such as FECD.

The first experimental chapter describes corneal development because it has been reported that wound healing in the mature cornea recapitulates some events in corneal embryogenesis (Cinrron, Covingron and Kublin, 1990). This provided baseline knowledge of corneal endothelial development, and also revealed features such as cell processes and extracellular matrix strings projecting from emerging endothelial cells in embryonic avian cornea at E4.5 using large-volume 3D reconstructions from SBF-SEM. Cell processes extended from the emerging corneal endothelial cells towards both primary stroma (distally) and the lens (proximally), while the matrix strings were observed extending through the loose collagenous matrix of the primary stroma up to the basement membrane of epithelium. The corneal endothelium assumes its typical morphology as development proceeds,

becoming an interlinked monolayer. The role of the matrix strings in corneal development and their impact on the endothelium is currently unknown; further studies using SBF-SEM and other techniques might clarify the situation more fully.

Following the investigation of the corneal endothelium in development (using the well-established chick model), TEM inspections of this cell monolayer in human corneas were conducted. This demonstrated changes in intracellular organelles within corneal endothelial cells of patients who received a corneal transplantation for FECD, supporting the hypothesis that ER stress has some involvement in FECD pathogenesis. Given the multifactorial nature of human disease, however, is likely that various other factors may be involved in the development of FECD and the precise mechanisms are yet to be determined.

Subsequent to the inspection of corneal endothelial development (in embryonic chick cornea) and changes during pathology (in FECD in human cornea), an investigation into the effects of a newly designed cryoprobe for removing endothelial cells via transcorneal freezing was conducted. The results demonstrated (see Appendix (Akhbanbetova *et al.*, 2017)) that the use of a 3.4 mm diameter cryoprobe with a concave profile, amongst other designs tested, was the optimal tool to consistently destroy endothelial cells in the central cornea, proposing the reliability of a minimally invasive procedure for removing FECD-diseased cells to stimulate healthy peripheral endothelial migration and subsequent treatment. Experiments also indicated that transcorneal freezing permitted the ingress of agents into the corneal stroma (see Appendix (Chan, Akhbanbetova, A. J. Quantock, *et al.*, 2016)).

The question, then, was how to encourage healthy corneal endothelial cells outside the diseased are to migrate and repopulate the central area of the inside of the cornea from which the diseased cells had been removed. To investigate this, *in vivo* studies on rabbit corneas demonstrated the extent of damage on other corneal layers affected by the freezing in the central region. The study suggested that the fast recovery of the epithelial cells was likely because the basement membrane remained intact. As expected, cells of all

corneal layers (epithelium, stroma, and endothelium) had recovered in the central zone within one-month post-freeze. The efficacy of the simple transcorneal freezing procedure for endothelial cell removal should be further studied in more sophisticated animal models and attempts made to prevent occurrence of fibrous tissue.

In conclusion, the application of Y27632 ROCK inhibitor enhances cell migration, adhesion, and cell survival in the corneal endothelium. It is likely that the ROCK inhibitor administration might be beneficial in assisting the restoration of mild endothelial dysfunctions such as early-stage FECD or cataract-surgery-related trauma (bullous keratopathy). Considering the typical age group of the late-stage FECD with lower proliferative endothelial capacity, additional cell-based therapy via *in vitro* cultured endothelial cell injection might be inevitable. The precise mechanism of these activities in endothelial wound healing is still yet to be understood and needs to be studied further. Conventional transmission electron microscopy and SBF/SEM could be useful approaches to visualise the bigger picture of endothelial cell injuries treated with the ROCK inhibitor, where interactions between migrating cells could be examined. Also, the long-term medical effect of Y27632 would need to be studied following treatment. Potentially, though, transcorneal freezing followed by ROCK inhibitor treatment would be simple, minimally invasive, and cost-effective approach for FECD treatment.

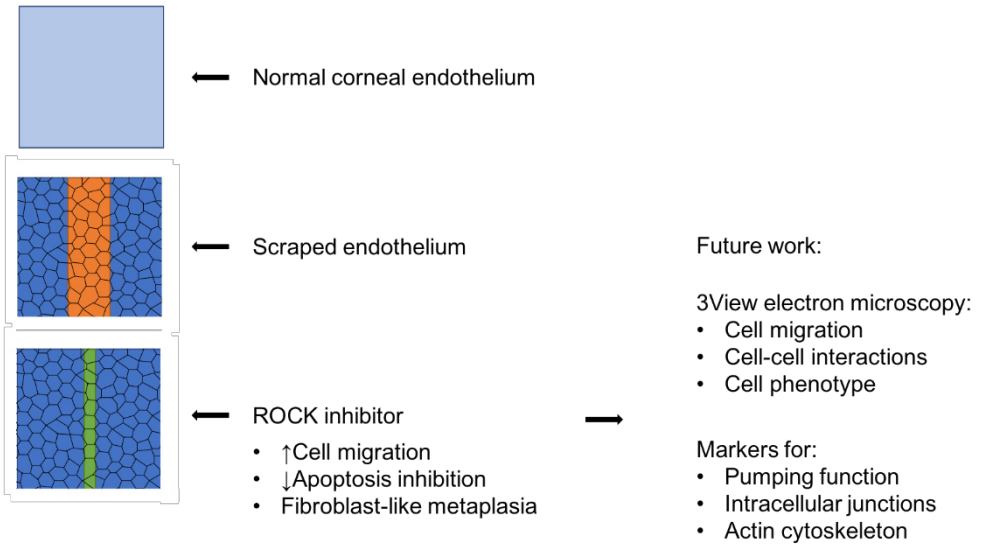

Figure 7.1 Schematic diagram of possible future work.

Chapter 8: References

Adamis, A. P., Filatov, V., Tripathi, B. J. and Tripathi, R. C. (1993) 'Fuchs' endothelial dystrophy of the cornea', *Survey of Ophthalmology*, 38(2), pp. 149–168.

Akanda, Z. Z., Naeem, A., Russell, E., Belrose, J., Si, F. F. and Hodge, W. G. (2015) 'Graft rejection rate and graft failure rate of penetrating keratoplasty (PKP) vs lamellar procedures: a systematic review', *PLoS ONE*. Edited by G. Brock. Public Library of Science, 10(3), p. e0119934. doi: 10.1371/journal.pone.0119934.

Akhbanbetova, A., Nakano, S., Littlechild, S. L., Young, R. D., Zvirgzdina, M., Fullwood, N. J., Weston, I., Weston, P., Kinoshita, S., Okumura, N., Koizumi, N. and Quantock, A. J. (2017) 'A surgical cryoprobe for targeted transcorneal freezing and endothelial cell removal', *Journal of Ophthalmology*. Hindawi, 2017, pp. 1–10. doi: https://doi.org/10.1155/2017/5614089.

Aldave, A. J., Rayner, S. A., Salem, A. K., Yoo, G. L., Kim, B. T., Saeedian, M., Sonmez, B. and Yellore, V. S. (2006) 'No pathogenic mutations identified in the COL8A1 and COL8A2 genes in familial Fuchs corneal dystrophy', *Investigative Ophthalmology and Visual Science*, 47(9), pp. 3787–3790. doi: 10.1167/iovs.05-1635.

Alkatan, H. (2017) 'Update on anterior segment development with emphasis on genetics and correlation with pathogenesis of developmental and primary open angle glaucoma', *Advances in Ophthalmology & Visual System*, 6(1), pp. 1–7. doi: 10.15406/aovs.2017.06.00164.

Armitage, W. J. (2003) 'Predicting endothelial cell loss and long-term corneal graft survival', *Investigative Ophthalmology and Visual Science*, 44(8), pp. 3326–3331. doi: 10.1167/iovs.02-1255.

Armitage, W. J., Hall, S. C. and Routledge, C. (2002) 'Recovery of endothelial function after vitrification of cornea at - 110°C', *Investigative Ophthalmology and Visual Science*, 43(7), pp. 2160–2164.

Armitage, W. J., Moss, S. J., Easty, D. L. and Bradley, B. A. (1990) 'Supply of corneal tissue in the United Kingdom', *British Journal of Ophthalmology*, 74(11), pp. 685–687. doi: 10.1136/bjo.74.11.685.

Bahar, I., Kaiserman, I. and Mcallum, P. (2008) 'Comparison of posterior lamellar keratoplasty techniques to penetrating keratoplasty', *Ophthalmology*, 115, pp. 1525–1533. doi: 10.1016/j.ophtha.2008.02.010.

Balachandran, C., Ham, L., Verschoor, C. a, Ong, T. S., van der Wees, J. and Melles, G. R. J. (2009) 'Spontaneous corneal clearance despite graft detachment in Descemet membrane endothelial keratoplasty.', *American Journal of Ophthalmology*, 148(2), p. 227–234.e1. doi: 10.1016/j.ajo.2009.02.033.

Baratz, K. H., Tosakulwong, N., Ryu, E., Brown, W. L., Branham, K., Chen, W., Tran, K. D., Schmid-Kubista, K. E., Heckenlively, J. R., Swaroop, A., Abecasis, G., Bailey, K. R. and Edwards, A. O. (2010) 'E2-2 protein and Fuchs's corneal dystrophy.', *The New England Journal of Medicine*, 363(11), pp. 1016–1024.

Bard, J. B. L. and Hay, E. D. (1975) 'The behavior of fibroblasts from the developing avian cornea: Morphology and movement in situ and in vitro', *Journal of Cell Biology*, 67(2), p. 400 418. doi: 10.1083/jcb.67.2.400.

Bee, J. A., Kuhl, U., Edgar, D. and Vandermark, K. (1988) 'Avian corneal nerves: Co-distribution with collagen type-IV and acquisition of substance-P immunoreactivity', *Investigative Ophthalmology and Visual Science*, 29(1), pp. 101–107.

Beebe, D. C. and Coats, J. M. (2000) 'The Lens Organizes the Anterior Segment: Specification of Neural Crest Cell Differentiation in the Avian Eye', *Developmental Biology*, 220(2), pp. 424–431. doi: 10.1006/dbio.2000.9638.

Ben-nun, J. and Barkana, Y. (2002) 'Nucleus cryoinversion for extraction of highly complicated cataracts', *Journal of Cataract and Refractive Surgery*. doi: 10.1016/S0886-3350(02)01272-5.

Biswas, S., Munier, F. L., Yardley, J., Hart-Holden, N., Perveen, R., Cousin, P., Sutphin, J. E., Noble, B., Batterbury, M., Kielty, C., Hackett, A., Bonshek, R., Ridgway, A., McLeod, D., Sheffield, V. C., Stone, E. M., Schorderet, D. F. and Black, G. C. M. (2001) 'Missense mutations in COL8A2, the gene encoding the alpha2 chain of type VIII collagen, cause two forms of corneal endothelial dystrophy', *Human Molecular Genetics*, 10(21), pp. 2415–2423. doi: 10.1093/hmg/10.21.2415.

Bonanno, J. A. (2012) 'Molecular mechanisms underlying the corneal endothelial pump.', *Experimental Eye Research*, 95(1), pp. 2–7. doi:

10.1016/j.exer.2011.06.004.

Borderie, V. M., Boëlle, P. Y., Touzeau, O., Allouch, C., Boutboul, S. and Laroche, L. (2009) 'Predicted long-term outcome of corneal transplantation', *Ophthalmology*, 116(12), pp. 2354–2360.

Bourne, W. M. (1998) 'Clinical estimation of corneal endothelial pump function.', *Transactions of the American Ophthalmological Society*, 96, pp. 229-39; discussion 239-42.

Bourne, W. M. (2003) 'Biology of the corneal endothelium in health and disease.', *Eye*, 17(8), pp. 912–8.

Bourne, W. M., Nelson, L. R. and Hodge, D. O. (1997) 'Central corneal endothelial cell changes over a ten-year period.', *Investigative Ophthalmology and Visual Science*, 38(3), pp. 779–82.

Bradford, S. M., Mikula, E. R., Juhasz, T., Brown, D. J. and Jester, J. V. (2018) 'Collagen fiber crimping following in vivo UVA-induced corneal crosslinking', *Experimental Eye Research*, 177(February), pp. 173–180. doi: 10.1016/j.exer.2018.08.009.

Buco, P., Van Horn, D. L., Schutten, W. H. and Cohen, K. (1973) 'Effects of transcorneal freezing on protein content of aqueous humor and intraocular temperature in rabbit and cat', *Investigative Ophthalmology and Visual Science*, 17(12), pp. 1199–1202.

Buddi, R., Lin, B., Atilano, S. R., Zorapapel, N. C., Kenney, M. C. and Brown, D. J. (2002) 'Evidence of oxidative stress in human corneal diseases', *Journal of Histochemistry & Cytochemistry*, 50(3), pp. 341–351. doi: 10.1177/002215540205000306.

Carlson, K. H., Bourne, W. M., McLaren, J. W. and Brubaker, R. F. (1988) 'Variations in human corneal endothelial cell morphology and permeability to fluorescein with age', *Experimental Eye Research*, 47(1), pp. 27–41. doi: 10.1016/0014-4835(88)90021-8.

Chan, W., Akhbanbetova, A., Quantock, A. J. A. J. and Heard, C. M. C. M. (2016) 'Topical delivery of a Rho-kinase inhibitor to the cornea via mucoadhesive film', *European Journal of Pharmaceutical Sciences*, 91, pp. 256–264. doi: 10.1016/j.ejps.2016.05.016.

Chan, W., Akhbanbetova, A., Quantock, A. J. and Heard, C. M. (2016) 'Topical delivery of a Rho-kinase inhibitor to the cornea via mucoadhesive film', *European Journal of Pharmaceutical Sciences*, 91, pp. 256–264. doi: 10.1016/j.ejps.2016.05.016.

Chang, Y. C. and Yu, C. H. (2013) 'Successful treatment of a large oral verrucous hyperplasia with photodynamic therapy combined with cryotherapy', *Journal of Dental Sciences*, 8(1), pp. 87–90. doi:

10.1016/j.jds.2012.09.024.

Chapman, S. C., Collignon, J., Schoenwolf, G. C. and Lumsden, A. (2001) 'Improved method for chick whole-embryo culture using a filter paper carrier', *Developmental Dynamics*, 220(3), pp. 284–289. doi: 10.1002/1097-0177(20010301)220:3<284::AID-DVDY1102>3.0.CO;2-5.

Chi, H. H. and Kelman, C. D. (1966) 'Effects of freezing on ocular tissues. I. Clinical and histologic study of corneal endothelium', *American Journal of Ophthalmology*, 61, pp. 630–641.

Chiou, A. G. Y., Kaufman, S. C., Beuerman, R. W., Ohta, T., Soliman, H. and Kaufman, H. E. (1999) 'Confocal microscopy in cornea guttata and Fuchs' endothelial dystrophy', *British Journal of Ophthalmology*, 83(2), pp. 185–189. doi: 10.1136/bjo.83.2.185.

Choi, H. J., Lee, J. J., Kim, D. H., Kim, M. K., Lee, H. J., Ko, A. Y., Kang, H. J., Park, C. and Wee, W. R. (2015) 'Blockade of CD40-CD154 costimulatory pathway promotes long-term survival of full-thickness porcine corneal grafts in nonhuman primates: Clinically applicable xenocorneal transplantation', *American Journal of Transplantation*, 15(3), pp. 628–641. doi: 10.1111/ajt.13057.

Chua, J. S., Liew, L. X. and Yim, E. K. F. (2013) 'Cultivation of human microvascular endothelial cells on topographical substrates to mimic the human corneal endothelium.', *Journal of Functional Biomaterials*, 4(1), pp. 38–58. doi: 10.3390/jfb4010038.

Cinrron, C., Covingron, H. I. and Kublin, C. L. (1990) 'Morphologic Analyses of Proteoglycons in Rabbit Corneal Scars', *Investigative Ophthalmology and Visual Science*, 31(9), pp. 1789–1798.

Cintron, C., Covington, H. I. and Kublin, C. L. (1988) 'Morphogenesis of rabbit corneal endothelium', *Current Eye Research*, 7(9), pp. 913–929.

Cotsarelis, G., Cheng, S. Z., Dong, G., Sun, T. T. and Lavker, R. M. (1989) 'Existence of slow-cycling limbal epithelial basal cells that can be preferentially stimulated to proliferate: Implications on epithelial stem cells', *Cell*, 57(2), pp. 201–209. doi: 10.1016/0092-8674(89)90958-6.

Cross, H. E., Maumenee, A. E. and Cantolino, S. J. (1971) 'Inheritance of Fuchs' Endothelial Dystrophy', *Archives of Ophthalmology*, 85(3), pp. 268–272. doi: 10.1001/archopht.1971.00990050270002.

Cui, Z., Zeng, Q., Liu, S., Zhang, Y., Zhu, D., Guo, Y., Xie, M., Mathew, S., Cai, D., Zhang, J. and Chen, J. (2018) 'Cell-laden and orthogonal-multilayer tissue-engineered corneal stroma induced by a mechanical collagen microenvironment and transplantation in a rabbit model', *Acta Biomaterialia*, 75, pp. 183–199. doi: 10.1016/j.actbio.2018.06.005.

Dandona, L., Naduvilath, T. J., Janarthanan, M., Ragu, K. and Rao, G. N. (1997) 'Survival analysis and visual outcome in a large series of corneal transplants in India', *British Journal of Ophthalmology*, 81(9), pp. 726–731. doi: 10.1136/bjo.81.9.726.

Dikstein, S. (1973) 'Efficiency and survival of the corneal endothelial pump', *Experimental Eye Research*, 15, pp. 639–644.

Dirisamer, M., Dapena, I., Ham, L., Van Dijk, K., Oganes, O., Frank, L. E., Van Der Wees, J. and Melles, G. R. J. (2011) 'Patterns of corneal endothelialization and corneal clearance after Descemet membrane endothelial keratoplasty for Fuchs endothelial dystrophy', *American Journal of Ophthalmology*, 152(4), pp. 543–555. doi: 10.1016/j.ajo.2011.03.031.

Eghrari, A. O., McGlumphy, E. J., Iliff, B. W., Wang, J., Emmert, D., Riazuddin, S. A., Katsanis, N. and Gottsch, J. D. (2012) 'Prevalence and severity of Fuchs corneal dystrophy in Tangier island', *American Journal of Ophthalmology*, 153(6), pp. 1067–1072. doi: 10.1016/j.ajo.2011.11.033.

Engler, C., Kelliher, C., Spitze, A. R., Speck, C. L., Eberhart, C. G. and Jun, A. S. (2010) 'Unfolded protein response in Fuchs endothelial corneal dystrophy: a unifying pathogenic pathway?', *American Journal of Ophthalmology*, 149(2), p. 194–202.e2. doi: 10.1016/j.ajo.2009.09.009.

Faber, C., Scherfig, E., Prause, J. U. and SÃ¸rensen, K. E. (2008) 'Corneal thickness in pigs measured by ultrasound pachymetry in vivo', *Scandinavian Journal of Laboratory Animal Sciences*, 35(1), pp. 39–43.

Faure, J. P., Kim, Y. Z. and Graf, B. (1971) 'Formation of giant cells in the corneal endothelium during its regeneration after destruction by freezing', *Experimental Eye Research*, 12, pp. 6–12.

Fitch, J. M., Birk, D. E., Linsenmayer, C. and Linsenmayer, T. F. (1991) 'Stromal assemblies containing collagen types IV and VI and fibronectin in the developing embryonic avian cornea', *Developmental Biology*, 144(2), pp. 379–391. doi: 10.1016/0012-1606(91)90430-B.

Fitch, J. M., Mentzer, A., Mayne, R. and Linsenmayer, T. F. (1988) 'Acquisition of type IX collagen by the developing avian primary corneal stroma and vitreous', *Developmental Biology*, 128(2), pp. 396–405. doi: 10.1016/0012-1606(88)90301-6.

Fraunfelder, F. W. (2008) *Liquid nitrogen cryotherapy for surface eye disease (an AOS thesis).*, *Transactions of the American Ophthalmological Society*.

Friedenwxald, H. and Friedenwvald, J. S. (1925) 'Epithelial dystrophy of the cornea', *The British Journal of Ophthalmology*, 9(1), pp. 14–20.

Fuchs, E. (1910) 'Dystrophia epithelialis corneae', *Albrecht von Græfe's*

Archiv für Ophthalmologie, 76(3), pp. 478–508. doi: 10.1007/BF01986362.

Fukata, Y., Kaibuchi, K., Amano, M. and Kaibuchi, K. (2001) 'Rho-Rho-kinase pathway in smooth muscle contraction and cytoskeletal reorganization of non-muscle cells', *Trends in Pharmacological Sciences*, 22(1), pp. 32–39. doi: 10.1016/S0165-6147(00)01596-0.

Fullwood, N. J., Davies, Y., Nieduszynski, I. A., Marcyniuk, B., Ridgway, A. E. A. and Quantock, A. J. (1996) 'Cell surface-associated keratan sulfate on normal and migrating corneal endothelium', *Investigative Ophthalmology and Visual Science*, 37(7), pp. 1256–1270.

Gain, P., Jullienne, R., He, Z., Aldossary, M., Acquart, S., Cognasse, F. and Thuret, G. (2016) 'Global survey of corneal transplantation and eye banking', *JAMA Ophthalmology*, 134(2), p. 167. doi: 10.1001/jamaophthalmol.2015.4776.

Galvis, V., Tello, A., Gomez, A. J., Rangel, C. M., Prada, A. M. and Camacho, P. A. (2013) 'Corneal transplantation at an ophthalmological referral center in Colombia: indications and techniques (2004-2011)', *The Open Ophthalmology Journal*, 7(August 2004), pp. 30–33. doi: 10.2174/1874364101307010030.

Garnock-Jones, K. P. (2015) 'Ripasudil: first global approval', *Drugs*, 75(15), pp. 1823–1830. doi: 10.1007/s40265-015-0477-8.

Germundsson, J., Karanis, G., Fagerholm, P. and Lagali, N. (2013) 'Age-related thinning of Bowman's layer in the human cornea in vivo', *Investigative Ophthalmology and Visual Science*, 54(9), pp. 6143–6149. doi: 10.1167/iovs.13-12535.

Geroski, D. H., Matsuda, M., Yee, R. W. and Edelhauser, H. F. (1985) 'Pump function of the human corneal endothelium: Effects of age and cornea guttata', *Ophthalmology*, 92(6), pp. 759–763. doi: 10.1016/S0161-6420(85)33973-8.

Goar, E. L. (1934) 'Dystrophy of the corneal endothelium. (Cornea guttata) with report of a histological examination', *American Journal of Ophthalmology*, 17(3), pp. 215–221. doi: 10.1016/S0002-9394(34)92584-8.

Gottsch, J. D., Sundin, O. H., Liu, S. H., Jun, A. S., Broman, K. W., Stark, W. J., Vito, E. C. L., Narang, A. K., Thompson, J. M. and Magovern, M. (2005) 'Inheritance of a novel COL8A2 mutation defines a distinct Early-onset subtype of fuchs corneal dystrophy', *Investigative Ophthalmology and Visual Science*, 46(6), p. 1934. doi: 10.1167/iovs.04-0937.

Gottsch, J. D., Zhang, C., Sundin, O. H., Bell, W. R., Stark, W. J. and Green, W. R. (2005) 'Fuchs corneal dystrophy: Aberrant collagen distribution in an L450W Mutant of the COL8A2 gene', *Investigative Ophthalmology and Visual Science*, 46(12), pp. 4504–4511. doi: 10.1167/iovs.05-0497.

Guindolet, D., Crouzet, E., He, Z., Herbepin, P., Jumelle, C., Perrache, C., Dumollard, J. M., Forest, F., Peoc'h, M., Gain, P., Gabison, E. and Thuret, G. (2017) 'Storage of porcine cornea in an innovative bioreactor', *Investigative Opthalmology and Visual Science*, 58(13), p. 5907. doi: 10.1167/iovs.17-22218.

Gupta, R., Kumawat, B. L., Paliwal, P., Tandon, R., Sharma, N., Sen, S., Kashyap, S., Nag, T. C., Vajpayee, R. B. and Sharma, A. (2015) 'Association of ZEB1 and TCF4 rs613872 changes with late onset Fuchs endothelial corneal dystrophy in patients from northern India', *Molecular Vision*, 21(April), pp. 1252–1260.

Han, S. B., Ang, H., Balehosur, D., Peh, G., Chaurasia, S. S., Tan, D. T. H. and Mehta, J. S. (2013) 'A mouse model of corneal endothelial decompensation using cryoinjury.', *Molecular Vision*, 19, pp. 1222–30.

Hara, H. and Cooper, D. K. C. (2011) 'Xenotransplantation - The future of corneal transplantation', *Cornea*, 30(4), pp. 371–378. doi: 10.1097/ICO.0b013e3181f237ef.XENOTRANSPLANTATION.

Hatami-Marbini, H., Etebu, E. and Rahimi, A. (2013) 'Swelling pressure and hydration behavior of porcine corneal stroma', *Current Eye Research*, 38(11), pp. 1124–1132. doi: 10.3109/02713683.2013.809769.

Hatta, K. and Takeichi, M. (1986) 'Expression of N-cadherin adhesion molecules associated with early morphogenetic events in chick development', *Nature*, 320(6061), pp. 447–449. doi: 10.1038/320447a0.

Hay, E. D. (1980) 'Development of the vertebrate cornea', *International Review of Cytology*, 63, pp. 263–322. doi: 10.1016/S0074-7696(08)61760-X.

Hay, E. D. and Revel, J. P. (1969) *Fine structure of the developing avian cornea*, *Monographs in Developmental Biology*.

Hayashi, K., Hayashi, H., Nakao, F. and Hayashi, F. (1996) 'Risk factors for corneal endothelial injury during phacoemulsification', *Journal of Cataract and Refractive Surgery*, 22(8), pp. 1079–1084. doi: 10.1016/S0886-3350(96)80121-0.

Hayashi, R., Ishikawa, Y., Sasamoto, Y., Katori, R., Nomura, N., Ichikawa, T., Araki, S., Soma, T., Kawasaki, S., Sekiguchi, K., Quantock, A. J., Tsujikawa, M. and Nishida, K. (2016) 'Co-ordinated ocular development from human iPS cells and recovery of corneal function', *Nature*, 531(7594), pp. 376–380. doi: 10.1038/nature17000.

Hemadevi, B., Srinivasan, M., Arunkumar, J., Prajna, N. V and Sundaresan, P. (2010) 'Genetic analysis of patients with Fuchs endothelial corneal dystrophy in India', *BMC Ophthalmology*, 10(1), p. 3. doi: 10.1186/1471-2415-10-3.

Hidayat, A. A. and Cockerham, G. C. (2006) 'Epithelial metaplasia of the corneal endothelium in Fuchs endothelial dystrophy.', *Cornea*, 25(8), pp. 956–9. doi: 10.1097/01.ico.0000228786.84581.ee.

Hirsch, M., Noske, W., Prenant, G. and Renard, G. (1999) 'Fine structure of the developing avian corneal stroma as revealed by quick-freeze, deep-etch electron microscopy', *Experimental Eye Research*, 69(3), pp. 267–277. doi: 10.1006/exer.1999.0695.

Hodge, R. G. and Ridley, A. J. (2016) 'Regulating Rho GTPases and their regulators', *Nature Reviews Molecular Cell Biology*. Nature Publishing Group, 17(8), pp. 496–510. doi: 10.1038/nrm.2016.67.

Van Horn, D. L. and Hyndiuk, R. a (1975) 'Endothelial wound repair in primate cornea.', *Experimental Eye Research*, 21(2), pp. 113–124.

Van Horn, D. L., Sendele, D. D., Seideman, S. and Buco, P. J. (1977) 'Regenerative capacity of the corneal endothelium in rabbit and cat', *Investigative Ophthalmology and Visual Science*, 16(7), pp. 597–613.

Ichijima, H., Petroll, W. M., Barry, P. A., Andrews, P. M., Dai, M., Cavanagh, H. D. and Jester, J. V. (1993) 'Actin filament organization during endothelial wound healing in the rabbit cornea: Comparison between transcorneal freeze and mechanical scrape injuries', *Investigative Ophthalmology and Visual Science*, 34(9), pp. 2803–2812.

Iliff, B. W., Riazuddin, S. A. and Gottsch, J. D. (2012) 'The genetics of Fuchs' corneal dystrophy.', *Expert Review of Ophthalmology*, 7(4), pp. 363–375. doi: 10.1586/eop.12.39.

Inoue, T., Kobayashi, T., Nakao, S., Hara, Y., Suzuki, T., Hayashi, Y., Zheng, X., Shiraishi, A. and Ohashi, Y. (2014) 'Horizontal intracorneal swirling water migration indicative of corneal endothelial function', *Investigative Ophthalmology and Visual Science*, 55(12), pp. 8006–8014. doi: 10.1167/iovs.14-14762.

Itoh, K., Yoshioka, K., Akedo, H., Uehata, M., Ishizaki, T. and Narumiya, S. (1999) 'An essential part for Rho–associated kinase in the transcellular invasion of tumor cells', *Nature Medicine*, 5(2), pp. 221–225. doi: 10.1038/5587.

Iwamoto, T. and Devoe, A. G. (1970) 'Electron microscopic studies on Fuchs' combined dystrophy I. Posterior portion of the cornea', *Investigative Ophthalmology and Visual Science*, 10(1), pp. 9–28.

Jakobiec, F. A. and Bhat, P. (2010) 'Retrocorneal membranes: A comparative immunohistochemical analysis of keratocytic, endothelial, and epithelial origins', *American Journal of Ophthalmology*, 150(2), pp. 230–242. doi: 10.1016/j.ajo.2010.03.011.

Jia, Y., Li, W., Duan, H., Li, Z., Zhou, Q. and Shi, W. (2018) 'Mini-sheet injection for cultured corneal endothelial transplantation', *Tissue Engineering Part C: Methods*, 24(8), pp. 474–479. doi: 10.1089/ten.tec.2018.0077.

Johnson, D. H., Bourne, W. M. and Campbell, J. (1982) 'The ultrastructure of Descement's membrane. I. Changes with age in normal corneas', *Archives of Ophthalmology*, 100, pp. 1942–1947.

Johnston, M. C. C., Noden, D. M. M., Hazelton, R. D. D., Coulombre, J. L. L. and Coulombre, A. J. J. (1979) 'Origins of avian ocular and periocular tissues', *Experimental Eye Research*, 29(1), pp. 27–43. doi: 10.1016/0014-4835(79)90164-7.

Joko, T., Shiraishi, A., Kobayashi, T., Ohashi, Y. and Higashiyama, S. (2017) 'Mechanism of proliferation of cultured human corneal', *Cornea*, 36(11), pp. 41–45.

Joyce, N. C. and Harris, D. L. (2010) 'Decreasing expression of the G1-phase inhibitors, p21Cip1 and p16INK4a, promotes division of corneal endothelial cells from older donors.', *Molecular Vision*, 16(November 2009), pp. 897–906.

Joyce, N. C., Meklir, B., Joyce, S. J. and Zieske, J. D. (1996) 'Cell cycle protein expression and proliferative status in human corneal cells', *Investigative Ophthalmology and Visual Science*, 37(4), pp. 645–655.

Joyce, N. C., Navon, S. E., Roy, S. and Zieske, J. D. (1996) 'Expression of cell cycle-associated proteins in human and rabbit corneal endothelium in situ.', *Investigative Ophthalmology and Visual Science*, 37(8), pp. 1566–1575.

Joyce, N. C., Zhu, C. C. and Harris, D. L. (2009) 'Relationship among oxidative stress, DNA damage, and proliferative capacity in human corneal endothelium.', *Investigative Ophthalmology and Visual Science*, 50(5), pp. 2116–22. doi: 10.1167/iovs.08-3007.

Jurkunas, U. V, Bitar, M. S., Funaki, T. and Azizi, B. (2010) 'Evidence of oxidative stress in the pathogenesis of fuchs endothelial corneal dystrophy.', *The American Journal of Pathology*, 177(5), pp. 2278–89. doi: 10.2353/ajpath.2010.100279.

Karnovsky, M. J. (1965) 'A formaldehyde-glutaraldehyde fixative of high osmolarity for use in electron microscopy', *Journal of Cell Biology*, 27, pp. 137–139.

Kaufman, H. E. and Katz, J. I. (1977) 'Pathology of the corneal endothelium.', *Investigative Ophthalmology and Visual Science*, 16(4), pp. 265–268.

Keenan, T. D. L., Carley, F., Yeates, D., Jones, M. N. A., Rushton, S. and Goldacre, M. J. (2011) 'Trends in corneal graft surgery in the UK', *British*

Journal of Ophthalmology, 95(4), pp. 468–472. doi: 10.1136/bjo.2010.182329.

Keenan, T. D. L., Jones, M. N. A., Rushton, S. and Carley, F. M. (2012) 'Trends in the indications for corneal graft surgery in the United Kingdom: 1999 through 2009.', *Archives Of Ophthalmology (Chicago, Ill.: 1960)*, 130(5), pp. 621–628. doi: 10.1001/archophthalmol.2011.2585.

Kidson, S. H., Kume, T., Deng, K., Winfrey, V. and Hogan, B. L. M. (1999) 'The forkhead/winged-helix gene, Mf1, is necessary for the normal development of the cornea and formation of the anterior chamber in the mouse eye', *Developmental Biology*, 211(2), pp. 306–322. doi: 10.1006/dbio.1999.9314.

Kim, M. D., Kolodziej, P. and Chiba, A. (2002) 'Growth cone pathfinding and filopodial dynamics are mediated separately by Cdc42 activation.', *The Journal of Neuroscience*, 22(5), pp. 1794–1806.

Kimura, K., Ito, M., Amano, M., Chihara, K., Fukata, Y., Nakafuku, M., Yamamori, B., Feng, J., Nakano, T., Okawa, K., Iwamatsu, A. and Kaibuchi, K. (1996) 'Regulation of myosin phosphatase by Rho and Rho-associated kinase (Rho- kinase)', *Science*, 273(5272), pp. 245–248. doi: 10.1126/science.273.5272.245.

Kinoshita, S., Adachi, W., Sotozono, C., Nishida, K., Yokoi, N., Quantock, A. J. and Okubo, K. (2001) *Characteristics of the human ocular surface epithelium*, *Progress in Retinal and Eye Research*. doi: 10.1016/S1350-9462(01)00007-6.

Kinoshita, S., Koizumi, N., Ueno, M., Okumura, N., Imai, K., Tanaka, H., Yamamoto, Y., Nakamura, T., Inatomi, T., Bush, J., Toda, M., Hagiya, M., Yokota, I., Teramukai, S., Sotozono, C. and Hamuro, J. (2018a) 'Injection of cultured cells with a ROCK inhibitor for bullous keratopathy', *New England Journal of Medicine*, 378(11), pp. 995–1003. doi: 10.1056/NEJMoa1712770.

Kinoshita, S., Koizumi, N., Ueno, M., Okumura, N., Imai, K., Tanaka, H., Yamamoto, Y., Nakamura, T., Inatomi, T., Bush, J., Toda, M., Hagiya, M., Yokota, I., Teramukai, S., Sotozono, C. and Hamuro, J. (2018b) 'Injection of Cultured Cells with a ROCK Inhibitor for Bullous Keratopathy', *New England Journal of Medicine*, 378(11), pp. 995–1003. doi: 10.1056/NEJMoa1712770.

Kitagawa, K., Kojima, M., Sasaki, H., Shui, Y. B., Chew, S. J., Cheng, H. M., Ono, M., Morikawa, Y. and Sasaki, K. (2002) 'Prevalence of primary cornea guttata and morphology of corneal endothelium in aging Japanese and Singaporean subjects', *Ophthalmic Research*, 34(3), pp. 135–138. doi: 10.1159/000063656.

Kivanany, P. B., Grose, K. C., Tippani, M., Su, S. and Petroll, W. M. (2018) 'Assessment of corneal stromal remodeling and regeneration after photorefractive keratectomy', *Scientific Reports*, 8(1), p. 12580. doi: 10.1038/s41598-018-30372-2.

Kobayashi, A., Fujiki, K., Murakami, A., Kato, T., Chen, L. Z., Onoe, H., Nakayasu, K., Sakurai, M., Takahashi, M., Sugiyama, K. and Kanai, A. (2004) 'Analysis of COL8A2 gene mutation in Japanese patients with Fuchs' endothelial dystrophy and posterior polymorphous dystrophy', *Japanese Journal of Ophthalmology*, 48(3), pp. 195–198. doi: 10.1007/s10384-003-0063-6.

Koizumi, N., Okumura, N. and Kinoshita, S. (2012) 'Development of new therapeutic modalities for corneal endothelial disease focused on the proliferation of corneal endothelial cells using animal models.', *Experimental Eye Research*, 95(1), pp. 60–7.

Koizumi, N., Okumura, N., Ueno, M. and Kinoshita, S. (2014) 'New therapeutic modality for corneal endothelial disease using Rho-associated kinase inhibitor eye drops', *Cornea*, 33(11), pp. 25–31.

Koizumi, N., Okumura, N., Ueno, M., Nakagawa, H., Hamuro, J. and Kinoshita, S. (2013) 'Rho-associated kinase inhibitor eye drop treatment as a possible medical treatment for Fuchs corneal dystrophy', *Cornea*, 32, pp. 1167–1170.

Koudouna, E., Mikula, E., Brown, D. J., Young, R. D., Quantock, A. J. and Jester, J. V. (2018) 'Cell regulation of collagen fibril macrostructure during corneal morphogenesis', *Acta Biomaterialia*, pp. 1–17. doi: 10.1016/j.actbio.2018.08.017.

Koudouna, E., Winkler, M., Mikula, E., Juhasz, T., Brown, D. J. and Jester, J. V. (2018) 'Evolution of the vertebrate corneal stroma', *Progress in Retinal and Eye Research*, 64(November 2017), pp. 65–76. doi: 10.1016/j.preteyeres.2018.01.002.

Krachmer, J. H., Purcell, J. J., Young, C. W. and Bucher, K. D. (1978) 'Corneal Endothelial Dystrophy', *Archives of Ophthalmology*, 96(11), p. 2036. doi: 10.1001/archopht.1978.03910060424004.

Kymionis, G. D., Liakopoulos, D. A., Grentzelos, M. A., Naoumidi, I., Kontadakis, G. A., Tsoulnaras, K. I. and Petrelli, M. K. (2017) 'Mini descemet membrane stripping (m-DMES) in patients with Fuchs' endothelial dystrophy: A new method', *Saudi Journal of Ophthalmology*, 31, pp. 275–279. doi: 10.1016/j.sjopt.2017.05.010.

Lai, J.-M., Hsieh, C.-L. and Chang, Z.-F. (2003) 'Caspase activation during phorbol ester-induced apoptosis requires ROCK-dependent myosin-mediated contraction.', *Journal of Cell Science*, 116(Pt 17), pp. 3491–501. doi: 10.1242/jcs.00660.

Laing, R. a, Sanstrom, M. M., Berrospi, a R. and Leibowitz, H. M. (1976) 'Changes in the corneal endothelium as a function of age.', *Experimental Eye Research*, 22(6), pp. 587–94.

Lang, G. K. and Naumann, G. (1987) 'The frequency of corneal dystrophies

requiring keratoplasty in Europe and the U.S.A.', *Cornea*, 6(3), pp. 209–211.

Le, R., Yucel, N., Khattak, S., Yucel, Y. H., Prud'homme, G. J. and Gupta, N. (2017) 'Current indications and surgical approaches to corneal transplants at the University of Toronto: A clinical-pathological study', *Canadian Journal of Ophthalmology*. Elsevier Inc., 52(1), pp. 74–79. doi: 10.1016/j.jcjo.2016.07.005.

Lechner, J., Dash, D. P., Muszynska, D., Hosseini, M., Segev, F., George, S., Frazer, D. G., Moore, J. E., Kaye, S. B., Young, T., Simpson, D. A., Churchill, A. J., H??on, E. and Willoughby, C. E. (2013) 'Mutational spectrum of the ZEB1 gene in corneal dystrophies supports a genotype-phenotype correlation', *Investigative Ophthalmology and Visual Science*, 54(5), pp. 3215–3223. doi: 10.1167/iovs.13-11781.

Lee, J. G. and Heur, M. (2014) 'Interleukin-1-induced Wnt5a enhances human corneal endothelial cell migration through regulation of Cdc42 and RhoA', *Molecular and Cellular Biology*, 34(18), pp. 3535–3545. doi: 10.1128/MCB.01572-13.

Lee, J. G., Jung, E. and Heur, M. (2018) 'Fibroblast growth factor 2 induces proliferation and fibrosis via SNAI1-mediated activation of CDK2 and ZEB1 in corneal endothelium', *Journal of Biological Chemistry*, 293(10), pp. 3758–3769. doi: 10.1074/jbc.RA117.000295.

Lee, S. E., Mehra, R., Fujita, M., Roh, D. S., Long, C., Lee, W., Funderburgh, J. L., Ayares, D. L., Cooper, D. K. C. and Hara, H. (2014) 'Characterization of porcine corneal endothelium for xenotransplantation', *Seminars in Ophthalmology*, 29(3), pp. 127–135. doi: 10.3109/08820538.2013.787104.

Lee, W. B., Jacobs, D. S., Musch, D. C., Kaufman, S. C., Reinhart, W. J. and Shtein, R. M. (2009) 'Descemet's stripping endothelial keratoplasty: safety and outcomes. A report by the American Academy of Ophthalmology', *Ophthalmology*, 116(9), pp. 1818–1830. doi: 10.1016/j.ophtha.2009.06.021.

Lee, W., Miyagawa, Y., Long, C., Zhang, M., Cooper, D. K. C. and Hara, H. (2016) 'Effect of Rho-kinase inhibitor, Y27632, on porcine corneal endothelial cell culture, inflammation and immune regulation', *Ocular Immunology and Inflammation*, 24(5), pp. 579–593. doi: 10.3109/09273948.2015.1056534.

Leung, E. W., Rife, L., Smith, R. E. and Kay, E. P. (2000) 'Extracellular matrix components in retrocorneal fibrous membrane in comparison to corneal endothelium and Descemet's membrane.', *Molecular Vision*, 6, pp. 15–23.

Li, S., Wang, C., Dai, Y., Yang, Y., Pan, H., Zhong, J. and Chen, J. (2013) 'The stimulatory effect of ROCK inhibitor on bovine corneal endothelial cells.', *Tissue and Cell*, 45(6), pp. 387–96.

Li, Y.-J., Minear, M. A., Rimmler, J., Zhao, B., Balajonda, E., Hauser, M. A., Allingham, R. R., Eghrari, A. O., Riazuddin, S. A., Katsanis, N., Gottsch, J. D., Gregory, S. G., Klintworth, G. K. and Afshari, N. A. (2011) 'Replication of

TCF4 through Association and Linkage Studies in Late-Onset Fuchs Endothelial Corneal Dystrophy', *PLoS ONE*. Edited by F. Kronenberg, 6(4), p. e18044. doi: 10.1371/journal.pone.0018044.

Lichtinger, A., Sandstedt, C. A., Padilla, K., Schwartz, D. M. and Chayet, A. S. (2011) 'Corneal endothelial safety after ultraviolet light treatment of the light-adjustable intraocular lens', *Journal of Cataract & Refractive Surgery*, 37(2), pp. 324–327. doi: 10.1016/j.jcrs.2010.08.033.

Lichtinger, A., Yeung, S. N., Kim, P., Amiran, M. D. and Rootman, D. S. (2012) 'The era of lamellar keratoplasty, evolving surgical techniques in corneal transplantation: The University of Toronto experience', *Canadian Journal of Ophthalmology*, 47(3), pp. 287–290. doi: 10.1016/j.jcjo.2012.01.001.

Lingor, P., Tönges, L., Pieper, N., Bermel, C., Barski, E., Planchamp, V. and Bähr, M. (2008) 'ROCK inhibition and CNTF interact on intrinsic signalling pathways and differentially regulate survival and regeneration in retinal ganglion cells', *Brain*, 131(1), pp. 250–263. doi: 10.1093/brain/awm284.

Linsenmayer, T. F., Fitch, J. M., Gordon, M. K., Cai, C. X., Igoe, F., Marchant, J. K. and Birk, D. E. (1998) 'Development and roles of collagenous matrices in the embryonic avian cornea', *Progress in Retinal and Eye Research*, 17(2), pp. 231–265. doi: 10.1016/S1350-9462(97)00010-4.

Liskova, P., Prescott, Q., Bhattacharya, S. S. and Tuft, S. J. (2007) 'British family with early-onset Fuchs' endothelial corneal dystrophy associated with p.L450W mutation in the COL8A2 gene.', *The British Journal of Ophthalmology*, 91(12), pp. 1717–8. doi: 10.1136/bjo.2007.115154.

Liu, C., Vojnovic, D., Kochevar, I. E. and Jurkunas, U. V. (2016) 'UV-A irradiation activates Nrf2-regulated antioxidant defense and induces p53/caspase3-dependent apoptosis in corneal endothelial cells', *Investigative Ophthalmology and Visual Science*, 57(4), pp. 2319–2327. doi: 10.1167/iovs.16-19097.

Lorenzetti, D. W., Uotila, M. H., Parikh, N. and Kaufman, H. E. (1967) 'Central cornea guttata. Incidence in the general population.', *American Journal of Ophthalmology*, 64(6), pp. 1155–8. doi: 10.1016/0002-9394(67)93073-5.

Lundberg, B., Jonsson, M. and Behndig, A. (2005) 'Postoperative corneal swelling correlates strongly to corneal endothelial cell loss after phacoemulsification cataract surgery', *American Journal of Ophthalmology*, 140(6), pp. 1171–1172. doi: 10.1016/j.ajo.2005.07.048.

Ma, R., Liu, Y., Zhang, L., Lei, Y., Hou, J., Shen, Z., Yi, X. and Wang, Y. (2018) 'Distribution and trends in corneal thickness parameters in a large population-based multicenter study of young chinese adults', *Investigative Opthalmology and Visual Science*, 59(8), p. 3366. doi: 10.1167/iovs.18-24332.

Maekawa, M. (1999) 'Signaling from Rho to the Actin Cytoskeleton Through Protein Kinases ROCK and LIM-kinase', *Science*, 285(5429), pp. 895–898. doi: 10.1126/science.285.5429.895.

Magovern, M., Beauchamp, G. R., McTigue, J. W., Fine, B. S. and Baumiller, R. C. (1979) 'Inheritance of Fuchs' combined dystrophy', *Ophthalmology*, 86(10), pp. 1897–1920. doi: 10.1016/S0161-6420(79)35340-4.

Mattila, P. K. and Lappalainen, P. (2008) 'Filopodia: Molecular architecture and cellular functions', *Nature Reviews Molecular Cell Biology*, 9(6), pp. 446–454. doi: 10.1038/nrm2406.

Maumenee, A. E. and Kornblueth, W. (1948) 'Regeneration of corneal stromal cells: I. Techniques for destruction of corneal corpuscles by application of solidified (frozen) carbon dioxide.', *American Journal of Ophthalmology*, 31(6), pp. 699–702.

Maurice, D. M. (1957) 'The structure and transparency of the cornea.', *The Journal of Physiology*, 136(2), pp. 263–286. doi: 10.1113/jphysiol.1957.sp005758.

Meek, K. M. and Boote, C. (2004) 'The organization of collagen in the corneal stroma', *Experimental Eye Research*, 78(3), pp. 503–512. doi: 10.1016/j.exer.2003.07.003.

Meek, K. M., Dennis, S. and Khan, S. (2003) 'Changes in the refractive index of the stroma and its extrafibrillar matrix when the cornea swells', *Biophysical Journal*, 85(4), pp. 2205–2212. doi: 10.1016/S0006-3495(03)74646-3.

Meek, K. M., Fullwood, N. J., Cooke, P. H., Elliott, G. F., Maurice, D. M., Quantock, A. J., Wall, R. S. and Worthington, C. R. (1991) 'Synchrotron x-ray diffraction studies of the cornea, with implications for stromal hydration', *Biophysical Journal*, 60(2), pp. 467–474. doi: 10.1016/S0006-3495(91)82073-2.

Melles, G. R. J., Lander, F., Beekhuis, W. H., Remeijer, L. and Binder, P. S. (1999) 'Posterior lamellar keratoplasty for a case of pseudophakic bullous keratopathy', *American Journal of Ophthalmology*, 127(3), pp. 340–341. doi: 10.1016/S0002-9394(98)00324-9.

Meng, H., Matthaei, M., Ramanan, N., Grebe, R., Chakravarti, S., Speck, C. L., Kimos, M., Vij, N., Eberhart, C. G. and Jun, A. S. (2013) 'L450W and Q455K Col8a2 knock-in mouse models of Fuchs endothelial corneal dystrophy show distinct phenotypes and evidence for altered autophagy.', *Investigative Ophthalmology and Visual Science*, 54(3), pp. 1887–97. doi: 10.1167/iovs.12-11021.

Mimura, T., Yamagami, S., Yokoo, S., Araie, M. and Amano, S. (2005) 'Comparison of rabbit corneal endothelial cell precursors in the central and peripheral cornea.', *Investigative Ophthalmology and Visual Science*, 46(10), pp. 3645–8. doi: 10.1167/iovs.05-0630.

Mimura, T., Yamagami, S., Yokoo, S., Yanagi, Y., Usui, T., Ono, K., Araie, M. and Amano, S. (2005) 'Sphere therapy for corneal endothelium deficiency in a rabbit model.', *Investigative Ophthalmology and Visual Science*, 46(9), pp. 3128–35.

Mimura, T., Yokoo, S., Araie, M., Amano, S. and Yamagami, S. (2005) 'Treatment of rabbit bullous keratopathy with precursors derived from cultured human corneal endothelium.', *Investigative Ophthalmology and Visual Science*, 46(10), pp. 3637–44.

Minkowski, J. S., Bartels, S. P., Delori, F. C., Lee, S. R., Kenyon, K. R. and Neufeld, a H. (1984) 'Corneal endothelial function and structure following cryo-injury in the rabbit.', *Investigative Ophthalmology and Visual Science*, 25(12), pp. 1416–25.

Mok, J. W., Kim, H. S. and Joo, C. K. (2009) 'Q455V mutation in COL8A2 is associated with Fuchs' corneal dystrophy in Korean patients', *Eye*, 23(4), pp. 895–903. doi: 10.1038/eye.2008.116.

Mukai, Y., Shimokawa, H., Matoba, T., Kandabashi, T., Satoh, S., Hiroki, J., Kaibuchi, K. and Takeshita, A. (2001) 'Involvement of Rho-kinase in hypertensive vascular disease: a novel therapeutic target in hypertension.', *FASEB journal : official publication of the Federation of American Societies for Experimental Biology*, 15(6), pp. 1062–4. doi: 10.1096/FJ.00-0735FJE.

Murphy, C., Alvarado, J. and Juster, R. (1984) 'Prenatal and postnatal growth of the human Descemet's membrane.', *Investigative Ophthalmology and Visual Science*, 25(12), pp. 1402–1415.

Musch, D. C., Niziol, L. M., Stein, J. D., Kamyar, R. M. and Sugar, A. (2011) 'Prevalence of corneal dystrophies in the United States: Estimates from claims data', *Investigative Ophthalmology and Visual Science*, 52(9), pp. 6959–6963. doi: 10.1167/iovs.11-7771.

Nieuwendaal, C. P., Lapid-Gortzak, R., Van Der Meulen, I. J. and Melles, G. J. R. (2006) 'Posterior lamellar keratoplasty using descemetorhexis and organ-cultured donor corneal tissue (Melles technique)', *Cornea*, 25(8), pp. 933–936. doi: 10.1097/01.ico.0000239002.92989.1a.

Okumura, N., Hashimoto, K., Kitahara, M., Okuda, H., Ueda, E., Watanabe, K., Nakahara, M., Sato, T., Kinoshita, S., Tourtas, T., Schlötzer-Schrehardt, U., Kruse, F. and Koizumi, N. (2017) 'Activation of TGF-β signaling induces cell death via the unfolded protein response in Fuchs endothelial corneal dystrophy', *Scientific Reports*, 7(1), p. 6801. doi: 10.1038/s41598-017-06924-3.

Okumura, N., Hayashi, R. and Koizumi, N. (2018) 'Perspective of future potent therapies for Fuchs endothelial corneal dystrophy', *The Open Ophthalmology Journal*, 12(Suppl-1, M4), pp. 154–163. doi: 10.2174/1874364101812010154.

Okumura, N., Kitahara, M., Okuda, H., Hashimoto, K., Ueda, E., Nakahara, M., Kinoshita, S., Young, R. D., Quantock, A. J., Tourtas, T., Schlötzer-Schrehardt, U., Kruse, F. and Koizumi, N. (2017) 'Sustained activation of the unfolded protein response induces cell death in Fuchs' endothelial corneal dystrophy', *Investigative Opthalmology and Visual Science*, 58(9), p. 3697. doi: 10.1167/iovs.16-21023.

Okumura, N., Koizumi, N., Kay, E. P., Ueno, M., Sakamoto, Y., Nakamura, S., Hamuro, J. and Kinoshita, S. (2013) 'The ROCK inhibitor eye drop accelerates corneal endothelium wound healing.', *Investigative Ophthalmology and Visual Science*, 54(4), pp. 2493–502.

Okumura, N., Koizumi, N., Ueno, M., Sakamoto, Y., Takahashi, H., Hirata, K., Torii, R., Hamuro, J. and Kinoshita, S. (2011) 'Enhancement of corneal endothelium wound healing by Rho-associated kinase (ROCK) inhibitor eye drops.', *The British Journal of Ophthalmology*, 95, pp. 1006–1009.

Okumura, N., Koizumi, N., Ueno, M., Sakamoto, Y., Takahashi, H., Tsuchiya, H., Hamuro, J. and Kinoshita, S. (2012) 'ROCK inhibitor converts corneal endothelial cells into a phenotype capable of regenerating in vivo endothelial tissue', *The American Journal of Pathology*, 181, pp. 268–277.

Okumura, N., Matsumoto, D., Fukui, Y., Teramoto, M., Imai, H., Kurosawa, T., Shimada, T., Kruse, F., Schlötzer-Schrehardt, U., Kinoshita, S. and Koizumi, N. (2018) 'Feasibility of cell-based therapy combined with descemetorhexis for treating Fuchs endothelial corneal dystrophy in rabbit model', *PLoS ONE*, 13(1), pp. 1–14. doi: 10.1371/journal.pone.0191306.

Okumura, N., Minamiyama, R., Ho, L. T., Kay, E. P., Kawasaki, S., Tourtas, T., Schlötzer-Schrehardt, U., Kruse, F. E., Young, R. D., Quantock, A. J., Kinoshita, S. and Koizumi, N. (2015) 'Involvement of ZEB1 and Snail1 in excessive production of extracellular matrix in Fuchs endothelial corneal dystrophy', *Laboratory Investigation*, pp. 1–14.

Okumura, N., Nakano, S., Kay, E. P., Numata, R., Ota, A., Sowa, Y., Sakai, T., Ueno, M., Kinoshita, S. and Koizumi, N. (2014) 'Involvement of Cyclin D and p27 in Cell Proliferation Mediated by ROCK Inhibitors Y-27632 and Y-39983 During Corneal Endothelium Wound Healing.', *Investigative Ophthalmology and Visual Science*, 55(1), pp. 318–29. doi: 10.1167/iovs.13-12225.

Okumura, N., Okazaki, Y., Inoue, R., Kakutani, K., Nakano, S., Kinoshita, S. and Koizumi, N. (2016) 'Effect of the Rho-associated kinase inhibitor eye drop (Ripasudil) on corneal endothelial wound healing', *Investigative Ophthalmology and Visual Science*, 57(3). doi: 10.1167/iovs.15-18586.

Okumura, N., Okazaki, Y., Inoue, R., Nakano, S., Fullwood, N. J., Kinoshita, S. and Koizumi, N. (2015) 'Rho-associated kinase inhibitor eye drop (Ripasudil) transiently alters the morphology of corneal endothelial cells', *Investigative Ophthalmology and Visual Science*, 56(12), p. 7560. doi: 10.1167/iovs.15-17887.

Okumura, N., Sakamoto, Y., Fujii, K., Kitano, J., Nakano, S., Tsujimoto, Y., Nakamura, S., Ueno, M., Hagiya, M., Hamuro, J., Matsuyama, A., Suzuki, S., Shiina, T., Kinoshita, S. and Koizumi, N. (2016) 'Rho kinase inhibitor enables cell-based therapy for corneal endothelial dysfunction', *Scientific Reports*, 6(April), p. 26113. doi: 10.1038/srep26113.

Okumura, N., Ueno, M., Koizumi, N., Sakamoto, Y., Hirata, K., Hamuro, J. and Kinoshita, S. (2009) 'Enhancement on primate corneal endothelial cell survival in vitro by a ROCK inhibitor.', *Investigative Ophthalmology and Visual Science*, 50(8), pp. 3680–7.

Olsen, E. G. and Davanger, M. (1984) 'The healing of human corneal endothelium. An in vitro study', *Acta Ophthalmologica*, 62(6), pp. 885–892.

Park, C. Y., Lee, J. K., Gore, P. K., Lim, C. Y. and Chuck, R. S. (2015) 'Keratoplasty in the United States: A 10-year review from 2005 through 2014', *Ophthalmology*, 122(12), pp. 2432–2442. doi: 10.1016/j.ophtha.2015.08.017.

Patel, S. V., Hodge, D. O. and Bourne, W. M. (2005) 'Corneal endothelium and postoperative outcomes 15 years after penetrating keratoplasty', *American Journal of Ophthalmology*, 139(2), pp. 311–319. doi: 10.1016/j.ajo.2004.09.045.

Peh, G. S. L., Adnan, K., George, B. L., Ang, H.-P., Seah, X.-Y., Tan, D. T. and Mehta, J. S. (2015) 'The effects of Rho-associated kinase inhibitor Y-27632 on primary human corneal endothelial cells propagated using a dual media approach', *Scientific Reports*, 5, pp. 1–10.

Petroll, W. M., Barry-Lane, P. a, Cavanagh, H. D. and Jester, J. V (1997) 'ZO-1 reorganization and myofibroblast transformation of corneal endothelial cells after freeze injury in the cat.', *Experimental Eye Research*, 64(2), pp. 257–267.

Pineros, O., Cohen, E. J., Rapuano, C. J. and Laibson, P. R. (1996) 'Long-term results after penetrating keratoplasty for Fuchs' endothelial dystrophy', *Archives of Ophthalmology*, 114(1), pp. 15–18. doi: 10.1001/archopht.1996.01100130013002.

Pipparelli, A., Arsenijevic, Y., Thuret, G., Gain, P., Nicolas, M. and Majo, F. (2013) 'ROCK inhibitor enhances adhesion and wound healing of human corneal endothelial cells.', *PLoS ONE*, 8(4), p. e62095.

Ramsay, A. S., Lee, W. R. and Mohammed, A. (1997) 'Changing indications for penetrating keratoplasty in the West of Scotland from 1970 to 1995', *Eye*, 11(3), pp. 357–360. doi: 10.1038/eye.1997.75.

Reinstein, D. Z., Archer, T. J., Gobbe, M., Silverman, R. H. and Coleman, D. J. (2008) 'Epithelial thickness in the normal cornea: three-dimensional display with very high frequency ultrasound', *Journal of Refractive Surgery*, 24(6), pp. 571–581. doi: 10.1016/j.bbi.2008.05.010.

Reneker, L. W., Silversides, D. W., Xu, L. and Overbeek, P. a (2000) 'Formation of corneal endothelium is essential for anterior segment development - a transgenic mouse model of anterior segment dysgenesis.', *Development*, 127(3), pp. 533–542.

Repp, D. J., Hodge, D. O., Baratz, K. H., McLaren, J. W. and Patel, S. V (2013) 'Fuchs' endothelial corneal dystrophy: subjective grading versus objective grading based on the central-to-peripheral thickness ratio.', *Ophthalmology*, 120(4), pp. 687–94.

Riazuddin, A. S., Vithana, E. N., Seet, L.-F., Liu, Y., Al-Saif, A., Koh, L. W., Heng, Y. M., Aung, T., Meadows, D. N., Eghrari, A. O., Gottsch, J. D. and Katsanis, N. (2010) 'Missense mutations in the sodium borate cotransporter SLC4A11 cause late-onset Fuchs corneal dystrophy.', *Human Mutation*, 31(11), pp. 1261–8. doi: 10.1002/humu.21356.

Riazuddin, A. S., Zaghloul, N. A., Al-Saif, A., Davey, L., Diplas, B. H., Meadows, D. N., Eghrari, A. O., Minear, M. A., Li, Y. J., Klintworth, G. K., Afshari, N., Gregory, S. G., Gottsch, J. D. and Katsanis, N. (2010) 'Missense mutations in TCF8 cause late-onset Fuchs corneal dystrophy and interact with FCD4 on chromosome 9p', *American Journal of Human Genetics*, 86(1), pp. 45–53. doi: 10.1016/j.ajhg.2009.12.001.

Riazuddin, S. A., Eghrari, A. O., Al-Saif, A., Davey, L., Meadows, D. N., Katsanis, N. and Gottsch, J. D. (2009) 'Linkage of a mild late-onset phenotype of Fuchs corneal dystrophy to a novel locus at 5q33.1-q35.2', *Investigative Ophthalmology and Visual Science*, 50(12), pp. 5667–5671. doi: 10.1167/iovs.09-3764.

Ringvold, a, Davanger, M. and Olsen, E. G. (1984) 'On the spatial organization of the cornea endothelium.', *Acta Ophthalmologica*, 62(6), pp. 911–8.

Robert, M. C., Choronzey, M. E., Lapointe, J., Gauvin Meunier, L. P., Harissi-Dagher, M., Germain, M., Mabon, M. and Brunette, I. (2015) 'Evolution of corneal transplantation in the province of Quebec from 2000 to 2011', *Cornea*, 34(8), pp. 880–887. doi: 10.1097/ICO.0000000000000481.

Rosenblum, P., Stark, W. J., Maumenee, I. H., Hirst, L. W. and Maumenee, A. E. (1980) 'Hereditary Fuchs' Dystrophy.', *American Journal of Ophthalmology*, 90(4), pp. 455–62. doi: 10.1016/S0002-9394(14)75011-1.

Ruiz-Ederra, J., García, M., Hernández, M., Urcola, H., Hernández-Barbáchano, E., Araiz, J. and Vecino, E. (2005) 'The pig eye as a novel model of glaucoma.', *Experimental Eye Research*, 81(5), pp. 561–9.

Savagner, P. (2001) 'Leaving the neighborhood: Molecular mechanisms involved during epithelial-mesenchymal transition', *BioEssays*, 23(10), pp. 912–923. doi: 10.1002/bies.1132.

Schröder, M. and Kaufman, R. J. (2005) 'ER stress and the unfolded protein

response', *Mutation Research - Fundamental and Molecular Mechanisms of Mutagenesis*, 569(1–2), pp. 29–63. doi: 10.1016/j.mrfmmm.2004.06.056.

Sebbagh, M., Renvoizé, C., Hamelin, J., Riché, N., Bertoglio, J. and Bréard, J. (2001) 'Caspase-3-mediated cleavage of ROCK I induces MLC phosphorylation and apoptotic membrane blebbing', *Nature Cell Biology*, 3(4), pp. 346–352. doi: 10.1038/35070019.

Shah, R. D., Randleman, J. B. and Grossniklaus, H. E. (2012) 'Spontaneous corneal clearing after Descemet's stripping without endothelial replacement', *Ophthalmology*, 119(2), pp. 256–260.

Staatz, W. D. and Van Horn, D. L. (1980) 'The effects of aging and inflammation on corneal endothelial wound healing in rabbits.', *Investigative Ophthalmology and Visual Science*, 19(8), pp. 983–986.

Steinberg, S., de Jong, S., Andreassen, O. A., Werge, T., Børglum, A. D., Mors, O., Mortensen, P. B., Gustafsson, O., Costas, J., Pietiläinen, O. P. H., Demontis, D., Papiol, S., Huttenlocher, J., Mattheisen, M., Breuer, R., Vassos, E., Giegling, I., Fraser, G., Walker, N., Tuulio-Henriksson, A., Suvisaari, J., Lönnqvist, J., Paunio, T., Agartz, I., Melle, I., Djurovic, S., Strengman, E., Jürgens, G., Glenthøj, B., Terenius, L., Hougaard, D. M., Ørntoft, T., Wiuf, C., Didriksen, M., Hollegaard, M. V., Nordentoft, M., van Winkel, R., Kenis, G., Abramova, L., Kaleda, V., Arrojo, M., Sanjuán, J., Arango, C., Sperling, S., Rossner, M., Ribolsi, M., Magni, V., Siracusano, A., Christiansen, C., Kiemeney, L. A., Veldink, J., van den Berg, L., Ingason, A., Muglia, P., Murray, R., Nöthen, M. M., Sigurdsson, E., Petursson, H., Thorsteinsdottir, U., Kong, A., Rubino, I. A., de Hert, M., Réthelyi, J. M., Bitter, I., Jönsson, E. G., Golimbet, V., Carracedo, A., Ehrenreich, H., Craddock, N., Owen, M. J., O'Donovan, M. C., Ruggeri, M., Tosato, S., Peltonen, L., Ophoff, R. A., Collier, D. A., St Clair, D., Rietschel, M., Cichon, S., Stefansson, H., Rujescu, D. and Stefansson, K. (2011) 'Common variants at VRK2 and TCF4 conferring risk of schizophrenia', *Human Molecular Genetics*, 20(20), pp. 4076–4081. doi: 10.1093/hmg/ddr325.

Stocker, F. W. and Irish, A. (1969) 'Ultimate fate of successful corneal grafts done for endothelial dystrophy (Fuchs's)', *Transactions of the American Ophthalmological Society*, 67.

Sundin, O. H., Broman, K. W., Chang, H. H., Vito, E. C. L., Stark, W. J. and Gottsch, J. D. (2006) 'A common locus for late-onset Fuchs corneal dystrophy maps to 18q21.2-q21.32', *Investigative Ophthalmology and Visual Science*, 47(9), pp. 3919–3926. doi: 10.1167/iovs.05-1619.

Sundin, O. H., Jun, A. S., Broman, K. W., Liu, S. H., Sheehan, S. E., Vito, E. C. L., Stark, W. J. and Gottsch, J. D. (2006) 'Linkage of late-onset Fuchs corneal dystrophy to a novel locus at 13pTel-13q12.13.', *Investigative Ophthalmology and Visual Science*, 47(1), pp. 140–5. doi: 10.1167/iovs.05-0578.

Tan, D. T. H., Dart, J. K. G., Holland, E. J. and Kinoshita, S. (2012) 'Corneal transplantation.', *Lancet*, 379(9827), pp. 1749–61. doi: 10.1016/S0140-

6736(12)60437-1.

Tan, J. C. H., Holland, S. P., Dubord, P. J., Moloney, G., McCarthy, M. and Yeung, S. N. (2014) 'Evolving indications for and trends in keratoplasty in British Columbia, Canada, from 2002 to 2011: A 10-year review', *Cornea*, 33(3), pp. 252–256. doi: 10.1097/ICO.0000000000000066.

Tang, H., Zhang, W., Yan, X.-M., Wang, L.-P., Dong, H., Shou, T., Lei, H. and Guo, Q. (2016) 'Analysis of SLC4A11, ZEB1, LOXHD1, COL8A2 and TCF4 gene sequences in a multi-generational family with late-onset Fuchs corneal dystrophy.', *International Journal of Molecular Medicine*, 37(6), pp. 1487–500. doi: 10.3892/ijmm.2016.2570.

Terry, M. a, Chen, E. S., Shamie, N., Hoar, K. L. and Friend, D. J. (2008) 'Endothelial cell loss after Descemet's stripping endothelial keratoplasty in a large prospective series.', *Ophthalmology*, 115(3), p. 488–496.e3. doi: 10.1016/j.ophtha.2007.10.035.

Thompson, R. W., Price, M. O., Bowers, P. J. and Price, F. W. (2003) 'Long-term graft survival after penetrating keratoplasty', *Ophthalmology*, 110(7), pp. 1396–1402. doi: 10.1016/S0161-6420(03)00463-9.

Thuret, G., Manissolle, C., Campos-Guyotat, L., Guyotat, D., Gain, P., Thuret, G., Manissolle, C., Campos-Guyotat, L., Guyotat, D. and Gain, P. (2005) 'Animal compound-free medium and poloxamer for human corneal organ culture and deswelling', *Investigative Ophthalmology and Visual Science*, 46(3), pp. 816–822. doi: 10.1167/iovs.04-1078.

Trelstad, R. L. and Coulombre, A. J. (1971) 'Morphogenesis of the collagenous stroma in the chick cornea', *Journal of Cell Biology*, 50(3), pp. 840–858. doi: 10.1083/jcb.50.3.840.

Tuft, S. J. and Coster, D. J. (1990) 'The corneal endothelium.', *Eye*, 4, pp. 389–424. doi: 10.1038/eye.1990.53.

Tuft, S. J., Williams, K. A. and Coster, D. J. (1986) 'Endothelial repair in the rat cornea.', *Investigative Ophthalmology and Visual Science*, 27(8), pp. 1199–204.

Uehata, M., Ishizaki, T., Satoh, H., Ono, T., Kawahara, T., Morishita, T., Tamakawa, H., Yamagami, K., Inui, J., Maekawa, M. and Narumiya, S. (1997) 'Calcium sensitization of smooth muscle mediated by a Rho-associated protein kinase in hypertension', *Nature*, 389(6654), pp. 990–994. doi: 10.1038/40187.

Ventura, a C., Wälti, R. and Böhnke, M. (2001) 'Corneal thickness and endothelial density before and after cataract surgery.', *The British Journal of Ophthalmology*, 85(1), pp. 18–20. doi: 10.1136/bjo.85.1.18.

Vithana, E. N., Morgan, P. E., Ramprasad, V., Tan, D. T. H., Yong, V. H. K.,

Venkataraman, D., Venkatraman, A., Yam, G. H. F., Nagasamy, S., Law, R. W. K., Rajagopal, R., Pang, C. P., Kumaramanickevel, G., Casey, J. R. and Aung, T. (2008) 'SLC4A11 mutations in Fuchs endothelial corneal dystrophy.', *Human Molecular Genetics*, 17(5), pp. 656–66. doi: 10.1093/hmg/ddm337.

Walshe, J., Richardson, N. A., Al Abdulsalam, N. K., Stephenson, S. A. and Harkin, D. G. (2018) 'A potential role for Eph receptor signalling during migration of corneal endothelial cells', *Experimental Eye Research*, 170(January), pp. 92–100. doi: 10.1016/j.exer.2018.02.017.

Wang, Z., Handa, J. T., Green, W. R., Stark, W. J., Weinberg, R. S. and Jun, A. S. (2007) 'Advanced glycation end products and receptors in Fuchs' dystrophy corneas undergoing Descemet's stripping with endothelial keratoplasty', *Ophthalmology*, 114(8), pp. 1453–1460. doi: 10.1016/j.ophtha.2006.10.049.

Waring, G. O., Bourne, W. M., Edelhauser, H. F. and Kenyon, K. R. (1982) 'The corneal endothelium: normal and pathologic structure and function', *Ophthalmology*, 89(6), pp. 531–590. doi: 10.1016/S0161-6420(82)34746-6.

Waring, G. O., Rodrigues, M. M. and Laibson, P. R. (1978) 'Corneal dystrophies. II. Endothelial dystrophies.', *Survey of Ophthalmology*, 23(3), pp. 147–68.

Watanabe, K., Ueno, M., Kamiya, D., Nishiyama, A., Matsumura, M., Wataya, T., Takahashi, J. B., Nishikawa, S., Nishikawa, S., Muguruma, K. and Sasai, Y. (2007) 'A ROCK inhibitor permits survival of dissociated human embryonic stem cells.', *Nature Biotechnology*, 25, pp. 681–686. doi: 10.1038/nbt1310.

Watson, S. L., Abiad, G. and Coroneo, M. T. (2006) 'Spontaneous resolution of corneal oedema following Descemet's detachment', *Clinical and Experimental Ophthalmology*, 34(8), pp. 797–799. doi: 10.1111/j.1442-9071.2006.01319.x.

Weiss, J. S., Møller, H. U., Aldave, A. J., Seitz, B., Bredrup, C., Kivelä, T., Munier, F. L., Rapuano, C. J., Nischal, K. K., Kim, E. K., Sutphin, J., Busin, M., Labbé, A., Kenyon, K. R., Kinoshita, S. and Lisch, W. (2015) 'IC3D classification of corneal dystrophies—edition 2', *Cornea*, 34(2), pp. 117–159. doi: 10.1097/ICO.0000000000000307.

WHO (2018) *Causes of blindness and visual impairment*, *World Health Organisation*. Available at: http://www.who.int/blindness/causes/en/%0A (Accessed: 6 September 2018).

Wieben, E. D., Aleff, R. A., Tosakulwong, N., Butz, M. L., Highsmith, W. E., Edwards, A. O. and Baratz, K. H. (2012) 'A common trinucleotide repeat expansion within the transcription factor 4 (TCF4, E2-2) gene predicts Fuchs corneal dystrophy', *PLoS ONE*, 7(11), pp. 5–12. doi: 10.1371/journal.pone.0049083.

Wolf, A. H., Welge-Lüen, U. C., Priglinger, S., Kook, D., Grueterich, M., Hartmann, K., Kampik, A. and Neubauer, A. S. (2009) 'Optimizing the deswelling process of organ-cultured corneas', *Cornea*, 28(5), pp. 524–529. doi: 10.1097/ICO.0b013e3181901dde.

Wulle, K. G. (1972) 'Electron microscopy of the fetal development of the corneal endothelium and Descemet's membrane of the human eye.', *Investigative Ophthalmology*, 11(11), pp. 897–904.

Yamamoto, M., Quantock, A. J., Young, R. D., Okumura, N., Ueno, M., Sakamoto, Y., Kinoshita, S. and Koizumi, N. (2012) 'A selective inhibitor of the Rho kinase pathway, Y-27632, and its influence on wound healing in the corneal stroma.', *Molecular Vision*, 18, pp. 1727–39.

Yamashita, K., Inagaki, E., Hatou, S., Higa, K., Ogawa, A., Miyashita, H., Tsubota, K. and Shimmura, S. (2018) 'Corneal endothelial regeneration using mesenchymal stem cell derived from human umbilical cord', *Stem Cells and Development*, 27(16), p. scd.2017.0297. doi: 10.1089/scd.2017.0297.

Yeh, C. J. (2000) 'Simple cryosurgical treatment for oral lesions', *International Journal of Oral and Maxillofacial Surgery*, 29(3), pp. 212–216. doi: 10.1016/S0901-5027(00)80096-X.

Yureeda, Q. and Hamrah, P. (2013) 'Corneal allograft rejection: immunopathogenesis to therapeutics', *Journal of Clinical & Cellular Immunology*, (Suppl 9), pp. 1–21. doi: 10.4172/2155-9899.S9-006.

Zafirakis, P., Kymionis, G. D., Grentzelos, M. A. and Livir-Rallatos, G. (2010) 'Corneal graft detachment without corneal edema after Descemet stripping automated endothelial keratoplasty', *Cornea*, 29, pp. 456–458.

Zhao, M., Thuret, G., Piselli, S., Pipparelli, A., Acquart, S., Peoc'H, M., Dumollard, J. M. and Gain, P. (2008) 'Use of poloxamers for deswelling of organ-cultured corneas', *Investigative Ophthalmology and Visual Science*, 49(2), pp. 550–559. doi: 10.1167/iovs.07-1037.

Ziaei, M., Barsam, A. and Mearza, A. A. (2013) 'Spontaneous corneal clearance despite graft removal in Descemet stripping endothelial keratoplasty in Fuchs endothelial dystrophy.', *Cornea*, 32(7), pp. e164--e166.

Zinn, K. M. (1970) 'Changes in corneal ultrastructure resulting from early lens removal in the developing chick embryo', *Investigative Ophthalmology and Visual Science*, 9(3), pp. 165–182.

Zoega, G. M., Fujisawa, A., Sasaki, H., Kubota, A., Sasaki, K., Kitagawa, K. and Jonasson, F. (2006) 'Prevalence and risk factors for cornea guttata in the Reykjavik eye study', *Ophthalmology*, 113(4), pp. 565–569. doi: 10.1016/j.ophtha.2005.12.014.

Appendix A: Publication 1

Chan, W., **Akhbanbetova, A**., Quantock, A. J. and Heard, C. M. (2016) 'Topical delivery of a Rho-kinase inhibitor to the cornea via mucoadhesive film', *European Journal of Pharmaceutical Sciences*, 91. doi: 10.1016/j.ejps.2016.05.016.

European Journal of Pharmaceutical Sciences 91 (2016) 256–264

Contents lists available at ScienceDirect

European Journal of Pharmaceutical Sciences

journal homepage: www.elsevier.com/locate/ejps

Topical delivery of a Rho-kinase inhibitor to the cornea via mucoadhesive film

Wendy Chan [a], Alina Akhbanbetova [b], Andrew J. Quantock [b], Charles M. Heard [a,*]

[a] School of Pharmacy and Pharmaceutical Sciences, Cardiff University, King Edward VII Avenue, Cardiff CF10 3NB, Wales, UK
[b] School of Optometry & Vision Sciences, Cardiff University, Maindy Road, Cardiff, CF24 4HQ, Wales, UK

ARTICLE INFO

Article history:
Received 7 March 2016
Received in revised form 29 April 2016
Accepted 14 May 2016
Available online 16 May 2016

Keywords:
ROCK inhibitor
Ocular delivery
Cornea
Cryoprobe
Diffusional release
Mucadhesive film
Topical delivery

ABSTRACT

The application of inhibitors of the Rho kinase pathway (ROCK inhibitors) to the surface of the eye in the form of eyedrops has beneficial effects which aid the recovery of diseased or injured endothelial cells that line the inner surface of the cornea. The aim of this study was to test the plausibility of delivering a selective ROCK inhibitor, Y-27632, to the cornea using a thin polymeric film. Mucoadhesive polymeric thin films were prepared incorporating Y-27632 and diffusional release into PBS was determined. Topical ocular delivery from the applied film was investigated using freshly excised porcine eyes and eyedrops of equivalent concentration acted as comparators; after 24 h the formulations were removed and the corneas extracted. Drug-loaded thin polymeric films, with high clarity and pliability were produced. ROCK inhibitor Y-27632 was weakly retained within the film, with release attaining equilibrium after 1 h. This in turn facilitated its rapid ocular delivery, and an approximately three-fold greater penetration of Y-27632 into cryoprobe-treated corneas was observed from the thin film ($p < 0.01$) compared to eyedrops. These findings support the further development of ROCK inhibitor delivery to the cornea via release from thin mucoadhesive films to treat vision loss cause by corneal endothelial dysfunction.

1. Introduction

The cornea of the eye, which is just over 0.5 mm thick in humans, owes its transparency to the characteristic spatial arrangement of its constituent collagens and other extracellular matrix components which make up much of its thickness (Knupp et al., 2009; Meek and Knupp, 2015). Lining the inner surface of the cornea is a single layer of metabolically active endothelial cells which separate the corneal matrix from the adjacent aqueous humor and prevent the ingress of fluid into the cornea (Hodson and Miller, 1976). If the endothelial cell layer is compromised the cornea swells and becomes oedematous, scatters light and loses its transparency. This results in severe vision loss and in most cases the only option is corneal transplant surgery. Typically, corneal endothelial dysfunction occurs because of an inherited disease called Fuch's endothelial corneal dystrophy (FECD) in which corneal endothelial cells deteriorate or are lost over the years. It can also occur as a result of accidental damage to the corneal endothelium during cataract surgery to remove or replace the lens of the eye, and this condition is often referred to as bullous keratopathy. Either way, the endothelial cell damage causes cornea to imbibe excess fluid and swell, making the cornea appear hazy (Fig. 1) clouding vision (Fig. 2) (Heiting, 2015; Royal National Institute of Blind People, 2015).

Techniques to treat vision loss caused by corneal endothelial dysfunction include an anterior corneal micropuncture and laser treatment to puncture the corneal epithelium. Although these procedures can be effective they carry a high risk of rejection and sometimes result in complications including corneal perforation and scarring (Rahman et al., 2008). But, by far the most common treatment for corneal endothelial dysfunction is a corneal graft, and the numbers of surgeries performed indicate the scale of the problem. The prevalence of FECD, generally, is estimated to be around 4% of individuals over the age of 40, but in inbred American, Singaporean and Icelandic populations this rises to 22%, 7% and 9% respectively (Zoega et al., 2006; Eghrari et al., 2012; Kitagawa et al., 2002).

In terms of drug therapy, the ROCK signaling pathway has received recent attention in light of the diverse therapeutic potential of changing cell behaviour in various diseases such as hypertension, vasospasm, and glaucoma (Arnold et al., 2013); and more recently FECD (Koizumi et al., 2013; Okumura et al., 2009, 2011, 2013, 2015; Nakagawa et al., 2015). ROCK inhibitors are protein serine/threonine kinases with various functions throughout the body (Riento and Ridley, 2003). Out of several different ROCK inhibitors with different therapeutic effects (Liao et al., 2007; Wang and Chang, 2014), a selective ROCK inhibitor Y-27632 was reported to have promoted the proliferation of corneal endothelial cells in vitro (Okumura et al., 2009) and the healing of the corneal endothelium in vivo (Okumura et al., 2011). Sufficient corneal endothelial cell density is crucial for the ionic pump and barrier functions (Okumura et al., 2013), which in FECD would lead to an increased overall cell size and cell shape alteration, resulting in endothelial

* Corresponding author.
E-mail address: heard@cardiff.ac.uk (C.M. Heard).

http://dx.doi.org/10.1016/j.ejps.2016.05.016

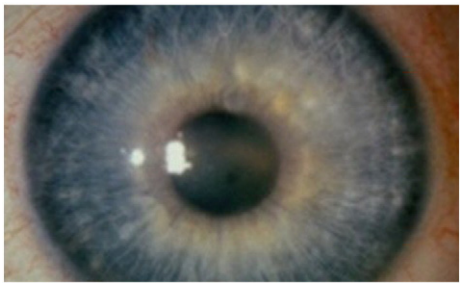

Fig. 1. Corneal haze of Fuchs Dystrophy.

dysfunction, and it was reported that Y-27632 was able to enhance cell density to the normal levels and resume the pump and barrier function, providing a functional recovery of the cornea. Koizumi et al. (2013) reported that some patients with FECD could be treated with ROCK inhibitor Y-27632 eye drops subsequent to transcorneal freezing to destroy damaged corneal endothelial cells.

The delivery of drugs to the eye is basically divided into three routes; topical, systemic and intraocular. The intraocular route involves an injection into the eye or use of implants, which is surgically fairly invasive, carries the risk if infection and is seen undesirable by patients. Systemic delivery is inefficient with potential unwanted side effects. The topical delivery of drugs to the eye is thus judged to be an attractive route. Examples of topical delivery include the use of eye drop solutions, ointments, suspensions and emulsions. Eye drops are widely used, but are easily washed out by blinking and nasolacrimal drainage; this means that only a small amount of the applied dose is likely to penetrate the cornea. Ointment, suspension and emulsion formulations are widely reported to cause ocular adverse effects, which include irritation and visual disturbance (Patel et al., 2013). Studies have been carried out on alternative topical approaches such as the OCUSERT® system, Topical Opthalmic Drug Delivery Device, medicated contact lenses and intraocular lenses (Morrison, 2015). However, none of these approaches are available commercially on the market. In this study, we investigated an alternative approach based upon drug-eluting thin polymeric muacoadhesive films that affix to the cornea, in an effort to improve the drawbacks of current methods. Our approach could conceivably lead to a more efficacious and user-friendly device capable of targeted delivery of ROCK inhibitors to attain improved clinical effect. Such therapy would also minimize wastage of costly ROCK inhibitor and avoid potential toxicity from dosing other tissues unnecessarily, in particular the tear duct and nasal cavity. Therefore, the hypothesis of this study is that topical delivery of ROCK inhibitor Y-27632 from thin mucoadhesive films is a superior alternative to eye drops for trans-corneal drug delivery. This study aimed to test the plausibility of topical delivery to the cornea from polymeric films by the fabrication of appropriate films, determination of drug release and finally the determination of trancorneal drug delivery in vitro.

Fig. 2. The hazy and clouded vision of a Fuchs patient (left) as compared to normal vision.

2. Materials and methods

2.1. Materials

ROCK inhibitor Y-27632 dihydrochloride (MW 247.3) was obtained from ApexBio Technology LLC (Houston, US). Acetonitrile (HPLC grade), water (HPLC grade) and phosphate buffered saline (PBS) tablets were obtained from Fisher Scientific (Loughborough, UK). Methylene blue (MW 319.9), polyethylene glycol 400 (PEG 400) and trifluoroacetic acid (≥99.0%) were from Sigma-Aldrich Company Ltd. (Poole, UK). Carbopol 917 (CP) was a gift from Noveon Inc. (Cleveland, U.S.) and hydroxyproplymethyl cellulose (HPMC) was a gift from Shin-Etsu Chemical Co. Ltd. (Tokyo, Japan). Porcine eyeballs were obtained from a local abattoir by blunt dissection, immediately following slaughter.

2.2. Preparation of thin films

Ingredients were weighed into a 250 mL conical flask as detailed in Table 1 to provide a 1% w/v polymeric solution loaded with either 1.7, 5.2 or 10 mg Y-27632·2HCl; the aqueous solubility of Y-27632·2HCl is reported as 14 mg/mL (Santa Cruz Biotechnology) and that of methylene blue 43.6 mg/L (Pubchem). The mixtures were stirred overnight on a magnetic stirrer at room temperature. The following day, the mixtures were placed in an ultrasonic bath for 2 h to further assist particle comminution, and to degas the solution. Next, 50 mL of the solutions were poured into Petri dishes and left to dry in an oven overnight set at 60 °C. Once completely dry, the clear films were carefully removed from the petri dish and checked for any imperfections – those that had bubbles or crystals were discarded.

2.3. Diffusional release from thin films

Ten 0.5 × 0.5 cm patches were excised from each drug loaded film and each patch was accurately weighed before being immersed in 1 mL of PBS solution in an Eppendorf tube for various durations (10 s, 20 s, 30 s, 1 min, 2 min, 5 min, 30 min, 1 h, 3 h and 6 h). The patches were then carefully removed from the PBS solution with forceps. The remaining solutions were transferred to autosampler vials, prior to analysis by HPLC (Section 2.8). The diffusional release was carried out over the timescale of up to 6 h to broadly simulate an overnight dosage

Table 1
Working formulae to produce methylene blue and ROCK inhibitor Y-27632 films.

Film	Working formula	
Methylene blue	HPMC	0.175 g
	PEG 400	0.25 g
	CP	0.075 g
	Methylene blue	0.01 g
	DI H_2O	to 50 mL
ROCK inhibitor Y-27632 10 mg	HPMC	0.175 g
	PEG 400	0.25 g
	CP	0.075 g
	Y-27632·2HCl	10 mg
	DI H_2O	to 50 mL
ROCK inhibitor Y-27632 5.2 mg	HPMC	0.175 g
	PEG 400	0.25 g
	CP	0.075 g
	Y-27632·2HCl	5.2 mg
	DI H_2O	to 50 mL
ROCK inhibitor Y-27632 1.7 mg	HPMC	0.175 g
	PEG 400	0.25 g
	CP	0.075 g
	Y-27632·2HCl	1.7 mg
	DI H_2O	to 50 mL

application. Preliminary method development experiments were carried out with methylene blue film.

2.4. Transcorneal freezing of porcine eyes

Transcorneal freezing has been used as a therapeutic modality prior to Y-27632 application in the form of eye drops (Koizumi et al., 2013). In the experiments described here, to test if cryoprobe-treated eyeballs achieved a better ingress of drug, transcorneal freezing was conducted (Fig. 3) by gently touching the tip of a newly designed cryoprobe onto the surface of freshly obtained porcine eyeballs for 3 s, which we have shown to be optimal to produce reliable and reproducible areas of corneal endothelial cell death. The cryoprobe tip is 3.4 mm in diameter and reaches −50 °C via the internal expansion of a cryogen (medical grade nitrous oxide), and is made of silver for heightened thermal conductivity. Six of 12 eyeballs used for the experiment underwent transcorneal freezing and six did not.

2.5. Formulation of eye drops

Eyedrops of equal concentration to the methylene blue and ROCK inhibitor Y-27632 film were formulated to act as a control. The working formulae of the eyedrops are detailed in Table 2. The concentration of Y-27632 incorporated was designed to replicate the concentration used previously, which is 10 mM (Koizumi et al., 2013).

2.6. Ocular delivery from applied formulations, in vitro

Freshly excised porcine eyeballs were placed, cornea uppermost, in a 6-well cell culture plate. Circular patches, 1 cm in diameter, were excised from the medicated (methylene blue or Y-27632) mucoadhesive films (n = 3) using a cork borer and applied to the corneas, which had been wetted beforehand with 300 μL PBS, and a combination of capillarity and film deformability ensured contact with the cornea. Eye drops of equal concentration were also applied to porcine eyeballs as a comparator (n = 3 for Y-27632, n = 2 for methylene blue). To simulate blinking and tearing, the eyes were periodically irrigated with 300 μL isotonic PBS. Y-27632 eye drops were used based on the dosing procedure reported by Koizumi et al. (2013), in which 50 μL of 10 mM Y-27632 was applied six times a day. To limit dehydration the eyeballs were placed in PBS, such that the solution reached half way up the eye (not contacting the cornea). The set-up was covered with a plastic lid to retain moisture and was incubated in a water bath at 37 °C overnight. The eyes were periodically bathed with aliquots of PBS in an effort to simulate tears (Chan et al., 2014).

After 24 h, films were carefully removed from the corneas using fine forceps and the corneal surface of eye-drop treated eyes were gently wiped with cotton buds. Corneas were then excised from the eyes and each was cut into small pieces before being comminuted to a fine powder using a mortar and pestle after being frozen in liquid nitrogen. The powders were carefully recovered and extracted into water after placing on a rotating blood tube mixer overnight. Tubes were then centrifuged at 5750 rpm for 30 min, the supernatant decanted and evaporated at 60 °C in an oven. The residue was reconstituted in 1 mL of deionised H_2O, prior to analysis by HPLC.

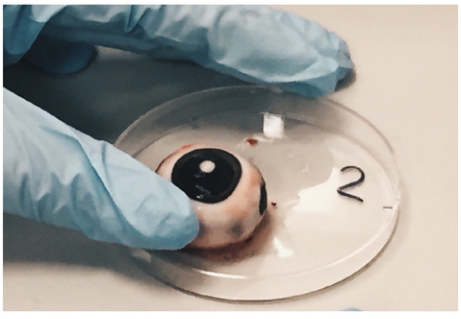

Fig. 3. Thaw forming in the middle of the eyeball, showing transcorneal freezing has taken place.

Table 2
Working formulae of methylene blue and ROCK inhibitor Y-27632 comparator eyedrops.

Eyedrops	Working formula	
Methylene blue	Methylene blue	87.7 mg
	DI H_2O	to 5 mL
ROCK inhibitor Y-27632	Y-27632	16 mg
	DI H_2O	to 5 mL

2.7. HPLC analysis of methylene blue and ROCK inhibitor Y-27632

The concentration of methylene blue and ROCK inhibitor Y-27632 released from each film and extracted from each cornea was quantified by reverse phase HPLC using an Agilent series 1100 HPLC system, fitted with a Phenomenex Kinetex 5μ C18 100 Å 150 × 4.6 mm column, eluted with a mobile phase comprised of H_2O:ACN (50:50 v/v) with 0.5% of TFA. The flow rate was 1 mL min^{-1}. For methylene blue the wavelength was 246 nm and the retention time 3.9 min; for Y-27632 the wavelength was 270 nm and retention time was 1.5 min. Calibration curves of methylene blue and ROCK inhibitor Y-27632 were constructed using standard solutions over the concentration range of 1–3.91 × 10^{-3} mM. The linearity of the curves was as follows: R^2 = 0.9999 for methylene blue; 0.9997 for Y-27632.

2.8. Statistical analysis

All data were analyzed using an InStat 3 statistical package (GraphPad Software Inc., San Diego, CA, U.S.A). Comparisons of concentration released from formulations into native and cryoprobe-treated corneas were determined using ANOVA (Analysis of variance) and Kruskal-Wallis post-tests, where $p < 0.05$ was considered statistically significant.

3. Results and discussion

3.1. Film preparation

Initially, a blank film (i.e. not loaded with any medication) was produced and was found to have good clarity, transparency and pliability, with the entire film weighing approximately 500 mg and having an average thickness of 0.1 mm as determined using a digital micrometer. Recovery (film mass/total mass of additives except water) was 98.3%. Representative images of the films loaded with methylene blue or ROCK inhibitor Y-27632 are shown in Fig. 4(a) and (b), respectively. The films appeared optically clear and were approximately 0.1 mm thick. Both films were pliable, which is important as they are to fit well to the curved cornea. Also, it was encouraging to find no evidence of drug crystals in the films at the levels added. Crystals would be potentially damaging to the cornea and would lead to unpredictable drug release rates.

Homogeneity and recovery were determined by sampling 5 × 1 cm diameter patches from across the film, dissolving in water and assaying for drug by HPLC – no statistically significant differences were found (not shown). The recovery of the methylene blue film was 111.8% while the recovery of the Y-27632 film was higher at 129.3%. Stability was determined by sampling the film stored at room temperature over an 8 week period and assaying, again with no statistically significant differences found. The recovery of the medicated films was higher than that of the blank film probably because the drugs attract a hydration shell, resulting in a higher water content. In the case of Y-27632, which was added as the hydrochloride salt, the positive charge would

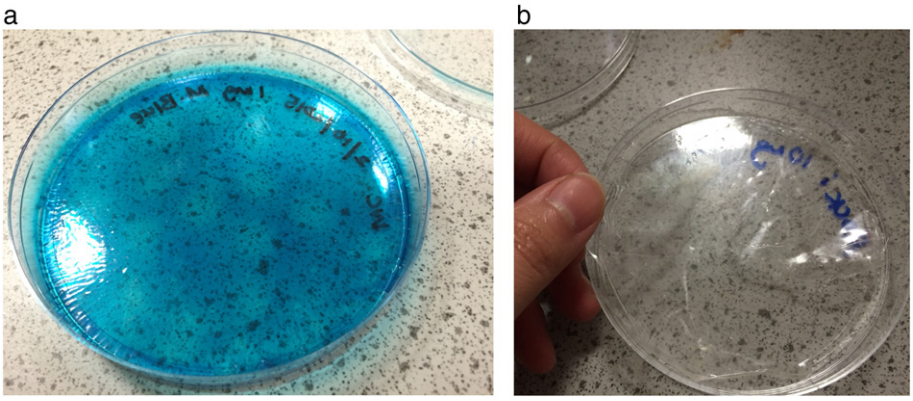

Fig. 4. (a) Methylene blue film. (b) ROCK inhibitor Y-27632 film.

attract even more water molecules. This analysis is supported by the fact that increasing the drying time did not significantly reduce the recovery.

The polymers hydroxyproplymethyl cellulose (HPMC), polyethylene glycol 400 (PEG 400) and Carbopol 917 (CP) were used in the film-forming excipients described here. The suitability of a HPMC film as a drug vehicle considered several factors, such as the mechanical properties, the swelling of films, and in vitro and in vivo bioadhesion evaluations (Peh and Wong, 1999). Compared to SCMC (sodium carboxymethyl cellulose) film, another polymer, HPMC films were shown to possess a greater bioadhesive strength value in vivo, and were reported to be tougher and more elastic. Consequently, we decided to use HPMC as our drug vehicle in this study. Moreover, PEG 400, a commonly used solubilizer which exists in liquid form, was included for its plasticizing properties, giving softness and pliability to the films to their fitting to the curved corneas. In previous experiments, PEG of a lower molecular weight (<300) had produced tough, brittle films that would not be suitable for ophthalmic applications (unpublished data). Our use of PEG 400 is supported by the work of Llabot et al. (2007) who revealed that its addition to films enhanced mucoadhesion as compared to the film without it. This can be explained by the diffusion theory of bioadhesion (Chickering and Mathiowitz, 1999) in which the intra-chain polymeric interaction is reduced in the presence of plasticizers, increasing the flexibility of the chains. This would result in strengthened mucoadhesive interactions by increasing the inter-penetration and entanglement of bioadhesive polymer chains with mucin. Carbopol is another polymer used to develop our polymeric film. It is a high molecular weight polymer containing a high content of carboxylic groups (Rowe et al., 2012), which is believed to contribute to the mucoadhesiveness of the film (Chickering and Mathiowitz, 1999). Carbopol plays an important role in increasing the softness, elasticity and bioadhesive strength of polymeric films (Lubrizol, 2015). Each of the polymers used is an approved excipient. In conclusion, the combination of HPMC, PEG 400 and CP provided homogeneous, stable, soft, pliable and mucoadhesive films, which are crucial properties of a viable product.

3.2. Diffusional release

Diffusional release is the process whereby drug molecules spontaneously migrate from the polymeric system to the exterior of the polymer and then into the release medium (Langer, 1990), which in our case was PBS to provide a basic model for tears. The diffusional release profiles of loaded drug characterize the amount of drug released from the film as a function of time into a given receiving medium. Low release is indicative of low drug loading or interaction and extensive retention of loaded drug within the film matrix; whilst this can reduce the dose delivered, it can also provide zero-order release. Zero-order kinetics is generally desirable in drug delivery systems, where drug levels released would remain constant throughout the delivery period (Ummadi et al., 2013). This is generally considered to be important in improving therapeutic outcomes and patient compliance and it also reduces the frequency of drug administration (Gokhale, 2014), which is discussed in Section 3.5. On the other hand, high release gives rise to 'burst' kinetics, and reflects excess drug added and/or weak retention within the polymer matrix – it is generally considered undesirable in drug delivery devices as it would not provide sustained release; furthermore excess drug is often present as crystals.

3.2.1. Methylene blue film

The purpose of producing a film containing methylene blue was to provide a model solute which was visible to the naked eye and allowed us to develop the film production technique – it is however, also used clinically as a photosensitizer (Tardivo et al., 2005). A diffusional release profile of methylene blue was constructed as cumulative mass and moles released, normalized per amount of film, hence, mass (mg drug mg^{-1} of film) and amount (μMol mg^{-1} of film) released are presented as a double-Y plot in Fig. 5; for further comparison purposes the percentage released (%) is also shown in Fig. 7 over the timescale of 6 h to reflect an overnight application. The intensity of the blue coloration of the receiving PBS solution visibly increased the longer the film was retained in the Eppendorf tube. From this observation it is deduced that an increased concentration of methylene blue diffused into PBS solution with increased contact time. This was verified following quantitative analysis by HPLC analysis as shown in Fig. 5, where the concentration of methylene blue released from film increased with increased immersion time. Fig. 5 shows an initial linear, or 0-order, relationship between cumulative amount and mass within the first 60 min. The rate constant, as determined from the plot gradient, was determined to be 0.0448 mg min^{-1}. The steady state phase was followed by a tailing off due to drug depletion. Methylene blue was detected in the first sample taken at 10 s as 0.22 μMol mg^{-1} (0.07 mg mg^{-1}) and at 6 h was 48.84 μMol mg^{-1} (15.62 mg mg^{-1}).

3.2.2. ROCK inhibitor Y-27632 film

Diffusional release profiles of ROCK inhibitor Y-27632 were constructed as cumulative mass (mg mg^{-1} of film) (Fig. 6a) and percentage released (%) (Fig. 6b). For further comparison purposes the percentage released (%) is also shown in Fig. 7. Drug was detected in the first samples taken at 10s (10 mg film; 1.94 mg mg^{-1}: 5.2 mg film; 1 mg mg^{-1}: 1.7 mg film; 0.99 mg mg^{-1}), with release increasing rapidly until it approaches equilibrium between 40 and 60 min (10 mg film; approximately 11.5 mg mg^{-1}: 5.2 mg film; 9 mg mg^{-1}: 1.7 mg film; 2.5 mg mg^{-1}). Thereafter, there was no major increase, and both amount and mass are proportionate to each other. Fig. 6 shows the cumulative concentration and mass of Y-27632 released over the 6 h test period. It is immediately apparent that the release profile for Y-27632 differed markedly to that of methylene blue, in that there was no

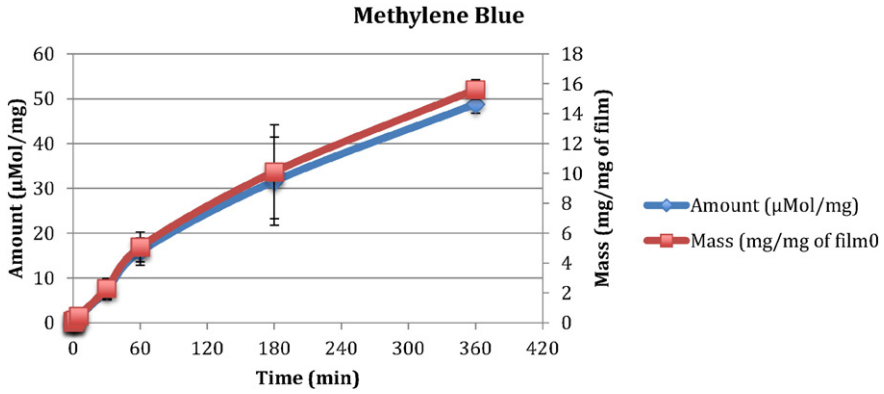

Fig. 5. Double Y-plot of methylene blue cumulative mass and μMol released over the timescale of 6 h, and normalized in terms of the mass of the film sample (n = 3 ± SD).

major steady state phase. Instead, there was a rapid rise or burst within the first 10 min.

The diffusional release of Y-27632 was replicated using three concentrations of Y-27632 films; 10 mg, 5.2 mg and 1.7 mg. The difference in concentrations has resulted in the difference in mass of Y-27632 released (Fig. 6a), so that the higher the concentration of Y-27632 within the film, the higher the mass of drug released. Interestingly, the difference between the 10 mg film and the 5.2 mg film was not large (the difference in mass was mostly kept within 2 mg mg^{-1}). However, the 10 mg film showed a clearer burst release. Mass released from the 1.7 mg film was much lower than the others where the highest mass released was only 2.8 mg mg^{-1}, but the overall release pattern was similar to both 5 mg and 10 mg films. Though concentrations varied, the percentage released was fairly similar (Fig. 6b). All three concentrations

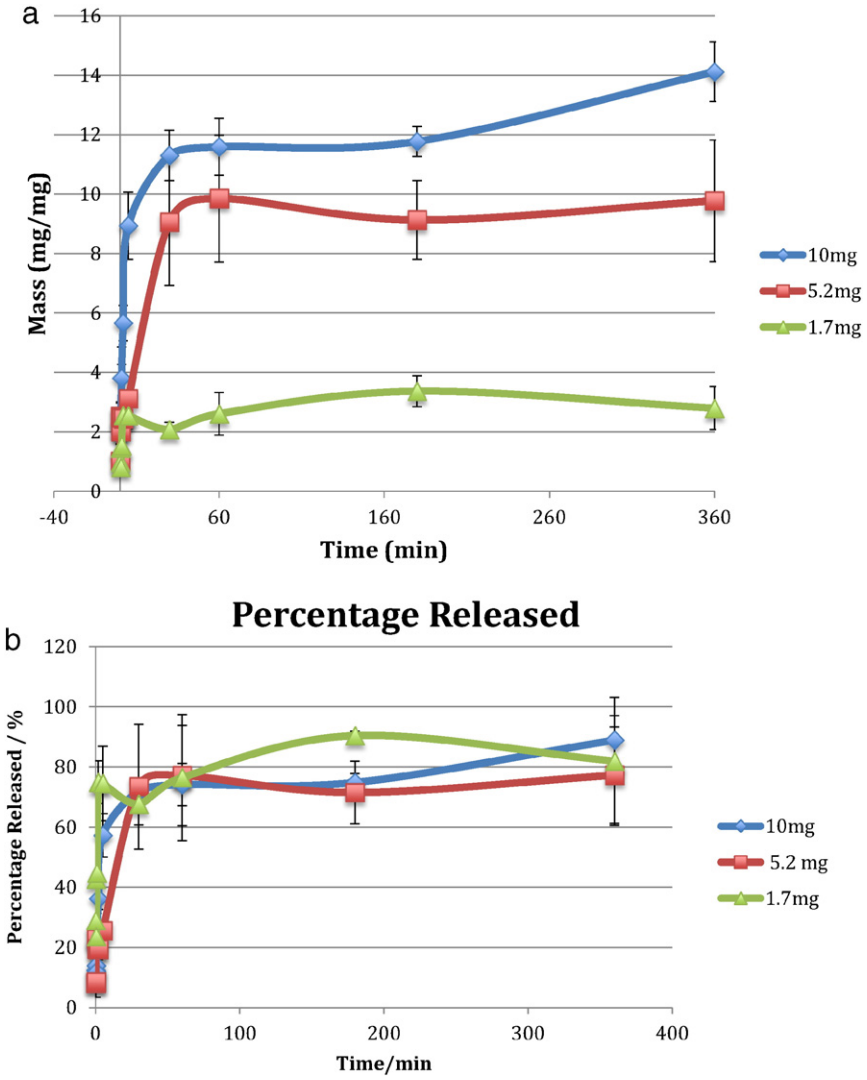

Fig. 6. (a) Cumulative drug release from thin films loaded with 1.7, 5.2 and 10 mg ROCK inhibitor Y-27632 over 6 h and normalized in terms of the mass of the film sample (n = 3 ± SD); (b) percentage of drug released from thin films loaded with 1.7, 5.2 and 10 mg ROCK inhibitor Y-27632 over 6 h (n = 3 ± SD).

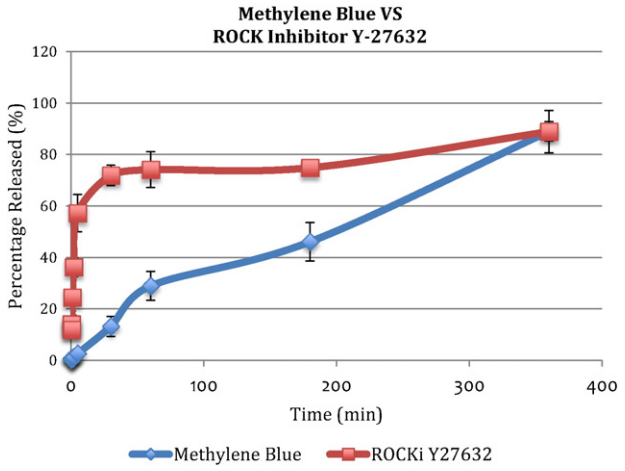

Fig. 7. Diffusional release profiles of methylene blue versus ROCK inhibitor Y-27632 in percentage released (%) (n = 2 or 3 ± SD).

showed rapid release up to approximately 70% within 30 min with a maximum release ≥80%. As the release kinetics were greatest from the 10 mg film, this was chosen to progress to the in vitro ocular delivery experiment.

3.3. Comparison of methylene blue and ROCK inhibitor Y-27632 release

Fig. 7 shows that both methylene blue and ROCK inhibitor Y-27632 were released from respective films up to approximately 90% after 6 h - the pathways appear very different, although further work will be needed to confirm this. High release indicates low retention of drug in the polymeric films, which is due to swelling and would be cost effective by reducing wastage of drugs to a minimal level. Y-27632 was found to be more weakly retained within the polymeric film than methylene blue, meaning it is more easily released, allowing more Y-27632 to penetrate the cornea; hence, a burst release from Y-27632 was observed. It is worth noting that the release of Y-27632 depleted after 40 min (approximately 80% has been released), which could have the potential benefit of getting more drugs into the eyes rapidly. While methylene blue displayed zero-order release kinetics over the 6 h timescale, Y-27632 showed mixed-order release, reaching equilibrium within 50 min. It is deduced that this is due to the lack of interaction of Y-27632 with the film polymers. It is assumed that methylene blue is able to form stronger bonds with the polymers (Chickering and Mathiowitz, 1999) and that this results in more entrapment in the polymeric film. It is also hypothesized that the burst release of Y-27632 was facilitated by its low molecular size and the presence of the charge, which the recovery data (Section 3.1) showed attracted more water. This, in turn, accelerated release of the hydrated complex into the aqueous receiving medium. It should also be borne in mind that such rapid release may be a concern if it gives rise to toxic levels in vivo (Shively et al., 1995; Jeong et al., 2000).

On a side note, methylene blue is used clinically as a visual guide during surgery or endoscopy (Tardivo et al., 2005), and is also a therapeutic agent for various conditions, including ifoasfamide-induced encephalopathy (Patel, 2006) and methemoglobinemia (Sikka et al., 2011) - the current delivery data of methylene blue using the thin film has potential relevance in such procedures.

3.4. Transcorneal freezing

As mentioned, transcorneal freezing achieved by touching the corneal surface with a cold probe can cause corneal endothelial cell death, either by forming intracellular ice that is lethal to the cell or by the formation of extracellular ice, which will create an osmotic imbalance leading to an increase in intracellular electrolytes and the collapse of cellular membranes. It was previously reported that corneal endothelial cells are expected to proliferate at the frozen wound sites after cryotherapy (Buco et al., 1978; Staatz and Van Horn, 1980), and potentially the application of Y-27632 eye drops enhances this recovery (Koizumi et al., 2013). Fig. 8 shows a picture taken upon the excision of a cryoprobe-treated cornea to which a methylene blue film had been applied. From this observation it was evident that penetration of methylene blue occurred predominantly at the centre of the cornea where transcorneal freezing took place.

3.5. Corneal penetration

As the corneal endothelium is the target site for Y-27632 following its surface application, it was important to ensure that the drug is penetrating towards the back of cornea to reach endothelial tissue. Since Y-27632 is colourless, methylene blue film was used as a model. Fig. 9 shows a schematic diagram of the cornea throughout its full thickness alongside a lateral view of the cornea from a cryoprobe-treated eyeball under a microscope. The endothelium is stained blue, depicting that drug is penetrating well through the cornea from the epithelial surface where the patch had been positioned on eye.

3.6. Ocular drug delivery

Koizumi et al. (2013) reported some patients with FECD who were successfully treated with ROCK inhibitor Y-27632 eye drops subsequent to transcorneal freezing to remove diseased and damaged corneal endothelial cells. While the reported results are encouraging, the eye drop application was repeated six times a day for 7 days. Eye drops have long been used to treat ocular pathology and injury, however, it is widely appreciated that upon application an eye drop dose is rapidly eliminated by dilution and washing out by tears and nasolacrimal drainage mechanisms. More often than not the instilled dose that enters ocular tissue is less than 1% (Morrison, 2015). Furthermore, ROCK inhibition is known to have a hypotensive effect and vascular resistance, which would result in potential adverse effects on unwanted systemic exposure (Hahmann and Schroeter, 2010). Another reported adverse effect of ROCK inhibitor eye drop application is ocular hyperemia because ROCK inhibitors are vasodilators, and this has been evident in ongoing clinical trials (Tanihara et al., 2013; Zhang et al., 2012). Drug wasted via eye drop delivery also represents sub-optimal drug therapy for the patient. Hence, the potential benefit of the development of a mucoadhesive film that is capable of sustained delivery of higher doses, specifically targeting the corneal endothelium.

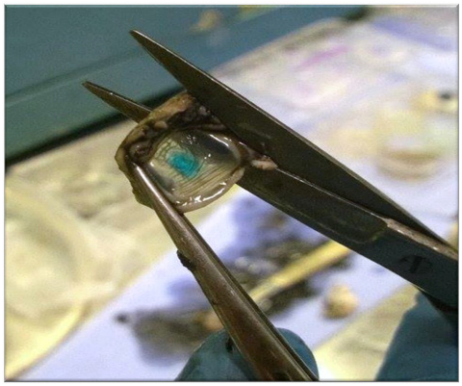

Fig. 8. Delivery of methylene blue to a cryoprobe-treated porcine cornea.

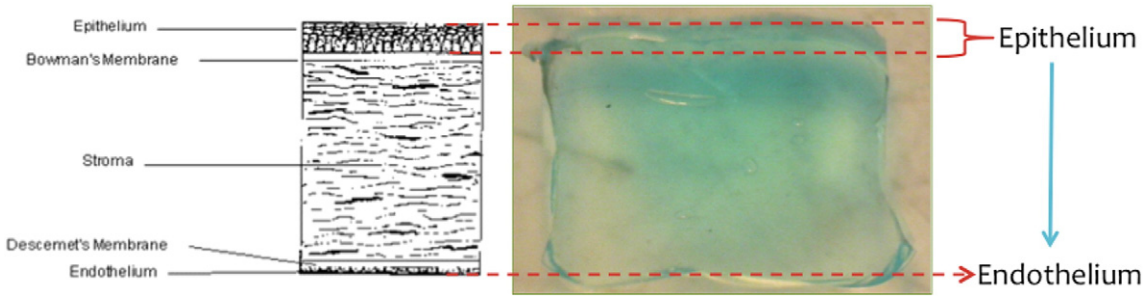

Fig. 9. Schematic diagram of the cornea layers and a microscopy lateral view of the cornea from a cryoprobe-treated porcine eyeball.

3.7. Run off and wash away

Run off of the dose applied as eyedrops is a well-known aspect of this mode of delivery and was vividly depicted in this work involving methylene blue (Fig. 10). In the experimental setup used, it was a challenge to accurately mimic the washing out action of tears and blinking. However, during the experiment the porcine eyeballs were periodically irrigated with 300 μL PBS in an effort to crudely simulate washing out. This revealed that methylene blue was visibly washed away on wetting as the intensity of the blueness decreased (as shown in Fig. 10). Methylene blue in films, on the other hand, remained and the drug did not drain away appreciably even after irrigation. This indicates a major advantage delivery via mucoadhesive films over eyedrops, whereby drug run off and washing away by tears are reduced, with the drug being retained at point of application.

3.8. Delivery of methylene blue to the cornea

The delivery of methylene blue from film and eye drops of equal concentrations to untreated in vitro porcine corneas and cryoprobe-treated porcine corneas (n = 2 or 3; ±SD) is shown in Fig. 11. It can be seen that methylene blue delivered from the thin film (0.072 mMol in untreated cornea and 0.081 mMol in cryoprobe-treated cornea) was significantly greater than the amount delivered from liquid eye drops (0.046 mMol in untreated cornea and 0.066 mMol in cryoprobe-treated cornea) for both untreated ($p < 0.01$) and cryoprobe-treated corneas ($p < 0.05$). The film delivered significantly more methylene blue to the cryoprobe-treated corneas as compared to native corneas ($p < 0.05$) and this was even more apparent for the eye drop-delivered agent ($p < 0.0001$). This is probably a consequence of the cryoprobe-treated corneas being more "leaky" owing to a modulation or disruption the cell and matrix components of the cornea cause by tissue freezing, which allows more drug to penetrate.

3.9. Delivery of ROCK inhibitor Y-27632 to the cornea

The corneal delivery of ROCK inhibitor Y-27632 from films and eye drops of equal concentration into native unfrozen porcine corneas and cryoprobe-treated porcine corneas (n = 2 or 3 ± SD) are shown in Fig. 12. It can be seen that for cryoprobe-treated corneas, the rapid diffusional release (Section 3.2.2) was manifested in the delivery of almost 3 times more Y-27632 (0.52 mMol) when compared to delivery via the equivalent eye drop solution (0.177 mMol) ($p < 0.01$). For native corneas, Y-27632 delivered from the thin film was greater than from liquid eye drops, although this was not statistically significant ($p > 0.05$). The films delivered significantly more Y-27632 to the cryoprobe-treated corneas (0.52 mMol) as compared to native corneas (0.23 mMol) ($p < 0.01$). The eye drops appeared to deliver more Y-27632 across the cryoprobe-treated corneas, although this was not statistically significant ($p > 0.05$). Prior to the development of a 10 mM Y-27632 film, a lower concentration Y-27632 film was produced (containing 10 mg of Y-27632). The delivery onto the cryoprobe-treated corneas of this was much lower (0.083 mMol) due to the lower concentration of the film (n = 3 ± SD).

Y-27632 has been reported to have no direct toxicity or significant effects on cell proliferation (Honjo et al., 2007), and a protective effect was observed for mouse motoneurons in a cytotoxicity assay following Y-27632 treatment (Günther et al., 2014). A clinical study involving another ROCK inhibitor, SNJ-1656 proved that it is a safe topical agent and effective in reducing intraocular pressure in the eyes of human volunteers (Tanihara et al., 2008).

4. Conclusions

This study has compared drug delivery to the cornea achieved via eye drops or release from mucoadhesive thin films. Initially, methylene blue as a model agent, followed by 10 mMol of selective ROCK inhibitor Y-27632, which is a drug used to treat vision loss caused by corneal endothelial dysfunction as would occur in FECD and/or bullous

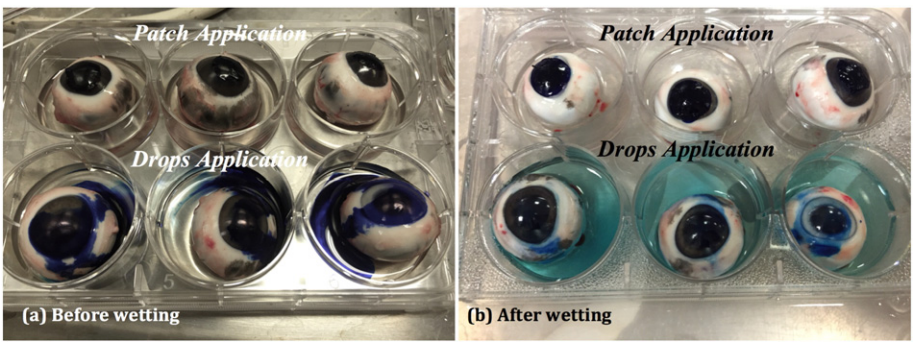

Fig. 10. Porcine eyeballs treated with film patch (upper) or equivalent 'eyedrop' solution (lower) immediately after application (left). Lower left clearly shows run off of significant amounts of MB immediately following application. Lower right shows that upon irrigation further MB is washed away from the eyeball dosed with eyedrops. In contrast, upper right shows no detectable wash out of MB from applied films following irrigation (3 determinations).

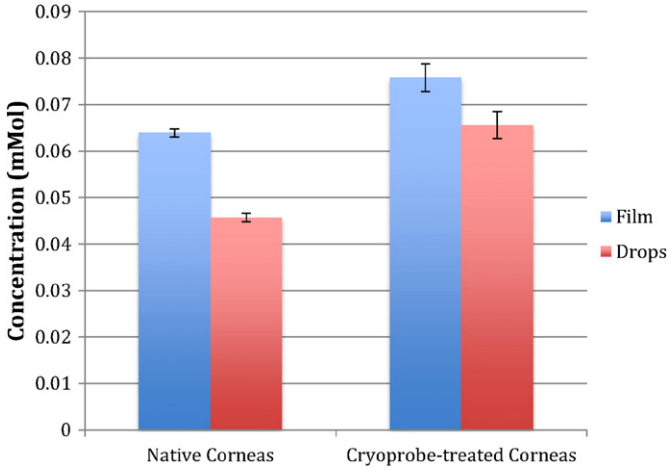

Fig. 11. The corneal delivery of methylene blue from film and 'eye drops' of equal concentration across native porcine corneas and cryoprobe-treated porcine corneas (n = 2 or 3 ± SD).

keratopathy. The major conclusions are: (1) drug delivery to the cornea via thin mucoadhesive films is a superior alternative to eye drop delivery because (at equal concentrations) significantly higher concentrations of Y-27632 were observed in the cornea after delivery from thin films compared to delivery via eye drops. This suggests the delivery of ROCK inhibitor from thin mucoadhesive films may produce better clinical results compared to eye drops. (2) thin mucoadhesive films have advantages over eye drops in that dose is well retained at point of application on thin film application, whereas eye drops are easily washed away by tearing and blinking of eyes. (3) thin films result in a 3-times higher delivery of Y-27632 over and above that achieved by eye drop delivery on cryoprobed-treated corneas. This suggests that targeted delivery of Y-27632 to the cryoprobe-treated, freeze-damaged tissue at the front of the cornea allows the ROCK inhibitor to penetrate more readily into and across cornea. Thus, a combination of transcorneal freezing and topical application of ROCK inhibitor via thin films is a potential non-invasive approach to deliver relatively higher concentrations of drugs into the corneal endothelium. In summary, findings from this study support the further development of mucoadhesive thin films as a modality for the targeted delivery of ROCK inhibitors to the cornea (with or without transcorneal freezing) to treat corneal endothelial dysfunction. The approach also has wider potential in the use of thin mucoadhesive films as an alternative to eye drop application in other scenarios, and could possibly apply to other ocular diseases by incorporating other disease-target drugs.

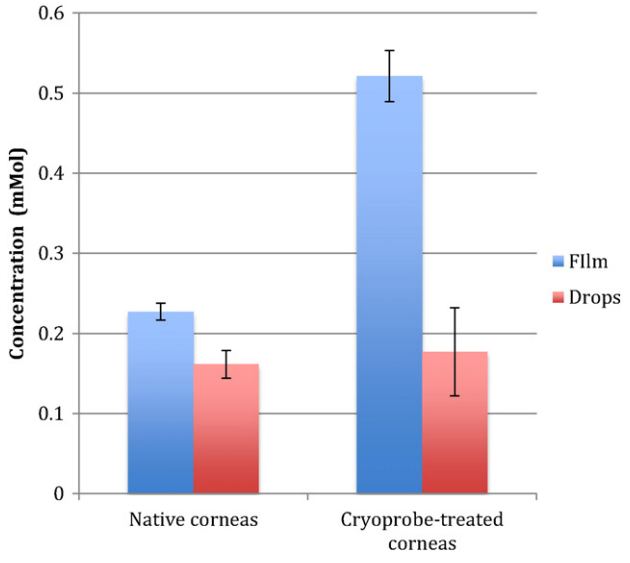

Fig. 12. The ocular delivery of ROCK inhibitor Y-27632 from film and eyedrops of equal concentration across native porcine corneas and cryoprobe-treated porcine corneas (n = 3 ± SD).

References

Arnold, J.J., Hansen, M.S., Gorman, G.S., Inoue, T., Rao, V., Spellen, S., Hunsinger, R.N., Chapleau, C.A., Pozzo-Miller, L., Stamer, W.D., Challa, P., 2013. The effect of Rho-associated kinase inhibition on the ocular penetration of timolol maleate. Invest. Ophthalmol. Vis. Sci. 54, 1118–1126.

Buco, P., van Horn, D.L., Schutten, W.H., Cohen, K., 1978. Effects of transcorneal freezing on protein content of aqueous humor and intraocular temperature in rabbit and cat. Invest. Ophthalmol. Vis. Sci. 17, 1199–1202.

Chan, K.Y., Cho, P., Boost, M., 2014. Corneal epithelial cell viability of an ex vivo porcine eye model. Clin. Exp. Optom. 97, 337–340.

Chickering, D.E., Mathiowitz, E., 1999. Definitions, mechanisms, and theories of bioadhesion. Bioadhesive Drug Delivery Systems: Fundamentals, Novel Approaches and Development. Marcel Dekker, New York (Available at:, https://books.google.co.uk/books?hl=en&lr=&id=d8-Eo7iGOTkC&oi=fnd&pg=PR3&dq=diffusion+theory+of+bioadhesion+(Chickering + and + Mathiowitz,+1999).&ots = i3HbEl6ep8&sig = _mgxm3f4KOk6XO2eFE5CSqwgUdQ#v = onepage&q&f = false Accessed: 5 December 2015).

Eghrari, A.O., McGlumphy, E.J., Iliff, B.W., Wang, J., Emmert, D., Riazuddin, S.A., Katsanis, N., Gottsch, J.D., 2012. Prevalence and severity of Fuchs corneal dystrophy in Tangier Island. Am J. Ophthalmol. 153, 1067–1072.

Gokhale, A., 2014. Achieving zero-order release kinetics using multi-step diffusion-based drug delivery. Pharm. Technol. ([Online] Available at: http://www.pharmtech.com/achieving-zero-order-release-kinetics-using-multi-step-diffusion-based-drug-delivery (Accessed: 12 December 2015)).

Günther, R., Saal, K.A., Suhr, M., Scheer, D., Koch, J.C., Bähr, M., Lingor, P., Tönges, L., 2014. The rho kinase inhibitor Y-27632 improves motor performance in male SOD1(G93A) mice. Front. Neurosci. 8, 304.

Hahmann, C., Schroeter, T., 2010. Rho-kinase inhibitors as therapeutics: from pan inhibition to isoform selectivity. Cell. Mol. Life Sci. 67, 171–177.

Heiting, G., 2015. Fuch's Corneal Dystrophy: 7 Things You Should Know [Online]. AllAboutVision, California (Available at: http://www.allaboutvision.com/conditions/fuchs-corneal-dystrophy.htm, Accessed: 6 December 2015).

Hodson, S., Miller, F., 1976. The bicarbonate ion pump in the endothelium which regulates the hydration of rabbit cornea. J. Physiol. 263, 563–577.

Honjo, M., Tanihara, H., Kameda, T., Kawaji, T., Yoshimura, N., Araie, M., 2007. Potential role of rho-associated protein kinase inhibitor Y-27632 in glaucoma filtration surgery. Investig. Opthalmol. Vis. Sci. 48, 5549–5557.

Jeong, B., Bae, Y.H., Kim, S.W., 2000. Drug release from biodegradable injectable thermosensitive hydrogel of PEG-PLGA-PEG triblock copolymers. J. Control. Release 63, 155–163.

Kitagawa, K., Kojima, M., Sasaki, H., Shui, Y.B., Chew, S.J., Cheng, H.M., Ono, M., Morikawa, Y., Sasaki, K., 2002. Prevalence of primary cornea guttata and morphology of corneal endothelium in aging Japanese and Singaporean subjects. Ophthalmic Res. 34, 135–138.

Knupp, C., Pinali, C., Lewis, P.N., Parfitt, G.J., Young, R.D., Meek, K.M., Quantock, A.J., 2009. The architecture of the cornea and structural basis of its transparency. Adv. Protein Chem. Struct. Biol. 78, 25–49.

Koizumi, N., Okumura, N., Ueno, M., Nakagawa, H., Hamuro, J., Kinoshita, S., 2013. Rho-associated kinase inhibitor eye drop treatment as a possible medical treatment for Fuchs Corneal Dystrophy. Cornea 32, 1167–1170.

Langer, R., 1990. New methods of drug delivery. Science 249, 1527–1533.

Liao, J.K., Seto, M., Noma, K., 2007. Rho kinase (ROCK) inhibitors. J. Cardiovasc. Pharmacol. 50, 17–24.

Llabot, J.M., Palma, S.D., Manzo, R.H., Allemandi, D.A., 2007. Design of novel antifungal mucoadhesive films: part II. Formulation and in vitro biopharmaceutical evaluation. Int. J. Pharm. 336, 263–268.

Lubrizol, 2015. https://www.lubrizol.com/PersonalCare/Products/Carbopol/default.html.

Meek, K.M., Knupp, C., 2015. Corneal structure and transparency. Prog. Retin. Eye Res. 49, 1–16.

Morrison, P., 2015. More Than Meets the Eye. United Kingdom and Ireland Controlled Release Society Newsletter, pp. 25–27.

Nakagawa, H., Koizumi, N., Okumura, N., Suganami, H., Kinoshita, S., 2015. Morphological changes of human corneal endothelial cells after rho-associated kinase inhibitor eye drop (ripasudil) administration: a prospective open-label clinical study. PLoS ONE 14, e0136802.

Okumura, N., Inoue, R., Okazaki, Y., Nakano, S., Nakagawa, H., Kinoshita, S., Koizumi, N., 2015. Effect of the Rho kinase inhibitor Y-27632 on corneal endothelial wound healing. Invest. Ophthalmol. Vis. Sci. 56, 6067–6074.

Okumura, N., Koizumi, N., Kay, E.P., Ueno, M., Sakamoto, Y., Nakamura, S., Hamuro, J., Kinoshita, S., 2013. The ROCK inhibitor eye drop accelerates corneal endothelium wound healing. Invest. Ophthalmol. Vis. Sci. 54, 2493–2502.

Okumura, N., Koizumi, N., Ueno, M., Sakamoto, Y., Takahashi, H., Hirata, K., Torii, R., Hamuro, J., Kinoshita, S., 2011. Enhancement of corneal endothelium wound healing by Rho-associated kinase (ROCK) inhibitor eye drops. Br. J. Ophthalmol. 95, 1006–1009.

Okumura, N., Ueno, M., Koizumi, N., Sakamoto, Y., Hirata, K., Hamuro, J., Kinoshita, S., 2009. Enhancement on primate corneal endothelial cell survival in vitro by a ROCK inhibitor. Invest. Ophthalmol. Vis. Sci. 50, 3680–3687.
Patel, A., Cholkar, K., Agrahari, V., Mitra, A.K., 2013. Ocular drug delivery systems: an overview. World Br. J. Pharmacol. 2 (2), 47–64.
Patel, P.N., 2006. Methylene blue for management of ifosfamide-induced encephalopathy. Ann. Pharmacother. 40, 299–303.
Peh, K.K., Wong, C.F., 1999. Polymeric films as vehicle for buccal delivery: swelling, mechanical, and bioadhesive properties. J. Pharm. Pharm. Sci. 2, 53–61.
Pubchem, d. Methylene blueAvailable at https://pubchem.ncbi.nlm.nih.gov/compound/methylene_blue#section=Top ([Accessed: 28 April 2016]).
Rahman, I., Carley, F., Hillarby, C., Brahma, A., Tullo, A.B., 2008. Penetrating keratoplasty: indications, outcomes, and complications. Eye 23, 1288–1294.
Riento, K., Ridley, A.J., 2003. ROCKs: multifunctional kinases in cell behavior. Nat. Rev. Mol. Cell Biol. 4, 446–456.
Rowe, R.C., Sheskey, P.J., Quinn, M.E., 2012. Carbomer. Handbook of Pharmaceutical Excipients. seventh ed. Pharmaceutical Press, London (Available at: https://www.medicinescomplete.com/mc/excipients/2012/1001935183.htm, Accessed: 10 December 2015).
Royal National Institute of Blind People., 2015. Corneal Dystrophies [Online]. Royal National Institute of Blind People, London (Available at:, http://www.rnib.org.uk/eye-health-eye-conditions-z-eye-conditions/corneal-dystrophies, Accessed: 5 December 2015).
Santa Cruz Biotechnology, Y-27632 dihydrochloride (CAS 129830-38-2), Available at: http://www.scbt.com/datasheet-281642.html, ([Accessed: 28 April 2016]).
Shively, M.L., Coonts, B.A., Renner, W.D., Bennett, A.T., 1995. Physicochemical characterization of polymeric injectable implant delivery system. J. Control. Release 33, 237–243.
Sikka, P., Bindra, V.K., Kapoor, S., Jain, V., Saxena, K.K., 2011. Blue cures blue but be cautious. J. Pharm. Bioall. Sci. 3, 542–545.
Staatz, W.D., van Horn, D.L., 1980. The effects of aging and inflammation on corneal endothelial wound healing in rabbits. Invest. Ophthalmol. Vis. Sci. 19, 983–986.
Tanihara, H., Inatani, M., Honjo, M., Tokushige, H., Azuma, J., Araie, M., 2008. Intraocular pressure-lowering effects and safety of topical administration of a selective ROCK inhibitor, SNJ-1656, in healthy volunteers. Arch. Ophthalmol. 126, 309–315.
Tanihara, H., Inoue, T., Yamamoto, T., Kuwayama, Y., Abe, H., Araie, M., 2013. Phase 1 clinical trials of a selective Rho kinase inhibitor, K-115. JAMA Ophthalmol. 131, 1288–1295.
Tardivo, J.P., del Giglio, A., Santos de Oliveira, C., Gabrielli, D.S., Junqueira, H.C., Tada, D.B., Severino, D., de Fátima Turchiello, R., Baptista, M.S., 2005. Methylene blue in photodynamic therapy: from basic mechanisms to clinical applications. Photodiagn. Photodyn. Ther. 2, 175–191.
Ummadi, S.B., Shravani, N.G., Raghavendra, R.M., Srikanth, R., Sanjeev, N.B., 2013. Overview on controlled release dosage form. Int. J. Pharm. Sci. Res. 3, 258–269.
Wang, S.K., Chang, R.T., 2014. An emerging treatment option for glaucoma: Rho kinase inhibitors. J. Clin. Ophthalmol. 8, 883–890.
Zhang, K., Zhang, L., Weinreb, R.N., 2012. Ophthalmic drug discovery: novel targets and mechanisms for retinal diseases and glaucoma. Nat. Rev. Drug Discov. 11, 541–559.
Zoega, G.M., Fujisawa, A., Sasaki, H., Kubota, A., Sasaki, K., Kitagawa, K., Jonasson, F., 2006. Prevalence and risk factors for cornea guttata in the Reykjavik Eye Study. Ophthalmology 113, 565–569.

Appendix B: Publication 2

Akhbanbetova, A., Nakano, S., Littlechild, S.L., Young, R.D., Zvirgzdina, M., Fullwood, N.J., Weston, I., Weston, P., Kinoshita, S., Okumura, N. and Koizumi, N. (2017). A surgical cryoprobe for targeted transcorneal freezing and endothelial cell removal. *Journal of Ophthalmology*, 2017.

Hindawi
Journal of Ophthalmology
Volume 2017, Article ID 5614089, 11 pages
https://doi.org/10.1155/2017/5614089

Research Article

A Surgical Cryoprobe for Targeted Transcorneal Freezing and Endothelial Cell Removal

Alina Akhbanbetova,[1] Shinichiro Nakano,[2] Stacy L. Littlechild,[1] Robert D. Young,[1] Madara Zvirgzdina,[1] Nigel J. Fullwood,[3] Ian Weston,[4] Philip Weston,[4] Shigeru Kinoshita,[5] Naoki Okumura,[2] Noriko Koizumi,[2] and Andrew J. Quantock[1]

[1]*Structural Biophysics Research Group, School of Optometry and Vision Sciences, Cardiff University, Maindy Road, Cardiff CF24 4HQ, UK*
[2]*Department of Biomedical Engineering, Faculty of Life and Medical Sciences, Doshisha University, 1-3 Miyakodami-Tatara, Kyoto 610-0321, Japan*
[3]*Division of Biomedical and Life Sciences, Faculty of Health and Medicine, Lancaster University, Lancaster LA1 4YQ, UK*
[4]*Network Medical Products Ltd. Coronet House, Kearsley Road, Ripon, North Yorkshire HG4 2SG, UK*
[5]*Department of Frontier Medical Science and Technology for Ophthalmology, Kyoto Prefectural University of Medicine, Hirokoji-Kawaramachi, Kyoto 602-0841, Japan*

Correspondence should be addressed to Andrew J. Quantock; quantockaj@cardiff.ac.uk

Academic Editor: Neil Lagali

Purpose. To examine the effects of transcorneal freezing using a new cryoprobe designed for corneal endothelial surgery. *Methods*. A freezing console employing nitrous oxide as a cryogen was used to cool a series of different cryoprobe tip designs made of silver for high thermal conductivity. In vitro studies were conducted on 426 porcine corneas, followed by preliminary in vivo investigations on three rabbit corneas. *Results*. The corneal epithelium was destroyed by transcorneal freezing, as expected; however, the epithelial basement membrane remained intact. Reproducible endothelial damage was optimally achieved using a 3.4 mm diameter cryoprobe with a concave tip profile. Stromal edema was seen in the pre-Descemet's area 24 hrs postfreeze injury, but this had been resolved by 10 days postfreeze. A normal collagen fibril structure was seen 1 month postfreeze, concurrent with endothelial cell repopulation. *Conclusions*. Transcorneal freezing induces transient posterior stromal edema and some residual deep stromal haze but leaves the epithelial basement membrane intact, which is likely to be important for corneal re-epithelialization. Localized destruction of the endothelial monolayer was achieved in a consistent manner with a 3.4 mm diameter/concave profile cryoprobe and represents a potentially useful approach to remove dysfunctional corneal endothelial cells from corneas with endothelial dysfunction.

1. Introduction

Corneal transparency is maintained in the healthy eye by a monolayer of endothelial cells on the inner surface of the cornea. Even though human corneal endothelial cells do not possess the capacity for proliferation in vivo, the endothelium as a whole has a functional reserve to cope with cell loss via the spreading and enlargement of cells adjacent to those lost [1, 2]. Excessive endothelial loss and deterioration caused by eye pathologies such as Fuchs' endothelial corneal dystrophy (FECD), however, lead to corneal edema, clouding, and eventually loss of vision. FECD is a progressive degenerative disorder that is a major indication for corneal transplant surgery. Surgical intervention in the form of a full-thickness-penetrating keratoplasty—or more commonly nowadays a posterior lamellar graft—is the main treatment option. But, despite the success of corneal graft surgery, some questions about the long-term survival of the donor tissue [3]

and the recurring problem of sufficient tissue availability remains. These limitations have led researchers to seek potential alternatives to corneal transplantation to treat corneal endothelial dysfunction.

One promising route involves the use of selective inhibitors of the Rho kinase pathway. The so-called ROCK inhibitors regulate the actin cytoskeleton and influence vital cell activities such as motility, proliferation, and apoptosis [4]. Owing to their demonstrable value, numerous studies have been conducted in recent years which focus on the effect of ROCK inhibitors on corneal endothelial cells both in vivo and ex vivo [5–9]. One approach involves transcorneal freezing to damage corneal endothelial cells in the central portion of the cornea in patients with FECD followed by the topical delivery of a ROCK inhibitor, Y27632, in the form of eye drops to encourage peripheral endothelial cells that had been unaffected by the freeze injury to repopulate the central zone of the corneal endothelium [10–12]. Freeze damage is achieved by application of a cold probe to the corneal surface. Another approach involves cell injection therapy whereby cultivated human corneal endothelial cells are injected into the anterior chamber of the eyes with FECD in a suspension that includes Y27632 ROCK inhibitor [13]. This agent has also been tested in the form of eye drops as a long-term pharmacological treatment for bullous keratopathy [14].

A small series of first-in-man surgeries to test the concept of transcorneal freezing followed by short-term ROCK inhibitor eye drop application for the treatment of FECD was conducted a few years ago and showed promise [10–12]. In this approach, the tip of a stainless steel rod, 2 mm in diameter, was immersed in liquid nitrogen at −196°C before being applied to the surface of the central cornea for an arbitrarily chosen time of 15 sec. The assumption was that central corneal endothelial cells located underneath the cold-rod applicator would be destroyed by freeze injury, although this could not be directly confirmed in the human subjects because the cloudy FECD corneas did not allow a view of the endothelium by specular microscopy. The freezing of corneal tissue has also been used as a modality to induce an injury to facilitate basic research into corneal wound healing [15–28]. If corneal freezing is to be used in a clinical setting, however, (either for the destruction of diseased cells in the central endothelium prior to ROCK inhibitor eye drop application for FECD as described above or to pretreat the cornea prior to targeted drug delivery to combat conditions such as fungal keratitis) we contend that it needs to be achieved in a more sophisticated, reliable, and reproducible manner than that achieved with an immersion-cooled steel rod. Here, we report the development and validation of a new cryoprobe based on the expansion of nitrous oxide as a cryogen and its effect, in vitro and in vivo, on the corneal epithelium, stroma, and endothelium.

2. Materials and Methods

2.1. Cryoprobe Development. A console that uses nitrous oxide as a cryogen was manufactured in conjunction with a series of cryoprobes with newly designed tips, some of which matched the cornea's curvature (Figure 1). This prototype project was carried out by Coronet Medical Technologies Ltd., the ophthalmic arm of Network Medical Products Ltd. Enclosed gas expanded within the tip and was recycled therein, achieving a low temperature based on the Joule/Thomson effect. The tip of the cryoprobe, used to contact the corneal surface, was circular around the probe's main axis and a number of designs were tested. Probe tips were 1.8 mm, 2.4 mm, or 3.4 mm in diameter and were manufactured from silver for high thermal conductivity. Larger diameter probe tips were not considered because of the option of multiple surface freeze placements should a wider area of the cornea need to be treated. Probes had either a flat surface profile or a concave one with a radius of curvature of 8 mm. For ease of use, a foot switch was incorporated into the design, which initiates cooling at the cryoprobe tip and maintains the reduced temperature throughout the whole time it is depressed. The foot switch is linked to a timer on the main console that provides a visual output of freezing time plus an audible signal (with a mute option) at 1 sec intervals when the foot switch is depressed. Freezing temperature at the probe tip (−50°C) is reached within 2 sec of depressing of the foot switch; after release, ambient room temperature is achieved within seconds. The hand-held cryoprobe has an ergonomic-angled design to allow easy application to the corneal surface (Figure 1). Probes should be thoroughly cleaned, inspected, and autoclaved prior to use.

2.2. Transcorneal Freezing In Vitro. The porcine cornea is comparable to that of the human cornea in terms of its structure and its overall dimensions and the pig eye is thus often used for practice by trainee corneal surgeons. The central corneal thickness in adult pigs is usually around 660 μm [29, 30], which approximates a representative measurement of edematous corneal thickness in individuals with FECD [31, 32]. The porcine eyes, therefore, were well suited for our investigations, and the intact eyeballs, including extraocular muscles, were obtained soon after slaughter at a local abattoir (W. T. Maddock, Kembery Meats, Maesteg, Wales, UK). These were brought to the laboratory on ice and experiments were begun within 2-3 h of death. When the eyes arrived at the home laboratory, ultrasound measurements of central corneal thickness were made with a Tomey SP-100 pachymeter (Erlangen, Germany), which revealed that the corneas had thickened (~1000 μm) postmortem compared to those of published values [31, 32]. Consequently, the eyes were placed in a humidified incubator (Brinsea Octagon 100, Egg Incubator, Sandford, UK) at 45°C for 30–45 min to reverse the postmortem swelling and attain a thickness similar to what might be expected in humans with FECD. In total, 426 porcine eyes were used for the in vitro experiments in which the corneal thickness ranged from 483 μm to 831 μm owing to differences in eye size and likely differential postmortem swelling and deswelling.

Immediately after an eye was removed from the humidified incubator, its central corneal thickness was recorded as an average of eight measurements. The cryoprobe tip was then applied to the corneal surface and cooling was activated by pressing the foot switch to control the flow of nitrous

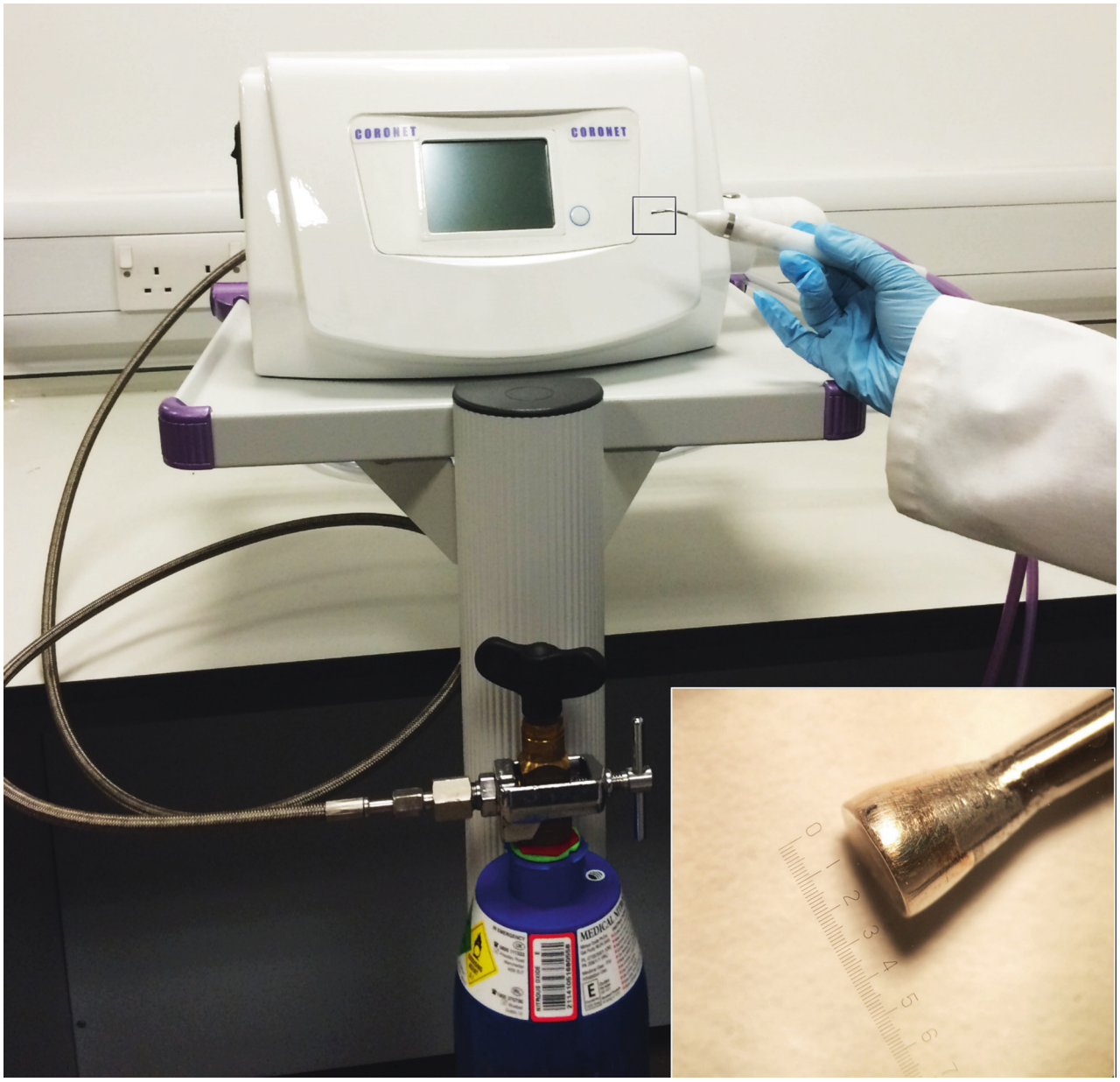

Figure 1: The transcorneal freezing machine attached to a cylinder of medical grade nitrous oxide (the cryogen), which comprises a main console with a monitor screen that illustrates freeze time, cryogen levels, and readiness for freeze plus interchangeable probe tips and a footswitch (not shown). Inset: the 3.4 mm diameter concave probe tip manufactured from silver for high thermal conductivity.

oxide gas. Freezing times of 3, 5, 9, and 13 sec were tested, allowing an additional 2 sec for the freezing temperature to be reached in all cases (thus, a 3 sec freeze required for a 5 sec application and foot-switch depression). The cornea was then carefully excised at the limbus after which staining solutions of 0.2% alizarin red (~1 ml) and 0.25% trypan blue were applied sequentially to the endothelial surface for 60–90 sec each to identify dead cells. The stains were then gently washed off using approximately 5 ml of 0.9% sodium chloride buffer solution, after which digital images of the corneal endothelial surface were captured on a Zeiss Stemi 1000 light microscope (Carl Zeiss, Jena, Germany). A successful freeze injury was deemed to have occurred when a clear circular wound area was seen. The endothelial wound area in each corneal image was manually traced and calculated using Image J software (http://imagej.nih.gov/ij/). Magnification was calibrated for each set of experiments using the image of an eyepiece graticule. Averages of three measurements were calculated and data were further collated using Microsoft Excel software (Microsoft Corp., Redmond, WA, USA).

2.3. Statistical Analysis. Statistical analyses were carried out operating IBM SPSS Statistics software (Version 23.0, IBM Corporation, New York, USA). Spearman's rank order correlation test was run to determine the relationship between central corneal thickness and endothelial wound areas induced by the freezing.

2.4. Scanning Electron Microscopy. To investigate the endothelial damage morphologically, four treated corneas were examined by scanning electron microscopy (SEM). Immediately after excision, the corneas were fixed in 2.5% glutaraldehyde and 2% paraformaldehyde in 0.1 M sodium cacodylate buffer, pH 7.3, for at least 2 h. Samples were then washed in PBS followed by the gradual dehydration through a graded ethanol series (from 50% to 100% in 30 min steps), after which the ethanol was replaced by hexamethyldisilazane for 20 min to minimize the shrinkage of the specimens. After drying, the corneas were placed on stubs (Agar Scientific, Stansted, UK) and sputter coated with gold (Edwards S150 sputter coater, Edwards High Vacuum Co. International, Wilmington, USA) to allow imaging in a JEOL JSM 5600 scanning electron microscope (JEOL Company, Tokyo, Japan) operating with a beam acceleration voltage of 15.0 kV.

2.5. Transcorneal Freezing In Vivo. Three adult New Zealand White rabbits were used to investigate corneal recovery after transcorneal freezing. At all stages, animals were treated in accordance with the ARVO Statement for the Use of Animals in Ophthalmic and Vision Research, and the research was approved by the IRB of Doshisha University. As reported later, the 3.4 mm concave cryoprobe was found to be the most effective in inducing endothelial damage in the porcine eye in vitro, but owing to the thinner cornea of the rabbit, the 2.4 mm concave cryoprobe was chosen for the in vivo transcorneal freezing experiments.

Under general anesthesia, a 2.4 mm probe was applied to the corneal surface of the rabbit eyes for a total of 5 sec. The contralateral eye was used as a control. Transcorneal freezing did not induce any severe general adverse effects. After 24 h, 10 days, and 1 month of treatment, the anterior segment of each eye was assessed by the use of a slit-lamp microscope and the rabbits were then euthanized. Corneal thickness was determined by the use of an ultrasound pachymeter (SP-2000; Tomey, Nagoya, Japan), and the mean of eight measured values was calculated. Intraocular pressure was measured by the use of a Tonovet tonometer (292000; KRUUSE, Langeskov, Denmark). Transmission electron microscopy (TEM) was conducted, as described below, on the corneas of the rabbits that were euthanized at 24 h- and 1-month time points after transcorneal freezing.

2.6. Transmission Electron Microscopy. The rabbit corneas were examined by TEM 24 h and 1 month postfreeze was conducted in Doshisha University, Japan. Briefly, after animals were euthanized, corneas were excised at the limbus and fixed in 2.5% glutaraldehyde and 2% paraformaldehyde in 0.1 M Sörensen buffer (pH 7.2–7.4) overnight at 4°C. Samples in fresh fixative were then express shipped to the UK. Full-thickness-dissected portions of the corneas were then subjected to alcohol dehydration and resin infiltration, after which they were embedded in epoxy resin (Araldyte CY212 resin, TAAB Laboratories, England, UK). Ultrathin sections were stained with uranyl acetate and lead citrate and examined on a JEOL 1010 microscope operating at 80 kV (JEOL Company, Tokyo, Japan).

3. Results

3.1. In Vitro Transcorneal Freezing. Initial experiments into the degree of endothelial damage caused by transcorneal freezing induced by four different types of cryoprobe tip—that is, 1.8 mm diameter/flat profile, 2.4 mm diameter/flat profile, 2.4 mm diameter/concave profile, and 3.4 mm diameter/concave profile—revealed that the time of contact with the corneal surface did not affect the area of endothelial damage, with freezing times of 3, 5, 9, and 13 sec tested (data not shown). Based on this outcome, a freezing time of 3 sec was chosen for all the in vitro experiments described herein. It also became apparent during the initial investigations that the probe tip had to be in contact with the corneal surface before the foot switch was depressed to initiate cooling. If the probe tip was cooled in air prior to being brought into contact with the cornea, no appreciable endothelial damage was seen; no matter how long, up to 15 sec, the probe remained in contact with the cornea.

Light microscopy of the endothelial surfaces of the post-freeze, trypan blue-stained corneas indicated the area of cell damage caused by the four different probes used in these experiments. Representative images of 426 technical replicates denoting the typical extent of endothelial damage are shown in Figure 2, with examples of what were considered to be successful or unsuccessful freeze injuries. A successful freeze injury was defined as one that resulted in a well-delineated circular area of cell damage. An unsuccessful freeze injury, on the other hand, was considered to have occurred either when there was no evidence of any cell damage or when the area of damage was irregular. Based on these criteria, only 14 of 102 eyes (14%) treated with the 1.8 mm diameter/flat profile probe were judged to have been successfully wounded, whereas 78 of 108 (72%) treated with the larger (i.e., 2.4 mm diameter) flat profile probe contained successful endothelial injuries. A similar number of the eyes exhibited corneal endothelial freeze damage—that is, 76 eyes of 108 (70%)—when the 2.4 mm diameter cryoprobe with a concave profile was used. Our data clearly indicated, however, that the 3.4 mm diameter/concave profile cryoprobe induced the most consistent endothelial damage with 90 eyes of 108 (83%) being successfully wounded in a reproducible manner (Table 1).

To quantify the extent of endothelial cell damage, we used Image J to manually trace around each wound deemed to have been successfully created (i.e., $n = 258$ of 426 technical replicates). The area of each wound was calculated, which, unsurprisingly, disclosed that larger probe tips led to more extensive endothelial damage (Table 1). All of the 426 corneas examined were subjected to multiple pachymetry measurements immediately prior to transcorneal freezing. This revealed that the average corneal thickness was 649 μm ($\pm$61 μm SD), which is a fair representative value for corneal edema in humans with endothelial dysfunction [31, 32]. Moreover, when the corneal thickness of the individual corneas was taken into account, a statistical Spearman's rank order correlation test identified that there was a weak relationship between central corneal thickness and endothelial damage when treated with the smallest and largest probes

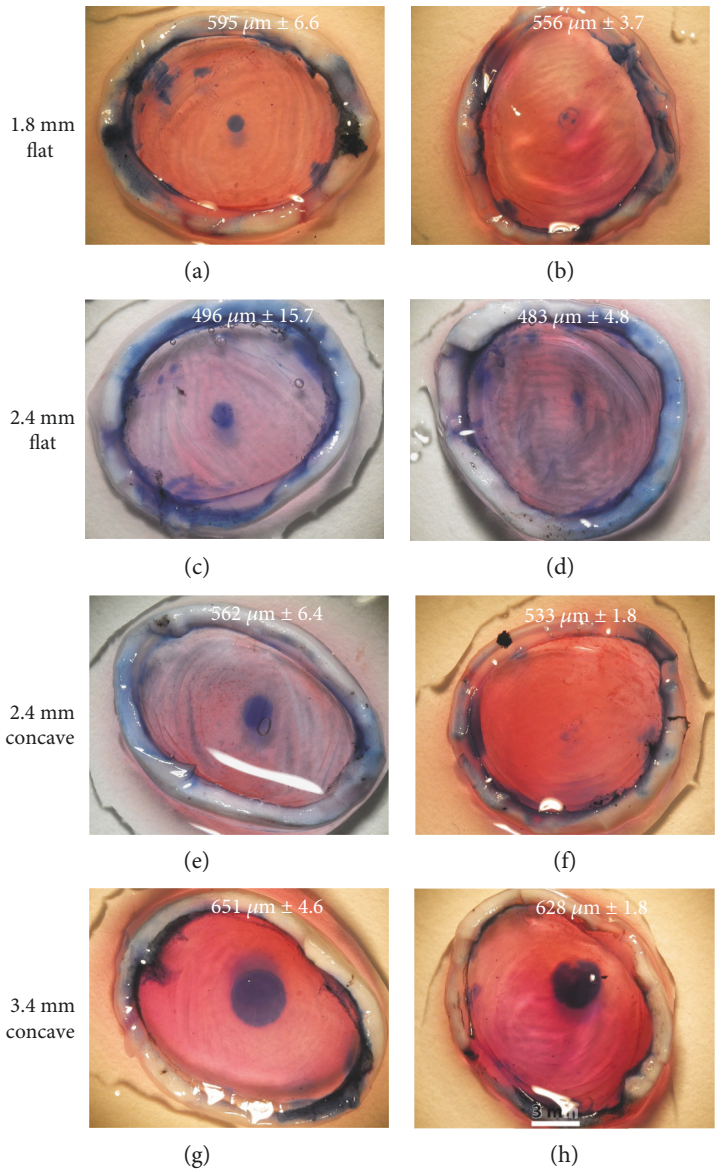

Figure 2: Representative images of corneal endothelial freeze injury on the pig eyes ex vivo induced by 3 sec freeze with four different cryoprobe tips and assessed by trypan blue staining. The thickness of each cornea is indicated on each panel (±SD) based on eight pachymetry readings. The area of cell damage is seen via the blue stain, and successful and non/less successful freeze injuries are shown in the left and right columns, respectively. Freezing with the 1.8 mm diameter/flat profile probe only rarely resulted in a reproducible wound (a and b). Endothelial freeze injury was more reliably achieved with 2.4 mm diameter probe tips with flat or concave profiles (c–f), but the optimal result and best consistency was achieved using the 3.4 mm diameter/concave profile cryoprobe (g and h). Scale bar, 3 mm. See Table 1 also.

Table 1: Data summary of transcorneal freezing for 3 sec on porcine eyes.

Probe tip (mm)/profile	Number of eyes	Number of eyes with successful freeze (%)	Mean/SD damaged area (mm^2)	Mean diameter (mm)	Mean/SD corneal thickness (nm)
1.8/flat	102	14 (14)	0.79/0.4	1.0	642/64
2.4/flat	108	78 (72)	2.12/1.0	1.6	650/71
2.4/concave	108	76 (70)	2.29/1.0	1.6	645/87
3.4/concave	108	90 (83)	6.91/1.9	2.9	654/59

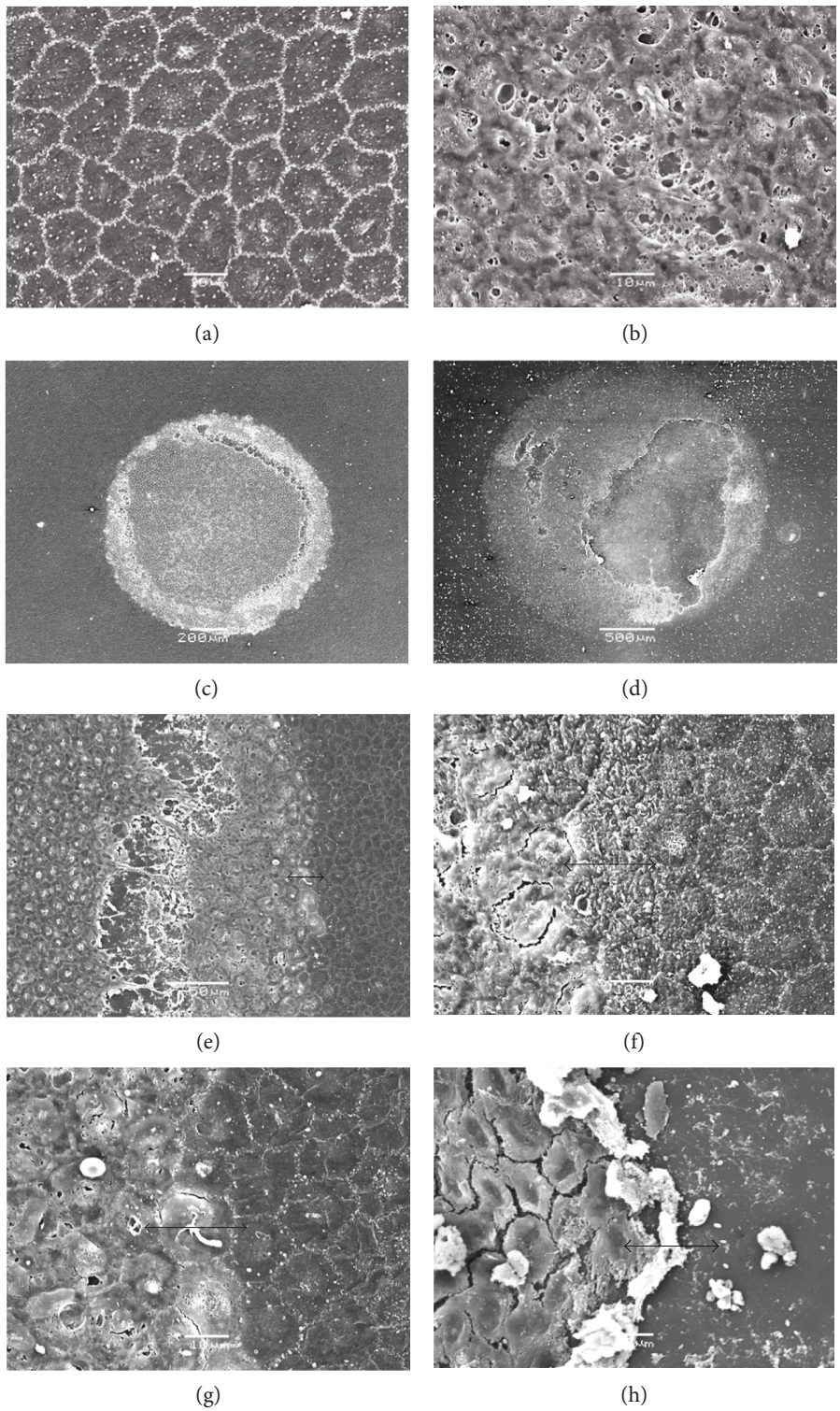

Figure 3: SEM of the endothelium of transcorneally frozen pig corneas. (a) An untreated pig cornea with cell boarders in white showing a characteristic hexagonal mosaic. The outline if the cell nucleus is evident as a slightly lighter area within each cell. Scale bar, 10 μm. (b) A representative image taken at the same magnification of the freeze-damaged area after treatment with a 2.4 mm diameter/concave profile tip, illustrating severe damage to endothelial cells by freezing. Scale bar, 10 μm. (c and d) Lower magnification images of endothelial freeze-injured wounds showing circular areas of endothelial cell damage including some endothelial debridement, exposing Descemet's membrane (c): 2.4 mm diameter/concave profile cryoprobe (scale bar, 200 μm); (d): 3.4 mm diameter/concave profile cryoprobe (scale bar, 500 μm). As expected, the larger probe induces more widespread damage (see Table 1 also). (e–h) Transition zones between unfrozen endothelial cells and those that were destroyed by freeze injury are often sharp (e) and (g); same area but different magnification (scale bars,10 μm, apart from (g) which is 50 μm).

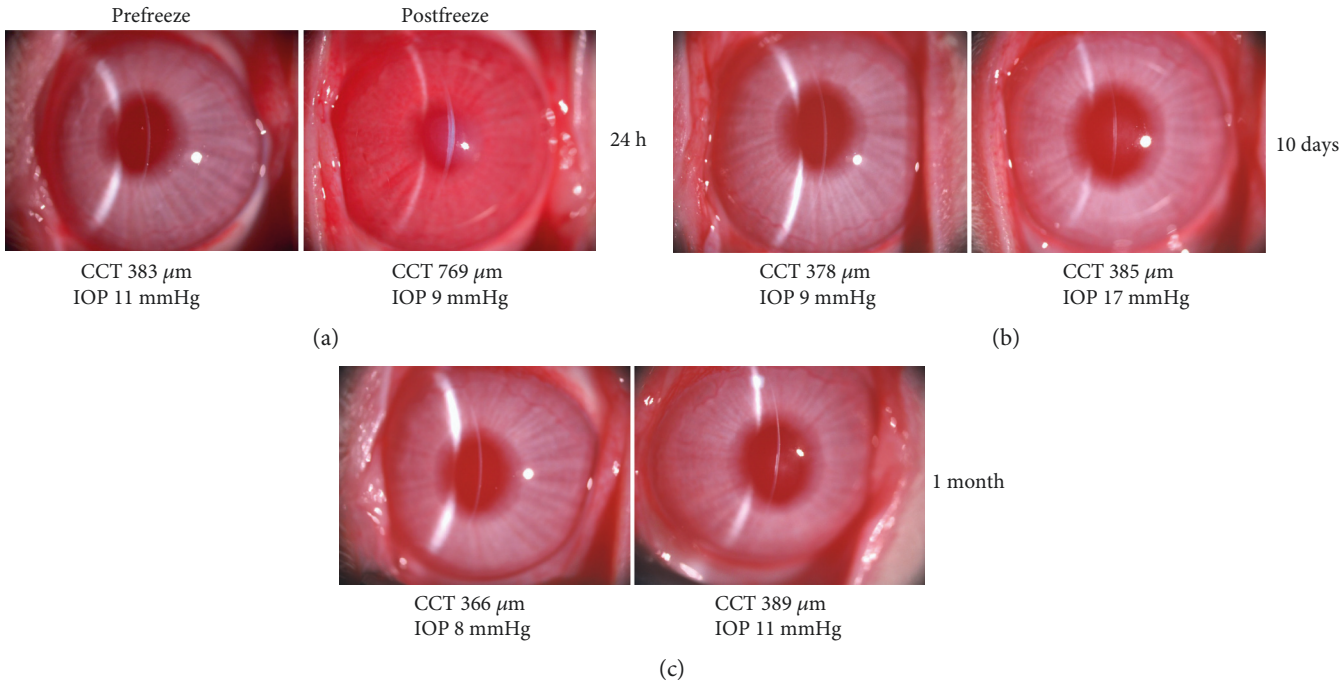

Figure 4: Effects of a 3 sec freeze on the rabbit cornea in vivo using the 2.4 mm diameter/concave profile cryoprobe tip. (a) 24 hrs after freeze, central corneal thickness (CCT) is increased considerably (769 μm) compared to that before freeze (383 μm), and the cornea is hazy, indicative of corneal endothelial damage, as well as epithelial and stromal cell damage. (b) 10 days after a freeze injury (in a different animal), CCT was at normal levels. (c) This was the case also, 1 month after treatment. (b and c) Some corneal haziness at the level of the posterior stroma or Descemet's membrane is evident at 10 days and 1 month.

(1.8 mm diameter ($r = -0.208$, $n = 102$, $p = 0.408$) and 3.4 mm diameter ($r = -0.258$, $n = 108$, $p = 0.007$) but a stronger relationship using the 2.4 mm diameter probe tips with concave and flat profiles ($r = -0.433$, $n = 108$, $p < 0.001$; 2.4 mm ($r = -0.466$, $n = 108$, $p < 0.001$, respectively) (Table 1).

To provide higher resolution information as to the status of the cells after freeze injury in the in vitro pig eye model, we conducted a series of SEM studies (Figure 3). This indicated that the corneal endothelial monolayer was severely disrupted in the central portion of the cornea beneath the site of the cryoprobe injury. Injured cells tended to become damaged and/or disassociated from each other, whereas noninjured cells adjacent to the area of damage exhibited classic hexagonal endothelial cell morphology. Interestingly, there appeared to be two transition zones between healthy nonfrozen cells and the more centrally damaged ones. The immediate transition at the inner edge of the morphologically normal cells was fairly abrupt; and in some cases, this was on a μm scale (Figures 3(e), 3(f), and 3(g)). More centrally, there was evidence of cellular dissociation (Figure 3(e)) and also total removal of large areas of frozen endothelial cells, exposing a bare Descemet's membrane (Figures 3(d) and 3(h)).

To investigate endothelial healing after transcorneal freeze, a small number of rabbit corneas were studied. For these investigations, a 2.4 mm diameter/concave profile cryoprobe was used rather than the 3.4 mm concave one owing to the relative thinness (approximately 350–400 μm) of the rabbit cornea compared to that of the pig (approximately 660 μm [29, 30]). This revealed that one day after a 3 sec surface freeze, the rabbit cornea had become significantly edematous, with its thickness approximately twice the normal value (Figure 4(a)). The central corneal thickness returned to normal values by day 7, and this was maintained up to one month post-freeze (Figure 4(c)). Slit-lamp images showed some evidence of corneal haze at the level of the posterior stroma or Descemet's membrane at 10 days and 1 month (Figures 4(b) and 4(c), resp.).

TEM examinations of rabbit corneas 24 hrs after freeze indicated that the corneal epithelium peripheral to the wound area was structurally normal, with typical epithelial stratification, cell-cell contact and surface microvilli (Figure 5(a)). As expected, the corneal epithelium was severely damaged in the central freeze-injured region of the cornea, with considerable cellular vacuolation and membrane destruction (Figure 5(b)). However, it was clear that the epithelial basement membrane remained intact, which presumably is important to aid subsequent epithelial resurfacing of the wound area. In the deep stroma, increased collagen fibril spacing accompanied by disorder in the fibril arrangement was sometimes observed focally 24 hrs post-freeze (Figure 5(c)), but this had been resolved by the 1-month timepoint at which time the stromal architecture appeared normal throughout the cornea (Figure 5(d)). These structural matrix changes likely contribute to the increased corneal thickness and opacity seen at 24 hrs (Figure 4(a)).

Just as with the corneal epithelium, the corneal endothelium in the periphery of the cornea away from the region of the tissue under the surface wound zone remained unaffected

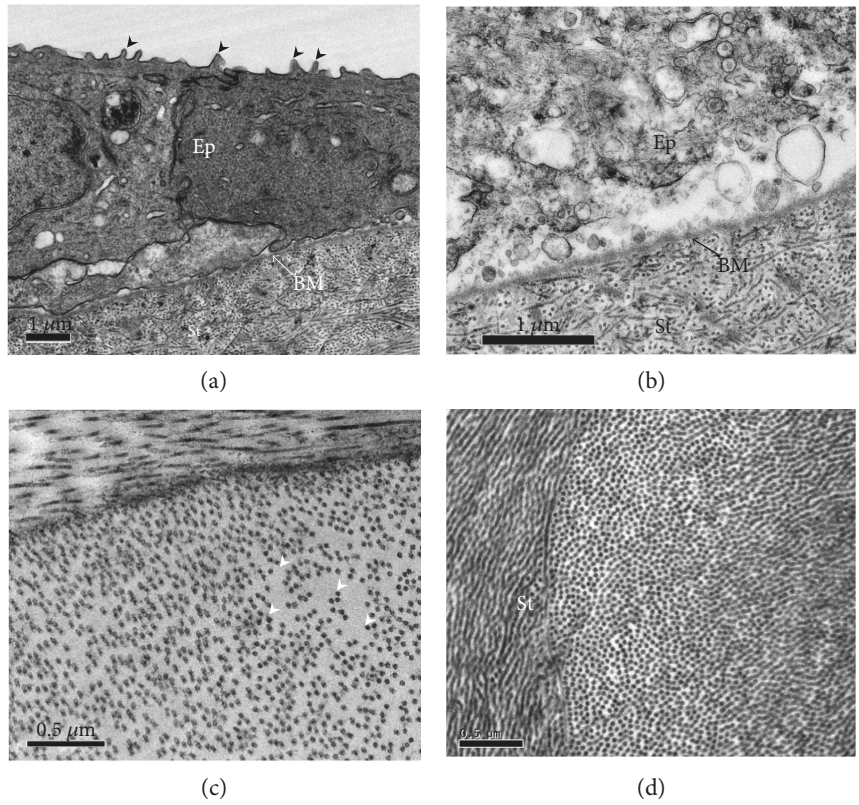

Figure 5: TEM of the corneal epithelium (Ep), epithelial basement membrane (BM), and stroma (St) following a 3 sec transcorneal freeze injury using a 2.4 mm diameter/concave profile cryoprobe on rabbit cornea in vivo. (a) The peripheral epithelium away from the wound zone, 24 hrs after the cryoprobe was applied and appeared morphologically normal. Arrowheads indicate microvilli on apical surface of epithelial cells. (b) Intact basement membrane is observed in the central freeze-injured area 24 hrs postfreeze. (c) After 24 hrs freeze injury, occasional focal regions of stromal matrix disruption were evident in the cornea, manifesting as tissue regions with increased spacing between collagen fibrils. (d) One month after the freezing, throughout the cornea, the spacing between collagen fibril appeared normal. Scale bars, 1 μm (a and b) and 0.5 μm (c and d).

24 hrs after transcorneal freeze of the central rabbit cornea (Figure 6(a)). The endothelium more centrally, however, began to exhibit clear signs of damage (Figure 6(b)). The central endothelium was often fully debrided with a bare Descemet's membrane that showed no apparent structural changes (Figure 6(c)). One month after freeze, the central corneal endothelium had reattained its normal character, although occasionally fibrous tissue deposition between Descemet's membrane and the recovered endothelium was observed (Figure 6(d)), which perhaps contributes to the deep stromal haze seen at this time (Figure 4(c)).

4. Discussion

A number of investigative surgical procedures, which utilize the selective ROCK inhibitor, Y27632, to combat FECD and bullous keratopathy are under investigation, including cell-injection therapy [10–14]. However, one alternative approach for FECD, especially in its early stage, involves freezing the central cornea using a cold probe to damage corneal endothelial cells beneath the surface contact area; this is then followed by the short-term delivery, for one week, of Y27632 in eye drop formulation [10–12]. In these surgeries, freezing was achieved by touching the corneal surface with a stainless steel rod, which had been immersed in liquid nitrogen. An arbitrary freezing time of 15 sec was chosen for these experiments, along with a 2 mm diameter for the steel rod. Encouragingly, the outcomes of these surgeries showed some promise, especially if the extent of the corneal endothelial dysfunction was not widespread, but if the approach is to be adopted more widely by the ophthalmic community, the corneal freeze would probably need to be achieved in a more reliable manner and with more knowledge of the nature and extent of the freeze damage.

Historically, and up to the present day, corneal freezing has been carried out by a variety of methods, most of which use it to induce an experimental injury for research into corneal wound healing [15–17, 28]. Freezing studies tend to employ either a brass rod or dowel, which had been immersed in liquid nitrogen [17–21] or similarly cooled steel ones [22, 23]. Retinal cryoprobes have also been used in investigational studies of transcorneal freezing [24, 33]. Here, we report the design and manufacture of a corneal cryoprobe that uses circulating nitrous oxide as a cryogen and report the type of freeze damage it induces.

Typically, the tips of cryoprobes that use high-pressure gas as a cryogen are made of stainless steel owing to the need to contain high-pressure gas safely. In our design, however,

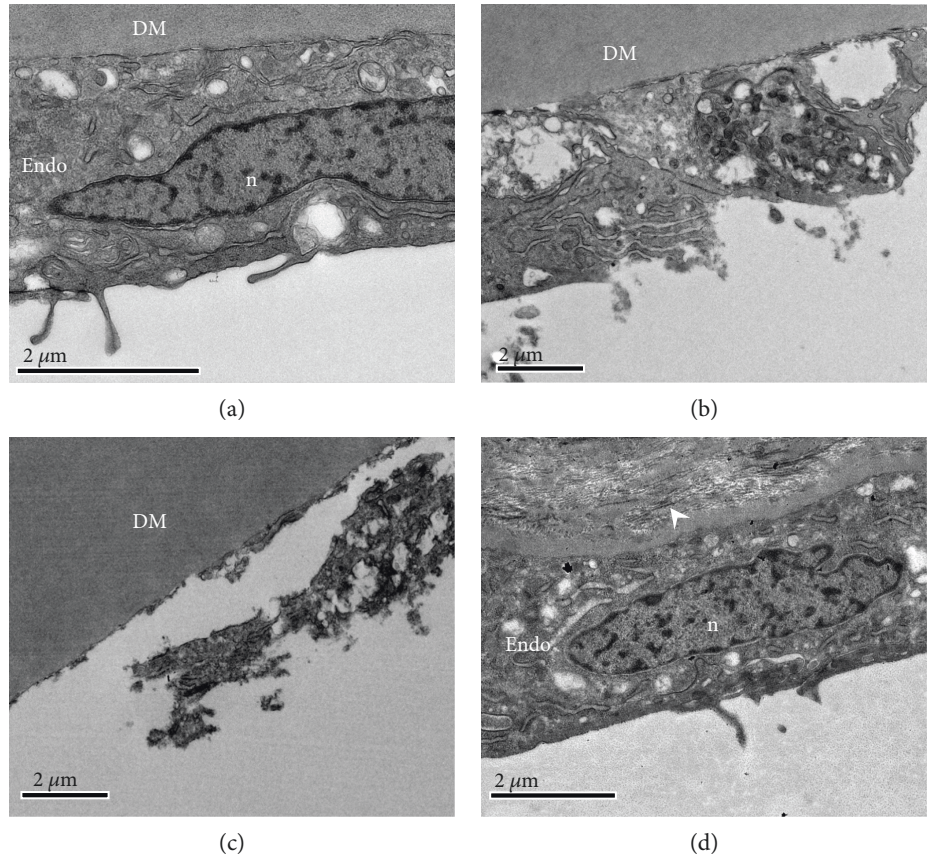

Figure 6: TEM of corneal epithelium following a 3 sec transcorneal freeze injury using a 2.4 mm diameter/concave profile cryoprobe on the rabbit cornea in vivo. (a) An endothelial cell (Endo) at 24 hrs postfreeze in a region peripheral to the freeze-injured area appeared morphologically normal, with normal organelles and nucleus (n). It adhered to Descemet's membrane (DM). (b) Closer to the region below the cryoprobe surface application, there were clear signs of cell damage including the destruction of the cell membrane, while even more centrally, (c) the cell damage was more extreme revealing a bare Descemet's membrane, consistent with the SEM analysis (Figure 3). (d) One month after the transcorneal freezing was performed, the central region of the inner cornea contained fairly normal endothelial cells that were sometimes accompanied by extracellular matrix material (white arrowheads) in the area posterior to Descemet's membrane. Scale bars, 2 μm.

the use of stainless steel would have resulted in a freeze that started in the center of the tip and thereafter spread, albeit quickly, to its outer circumference at a speed which relies on the thermal conductivity of the metal. To achieve a more uniform cooling across the probe tip, we manufactured a cryoprobe tip out of silver, which has a higher thermal conductivity than that of steel. The benefit of this design feature is that the diameter of the freeze in the cornea is decoupled from the depth of the freeze. Cooling in this design is based on the expansion and internal recycling of nitrous oxide inside the cryoprobe tip. At the point of its transition from liquid to gas, nitrous oxide exists at a temperature of −88.5°C, and this transition, which occurs inside our probe tip, of course, rapidly cools it. Owing to thermal conductivity within the whole probe and thermal loss at ambient room temperature, an equilibrium is reached, which in our design means that the temperature at the outer surface of the probe tip reaches −50°C.

The response of a cell to freezing is explained by Fraunfelder in his comprehensive review of corneal cryotherapy, the main mechanisms of cell damage being a piercing of the cell membrane by ice crystals or the creation of a sizeable osmotic imbalance between the inside and outside of the cell because of the removal of liquid water into the ice crystals [34]. Armitage also describes, from the other side of the coin, how careful freezing using time-mediated freeze-thaw protocols accompanied by the use of cryoprotectants can lead to cell survival [35]. The freezing we achieve here can probably be thought of as being fairly conservative in terms of the rate of endothelial cooling, but our current observations clearly indicate that sufficient levels of endothelial damage are achieved after a single freeze treatment. Experiments that applied additional treatments to the same surface location did not enhance the extent of the freeze injury (data not shown). We also found that if the foot switch was depressed to initiate cooling of the probe tip before it was brought into contact with the corneal surface, then no appreciable endothelial freeze damage was seen, even if the cryoprobe was kept in contact with the cornea for periods up to 15 sec. It is not immediately clear why this is the case, but perhaps, frosting of the probe tip when it is cooled in the moist air could contribute to this. This likely lack of frosting also might help facilitate the easy

release of the probe tip from the corneal surface after the foot switch is released, which we found to happen within a second or two of the cryogen circulation being suspended.

In the experiments described here, the central corneal epithelium was destroyed by the application of the cryoprobe, as we would expect. But, it is of potential importance that the corneal epithelial basement membrane remains intact as seen by TEM. The lack of epithelial basement membrane damage will presumably aid the epithelial resurfacing of the debrided epithelial area. Fibril arrangement changes are also apparent focally in the stromal matrix after the in vivo rabbit freeze injury, but these are transient, and the increased collagen fibril separation and disorganization which are seen 24 hrs after the treatment subsequently decrease as corneal thickness reduces. The obvious conclusion is that the recovering endothelium is mostly responsible. Of course, the in vivo healing studies reported here do not reflect the situation in the human cornea because of the different behavior of the endothelial cells and their limited replicative ability in humans. TEM also discloses the presence of fibrotic extracellular matrix tissue in the region of Descemet's membrane one month after freeze injury (Figure 6(d)). This might contribute to the deep stromal haze seen at this time, although a potential contribution to light scatter by freeze-damaged keratocytes cannot be discounted.

As mentioned, the use of ROCK inhibitors has aided the recovery of the corneal endothelium in situations where diseased corneal endothelial cells have been scraped away surgically [13] or frozen with a cooled steel rod applied to the corneal surface [10–12]. A report by Balachandran et al. [36] and Shah and associates also suggests that corneal endothelial cells can repopulate in FECD patients after damage alone [37–39]. The data presented here show that endothelial cells can be functionally damaged and/or removed by the application of a cryogenic cold probe and that this can be done in a targeted and reproducible manner with cell damage restricted to the area below the surface contact. Of course, the transcorneal freezing technique is unlikely to induce any significant change to the guttae which exist in FECD and their continued presence will conceivably hinder the reformation of a normal endothelial layer. Nevertheless, cell damage can be achieved through use of a silver 3.4 mm diameter cryoprobe with a concave profile, which was discovered to be the optimal design of the cryoprobes tested in the experiments described here. It thus has the potential to rapidly and reliably induce damage to the human corneal endothelium via transcorneal freezing, leaving the epithelial basement membrane intact. This has the potential to be used prior to the application of ROCK inhibitors to the eye in the form of eye drops [10–12] or as slow-release chemicals from thin films [40] to aid the recovery of corneal endothelial function.

Disclosure

The technology, the use of our freezing device coupled with the application of a Rho-kinase inhibitor for the nonevasive treatment of endothelial dysfunction, is the subject of patent (WO2013034907) currently under examination in Europe, Japan, and the United States of America. Preliminary results of this study were presented at the ARVO Annual Meeting, Seattle, USA, 1–5 May 2016.

Conflicts of Interest

The authors declare that there is no conflict of interest regarding the publication of this paper.

Acknowledgments

This research was supported by a Wellcome Trust Health Innovation Challenge Fund grant (HICF-T4-277 to Andrew J. Quantock, Noriko Koizumi, and Shigeru Kinoshita) and a Ph.D. Studentship to Alina Akhbanbetova and Andrew J. Quantock funded by the Life Science Research Network Wales, an initiative funded through the Welsh Government's Ser Cymru programme. The corneal programme at Cardiff University is funded by the BBSRC and MRC.

References

[1] W. M. Bourne, "Biology of the corneal endothelium in health and disease," *Eye*, vol. 17, no. 8, pp. 912–918, 2003.

[2] H. E. Kaufman and J. I. Katz, "Pathology of the corneal endothelium," *Investigative Ophthalmology & Visual Science*, vol. 16, no. 4, pp. 265–268, 1977.

[3] V. M. Borderie, P. Y. Boëlle, O. Touzeau, C. Allouch, S. Boutboul, and L. Laroche, "Predicted long-term outcome of corneal transplantation," *Ophthalmology*, vol. 116, no. 12, pp. 2354–2360, 2009.

[4] C. D. Nobes and A. Hall, "Rho, rac, and cdc42 GTPases regulate the assembly of multimolecular focal complexes associated with actin stress fibers, lamellipodia, and filopodia," *Cell*, vol. 81, no. 1, pp. 53–62, 1995.

[5] S. Li, C. Wang, Y. Dai et al., "The stimulatory effect of ROCK inhibitor on bovine corneal endothelial cells," *Tissue & Cell*, vol. 45, no. 6, pp. 387–396, 2013.

[6] N. Okumura, M. Ueno, N. Koizumi et al., "Enhancement on primate corneal endothelial cell survival in vitro by a ROCK inhibitor," *Investigative Ophthalmology & Visual Science*, vol. 50, no. 8, pp. 3680–3687, 2009.

[7] N. Okumura, N. Koizumi, M. Ueno et al., "ROCK inhibitor converts corneal endothelial cells into a phenotype capable of regenerating in vivo endothelial tissue," *The American Journal of Pathology*, vol. 181, no. 1, pp. 268–277, 2012.

[8] G. S. L. Peh, K. Adnan, B. L. George et al., "The effects of Rho-associated kinase inhibitor Y-27632 on primary human corneal endothelial cells propagated using a dual media approach," *Scientific Reports*, vol. 5, p. 9167, 2015.

[9] A. Pipparelli, Y. Arsenijevic, G. Thuret, P. Gain, M. Nicolas, and F. Majo, "ROCK inhibitor enhances adhesion and wound healing of human corneal endothelial cells," *PLoS One*, vol. 8, no. 4, articlsse e62095, 2013.

[10] N. Okumura, N. Koizumi, E. P. Kay et al., "The ROCK inhibitor eye drop accelerates corneal endothelium wound healing," *Investigative Ophthalmology & Visual Science*, vol. 54, no. 4, pp. 2493–2502, 2013.

[11] N. Koizumi, N. Okumura, M. Ueno, H. Nakagawa, J. Hamuro, and S. Kinoshita, "Rho-associated kinase inhibitor

eye drop treatment as a possible medical treatment for Fuchs corneal dystrophy," *Cornea*, vol. 32, no. 8, pp. 1167–1170, 2013.

[12] N. Koizumi, N. Okumura, M. Ueno, and S. Kinoshita, "New therapeutic modality for corneal endothelial disease using Rho-associated kinase inhibitor eye drops," *Cornea*, vol. 33, Supplement 11, pp. S25–S31, 2014.

[13] N. Okumura, S. Kinoshita, and N. Koizumi, "Cell-based approach for treatment of corneal endothelial dysfunction," *Cornea*, vol. 33, Supplement 11, pp. S37–S41, 2014.

[14] N. Okumura, R. Inoue, Y. Okazaki et al., "Effect of the Rho kinase inhibitor Y-27632 on corneal endothelial wound healing," *Investigative Ophthalmology & Visual Science*, vol. 56, no. 10, pp. 6067–6074, 2015.

[15] A. E. Maumenee and W. Kornblueth, "Regeneration of corneal stromal cells: I. Technique for destruction of corneal corpuscles by application of solidified (frozen) carbon dioxide," *American Journal of Ophthalmology*, vol. 31, no. 6, pp. 699–702, 1948.

[16] J. P. Faure, Y. Z. Kim, and B. Graf, "Formation of giant cells in the corneal endothelium during its regeneration after destruction by freezing," *Experimental eye Research*, vol. 12, no. 1, pp. 6–12, 1971.

[17] D. L. Van Horn, D. D. Sendele, S. Seideman, and P. J. Buco, "Regenerative capacity of the corneal endothelium in rabbit and cat," *Investigative Ophthalmology & Visual Science*, vol. 16, no. 7, pp. 597–613, 1977.

[18] J. S. Minkowski, S. P. Bartels, F. C. Delori, S. R. Lee, K. R. Kenyon, and A. H. Neufeld, "Corneal endothelial function and structure following cryo-injury in the rabbit," *Investigative Ophthalmology & Visual Science*, vol. 25, no. 12, pp. 1416–1425, 1984.

[19] P. Buco, D. L. Van Horn, W. H. Schutten, and K. Cohen, "Effects of transcorneal freezing on protein content of aqueous humor and intraocular temperature in rabbit and cat," *Investigative Ophthalmology & Visual Science*, vol. 17, no. 12, pp. 1199–1202, 1973.

[20] T. Mimura, S. Yokoo, M. Araie, S. Amano, and S. Yamagami, "Treatment of rabbit bullous keratopathy with precursors derived from cultured human corneal endothelium," *Investigative Ophthalmology & Visual Science*, vol. 46, no. 10, pp. 3637–3644, 2005.

[21] T. Mimura, S. Yamagami, S. Yokoo et al., "Sphere therapy for corneal endothelium deficiency in a rabbit model," *Investigative Ophthalmology & Visual Science*, vol. 46, no. 9, pp. 3128–3135, 2005.

[22] H. Ichijima, W. M. Petroll, P. A. Barry et al., "Actin filament organization during endothelial wound healing in the rabbit cornea: comparison between transcorneal freeze and mechanical scrape injuries," *Investigative Ophthalmology & Visual Science*, vol. 34, no. 9, pp. 2803–2812, 1993.

[23] W. M. Petroll, P. A. Barry-Lane, H. D. Cavanagh, and J. V. Jester, "ZO-1 reorganization and myofibroblast transformation of corneal endothelial cells after freeze injury in the cat," *Experimental eye Research*, vol. 64, no. 2, pp. 257–267, 1997.

[24] S. J. Tuft, K. A. Williams, and D. J. Coster, "Endothelial repair in the rat cornea," *Investigative Ophthalmology & Visual Science*, vol. 27, no. 8, pp. 1199–1204, 1986.

[25] S. B. Han, H. Ang, D. Balehosur et al., "A mouse model of corneal endothelial decompensation using cryoinjury," *Molecular Vision*, vol. 19, pp. 1222–1230, 2013.

[26] H. H. Chi and C. D. Kelman, "Effects of freezing on ocular tissues. I. Clinical and histologic study of corneal endothelium," *American Journal of Ophthalmology*, vol. 61, no. 4, pp. 630–641, 1966.

[27] N. J. Fullwood, Y. Davies, I. A. Nieduszynski, B. Marcyniuk, A. E. A. Ridgway, and A. J. Quantock, "Cell surface-associated keratan sulfate on normal and migrating corneal endothelium," *Investigative Ophthalmology & Visual Science*, vol. 37, no. 7, pp. 1256–1270, 1996.

[28] D. L. Van Horn and R. A. Hyndiuk, "Endothelial wound repair in primate cornea," *Experimental eye Research*, vol. 21, no. 2, pp. 113–124, 1975.

[29] C. Faber, E. Scherfig, J. U. Prause, and K. E. Sørensen, "Corneal thickness in pigs measured by ultrasound pachymetry in vivo," *Scandinavian Journal of Laboratory Animal Science*, vol. 35, no. 1, pp. 39–43, 2008.

[30] I. Sanchez, R. Martin, F. Ussa, and I. Fernandez-Bueno, "The parameters of the porcine eyeball," *Graefe's Archive for Clinical and Experimental Ophthalmology*, vol. 249, no. 4, pp. 475–482, 2011.

[31] L. J. Kopplin, K. Przepyszny, B. Schmotzer et al., "Relationship of Fuchs endothelial corneal dystrophy severity to central corneal thickness," *Archives of Ophthalmology (Chicago, Ill. 1960)*, vol. 130, no. 4, pp. 433–439, 2012.

[32] D. J. Repp, D. O. Hodge, K. H. Baratz, J. W. McLaren, and S. V. Patel, "Fuchs' endothelial corneal dystrophy: subjective grading versus objective grading based on the central-to-peripheral thickness ratio," *Ophthalmology*, vol. 120, no. 4, pp. 687–694, 2013.

[33] E. G. Olsen and M. Davanger, "The healing of human corneal endothelium. An in vitro study," *Acta Ophthalmologica*, vol. 62, no. 6, pp. 885–892, 1984.

[34] F. W. Fraunfelder, "Liquid nitrogen cryotherapy for surface eye disease (an AOS thesis)," *Transactions of the American Ophthalmological Society*, vol. 106, no. 1, pp. 301–324, 2008.

[35] W. J. Armitage, "Cryopreservation for corneal storage," *Developments in Ophthalmology*, vol. 43, pp. 63–69, 2009.

[36] C. Balachandran, L. Ham, C. A. Verschoor, T. S. Ong, J. van der Wees, and G. R. J. Melles, "Spontaneous corneal clearance despite graft detachment in Descemet membrane endothelial keratoplasty," *American Journal of Ophthalmology*, vol. 148, no. 2, pp. 227–234, 2009, e1.

[37] R. D. Shah, J. B. Randleman, and H. E. Grossniklaus, "Spontaneous corneal clearing after Descemet's stripping without endothelial replacement," *Ophthalmology*, vol. 119, no. 2, pp. 256–260, 2012.

[38] V. Galvis, A. Tello, and G. Miotto, "Human corneal endothelium regeneration," *Ophthalmology*, vol. 119, no. 8, pp. 1714–1715, 2012.

[39] E. Manche and A. Chan, "Preoperative pupil size and LASIK," *Ophthalmology*, vol. 118, no. 12, pp. 2526–2526, 2011, author reply 2526-7.

[40] W. Chan, A. Akhbanbetova, A. J. Quantock, and C. M. Heard, "Topical delivery of a Rho-kinase inhibitor to the cornea via mucoadhesive film," *European Journal of Pharmaceutical Sciences*, vol. 91, pp. 256–264, 2016.